

1-1-2012

# Towards Smart Drug Delivery: Exploration Of A Molecularly Imprinted Polymer Network

Anessa Khan  
*Ryerson University*

Follow this and additional works at: <http://digitalcommons.ryerson.ca/dissertations>

 Part of the [Polymer Science Commons](#)

---

## Recommended Citation

Khan, Anessa, "Towards Smart Drug Delivery: Exploration Of A Molecularly Imprinted Polymer Network" (2012). *Theses and dissertations*. Paper 1527.

This Thesis is brought to you for free and open access by Digital Commons @ Ryerson. It has been accepted for inclusion in Theses and dissertations by an authorized administrator of Digital Commons @ Ryerson. For more information, please contact [bcameron@ryerson.ca](mailto:bcameron@ryerson.ca).

**TOWARDS SMART DRUG DELIVERY: EXPLORATION OF A MOLECULARLY  
IMPRINTED POLYMER NETWORK**

by

**Aneesa Khan**

B.Sc., Applied Chemistry and Biology,  
Ryerson University, Toronto, June 2008

A thesis

presented to Ryerson University

in partial fulfillment of the requirements for the degree of

Master of Science

in

Molecular Science

Toronto, Ontario, Canada, 2012

© Aneesa Khan 2012

## **AUTHOR'S DECLARATION**

I hereby declare that I am the sole author of this thesis.

I authorize Ryerson University to lend this thesis to other institutions or individuals for the purpose of scholarly research.

I further authorize Ryerson University to reproduce this thesis by photocopying or by other means, in total or in part, at the request of other institutions or individuals for the purpose of scholarly research.

I understand that my thesis may be made electronically available to the public.

## **ABSTRACT**

### **TOWARDS SMART DRUG DELIVERY: EXPLORATION OF A MOLECULARLY IMPRINTED POLYMER NETWORK**

**Aneesa Khan**

Master of Science in Molecular Science, Ryerson University, 2012

The current study explores the concept of Molecular Imprinting Technology (MIT) and evaluates the ability of a molecularly imprinted hydrogel polymer (MIP) to preferentially uptake the template drug propranolol from aqueous solution. The extent of the molecular affinity and recognition was challenged by introducing a secondary competing structure during uptake. The release of propranolol as a response to environmental stimuli was investigated. The MIP was synthesized with copolymers methyl methacrylate (MMA) and N,N-dimethyl acrylamide (DMAA). Morphology was studied by scanning electron microscopy (SEM), uptake, displacement, and release experiments were studied by fluorescence spectroscopy. The SEM studies did not indicate the presence of molecularly imprinted cavities. The MIPs demonstrated preferential uptake in comparison to the non-imprinted (NIP) counterpart. The displacement studies revealed that uptake by the MIP is not very selective. The release studies demonstrated that propranolol release can be tailored to respond to environmental stimuli such as temperature and, especially, pH.



## ACKNOWLEDGMENTS

It is my pleasure to express my gratitude to the following people, without whom this thesis would not have been possible.

I would like to sincerely thank Dr. Christopher Evans, my graduate supervisor, for his encouragement, support and for the opportunity to allow me to research a field of chemistry that I am most passionate about. I am truly grateful for the patience and guidance that Dr. Evans displayed towards me. I am honoured to have had the privilege of being a graduate student under his supervision and also thankful for his financial support.

I would also like to extend my gratitude to Dr. Daniel Foucher and Dr. Stephen Wylie for the privilege that it has been to have them on my Supervisory Committee. Dr. Foucher's commitment to my project and ultimately my success, his vast knowledge on the topics and his ongoing encouragement have allowed me to reach the point of submitting my thesis. Dr. Wylie's guidance and his willingness to discuss strategies and provide innovative solutions that are without a doubt a major contributing factor to this project.

I would also like to express my appreciation to Dr. Ana Pejovic-Milic from the physics department for access to the equipment in her lab, and to Mr. Qiang Li for his assistance and his extensive expertise on the Scanning Electron Microscope. Also, a sincere thanks to Mr. Shawn McFadden for his patience and assistance with the instruments in the Ryerson University Analytical Centre.

I would like to sincerely thank Dr. Debora Foster for her ongoing support and for being more than just an educator. I am really thankful for her willingness to lend an ear and offer direction and guidance. It is my pleasure to thank Maria Landau, her dedication to the success of her students is admirable. I really appreciate her positivity and her willingness to assist in any situation.

I would like to thank Ryerson University and the Ontario Ministry of Education for financial support.

I would like to thank my colleagues Sofija Katic, Kristin McBain, and Muhammad Ali Naqvi for their guidance, assistance and support throughout my research project.

I would like to express my gratitude to my parents, Amir and Shaheen Khan, my siblings, Ruqaiya and Aysha Khan, Faysal Motaleb and my nephew, Yusuf Hamza Motaleb for their unconditional love and their support that has allowed me to complete this project. I am blessed to have a family that has always stood by my side and encouraged me to fulfill my aspirations. Thank you for all the big and small things each of you have done for me that has allowed me to achieve this milestone.

I would like to extend my gratitude to my friend and cousin, Soaleha Shams, who has always inspired me to achieve nothing short of success and has supported and encouraged me through all obstacles.

Also a special thanks to my cousins Nida, Waqqas and Ghayas Shams, my dear friends Shahid Amlani, Charlene Sethi, Matt Cadorin, and Hiona Murray.

Lastly, I would like to express my appreciation to Ahmer Chowdhery for the continuous support and encouragement, but most of all for believing in me.

## TABLE OF CONTENTS

ABSTRACT	iii
ACKNOWLEDGEMENTS	iv
LIST OF TABLES	xii
LIST OF FIGURES	xiii
LIST OF ACRONYMS AND ABBREVIATIONS	xvii
1. Introduction	1
1.1. Supramolecular Chemistry	2
1.1.1. Molecular Recognition	3
1.1.2. Self Assembly	8
1.1.3. Host-Guest Complexation/Inclusion Complexation	10
1.2. Molecular Imprinting	16
1.2.1. Imprinting Approaches	16
1.2.2. Preparation Technique	18
1.2.3. Components of Imprinting	21
1.2.3.1. Backbone Monomers	21
1.2.3.2. Functional Monomers	22
1.2.3.3. Cross-Linker	24
1.2.3.4. Template	27
1.2.3.5. Photo-initiator	28
1.2.4. Polymerization	31
1.2.5. Extraction	33
1.2.6. Applications	38

1.2.6.1.	Separation Techniques	40
1.2.6.2.	Chemical Sensors and Biosensors	40
1.2.6.3.	Catalysis	41
1.2.6.4.	Tissue Engineering	42
1.2.6.5.	Drug Delivery	44
1.2.6.6.	Hydrogels	44
1.3.	MIPs, Drug Delivery and Pharmacology	51
1.3.1.	Pharmacology and Pharmacokinetics	51
1.3.2.	Important Principles of Pharmacology	52
1.3.2.1.	Drug Administration	52
1.3.3.	Important Principles of Pharmacokinetics	53
1.3.3.1.	Drug Absorption	53
1.3.3.2.	Drug Distribution	55
1.3.3.3.	Drug Metabolism	56
1.3.3.4.	Drug Excretion	57
1.3.3.5.	Half Life	58
1.3.3.6.	Blood Drug Levels	58
1.3.3.7.	Bioavailability	60
1.3.3.8.	Factors of Individual Variation	60
1.4.	Improving Drug Delivery <i>via</i> Molecular Imprinting	61
1.4.1.	Experimental Polymer System	63
1.4.2.	Template Drug	66
1.4.3.	Additional Materials Used	69

1.4.3.1.	Benzoic Acid	69
1.4.3.2.	Naproxen	70
1.4.3.3.	Timolol	71
1.4.3.4.	1-Naphthol	72
1.4.4.	Experimental Design	74
1.4.4.1.	Scanning Electron Microscopy	74
1.4.4.2.	Fluorescence Spectroscopy	76
1.5.	Research Objectives	78
2.	Experimental	80
2.1.	Materials	80
2.2.	Instrumentation	81
2.3.	Analysis	82
2.4.	Methods	83
2.4.1.	Polymer Synthesis	83
2.4.2.	Polymer Washing	84
2.4.3.	Polymer Drying	84
2.4.4.	Morphology Studies	85
2.4.5.	Shearing Experiments	85
2.4.6.	Probe Studies	86
2.4.7.	Degradation of Propranolol	86
2.4.8.	Uptake	87
2.4.9.	Preferential Uptake	88
2.4.10.	Polymer Form Variation	88

2.4.11. Effects of Centrifugation	88
2.4.12. Maximum Adsorption	89
2.4.13. Higher Polymer Concentrations	89
2.4.14. Cavities as Limiting Factor	89
2.4.15. Displacement Studies	90
2.4.16. Release Studies	90
3. Results	92
3.1. Morphology Studies	92
3.1.1. Effects of Cleaning Methods on Polymer Morphology	94
3.1.2. Effects of Shearing on Polymer Morphology	99
3.1.3. Probe Studies	101
3.1.4. Effects of Shearing in the presence of the Probe	103
3.2. Degradation of Propranolol	105
3.3. Uptake of Propranolol by Polymer Systems	107
3.3.1. Preferential Uptake	110
3.3.2. Structure Variation	114
3.3.3. Effects of Centrifugation on Uptake	117
3.3.4. Maximum Adsorption	120
3.3.5. Higher Concentrations	123
3.3.6. Cavities as Limiting Factor	128
3.4. Displacement	132
3.4.1. Non-Complementary Structures	132
3.4.1.1. Benzoic Acid	132

3.4.1.2. Naproxen	136
3.4.2. Complementary Structures	139
3.4.2.1. Timolol	139
3.4.2.2. 1-Naphthol	144
3.5. Release Studies	148
3.5.1. Temperature	148
3.5.2. Agitation	151
3.5.3. pH	154
4. Discussion	159
4.1. Morphology Studies	159
4.1.1. Cleaning	162
4.1.2. Shearing	164
4.1.3. Probe	165
4.2. Degradation of Propranolol	167
4.3. Uptake Experiment	167
4.3.1. Preferential Uptake	168
4.3.2. Structure Variation	169
4.3.3. Centrifugation	170
4.3.4. Maximum Adsorption	170
4.3.5. High Concentrations	171
4.3.6. Cavities as limiting Factor	172
4.4. Displacement	174
4.4.1. Non Complementary Structures	174

4.4.2. Complementary Structures	176
4.5. Release	178
5. Conclusion	181
6. Future Studies	184
APPENDIX	190
REFERENCES	192



## LIST OF TABLES

Table 1.1: Types of Interactions that take place in Molecular Recognition Processes	5
Table 1.2: Necessary Features of a Host Molecule for Crystalline Inclusion to occur	15
Table 1.3: Summary of Polymerization Processes for MIPs	32
Table 1.4: Advantages and Disadvantages of Soxhlet Extraction	35
Table 1.5: Design Criteria for Hydrogel for Drug Delivery Systems	50
Table 1.6: Key MIP Considerations for Developing an Effective DDS	62
Table 1.7: Components of Experimental System used in this study	65
Table 1.8: Structure, Molecular Formula, Molecular Weight, and pKa of Templates	73
Table 3.1: Comparison of release method on propranolol release from MIP; 250 $\mu$ M propranolol solution at 72 hours	158

## LIST OF FIGURES

Figure 1.1: Schematic representation of Emil Fischer's Lock and Key Complementarity Arrangement	7
Figure 1.2: A Schematic Interpretation of Molecular Recognition	7
Figure 1.3: Schematic Representation of Self-Assembly of A Supramolecular Aggregate	9
Figure 1.4: Common Hosts used in host-guest complexation	12
Figure 1.5: Schematic Representation of $\beta$ -Cyclodextrin	12
Figure 1.6: Schematic Illustration of the association of host-guest interaction	13
Figure 1.7: Schematic Interpretation of MIT	20
Figure 1.8: Commonly used Functional Monomers	23
Figure 1.9: Cross-Linkers most commonly used	26
Figure 1.10: Animated representation of Photoinitiated Polymerization	30
Figure 1.11: Type I Photoinitiation Mechanism of Benzoin	30
Figure 1.12: Conventional Soxhlet Extraction Set-Up	34
Figure 1.13: Schematic of Potential Changes to MIP's Induced by Template Extraction	37
Figure 1.14: Five Common Applications of MIT	39
Figure 1.15: SEM Images of Tissue Scaffolds	43
Figure 1.16: Swollen and Collapsed Hydrogel State	46
Figure 1.17: Schematic of Swelling of Ionic Hydrogels as a function of pH	48
Figure 1.18: Generic Time Response Curve	59
Figure 1.19: Chemical structure of Propranolol and Related compounds	68
Figure 1.20: Chemical structure of Propranolol Metabolites	68
Figure 1.21: Major components in a Scanning Electron Microscope set-up	75

Figure 1.22: Jablonski Diagram	77
Figure 3.1: Scanning Electron Microscope images of ProMIPs	93
Figure 3.2: SEM images of NIP – Un-cleaned	95
Figure 3.3: SEM images of ProMIP – Un-cleaned	95
Figure 3.4: SEM images of NIP - Cleaned	96
Figure 3.5: SEM images of ProMIP – Cleaned	96
Figure 3.6: SEM images of NIP morphology	98
Figure 3.7: SEM images of ProMIP morphology	98
Figure 3.8: SEM images of NIP samples with shearing	100
Figure 3.9: SEM images of ProMIP samples -shearing	100
Figure 3.10: SEM images of NIP samples with probe	102
Figure 3.11: SEM images of ProMIP samples with probe	102
Figure 3.12: SEM images of NIP samples with shearing and probe	104
Figure 3.13: SEM images of ProMIP samples with shearing and probe	104
Figure 3.14: Photolysis of Propranolol	106
Figure 3.15: Explanation of Graph Interpretation	109
Figure 3.16: Propranolol preferential uptake by NIP	111
Figure 3.17: Propranolol preferential uptake by ProMIP	112
Figure 3.18: Comparison of preferential uptake by NIP and ProMIP	113
Figure 3.19: Comparison of propranolol uptake by HF and PF in NIP	115
Figure 3.20: Comparison of propranolol uptake by HF and PF in ProMIP	116
Figure 3.21: Centrifugation effects on NIP hydrogel network	118
Figure 3.22: Centrifugation effects on ProMIP hydrogel network	119

Figure 3.23: Propranolol Uptake maximum of 168 hours in NIP	121
Figure 3.24: Propranolol Uptake maximum of 168 hours in ProMIP	122
Figure 3.25: NIP behaviour at high concentrations (above 100 $\mu\text{M}$ )	125
Figure 3.26: ProMIP behaviour at high concentrations (above 100 $\mu\text{M}$ )	126
Figure 3.27: A comparison of propranolol uptake between the NIP and ProMIP	127
Figure 3.28: ProMIP Uptake of 10 $\mu\text{M}$ Propranolol Solution in varying quantities of Polymer	129
Figure 3.29: ProMIP Uptake of 25 $\mu\text{M}$ Propranolol Solution in varying quantities of Polymer	130
Figure 3.30: ProMIP Uptake of 50 $\mu\text{M}$ Propranolol Solution in varying quantities of Polymer	131
Figure 3.31: Non-Competitive Displacement of Propranolol in a MIP network by Benzoic Acid.	134
Figure 3.32: Competitive Displacement of Propranolol in a MIP network by Benzoic Acid.	135
Figure 3.33: Non-Competitive Displacement of Propranolol in a MIP network by Naproxen.	137
Figure 3.34: Competitive Displacement of Propranolol in a MIP network by Naproxen.	138
Figure 3.35: Non-Competitive Displacement of Propranolol in a MIP network by Timolol.	141
Figure 3.36: Competitive Displacement of Propranolol in a MIP network by Timolol.	142
Figure 3.37: Corrected Competitive Displacement of Propranolol in a MIP network by Timolol.	143
Figure 3.38: Non-Competitive Displacement of Propranolol in a MIP network by 1-Naphthol.	145
Figure 3.39: Competitive Displacement of Propranolol in a MIP network by 1-Naphthol.	146

Figure 3.40: Corrected Competitive Displacement of Propranolol in a MIP network by 1-Naphthol	147
Figure 3.41: Release of Propranolol from the MIP network at RT	149
Figure 3.42: Release of Propranolol from the MIP network at 37 °C	150
Figure 3.43: Release of Propranolol from the MIP network with shaking at 37°C	152
Figure 3.44: Release of Propranolol from the MIP network with sonicator at 37°C	153
Figure 3.45: Ionic release of propranolol from MIP network at pH 12	155
Figure 3.46: Ionic release of propranolol from MIP network at pH 3	156
Figure 3.47: Release of Propranolol from MIP network for all methods, room temperature, heating at 37 °C, shaking, sonication, pH 12 and pH 3	157
Figure 6.1: Schematic representation of the burst effect in a zero-order (constant drug delivery) controlled release system	185
Figure 6.2: Potential alternative approaches available for template extraction	188
Figure A.1: Calibration curve	191

## **LIST OF ACRONYMS AND ABBREVIATION**

AFM – Atomic Force Microscopy

BA – Benzoic Acid

BSE - Back-Scattered Electrons

CEC - Capillary Electro-Chromatography

Cent - Centrifuged

CSP – Chiral Stationary Phases

CS - Complementary Structures

CD - Competitive Displacement

[conc] – concentration

CD – Cyclodextrin

COX - Cyclo-oxygenase

DMAA – N,N-dimethyl acrylamide

DCM - dichloromethane

DMSO - di-methyl sulfoxide

DDS - Drug Delivery Systems

DMMS - drug microsomal metabolizing system

EGDMA – ethylene glycol dimethacrylate

EPI - epinephrine

FRP – free radical polymerization

GI - gastrointestinal

HPLC - High Performance Liquid Chromatography

HF – hydrogel form

IM - intramuscular

IV - intravenous

LC - Liquid Chromatography

MAA – methacrylic acid

MeCN - acetonitrile

MIP – molecularly imprinted polymers

MISPE - molecularly imprinted polymers for Solid-Phase Extraction

MIT – molecular imprinting technology

MEHQ - monomethyl ether hydroquinone

MMA – methyl methacrylate

NIP – non-imprinted polymer

NE - norepinephrine

NCS - Non-Complementary Structures

NCD - Non-Competitive Displacement

NCent – Non centrifuged

NSAID - non-steroidal anti-inflammatory drugs

ppm – parts per million

PF – powder form

Pro-MIP – molecularly imprinted with propranolol

ROMP – ring-opening metathesis polymer

rpm - revolutions per minute

RT – Room temperature

SEM – Scanning Electron Microscopy

Solid Phase Extraction (SPE)

TEM – Transmission Electron Microscopy

TRIM - trimethylpropane trimethacrylate

UV - ultra-violet

Vis – visible



## 1. INTRODUCTION

The field of drug delivery has become a well-studied science in the last forty years.<sup>1</sup> Significant advances have been made in the development of new technologies that allow for optimized drug delivery.<sup>2</sup> For example, intelligent release of a therapeutic agent, which occurs as a response to a specific stimulus, can allow for controlled drug delivery.<sup>3</sup> The design and synthesis of biocompatible materials useful in sustained drug delivery are still under development despite receiving an overwhelming level of attention, especially in the past decade.<sup>4, 5</sup>

The challenges that surround pharmaceutical drug delivery, such as first pass metabolism and premature biotransformation can be controlled through modification of the delivery vehicles. Through implementation of better formulation strategies, the specific demands of a drug delivery system and improved performance of already established medicines can be achieved.<sup>6</sup> The development of superior delivery systems would allow better regulation of the rate of release, reduce the adverse effects, prolong the duration of pharmacological action, and enhance loading capacity, which would minimize the dosing frequency and overall improved patient compliance.<sup>7</sup>

This paper explores the potential to alleviate some of the limitations encountered in drug administration by developing a smart drug delivery vehicle for intelligent release using molecular imprinting technology. In a nutshell, the molecular imprinting technique involves synthesis of a cross-linked polymer in the presence of a target drug molecule (the “template”). According to the conventional model of molecular imprinting, this approach to synthesis creates cavities within the

polymer network with structures complementary to features on the template molecule, thus they are tailored to interact specifically and selectively with the template. Such material is expected to be a highly efficient binding medium for the template. Depending on the choice of network polymer, such an imprinted system may be useful to deliver the template drug in a pharmaceutical context. This chapter defines and discusses the various concepts that are related to molecular imprinting and its basis as a mode for drug delivery. In the present study, the polymer chosen was composed of methacrylic acid, N,N-dimethyl acrylamide, and methyl methacrylate as monomers, cross-linked with ethylene glycol dimethacrylate, and the template was the conventional anti-hypertensive compound propranolol.

### **1.1. Supramolecular Chemistry**

A key concept in the conventional model of molecular imprinting is that there must be some form of interaction between the template molecule and the components of the polymer to be synthesized. This set of interactions ensures that the template influences the formation of the polymer in such a way that the cavities alluded to above are created during the process of synthesis. In most cases, the interactions used for imprinting are non-covalent, inter-molecular interactions. Thus, imprinting can be viewed as a sub-set of supramolecular chemistry.

Supramolecular chemistry is a branch of chemistry that examines the association of molecules into non-covalent arrays or aggregates.<sup>8</sup> In more general terms it has been defined as “Chemistry beyond the Molecule”.<sup>9, 10</sup> Supramolecular chemistry refers to the association of two or more chemical species and the

structures and functions that govern the formation of those entities.<sup>9</sup> The discovery of “crown ethers”, “cryptands”, and “spherands” by Pedersen,<sup>11</sup> Lehn,<sup>9</sup> and Cram<sup>12</sup> respectively, won them the Nobel Prize in 1987.<sup>13</sup> This work developed a vast interest in small, complementary molecules that could be designed to recognize each other through non-covalent interactions such as hydrogen bonding, charge-charge, donor-acceptor,  $\pi$ - $\pi$ , and van der Waals.<sup>14</sup>

The design and production of distinct molecular assemblies that have the ability to selectively recognize molecules as well as signal the presence of specific analyte(s) is a major achievement of supramolecular chemistry.<sup>15</sup> It is due to such achievements that molecular recognition and supramolecular chemistry have been used interchangeably by some,<sup>8</sup> however, others characterize molecular recognition as an essential *principle* that governs the formation of supramolecular entities.<sup>15, 16</sup> Self-assembly is also a factor in the formation of supramolecular entities.<sup>17, 18</sup> Molecular recognition and self-assembly are intrinsic features of supramolecular chemistry that are interdependent on each other and are described further in detail in the next section.<sup>19, 20</sup>

#### 1.1.1. *Molecular Recognition*

The phrase “Molecular Recognition” refers to specific affinities and structural complementarity between pairs of molecules and it occurs as a result of a pattern of favourable interactions between the molecules concerned.<sup>21, 22</sup> Such phenomena are intrinsic features of several biochemical systems, as the interaction between various biochemical materials occurs on the basis of highly specific recognition, reaction,

transport, and regulation.<sup>16</sup> A few examples of such processes that occur in nature include substrate binding to a receptor protein, enzymatic reactions, assembling of protein-protein complexes, intermolecular reading, translation and transcription of the genetic code, etc.<sup>9, 23</sup> A perfect model of such an interaction based on the strong affinity between two bio-molecules is the specific interaction between an antigen and its respective antibody.<sup>24, 25</sup>

Molecular recognition explores and exploits both intramolecular and intermolecular interactions through non-covalent bonding. An exquisite demonstration of such an intramolecular process related to molecular recognition is protein folding.<sup>21</sup> Non-covalent interactions range from very weak interactions where the binding energy is 4.18-41.8 kJ/mol, to rather strong interactions where binding energy ranges from 41.8-377 kJ/mol.<sup>26</sup> Some of the weak interactions include, but are not limited to: hydrophobicity,<sup>27-29</sup> dipole-dipole, cation- $\pi$  interactions, charge transfer ( $\pi$ - $\pi$  staking), and hydrogen bonding.<sup>30, 31</sup> Hydrogen bonds are in the energy range from 5-30 kJ/mol, weaker than ionic bonds but stronger than van der Waals forces.<sup>15</sup> They are attributed to the interaction of an electron cloud polarized by nuclei with the energy less than 5 kJ/mol.<sup>32</sup> Ion-Ion interactions are the strongest among non-covalent bonds, followed by ion-dipole effects, which are about 14.64 kJ/mol for molecular recognition in both aqueous and organic media.<sup>33</sup> A summary of the interactions involved in molecular recognition processes is displayed in Table 1.1.

**Table 1.1:** Types of interactions that take place in Molecular Recognition processes  
(Adapted from König, 1995).<sup>34</sup>

Interaction	Example
metal-ligand	metal salts, organometallic coordination compounds, metalloproteins
hydrogen bonds	nucleotide base pairs, melamine-cyanuric acid structures, amide dimerization in solution
electronic interactions	salt bridges in proteins, carboxylate – guanidinium interaction
dipole-dipole interactions	e.g. $-I \cdots NC-$ or $-I \cdots O_2N-$ interaction in the solid state
hydrophobic interactions	cyclodextrin inclusion complexes, micelles, amphiphilic monolayers
van der Waals interactions	urea inclusion complexes
$\pi$ -stacking and charge-transfer interactions	nucleic acids in the DNA, porphyrins in the solid state
covalent bonds, that can be reversibly formed and broken	disulfides, borate esters

Molecular Recognition is also influenced by geometrical and electronic complementarity of size, shape, and chemical functionalities.<sup>8</sup> The fundamental principles of molecular recognition date back to the late 19<sup>th</sup> century and were described in the context of the “lock and key” analogy by Emil Fischer in 1894 and Paul Ehrlich in 1906. Fischer’s famous lock and key analogy, demonstrating the specificity of enzyme reactions<sup>35</sup> shown in Figure 1.1, has created a mental picture of molecular recognition processes for successive generations of scientists.<sup>36</sup> Some scientists believe that Fischer’s model shaped to a “marked degree” the development of organic chemistry.<sup>37</sup> The lock depicts the molecular receptor, a protein or an enzyme, and the key depicts the substrate that is recognized to give a defined receptor-substrate complex.<sup>38</sup>

Although widely accepted, the lock and key analogy is an oversimplified model and has several limitations, and therefore does not adequately describe molecular recognition systems. One limitation is the fact that the model takes only the enthalpic driving force for binding into account and ignores entropy.<sup>15</sup> Another limitation is that the lock and key model suggests a one point binding system, one key (or substrate) to one lock (or receptor), which in many molecular recognition systems is not the case, as can be seen in Table 1.1. Thus the implication of the one point binding system of the lock and key analogy is misleading.<sup>39</sup> The schematic representation of molecular recognition as seen in Figure 1.2 is a more accurate interpretation of the types of binding systems; it is indicative of the multiple binding sites that may be available.

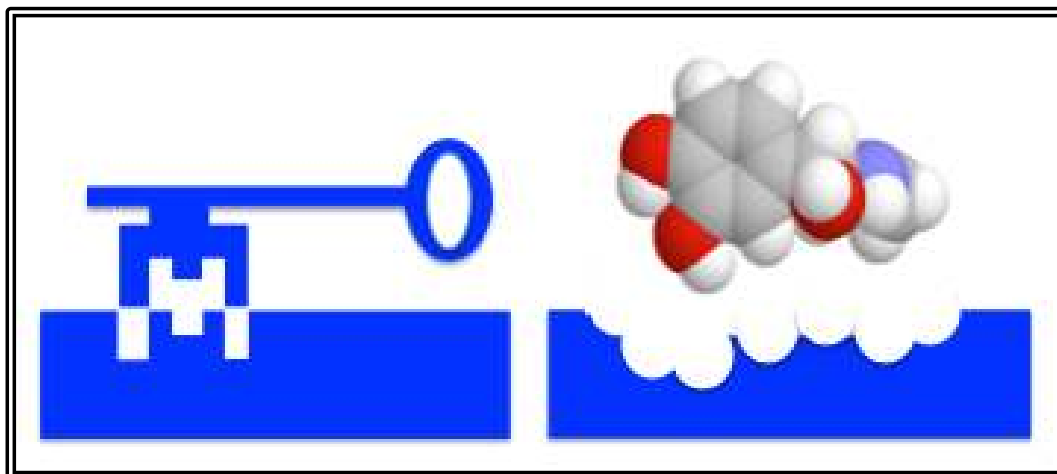


**Figure 1.1:** Schematic representation of Emil Fischer's Lock and Key complementarity arrangement.<sup>40</sup>

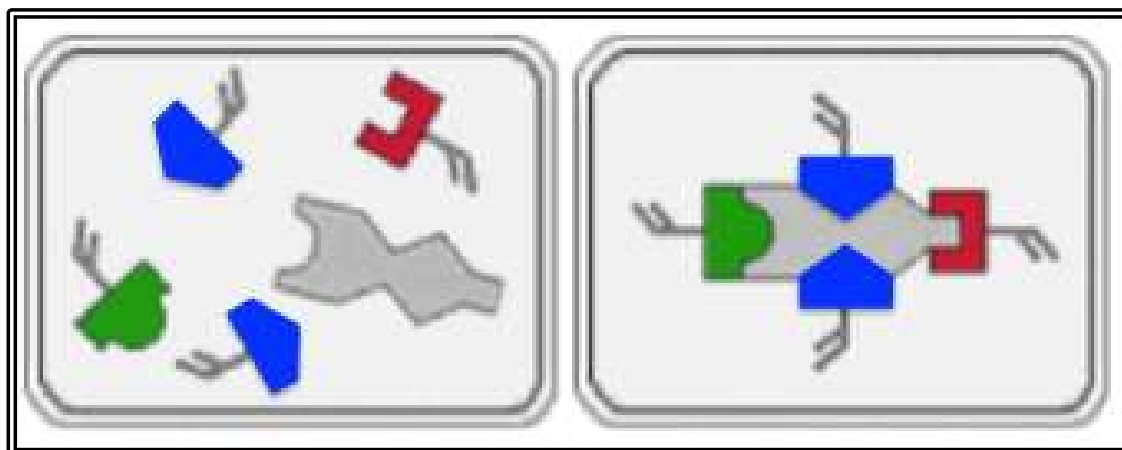


**Figure 1.2:** A schematic interpretation of Molecular Recognition (adapted from Henzte, 2001).<sup>41</sup>

### *1.1.2. Self Assembly*

Molecular self-assembly is an organized, yet spontaneous, association of molecules under equilibrium conditions, into stable and structurally well-defined aggregates from its components joined by non-covalent bonds.<sup>20, 42</sup>

Self-assembly allows for the production of higher ordered molecular architectures. These structures can consist of complementary molecules or multiple copies of a self-complementary molecule.<sup>43</sup> In order for a group of molecules to self-assemble, they must first aggregate. Aggregation is a result of molecules selectively binding to form well defined structures held together by intermolecular forces.<sup>44</sup>

Figure 1.3 demonstrates the importance of complementarity in the process of aggregation.



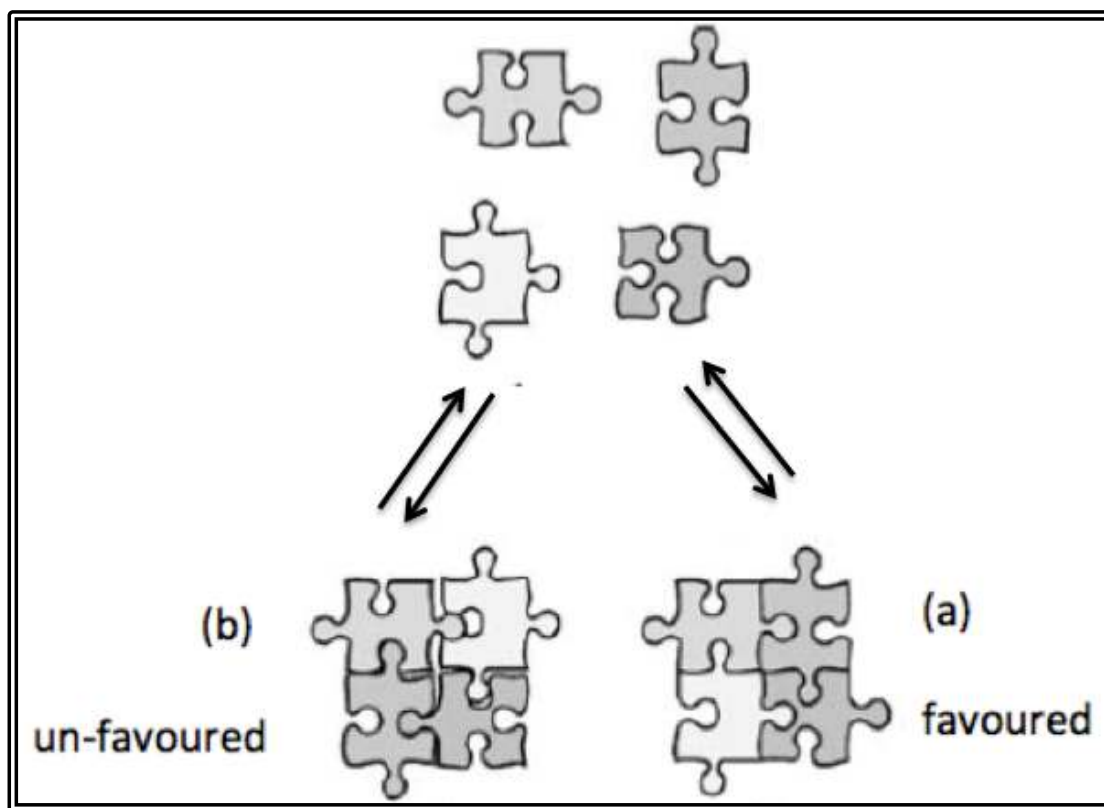


**Figure 1.3:** Schematic representation of self-assembly of a supramolecular aggregate.<sup>15</sup> (a) Binding among complementary units leads to strong aggregation. On a molecular level the thermodynamically most favoured species and the most stable one is obtained in a thermodynamically controlled system. (b) Poor complementarity of the building blocks destabilizes the obtained aggregate. Note: In a reversible process (b) can be converted into the more preferred aggregate (a).

Such phenomena are well documented in biology and as such the virtues of self-assembly were originally established through understanding biological systems.<sup>16, 22, 45</sup> Since molecular self-assembly is ubiquitous in biological systems, it underlies the creation of a range of complex biological structures.<sup>20</sup> In classic biological examples, self-assembly:

- i. minimizes information through the use of binding subunits,
- ii. establishes control of assembly and disassembly by virtue of multiple bonds of low energy,
- iii. exploits error-checking through reversible interactions,
- iv. maintains a level of architectural control and efficiency

The idea of self-assembly has also evolved into an attractive strategy with respect to synthetic chemistry.<sup>44</sup> All of the features mentioned above are however without parallel in synthetic chemical environments.<sup>22, 43, 46</sup> A significant amount of effort in establishing synthetic chemical systems as self-assembly paradigms has been put forth by various research groups including Lehn,<sup>47, 48</sup> Raymond,<sup>49-51</sup> Albrecht,<sup>15, 52, 53</sup> Stang,<sup>54-57</sup> and Severin.<sup>14</sup> Self-assembly can involve non-covalent and/or covalent bonds. Molecular recognition is one manifestation of non-covalent self-assembly.<sup>58</sup>

### *1.1.3. Host-Guest Complexation/ Inclusion Complexation*

Host-guest complexation or inclusion complexation (often used interchangeably), like self-assembly, is another phenomenon that can be categorized as a type of supramolecular association. Although the lock and key model described earlier, and shown in Figure 1.1, does not sufficiently characterize supramolecular

association, it certainly laid the groundwork for the concept of host-guest complexation. Host-guest interactions have been reported as early as the 19<sup>th</sup> century, and are said to have been discovered mostly by accident at the time of clathrate chemistry,<sup>59</sup> originating from the discovery of “cellulosine” (now known as cyclodextrin) by Villiers in 1891.<sup>60</sup>

Generally host-guest interactions involve two or more molecules: a host and one or more guests, which form a supramolecular complex. Materials that have commonly been used as hosts include crown ethers,<sup>61-63</sup> cyclodextrins,<sup>64-66</sup> calixarenes,<sup>67-69</sup> porphyrins<sup>70-72</sup> and cryptophanes<sup>73-75</sup> which are shown in Figure 1.4 (Note – The structures shown are adapted from the cited references for these various hosts).

Figure 1.4 demonstrates that hosts are three-dimensional supramolecular cages that have well defined cavities that may serve as sites for selective binding of guests. The general shape of the cage/cavity that is formed varies from one host molecule to the next. In the case of cyclodextrin,<sup>76</sup> shown in Figure 1.5 the shape of the cavity has been described as a toroidal shape and more commonly called a “donut”.<sup>77</sup> An inclusion complex, such as the one in Figure 1.6,<sup>76</sup> is formed when a host, such as cyclodextrin, spatially encloses the guest molecule. The cavity of the host is often not altered, or very slightly altered upon complexation.<sup>78</sup>

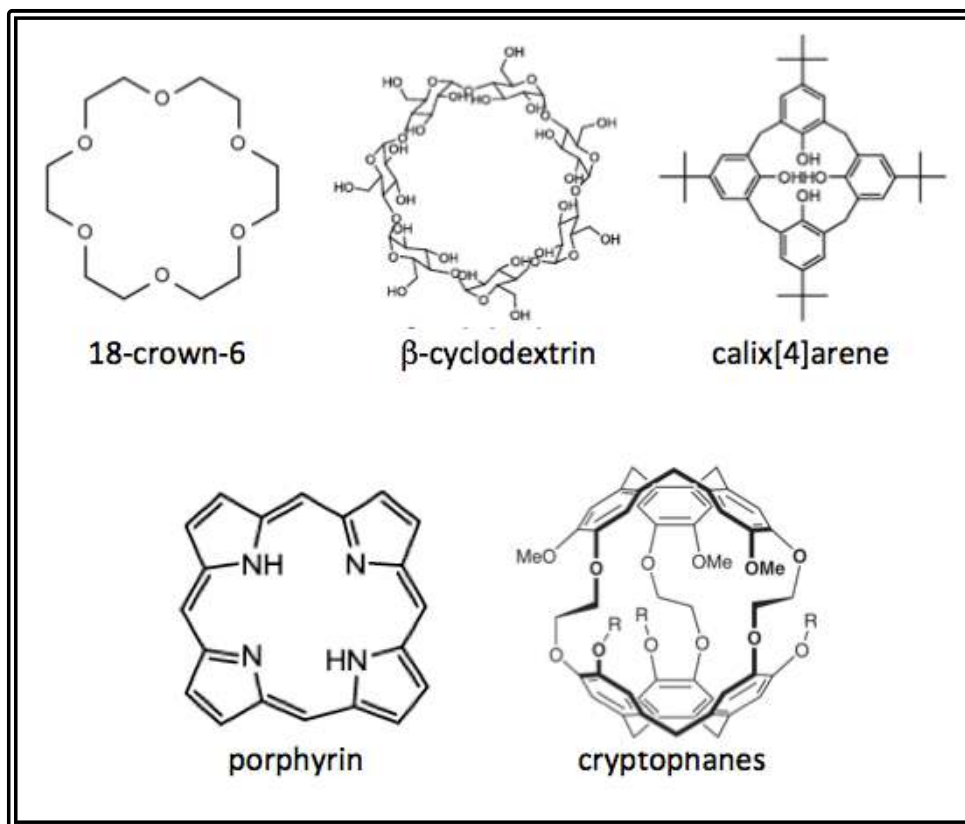


**Figure 1.4:** Common hosts used in host-guest complexation.

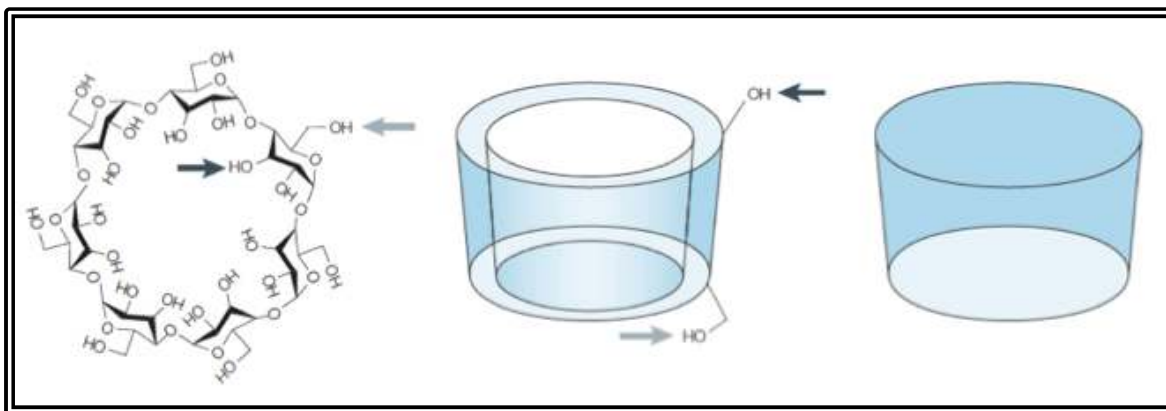


**Figure 1.5:** Schematic representation of β-cyclodextrin in its toroidal cavity formation.<sup>76</sup> The positions of the two highlighted hydroxyl groups from the structure are indicated on the schematic configuration.

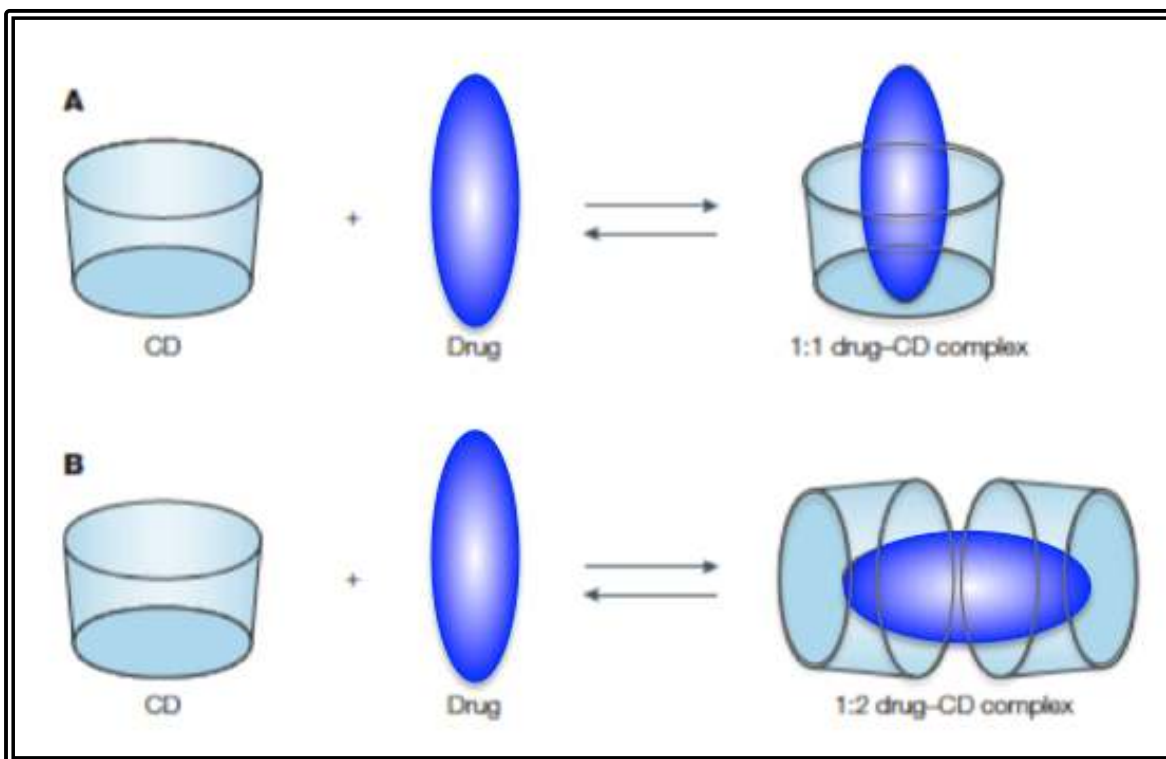


**Figure 1.6:** Schematic illustration of the association of free host, cyclodextrin (CD) and a drug as a guest molecule.<sup>76</sup> **A:** The drug is included by cyclodextrin in a 1:1 ratio **B:** The drug is included by two cyclodextrins in a 1:2 ratio.

The encapsulation of a guest molecule often causes changes to the physiochemical properties and chemical reactivity of the guest. One such change that has been highly beneficial in pharmaceutical applications is that a hydrophobic guest becomes hydrophilic.<sup>76</sup> The unique capability of being able to alter properties of guest molecules, by means of complexation, has allowed host-guest interactions to be applied in a variety of contexts. In 1989, Weber<sup>79</sup> *et al.* described criteria that were necessary in a host in order for crystalline inclusion to occur, which are outlined in Table 1.2.

**Table 1.2:** Necessary features of a host molecule for crystalline inclusion to occur (adapted from Weber *et al.*, 1989).<sup>80</sup>

Bulky	Host must be bulky in composition, to provide low density packing in the crystal
Rigid	Host must have a rigid conformation to maintain the cavity structure (not collapse)
Placement	Host must be appropriately placed to allow for interaction between functional groups
Balance	The host should allow for an overall balanced shape of the molecule to help stabilize the crystal packing in general

## 1.2. Molecular Imprinting

Molecular Imprinting Technology (MIT) utilizes supramolecular processes that feature elements of molecular recognition and self-assembly to form a set of host-guest complexes which are then “frozen” into a polymer network. MIT as first developed by Wulff<sup>81-83</sup> in 1972 and Mosbach<sup>84-86</sup> in 1981, allows for the production of pre-organized spaces, specific to a molecule of interest (template), within a cross-linked polymer network.<sup>87, 88</sup> The developed synthetic polymer is capable of predetermined selective recognition originating from the interaction between the template molecule and the polymer building blocks.<sup>89, 90</sup> By exploiting the template-mediated polymerization mechanisms in the fabrication of molecularly imprinted polymers (MIP), the resulting synthetic networks not only have tailored selectivity, but they also possess affinity for the template molecule.<sup>91</sup> The sequence of events just described can be referred to as the conventional model of molecular imprints.

### 1.2.1. *Imprinting Approaches*

Specific recognition is influenced by the type of interaction established between the template and the monomers prior to polymerization, which could be covalent, non-covalent or a combination of the two.<sup>2</sup> Among these types of interactions, covalent interactions are the strongest and most selective, however, the approach is limited to a few specific functional groups.<sup>92</sup> The covalent technique, developed by Wulff<sup>81, 82, 83</sup> and his colleagues, allowed the template and the monomer to undergo reversible covalent binding prior to polymerization, which results in the covalent bond remaining intact. The binding of this type of polymer



depends on the reversibility of the covalent bonds. In order to cleave the covalent bonds between the template and the functional monomer, harsh conditions are generally required (acid hydrolysis), greater extraction times, and can be costly.<sup>85</sup> The mechanism of this interaction is well understood despite the fact that suitable reversible covalent interactions with polymerizable monomers are few.

Alternatively, a greater variety of functionality can be introduced into MIP cavities *via* non-covalent interactions. The non-covalent protocol is considered to be simpler as the extraction of the template can often be carried out by rinsing with suitable polar or non-polar solvents rather than with harsh chemistry<sup>93, 94</sup> and with minimal damage to the imprinted cavities. Hence the non-covalent protocol is the favoured process over covalent imprinting.<sup>95</sup> In the non-covalent approach the functional monomer interacts with the template through weak intra-molecular forces such as hydrogen bonding, van der Waals forces, and electrostatic forces.<sup>85</sup> The binding of this type of polymer relies on the special binding sites that are formed by the self-assembly between the template and monomer following a cross-linked co-polymerization. Molecular recognition is driven, largely by non-covalent forces which are relatively weak, thus specificity against competitor binding substances may pose a challenge.<sup>96</sup>

The requirements of the covalent MIP protocol differ from that of the non-covalent method in the ratios of the components (functional monomer, cross-linker, and template) that are utilized. With non-covalent interactions, an excess of functional monomer is required in the polymerization mixture to ensure that the binding sites in the template are fully saturated at equilibrium.<sup>83, 97</sup>

Combined covalent and non-covalent strategies have also been employed. These utilize covalent interactions in the creation of the imprinted step and non-covalent interactions in the rebinding of the ligand. The combinational technique has proved to be useful by manipulating the advantages of both techniques, however, it is restricted to cases where the template molecule needed to be modified prior to polymerization.<sup>98</sup>

### *1.2.2. Preparation Technique*

The preparation of the MIP is relatively straightforward and an inexpensive procedure. The traditional methodology, involves preparing a monomer solution, consisting of backbone monomer, functional monomers (i.e., the component that introduces the complementary functionalities) and cross-linker in the presence of the molecule of interest; the template molecule.<sup>99</sup> The template is allowed to interact with functional groups on one or more of the polymer components (usually the functional monomer) in order to form a stable self-assembled complex around the template.<sup>4, 100</sup> The sequence and the spatial arrangement of the polymer network are then fixed upon polymerization<sup>90</sup> with the assistance of an initiator. Following polymerization, the template molecules are extracted from the MIP, resulting in highly specific and selective recognition sites that are complementary and have affinity for the original template.<sup>90, 101, 102</sup> The cavities produced re-binds the template when the imprinted polymer is re-introduced to the template under favourable binding conditions.<sup>89, 103</sup> The corresponding non-imprinted polymer (NIP) is prepared in the same manner described for the MIP, however, the template

molecule is not used. Therefore, the NIP should not have complementary binding sites for the template drug. Figure 1.7 depicts schematically the process of molecular imprinting<sup>7</sup> that is described above.

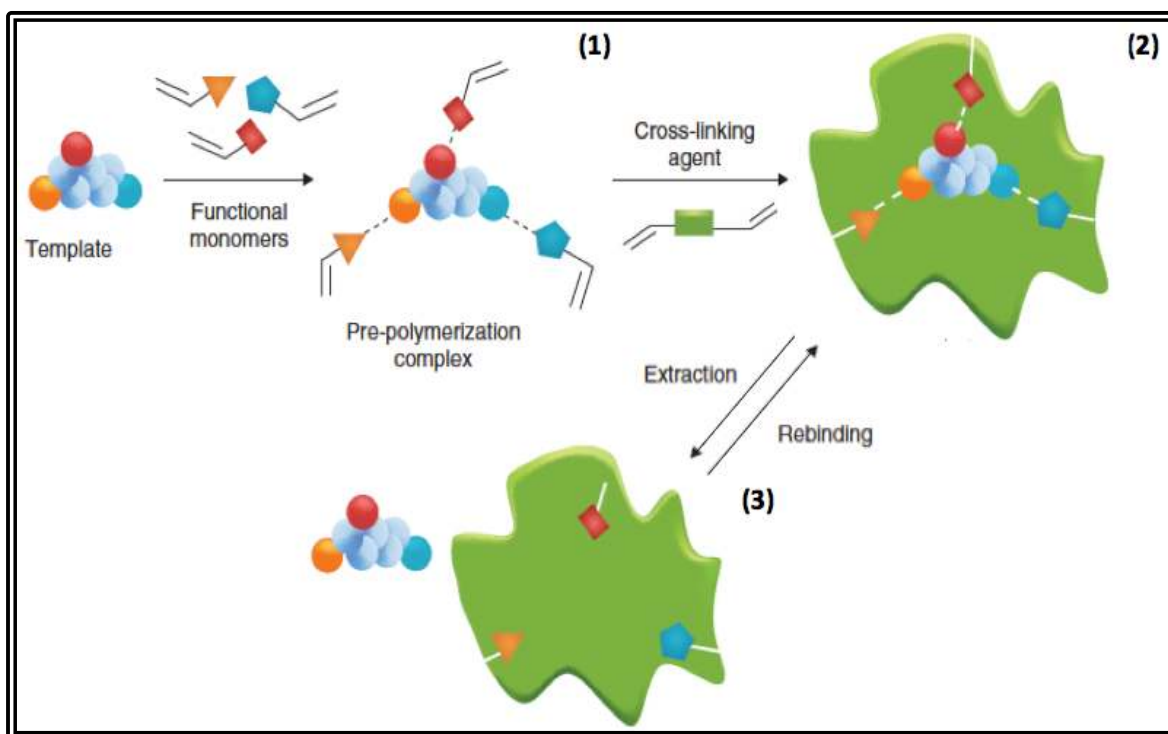


**Figure 1.7:** Schematic interpretation of MIT<sup>7</sup>. There are three essential processes (1) the assembly of the pre-polymerization complex, (2) polymerization, and (3) the extraction of the template liberating the binding site.

### *1.2.3. Components of Imprinting*

Each component in the system has a specific role and modifications in the quantities of backbone monomers, functional monomers, and/or the cross-linkers can render very different polymers despite the mixture constituents being the same.

#### *1.2.3.1. Backbone Monomers*

Backbone monomers determine the capacity of the polymer to bind to the template molecule, though, they do not interfere in the template binding process itself (or at most, backbone monomers may offer non-specific binding opportunities). The backbone monomers may also affect the degree of swelling of the system in a hydrogel. The intensity of the swelling effect is dependent on the nature of the monomers used.<sup>104</sup> The backbone monomers also influence the way in which the template is released from the polymer matrix.<sup>105</sup> According to developments in the statistical mechanics of polymers, molecular imprinting is favoured by heteropolymer systems (i.e. there should be more than one monomer species).<sup>106</sup> Since a single type of functional monomer (described in the next section) does not provide optimal interactions between the polymer chains as well as the template. Imprinting can manage the monomers in an energetically favoured conformation that facilitates multiple point complexation with the template<sup>107</sup> and increases the potential for growth of the polymer chain with increased “memorization” and enhanced template binding.<sup>108</sup>

#### 1.2.3.2. *Functional Monomers*

The role of the functional monomer in the production of MIPs is to interact with the template prior to and during polymerization. The selection of the functional monomer is crucial as it is responsible for the formation of cavities and much of the selectivity of a MIP arises from its interaction with the template.<sup>109</sup> To maximize the cavity formation and the overall imprinting effect, the functionality of the functional monomer should complement the functionality of the template in a coordinating fashion. For instance, if the template is a hydrogen bond donor, pairing it for polymerization with a functional monomer that is a hydrogen bond acceptor would be most beneficial for imprinting efficacy.<sup>110</sup>

A comprehensive listing of functional monomers that are commonly used in non-covalent molecular imprinting<sup>3, 110</sup> is provided in Figure 1.8. Methacrylic acid (MAA) is the most commonly used functional monomer as it is able to participate in ion-ion, ion-dipole, and dipole-dipole interactions.<sup>111</sup> In non-covalent imprinting protocols, functional monomers are used in excess relative to the template to drive the formation of template-functional monomer assemblies.<sup>108</sup> The optimal template/monomer ratio is achieved empirically by evaluating several polymers generated with various formulations and increasing the template – a systematic trial and error approach.<sup>112</sup> The optimal concentration ratio of functional monomer to the template was determined to be 4:1.<sup>83, 97</sup> In covalent imprinting, tweaking the quantities of the components to determine the optimal ratio is not necessary as the template dictates the number of functional monomers that can be covalently attached in a stoichiometric manner.

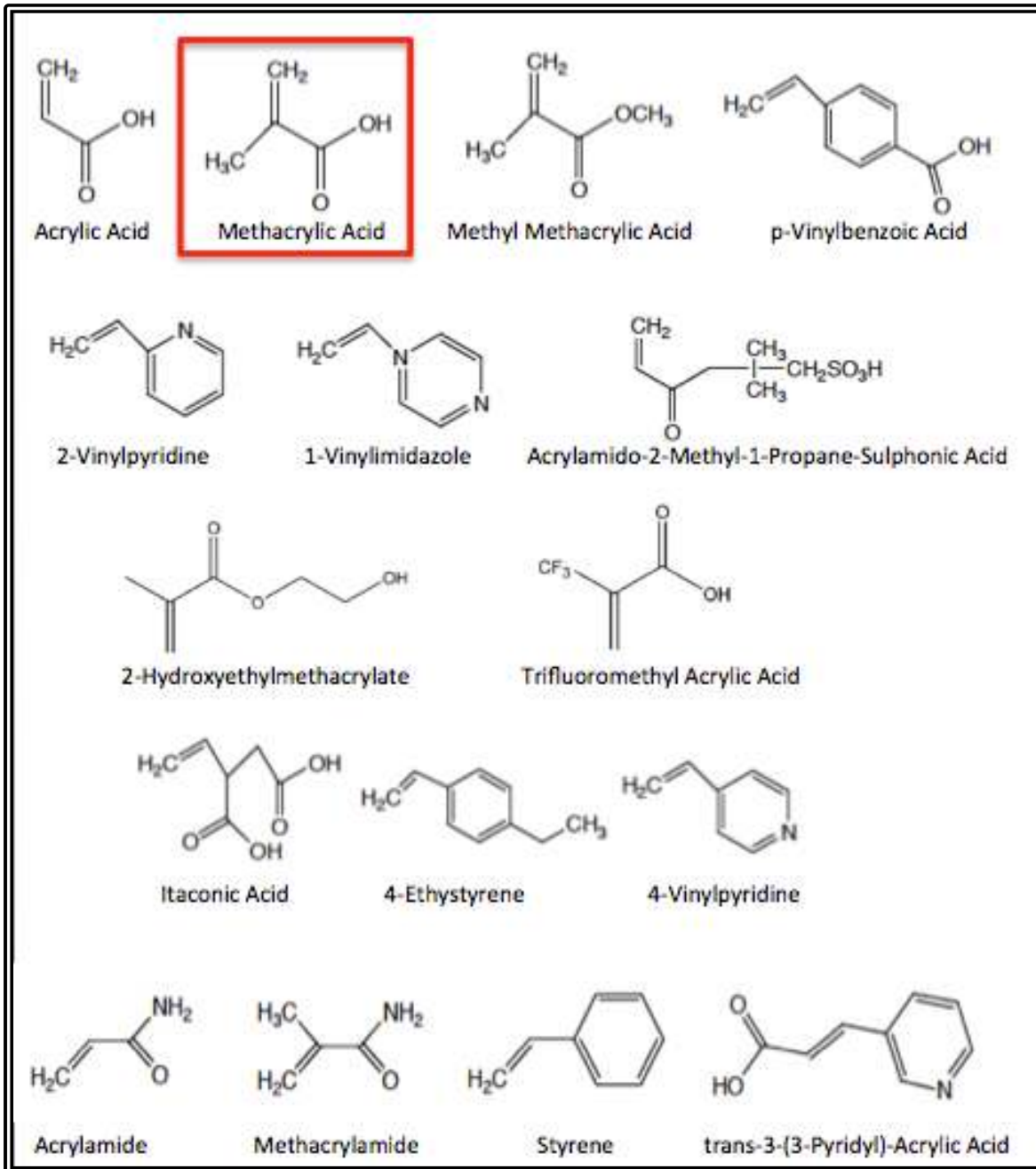


**Figure 1.8:** A list with the structures for commonly used functional monomers (adapted from Vasapollo, 2011, and Yan, 2006).<sup>3, 110</sup> Methacrylic acid is one of the most commonly used and is also used in the present study.

#### 1.2.3.3. *Cross-Linkers*

The influential factor for high selectivity is the type and quantity of the cross-linking agent used in the production of the polymer.<sup>113</sup> The cross-linker controls the morphology of the polymer matrix, dictating whether it is a gel-type, macroporous or a microgel powder,<sup>110</sup> and is not always uniformly manufactured.<sup>114</sup> The cross-linker is also responsible for locking the spatial orientation of the functional monomer relative to the template and to provide structural scaffolding<sup>105</sup> and providing rigidity to the polymer to allow for durable recognition cavities to be formed.<sup>89</sup> The mechanical stability of the polymer network (i.e. stiff/flexible) and the conformation of imprinted sites are also established by the cross-linker.<sup>115</sup> A high cross-linker proportion results in a stiff network with functional groups fixed in a strictly defined and optimal position in the recognition site.<sup>116</sup>

The quantity of the cross-linking agent should be high enough to maintain the stability of the recognition sites complementary to the template (both chemically and in terms of shape) following template removal.<sup>3, 115</sup> Most MIP systems for analytical applications require around 25-90%<sup>117</sup> of cross-linker agent. Systems with higher cross-linker ratios are denser polymer networks and increase the number of imprinted sites and therefore establish high template specificity, which is preferred, however, they are very rigid and are difficult to manipulate.<sup>115</sup> Furthermore, as a result of strong templating, the release profiles are significantly slower.<sup>111</sup> The opposite is also true – weakly cross-linked systems reflect a low specificity for the template but are able to bind and release the template effortlessly.<sup>118</sup>



Polymer systems with cross-link ratios in excess of 80% have become increasingly common. Research findings by some groups have found that the cross-linker has a distinct effect on the physical characteristics of the polymer but a much less impact on the specific interactions between the template and functional monomers.<sup>119, 120</sup> Some of the most frequently used cross-linkers are outlined in Figure 1.9, of which ethylene glycol dimethacrylate (EGDMA) and trimethylpropane trimethacrylate (TRIM) are the two most commonly utilized. Quite a few cross-linkers are capable of simultaneously complexing with the template, and thus, also act as functional monomers.

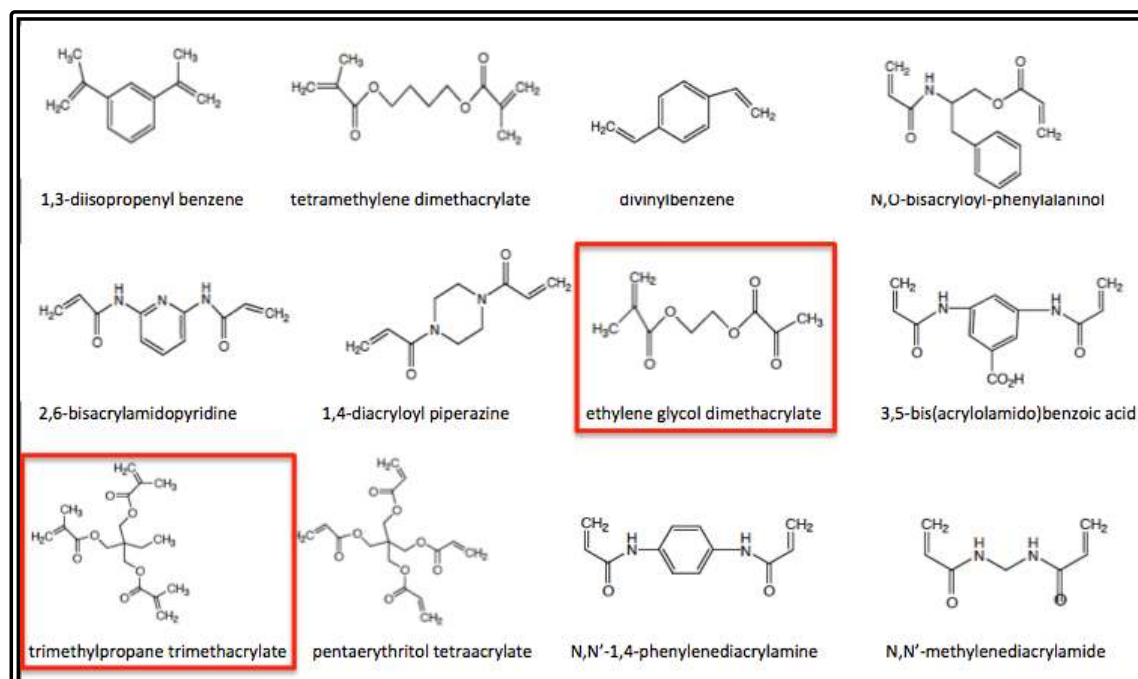


**Figure 1.9:** Commonly used cross-linkers,<sup>110</sup> of which the two outlined are the most popular agents. Ethylene glycol dimethacrylate (EGDMA) is the cross-linker used in the present study.

#### 1.2.3.4. *Templates*

The template is of vital importance as it directs the organization of the functional groups of the functional monomers in all molecular imprinting processes,<sup>110</sup> which is applicable to a broad range of template molecules.<sup>121</sup> Prior to selection of a template one should consider the following:

- Are there any polymerizable groups within the template?
- Does the template contain functionality that could potentially inhibit or hinder a free radical polymerization?
- Whether the template is stable and able to tolerate moderately elevated temperatures or exposure to UV radiation?

These three points are legitimate concerns as they can impact the polymer synthesis in an undesirable manner.<sup>110</sup> Templates should ideally be chemically inert during polymerization to prevent participation of the template in polymerization reactions.

The extent of template binding at equilibrium is governed by the change in Gibbs free energy of formation of template-functional monomer interaction.<sup>122</sup> The bond between the template and the functional monomer should be as strong as possible while polymerizing the system to allow the template to be fixed in a definite orientation. However, by the same token it should also be possible to extract the template as completely as possible.<sup>83</sup>

The most attractive feature about this technology is that it is widely applicable and can be utilized with a diverse range of analytes. MIT routinely imprints small organic molecules such as pharmaceuticals, pesticides, amino acids, peptides, and sugars. Imprinting with larger templates is challenging as they are

more flexible and unable to effectively generate well defined cavities. Furthermore, re-binding is also more challenging as permeation into the polymer network is difficult with larger molecules.

#### *1.2.3.5. Photo-initiators*

A photo-initiator is a molecule or a combination of molecules that upon the absorption of light initiate polymerization.<sup>123</sup> Essentially, photons are absorbed by the photo-initiator and promote it to a singlet state and then to a triplet state by intersystem conversion, from which chemical reactions start.<sup>124</sup> Several photo-initiators with various chemical properties can be used as the radical source in free radical polymerization. This process is the most widely used for manufacturing polymers<sup>125</sup> and is described in the next section. Photo-initiators affect the cure speed of a system and yellowing.<sup>126</sup> The photophysical and photochemical properties of the photo-initiators are crucial in controlling the reactivity of the system. Photo-initiators should possess the following properties:<sup>127</sup>

- i. High absorptivity in the region of activation (depend on the application and light source used);
- ii. High quantum yield for free radical formation;
- iii. Adequate solubility in the resin system used;
- iv. High storage stability;
- v. Odourless and non-yellowing;
- vi. Non-toxic, cheap and ease in handling

There are benefits and limitations to each photo-initiator, thus the selection of the photo-initiator should consider the requirements of its specific application. For instance, photo-initiators used in MIP synthesis for biosensors, drug-delivery, or tissue scaffolding must be carefully selected, to avoid any toxicity in precursor or radical form,<sup>128</sup> in order to ensure biocompatibility.

The general representation of photo-initiated polymerization<sup>129</sup> is depicted in Figure 1.10. There are two basic categories of photo-initiators that meet the above requirements<sup>130</sup> and are classified as  $\alpha$ -cleavage (Type I) and H-abstraction (Type II) initiators.<sup>131, 132</sup> The majority of cleavage initiators are aromatic carbonyl compounds with appropriate substitutions. They are based on the acetophenone (benzoyl) functionality which is essential in their mechanism of action.<sup>133-135</sup> The photo-initiator used in this study, Darocur 1173 is this type of compound and is a Type I photo-initiator. Benzoin and its derivatives; benzyl ketals, acetophenones, aminoalkylphenones, O-acyl-R-oximino ketones, R-hydroxyalkyl ketones, and acyphosphine oxides absorb light in the ultra-violet (UV) range and undergo spontaneous homolytic bond cleavage, resulting in two free radicals.<sup>136</sup> A depiction of such radical cleavage is shown in Figure 1.11<sup>129</sup> with benzoin as an example.<sup>137</sup>

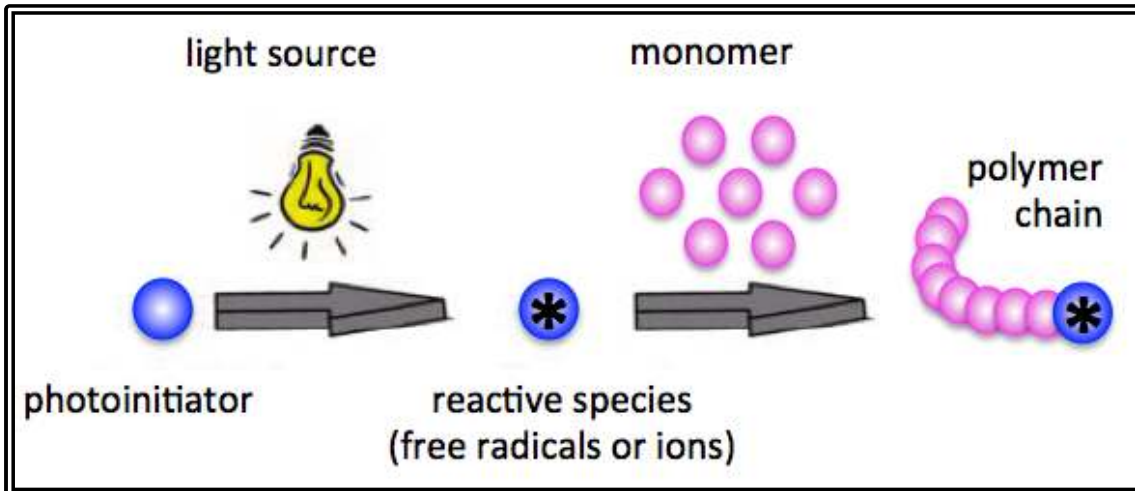


**Figure 1.10:** Animated representation of photo-initiated polymerization.<sup>129</sup> Upon absorption of light of the proper wavelength an excited singlet state is produced which undergoes rapid and efficient intersystem crossing to the lowest excited triplet state from which the actual photochemical reactions take place.<sup>138</sup>

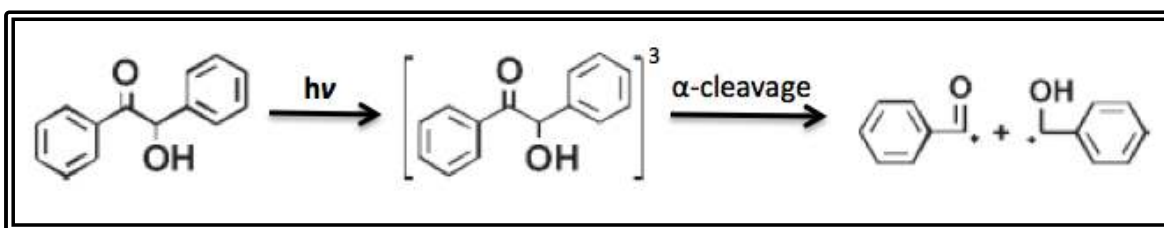


**Figure 1.11:** Type I photo-initiation mechanism of benzoin.<sup>129</sup> Benzoin and byproducts are the most widely used photo-initiators for free radical polymerization because they exhibit high reactivity arising from the high electron density and due to favourable steric conditions.<sup>139</sup>

#### 1.2.4. Polymerization

Most polymers are produced *via* free-radical polymerization, due to simplicity, convenience, and because it is much less sensitive to impurities within the monomers.<sup>125</sup> These advantages generally outweigh the limitations of irregularity of the particles produced, the waste of polymer product and the limited control in the process.<sup>2</sup>

Free radical polymerizations are usually performed using one of methods listed in Table 1.3. Various studies have indicated that polymerization of MIPs carried out at lower temperatures produces polymers with greater selectivity than the polymers manufactured at elevated temperatures.<sup>136, 140</sup> The polymerization reaction is very fast at elevated temperatures and this adversely impacts the stability of the complex, reducing the reproducibility of the MIP. Furthermore, where complexation is driven by hydrogen bonding (non-covalent imprinting), lower temperatures are preferable so not to increase the kinetic energy of the functional monomer-template complex and inadvertently shift the equilibrium towards uncomplexed species.<sup>141</sup>

**Table 1.3:** Summary of polymerization processes for MIPs (adapted from Yan, 2003).<sup>110</sup> Depending on the objective of the polymer synthesis, a specific polymerization method may be utilized in favor of another to achieve the desired outcome.

<b>Polymerization Type</b>	<b>Benefits</b>	<b>Limitations</b>
<b>Bulk Polymerization</b>	<ul style="list-style-type: none"> <li>• Simplicity</li> <li>• Universality</li> <li>• No particular skills or sophisticated instrumentation</li> </ul>	<ul style="list-style-type: none"> <li>• Tedious procedure of grinding, sieving, and column packing</li> <li>• Irregular particle in size and shape, low performance</li> </ul>
<b>Suspension Polymerization</b>	<ul style="list-style-type: none"> <li>• Spherical particles</li> <li>• Highly reproducible results</li> <li>• Large scale possible</li> </ul>	<ul style="list-style-type: none"> <li>• Phase partitioning of complicates system</li> <li>• Water is incompatible with most MIP protocols</li> <li>• Special surfactant polymer required</li> </ul>
<b>Multi-Step Swelling Polymerization</b>	<ul style="list-style-type: none"> <li>• Monodispersed beads of controlled diameter</li> <li>• Excellent for high performance liquid chromatography HPLC</li> </ul>	<ul style="list-style-type: none"> <li>• Complicated procedure and reaction conditions</li> <li>• Need for aqueous emulsions</li> </ul>
<b>Precipitation Polymerization</b>	<ul style="list-style-type: none"> <li>• Imprinted microspheres</li> <li>• Uniform size and high yields</li> </ul>	<ul style="list-style-type: none"> <li>• Large amount of template</li> <li>• High dilution factor</li> </ul>
<b>Surface Polymerization</b>	<ul style="list-style-type: none"> <li>• Monodispersed product</li> <li>• Thin imprinted layers</li> </ul>	<ul style="list-style-type: none"> <li>• Complicated system</li> <li>• Time consuming</li> </ul>
<b>In-situ Polymerization</b>	<ul style="list-style-type: none"> <li>• One-step, in-situ polymerization</li> <li>• Cost-efficient</li> <li>• Good porosity</li> </ul>	<ul style="list-style-type: none"> <li>• Extensive optimization required for each new template system</li> </ul>



### 1.2.5. *Extraction*

In order for successful selective recognition of template molecules to occur, it is essential that the template utilized in the polymerization process is completely removed from the binding cavity. This ensures that the cavities of the imprinted polymer are free and available to interact with the template during re-uptake.<sup>142</sup> For an adequate comparison to be made, the MIP and the corresponding NIP both undergo the extraction process. Of the various cleaning methods available, Soxhlet extraction is a standard method that has been utilized for nearly 135 years<sup>143</sup> and the general set up is depicted in Figure 1.12.<sup>144</sup>

The technique consists of placing MIP particles into a porous cartridge inside the extraction chamber. The extracting solvent is poured into a flask connected to the lower part of the extraction chamber. The solvent is heated and as it becomes volatilized, it goes up into the extraction chamber. The condensed vapour drips into the cartridge and comes into contact with the MIP particles and removes the template. After a particular level of liquid is reached, the solvent, along with the dissolved template, enters into the flask at the bottom through a siphon. The process is repeated for several hours, re-circulating the solvent through the MIP particles. The process can be optimized by changing continuous extraction solvent to fresh solvent, allowing clean solvent to circulate to the MIP and removing template molecules that are still bound. The Soxhlet process has both advantages and disadvantages associated with it, which are briefly outlined in Table 1.4.

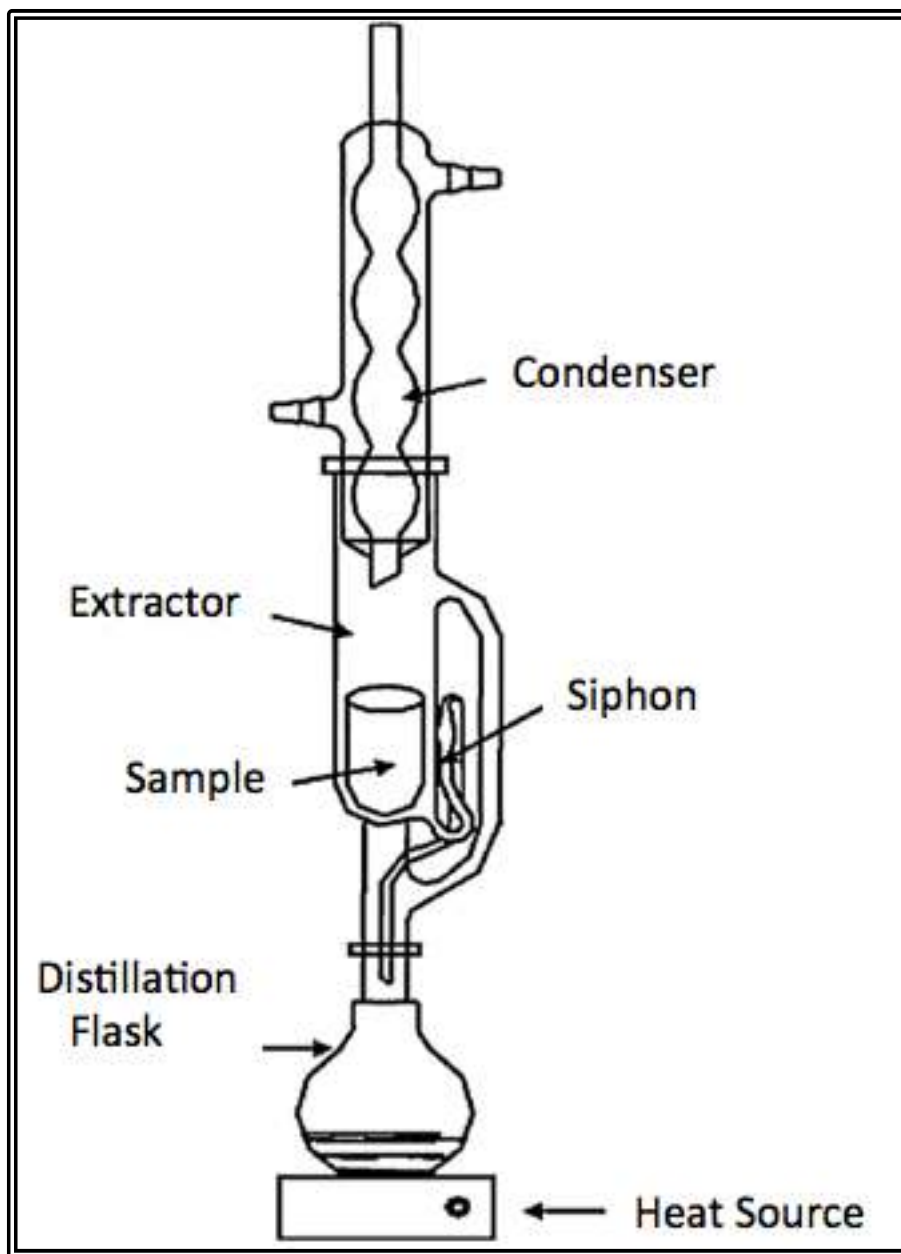


**Figure 1.12:** Conventional Soxhlet extraction set-up.<sup>144</sup> The sample to be distilled is placed in the extractor usually in a thimble. The extraction solvent is placed in the distillation flask, and drips down from the condenser as it is heated. Tubes connect to the condenser. The tube at the top is connected to a water source and allows water to flow through the condenser. The tube connected to the bottom is secured to a drain to discard the water. This is to ensure that the solvent cools down and drips back down through the sample.

**Table 1.4:** Advantages and disadvantages of Soxhlet extraction (adapted from Lorenzo *et al.*, 2011).<sup>101</sup>

Advantages	Disadvantages
MIP particles are repeatedly washed with fresh portions of the extracting solvent	Time consuming process as long extraction times are required
The extraction is carried out with a hot solvent, which favours solubilization of the template	Large quantities of organic solvents are required which is not environmentally friendly
Filtration is not required following extraction to collect the MIP particles	Temperature induced degradation of labile template is a risk
The equipment is affordable and training an operator is easy	MIP particles remain mostly static during the process, preventing flow of solvent around them, and extending extraction process
The process is versatile and can be applied to almost any polymer system	Automation is difficult

Theoretically, the extraction process in non-covalent imprinting is supposed to occur with ease because the interactions are weaker than those in covalent imprinting. However, there are various challenges associated with template extraction that can ultimately induce changes to the MIP system. Five potential outcomes of Soxhlet extraction are described in Figure 1.13,<sup>101</sup> of which only one, the adequate removal, is the desired outcome.

It is possible during template removal for the imprinted cavity, to rupture or for the template to remove partially and become locked into a new position. It is also possible for the binding cavity to become distorted and for the binding points to lose their positions. Collapse of the imprinted binding sites has also been reported. Each of these scenarios would render template re-uptake impossible and at the very least problematic.

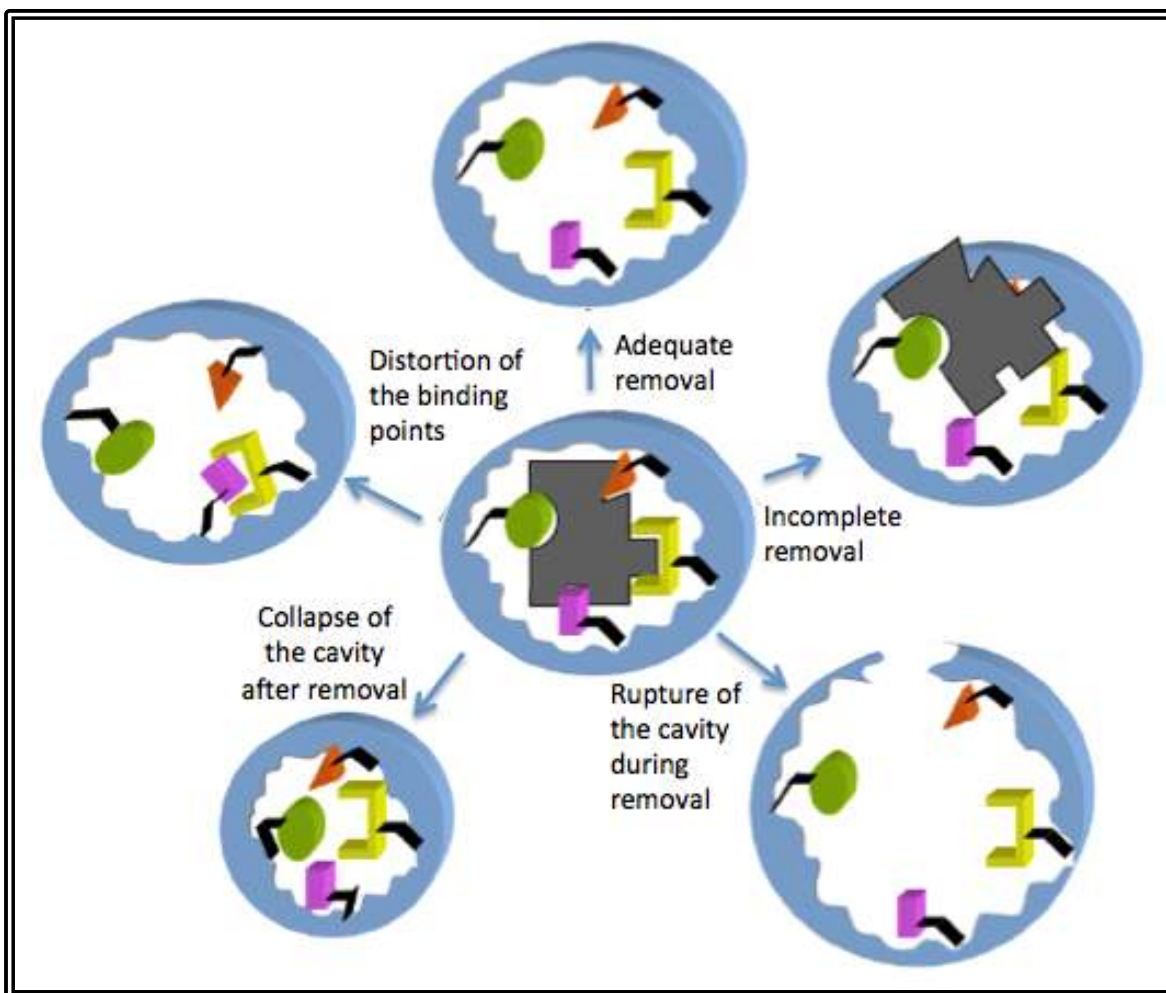


**Figure 1.13:** Schematic of potential changes to MIP's induced by template extraction.<sup>101</sup> Clockwise from the top: the template could be removed adequately; the template could be removed impartially; the cavity could rupture as a result of extraction; the walls of the cavity can collapse from removal of the template; and the binding sites can become distorted.

#### *1.2.6. Applications*

Research efforts over the past forty years have allowed MIPs to develop into a prominent tool applicable in various fields. MIPs are very versatile and their applications include, but are not limited to, industries such as environmental, food, chemical, biomedical and pharmaceutical. The unique properties of MIPs have made them a useful tool for various applications, such as separation science and purification, sensors and biosensors, catalysis, tissue engineering and drug delivery.

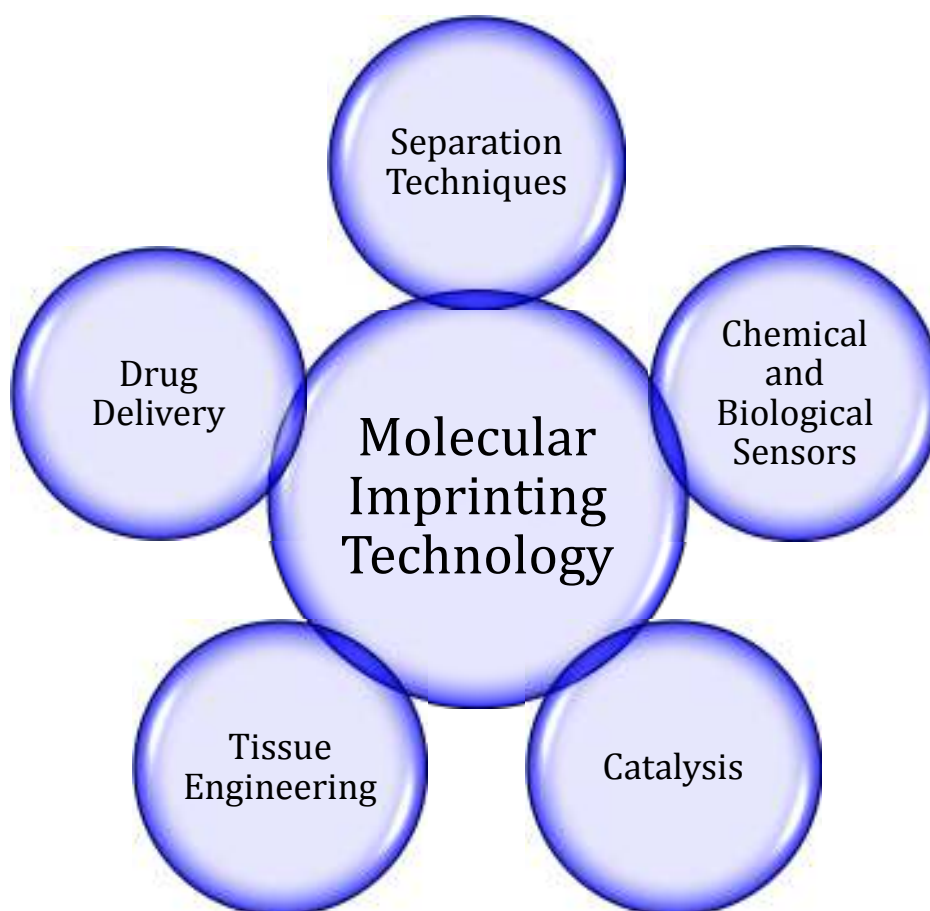


**Figure 1.14:** Five common applications of MIT. Clockwise from the top: separation techniques, chemical and biological sensors, catalysis, tissue engineering, and drug delivery.

#### *1.2.6.1. Separation Techniques*

In separation techniques, MIPs can be used in remediation to separate contaminants from a sample,<sup>145</sup> resolution of racemic drugs, and purification of samples.<sup>146, 147</sup> Molecular imprinting chromatography is one of the most extensively studied and traditional application areas of MIT,<sup>148</sup> especially for Liquid Chromatography (LC).<sup>149</sup> Due to the demand for optically pure compounds MIPs are frequently used as Chiral Stationary Phases (MIP-CSP) in High Performance Liquid Chromatography (HPLC).<sup>150-152</sup> MIPs have also been used as media for Capillary Electrochromatography (CEC) which is a hybrid separation technique that combines the stationary phase of LC with the electrosmotically driven mobile-phase of electrophoresis.<sup>153, 154</sup> MIPs for Solid-Phase Extraction (MISPE) has also shown promise and gained popularity as an analytical tool.<sup>155, 156</sup> The principle of MISPE is based on the four steps as in traditional Solid-Phase Extraction (SPE): conditioning of the sorbent, loading of the sample, washing away interferences and elution of the target analytes. MISPE has been applied to the extraction of compounds in different sample networks such as biological,<sup>157-159</sup> environmental samples,<sup>160-162</sup> and also in food analysis.<sup>163-165</sup>

#### *1.2.6.2. Chemical Sensors and Biosensors*

MIPs have gained increasing attention in the last few years as chemical sensors and biosensors, as can be seen from the growing number of publications in this field. New demands stemming from clinical diagnostics, environmental analysis, and food analysis are to attribute for the spike in popularity. An effort to synthesize



artificial receptors capable of binding a target analyte with comparable affinity and selectivity to natural antibodies or enzymes has been put forth.<sup>3</sup>

MIT has potential to establish antibody-like materials with high selectivity and sensitivity, along with long-term stability, chemical inertness and insolubility in water and most organic solvents.<sup>166</sup> Despite the significant amount of effort in the field, MIP-based biomimetic sensors are still inferior to biosensors and are unable to reproduce the same level of selectivity as their naturally occurring counterparts.

#### 1.2.6.3. *Catalysis*

The potential for MIPs in catalytic applications has been investigated extensively by Piletsky *et al.*,<sup>167-170</sup> Longo *et al.*,<sup>171-174</sup> Mosbach *et al.*,<sup>95, 175-177</sup> and Sellergren *et al.*<sup>109, 178-180</sup> The level of interest and quantity of literature available is overwhelming, which is attributed to the high selectivity and strength that these polymers exhibit. This allows them to be useful at elevated temperatures and pressures, in the presence of several organic solvents, as well as under acidic and basic reaction conditions. While natural catalytic molecules may undergo decomposition or degradation under these harsh conditions, catalytic MIPs can be engineered to withstand such conditions.

MIP catalysts are able to replicate the selectivity and stereospecificity of the binding sites of antibodies and enzymes, which are commonly used in reactions. Catalytic MIPs can be generated using analogues of substrates, transition states or products as templates during the imprinting process.<sup>181</sup> The polymer matrix that is obtained has binding sites with a shape similar to that of the template. Thus, when

the catalytic groups are introduced in the correct binding sites of the MIP they behave catalytically in the presence of the true substrate.<sup>182</sup>

#### *1.2.6.4. Tissue Engineering*

In the field of regenerative medicine, MIPs have shown potential to be used as scaffolds to provide structural integrity and morphogenic guidance, serve as tissue barriers and bioadhesives, and to encapsulate and deliver cells to stimulate the natural repair processes. Langer and Vacanti<sup>183</sup> paved the way in developing the basic techniques used in tissue engineering to repair damaged tissues as well the way in which the technique utilizes MIPs.<sup>184</sup>

Tissue engineering and design can be carried out using MIPs as a material, due to their mechanical properties that can be manipulated to mimic natural tissues. The main objective of a tissue scaffold, displayed in Figure 1.15,<sup>185</sup> is to maintain cellular proliferation and desired cellular distribution for the set life expectancy of the construct.<sup>186</sup> Generally, scaffolds are designed to maintain a specific life expectancy. The life expectancy is a crucial aspect in the engineering process. It is essential to ensure that degradation of the scaffold commences when the emergent tissue is at a durable stage in the healing process.<sup>187, 188</sup>

Various elements need to be present for the successful implementation of MIPs for regenerative scaffolds and tissue repair. The polymers should be biodegradable to optimize proliferation of regenerative tissues<sup>189</sup> and biocompatible to maintain safety and avoid any toxic effects on surrounding tissues.

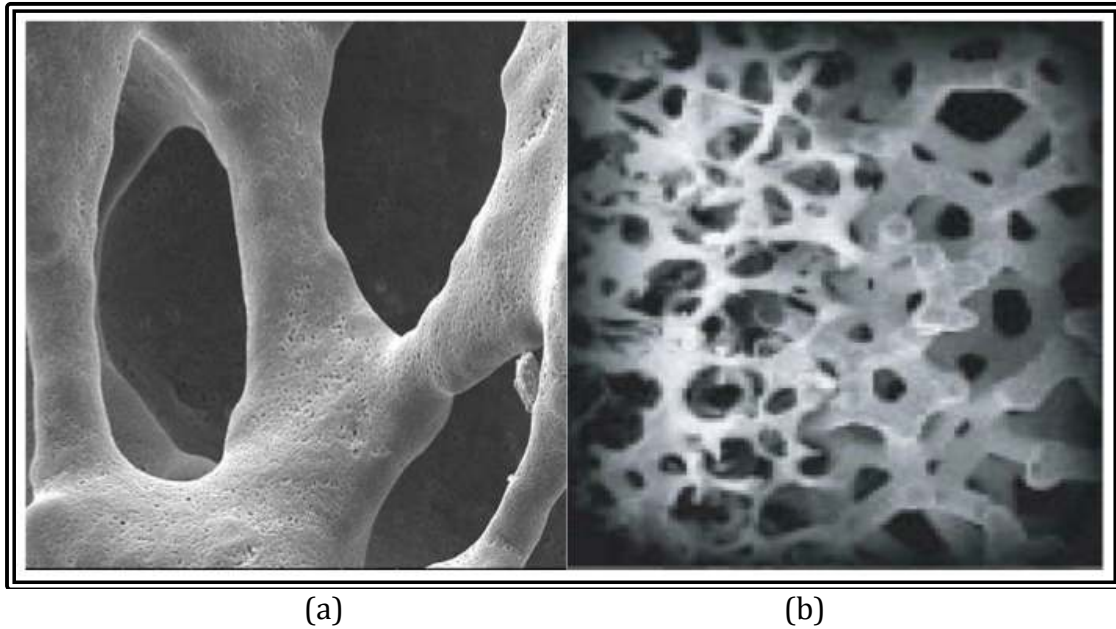


**Figure 1.15:** SEM images of tissue scaffolds.<sup>185</sup> There are two categories of scaffolds; permanent and temporary, also commonly referred to as (a) hard and (b) soft. Different materials are used to form these classes of scaffolds. For instance, in bone engineering, hard scaffolding is required and a metallic scaffold as seen in (a) is used.<sup>190</sup> The scaffold in (b) is a soft urea based tissue scaffold, which would be applicable in cartilage repair.<sup>191</sup>

#### 1.2.6.5. *Drug Delivery*

The ability of MIPs to strongly and selectively bind bioactive molecules, with high loading capacities, and the potential for prolonged release times are all characteristic features that make them suitable for drug delivery devices.<sup>142, 192, 193</sup> The physiochemical properties of MIPs protect the drug from degradation by enzymes during transportation in the body, which creates the potential to limit premature drug metabolism and biotransformation.<sup>194</sup> Several drugs have been used as templates to develop MIPs that prolong the release profile of specific therapeutic agents with enhanced performance in comparison to traditional delivery devices.<sup>195</sup>

Imprinted drug delivery devices have not reached clinical applications and therefore, only achieved limited commercial success due to safety and toxicity concerns. Since these MIPs interact with biological tissues, it is necessary to ensure that they do not exhibit any toxicological effects.<sup>115</sup>

#### 1.2.6.6. *Hydrogels*

One type of synthetic polymer systems that has been favoured by drug delivery researchers is hydrogels. The polymer system used in the present study is a hydrogel. For these reasons, it is appropriate to describe the properties of hydrogel polymers and their potential applications for drug delivery in some detail.

Hydrogels are three-dimensional, hydrophilic, homopolymer or copolymer systems, capable of swallowing large amounts of water or biological fluids,<sup>196-198</sup> giving them the ability to swell and shrink under different moisture conditions.<sup>199</sup>

They are insoluble due to the presence of chemical or physical cross-links.<sup>200</sup> The physical cross-links can be entanglements, crystallites, or weak associations such as van der Waals forces or hydrogen bonds.<sup>201</sup> Cross-links provide the network structure and physical integrity.<sup>196</sup>

Hydrogels can be classified based on their network structures as macroporous, microporous, or nanoporous. As the names imply, these hydrogels are based on size of their respective pores. Macroporous hydrogels have large pores, ranging between 0.1 – 1  $\mu\text{m}$  and are generally much larger than the diffusion species. Microporous hydrogels range from 100 – 1000  $\text{\AA}$  and in nanoporous hydrogels the pore size range from 10 – 100  $\text{\AA}$ .<sup>202</sup> Hydrogels can be neutral or ionic based on the type of charges of their pendent groups.<sup>203</sup> A variety of pH-responsive and biocompatible polymers exhibit anionic or cationic properties allowing these hydrogel networks to be tailored or modified to exhibit desirable physiochemical properties appropriate for specific application conditions.<sup>196</sup>

By incorporating hydrogels in molecular imprinting processes, they can be templated with various macromolecules. Hydrogels exhibit a thermodynamic compatibility with water, which allows them to swell in aqueous media.<sup>204</sup> This change in the degree of swelling can be controlled and used to modulate the capture and release of the imprinted template molecule.<sup>105</sup> Figure 1.16 indicates the relative position of hydrogel constituents in MIP while in a swollen and collapsed state.

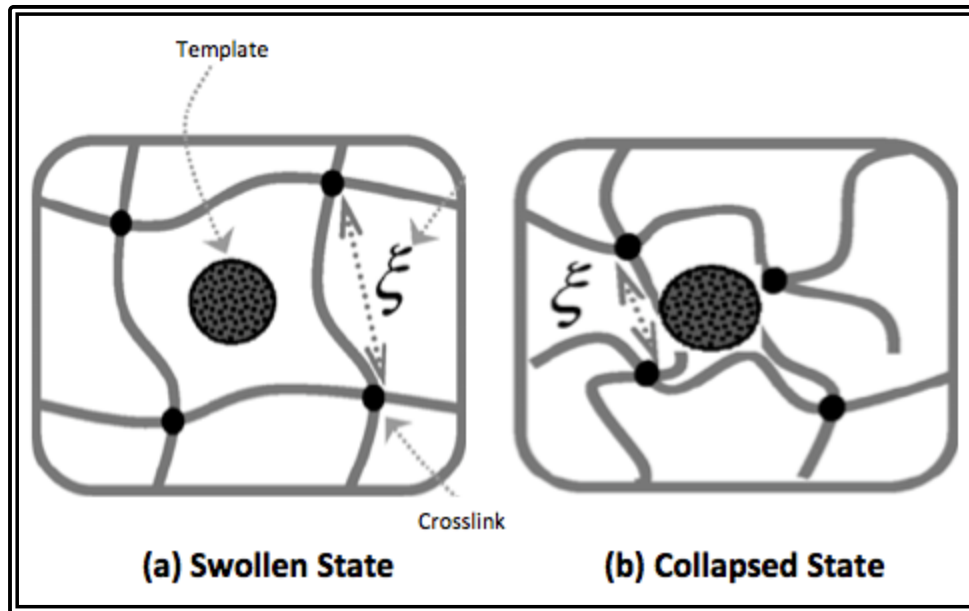


**Figure 1.16:** Swollen and collapsed hydrogel state (adapted from Lowman, 1999, and Lin, 2006).<sup>200, 205</sup> The hydrogels ability to absorb large amounts of water is the cause for the (a) swollen state. In the absence of water, the hydrogel could enter a (b) collapsed state.<sup>206</sup>

As such, there are several applications of these hydrogels, in particular, in the biomedical and pharmaceutical sectors,<sup>207</sup> and can be used as contact lenses, membranes for biosensors, linings for artificial hearts, materials for artificial skin, and drug delivery devices.<sup>203, 208</sup>

Hydrogels are often employed as carriers for controlled release of therapeutic compounds<sup>209, 210</sup> because they are hydrophilic and their soft consistency is more similar to natural tissue<sup>211</sup> than any other class of synthetic biomaterials, which contributes to their biocompatibility.<sup>212, 213</sup> Macromolecular drugs such as proteins or oligonucleotides that are hydrophilic are innately compatible with hydrogels used in drug delivery due to the high water content.<sup>214</sup> Hydrogel based drug delivery systems can be used for oral, rectal, ocular, epidermal, and subcutaneous administration.<sup>215-217</sup>

By controlling the degree of swelling, crosslinking density, and degradation rate, the kinetics of release can be engineered to follow a desired drug release schedule.<sup>218</sup> Drug release rates can be controlled<sup>219</sup> and triggered intelligently *via* interactions with biomolecular stimuli.<sup>220-223</sup> The swelling behaviour and associated release kinetics<sup>224</sup> could be elicited by pH, temperature, ionic strength, or drug concentration.<sup>225-227</sup> For example, in the case of anionic hydrogels that consists of functional groups that can ionize into negatively charged moieties, they swell at pH levels above the  $pK_a$  of the given functional groups due to the charge repulsion between deprotonated moieties and greater hydrophilicity.<sup>228</sup> The relationship between pH environment and swelling behaviour of ionic hydrogels is depicted in Figure 1.17.

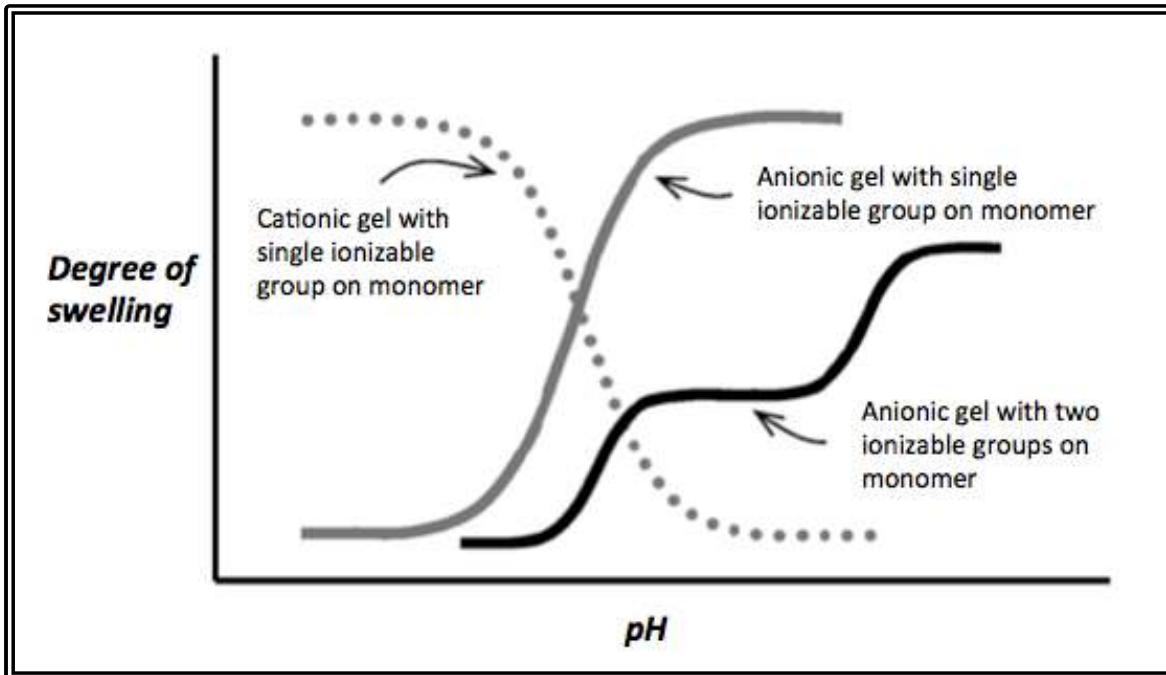


**Figure 1.17:** Schematic of swelling of ionic hydrogels as a function of pH.<sup>205</sup> Ionic hydrogels contain pendent groups that are either cationic or anionic in nature. For anionic gels, the side groups of the gel are un-ionized below the  $pK_a$  and the swelling of the gel is dictated by thermodynamic compatibility of the polymer and the swelling agent. Above the  $pK_a$  of the network, the pendent groups are ionized and the gels swell to a large degree due to the development of a large osmotic swelling force due to the presence of ions. In cationic gels, the pendent groups are un-ionized above the  $pK_b$  of the network. When the gel is placed in a fluid of pH less than this value, the basic groups are ionized and the gels swell to a large degree.<sup>200</sup>



As the ionic content of a hydrogel is increased, in response to an environmental stimulus, the repulsive forces increase and the network becomes more hydrophilic. Hydrophilicity results in a higher degree of swelling.<sup>200</sup>

It is crucial to realize that when the polymer is swollen, it increases the free volume available for template transport, and although transport may be effective the effect of imprinting is decreased under these conditions.<sup>229</sup> Although a wide range of cross-linked hydrogels have been reported to be useful as drug delivery platforms,<sup>230, 231</sup> molecular imprinting in water is still under development. Imprinting in water can reduce the effectiveness of electrostatic and hydrogen-bonding interactions and decrease the overall affinity and selectivity of the MIP for the template.<sup>115</sup> Also, a hydrogel system can interact very well with a given template but biocompatibility can pose limitations.<sup>202, 215, 225</sup>

Despite the limitations of hydrogels, their unique swelling properties can be an asset in developing an effective MIP for use as a drug delivery device. Table 1.5 outlines the design considerations to be made when developing a hydrogel for drug delivery.

**Table 1.5:** Design criteria for hydrogel for drug delivery systems (adapted from Lin, 2006).<sup>205</sup> There are three general categories for consideration, transport properties, physical properties, and biological properties.

Design Criteria	Design Variables
<b>Transport Properties</b>	Molecular weight and size of protein
Molecule diffusion	Molecular weight of polymer
	Cross-linking density
	Polymer-protein interactions
	Hydrogel degradation rate
	Additional functionalities
<b>Physical Properties</b>	Polymer/crosslinker/initiator
Gelling mechanisms/conditions	concentrations
Structural Properties	Temperature, pH, ionic strength
Biodegradability	Molecular weight of polymer
Stimuli-responsiveness	Mechanical strength
	Concentration of degradable groups
	Concentration of responsive groups
<b>Biological Properties</b>	Cytotoxicity of the hydrogel
Biocompatibility	Capsule formation

### **1.3. MIPs, Drug Delivery and Pharmacology**

As noted above, the application of MIT in pharmaceuticals and MIPs' ability to behave as drug delivery vehicles has resulted in a profound level of interest and is the main topic of interest of this paper. However, before one can establish the extent of influence MIT has on the pharmaceutical industry, an understanding of pharmaceuticals and limitations surrounding them must first be established.

#### *1.3.1. Pharmacology and Pharmacokinetics*

Pharmacology is the science that investigates drugs. A drug can be broadly classified as a substance that is administered to a living organism for medicinal purposes and produces a desired pharmacological effect. The last half of the twentieth century witnessed a revolution in pharmacology, making pharmaceuticals a multi-billion dollar industry.<sup>232</sup> As such, the use of medicinal products has become increasingly common and the advancement of the field has been tremendous. Although there has been a profound level of knowledge that has been acquired through research, pharmacology is an ever-changing and growing field and continual effort is directed at further innovation.

The commercial success of the industry has resulted in the misinterpretation of the level of complexity and how profoundly challenging it is to formulate a pharmaceutical product. A given pharmaceutical is often required to be multi-faceted, deliver a specific dose, to the specific target organ, to achieve the intended therapeutic effect for a specified period of time that has minimal side effects, adverse effects, and/or toxic effects to the patient. It is these sometimes competing

imperatives that have driven much innovation in the pharmaceutical sector. The present work also tries to address some of these issues using a MIP approach.

Of particular interest are intelligent drug delivery systems that are able to respond to biological cues for target specific delivery. Molecular design of intelligent delivery systems must consider aspects of pharmacokinetics. Pharmacokinetics is the study of drug absorption, distribution, metabolism and excretion processes. By managing and controlling the level and location of pharmatherapeutics within the body, harmful side effects can be minimized.<sup>233-235</sup>

### *1.3.2. Important Principles of Pharmacology*

#### *1.3.2.1. Drug Administration*

A specific area of pharmacology that has gained significant research attention is drug delivery, due to the limitations associated with current modes of administration. A crucial aspect that affects drug action is the route of drug administration. Also, the route determines the rate of drug absorption, which in turn influences the rate of entrance of a drug into the bloodstream and its distribution to the body. There are fundamentally two routes of drug administration; oral or parenteral. Oral administration includes tablets, capsules, troches, and enteric-coated products, etc. Parenteral administration implies any route that does not involve the GI tract. Parenteral modes of administration include, intramuscular (IM), intravenous (IV), inhalation, and transdermal, etc.

Oral administration is the safest and most convenient method for patients. However, with oral administration the drug is swallowed by mouth and passes

through various pH environments within the body that can result in premature drug metabolism. Premature drug metabolism reduces bioavailability, the percentage of the dose of the drug that is absorbed into the bloodstream. The other modes of administration mentioned above also have limitations associated with them. With IM injections, extreme caution must be observed to avoid injury to the sciatic nerve, however the onset of action is within minutes. In the case of IV injections, it usually requires assistance from a health care professional and as such are generally inconvenient to patients. However as an advantage, it is the fastest means of drug absorption as the drug is delivered directly into the bloodstream. Transdermal products are administered through a bandage or a patch system and absorbed through the skin into the systemic circulation. This can often lead to irritation and even bruising of the skin, however, this can provide continuous administration of a drug dosage over a given period of time.

### *1.3.3. Important Principles of Pharmacokinetics*

Examining the relationship between the dose of a specific drug and its concentration in the body over time is the study of pharmacokinetics. Factors that induce changes in drug concentration over a given time play a significant role in drug delivery and must be considered for effective design of a drug delivery device.

#### *1.3.3.1. Drug Absorption*

Drug absorption refers to the passage of a drug from the site of administration into the blood-stream. In order for absorption to be effective the administered drug must dissolve in the body fluids and must pass through the

membranes of the GI lining and blood vessels to gain access to the blood-stream.<sup>236</sup>

In the case of IV administration, the drug enters the blood-stream directly.

Transport mechanisms that allow substances, such as drugs, to pass through cell membranes include filtration, passive transport, and active transport. A majority of drugs are absorbed by passive diffusion.<sup>237</sup> In passive transport drug molecules pass from an area of high concentration to an area of low concentration, based on the law of diffusion. For instance, following oral administration, a large amount of the drug is in the GI tract and no drug has reached the bloodstream at this point. Thus, the drug molecules have a natural tendency to diffuse from the GI tract into the blood.<sup>238</sup> The rate of diffusion depends on chemical properties of the drug and the site of administration.<sup>239</sup> The properties of the drug that most influence absorption are lipid solubility and the degree of ionization.

*i. Lipid Solubility*

The cell membrane is highly permeable to lipid-soluble substances. Therefore the higher lipid content of a drug, the faster it passes through the cell membrane.

*ii. Drug Ionization*

Ionized drug molecules do not readily cross through the cell membrane. The uncharged/un-ionized form of the drug is required in order for absorption to occur. Also, it is noteworthy that basic drugs are absorbed more slowly than acidic drugs and to a less extent because they are the ionized form in many cases.

### *iii. Drug Formulation*

As previously stated, drugs must dissolve into the body fluid before they can be absorbed into the bloodstream. Thus, solid forms such as capsules and tablets require time for dissolution to occur. As such liquid doses are absorbed faster. Also, the particle size of a drug can influence the rate of absorption such that the smaller the particle size the faster the absorption.

#### *1.3.3.2. Drug Distribution*

Once the drug passes through to the bloodstream it is distributed to the organs and tissues through the circulatory system.<sup>240</sup> The main factors that determine how much drug is distributed to a given organ or area of the body are plasma protein binding, blood flow, and the presence of specific tissue barriers.

##### *i. Plasma Protein Binding*

Plasma proteins consist of several different proteins (e.g. albumin and globulins) that make up a circulation protein pool. These plasma proteins regulate osmotic pressure in the blood. Drugs are attracted to the plasma proteins, especially albumin. As such, some drug molecules are bound to plasma proteins. This is problematic since bound drugs cannot exert a pharmacological effect.

##### *ii. Blood Flow*

Different quantities of blood are delivered to various organs within the body; the organs that receive the largest supply include the liver, kidneys, and the brain. These organs therefore come into contact with the largest amount of drug.

### iii. Blood-Brain Barrier

The blood brain barrier is a membrane that protects the brain by preventing the passage of electrolytes and other water-soluble substances. This is necessary since the brain is comprised of a large amount of lipid, lipid-soluble drugs would readily pass into the brain.

#### 1.3.3.3. Drug Metabolism

Drug metabolism, commonly known as biotransformation, is the enzyme-catalyzed conversion of drugs to their metabolites. The liver is the main organ involved in biotransformation *via* the drug microsomal metabolizing system (DMMS). The DMMS is comprised of a group of enzymes that specifically functions to metabolize drugs, and chemically alter lipid-soluble drugs to become water-soluble compounds. Water-soluble drug metabolites are excreted by the kidneys.

Following oral administration, drugs that are absorbed from the GI tract reach the liver through the hepatic portal vein before entering the systemic circulation which transports the drugs to the liver before they are distributed throughout the body. Some drugs are converted to inactive metabolites as they pass through the liver this first time. This undesirable phenomenon is referred to as *first-pass metabolism*. When a drug is administered orally, first pass metabolism can reduce the amount of active drug to less than 50%.<sup>237</sup>



#### *1.3.3.4. Drug Excretion*

The most common pathways for drug excretion include renal (urine), GI (feces), and respiratory (exhaled gases), exiting the body as a drug compound or a drug metabolite. While the liver is the most important organ pertaining to drug metabolism, the kidney is the most important organ for drug excretion. Drugs undergo glomerular filtration, active tubular secretion, and passive tubular reabsorption during filtration by the kidneys. Most drugs exhibit first-order excretion kinetics, in which the rate of elimination is proportional to the plasma drug concentration.<sup>237</sup>

##### *i. Renal Excretion*

Blood is filtered through the glomeruli of the kidneys; most of the filtered substances are eventually reabsorbed into the blood excluding urinary waste products. In order for drug excretion to occur, the drug or drug metabolite must be water soluble.

##### *ii. Gastrointestinal Tract*

Following oral administration, a portion of the drug passes through the GI tract and is excreted in the feces. Certain drugs (lipid-soluble) can enter the intestines by way of the biliary tract. After the drug is released into the intestines it may be absorbed into the blood again. This is referred to as the enterohepatic cycle in which the duration of action is greatly prolonged.

### *iii. Respiratory Excretion*

The respiratory system usually does not have a significant role in drug excretion. There are a few drugs that metabolize to products that are exchanged from the blood to the respiratory tract.

### *iv. Miscellaneous*

Drugs and their metabolites can also be found to, although uncommon, excrete through perspiration, saliva, and lactation.

#### *1.3.3.5. Half Life*

The half-life of a drug is the time necessary for the blood or plasma concentration of the drug to fall to half of its original level. This is crucial in determining the frequency of drug administration. The major factors that influence half-life of a drug are drug metabolism and excretion.

#### *1.3.3.6. Blood Drug Levels*

The intensity of a drug effect is influenced by the concentration of drug in the blood or plasma. The amount of drug in the plasma is determined by pharmacokinetic processes (absorption, distribution, metabolism and excretion). As a drug is absorbed and distributed, the liver and kidneys begin the processes of metabolism and excretion. Thus the plasma level of the drug is constantly changing as depicted in Figure 1.18.

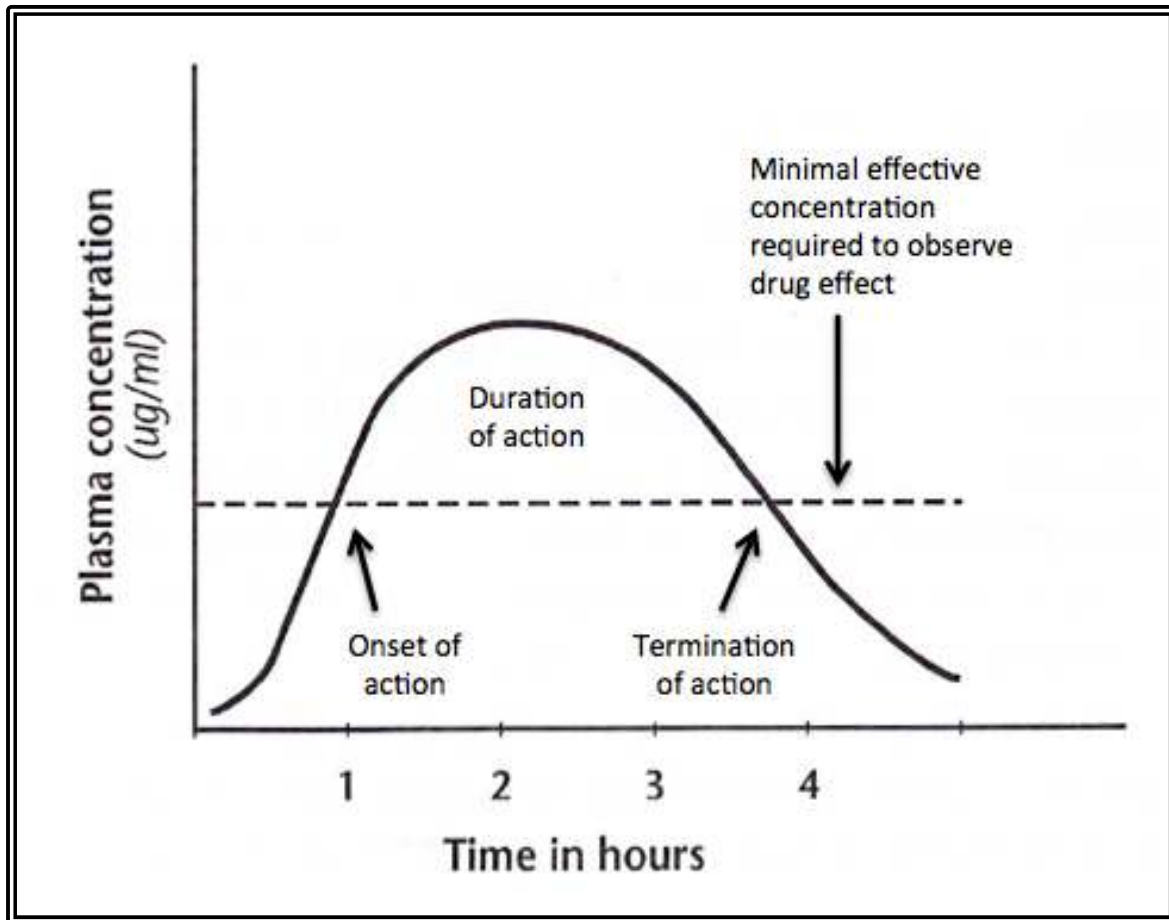


**Figure 1.18:** Generic time response curve. As the plasma level increases absorption and distribution predominate. Later, as the plasma level decreases drug metabolism and excretion predominate.<sup>237, 241</sup>

#### *1.3.3.7. Bioavailability*

Bioavailability is the percentage of the administered dose of a drug that is absorbed into the systemic circulation in active form.<sup>242</sup> The bioavailability of orally administered drugs can be reduced by pharmaceutical factors such as the rate and extent of tablet disintegration or drug dissolution. Bioavailability can also be reduced by biological factors such as: the effects of food that can sequester or inactivate a drug; the effects of gastric acid can also inactivate a drug; and liver enzymes, which can biotransform a drug during absorption.

#### *1.3.3.8. Factors of Individual Variation*

Various factors pertaining to the individual consuming the pharmaceutical product can influence the pharmacokinetics. These factors include age, weight, sex, genetic variation, emotional state, placebo effect, presence of disease, and patient compliance.<sup>142</sup>

An exhaustive understanding of pharmacokinetics and related principles have been established in this section. The fact remains that despite the advantages of the other modes of administration, oral drug delivery is by far the most common and most convenient for patient use. Since it is the most common means of drug administration, a large amount of effort has gone into reducing the limitations associated with oral administration through the use of “smart polymers”<sup>243-245</sup> which is the focus of this paper.

#### **1.4. Improving Drug Delivery *via* Molecular Imprinting Technique**

MIT has an enormous potential to create drug delivery systems (DDS) that can adjust the desired drug release, improve storage stability, and develop strategies for site specific and intelligent drug delivery.<sup>115, 246</sup> Various factors contribute to a successful DDS. These factors include, the DDS produces the desired rate of release (delayed or extended), delivers to the target site, reduces adverse effects, requires the fewest dosages, and enhances patient compliance. Another very attractive possibility with DDS is the potential to divert the portion of the dosage that is responsible for causing the adverse effects. This diversion could ultimately reduce toxic effects experienced by patients entirely. Many have argued that developing a system that incorporates all of the desired features into a DDS is highly ambitious, and as such has received limited commercial success to date.

Two of the major benefits of intelligent, pH-responsive, or other stimuli sensitive, MIP-based delivery systems are that they have large loading capacities (that can carry potent therapeutics)<sup>247</sup> and that they exhibit physiochemical characteristics that can be manipulated.<sup>248</sup> These key features allow for efficient delivery at a target site, thereby avoiding accumulation in non-target tissues, lowering therapeutic dosage, and minimizing harmful side effects.<sup>249</sup>

Selective delivery of pharmaceuticals depends on safe, efficient and precise delivery vehicles.<sup>250, 251</sup> Furthermore, considerations that should be taken into account during polymer design<sup>82</sup> to include the polymer properties listed in Table 1.6.

**Table 1.6:** Key MIP considerations for developing an effective DDS.<sup>82</sup>

<i>Stiffness of the polymer structure</i>	Stiffness allows the cavities to retain their shape following the removal of the template, thus giving high selectivity
<i>High flexibility</i>	Flexibility of the polymer structure works against the above, but is essential for the kinetics, to give rapid equilibration with the substrate to be embedded
<i>Good accessibility</i>	Access to as many cavities as possible in the highly cross-linked polymer can be achieved by forming a particular polymer morphology <sup>252</sup>
<i>Mechanical Stability</i>	Stability of the polymer particles is of great importance for many applications, for example, for use in an HPLC column at high pressure or as a catalyst in a stirred reactor
<i>Thermal Stability</i>	Of the polymers enables them to be used at higher temperatures, at which the kinetics are considerably more favorable
<i>Chemical Stability</i>	For use as a biological sensor or in drug delivery the MIP should be stable enough to resist enzymatic and chemical attack. The device is exposed to biological fluids of complex composition and of different pH, in which the enzymatic activity is intense <sup>115</sup>

A balance between flexibility and polymer stiffness is essential. If the polymer is not sufficiently rigid, the imprinted cavities are not stable enough to retain their conformation in the absence of the template.<sup>253</sup> However, if the polymer is not flexible enough, it is unable to facilitate the completion of rapid equilibrium between the release and re-uptake of the template.<sup>115</sup> These two properties contradict each other, and a careful optimization is necessary.<sup>110</sup>

Furthermore, MIPs for drug delivery must be safe and non-toxic. The delivery vehicle or any of its components, residual monomers, impurities, or potential degradation products cannot be toxic, as they come in contact with sensitive tissues.<sup>254, 255</sup> Thus, to ensure biocompatibility employing MIT on already tested materials instead of developing a new polymeric system can be advantageous.

#### *1.4.1. Experimental Polymer System for this Study*

The selection of monomers is crucial as the selectivity of the MIP is attributed to the interaction between the template and the monomer. As such it is essential that the functionalities of the monomers complement the functionalities of the template. The backbone monomers in the present system are Methyl methacrylate (MMA) and N,N-dimethyl acrylamide (DMAA), and the functional monomer is Methacrylic acid (MAA). The cross-linker serves to spatially lock the position of the backbone and functional monomers in relation to the template generating recognition sites in the polymer. The cross-linker used to form the recognition sites is ethylene glycol dimethacrylate (EGDMA).<sup>89</sup> The initiator used to induce free

radical polymerization is 2-hydroxy-2-methyl-1-phenyl-1-propanone (Darocur 1173).

DMAA plays an important role as a free radical polymerization monomer, but also as an effective dispersant and stabilizer.<sup>256</sup> The MMA-DMAA co-polymer is reported to have a strong imprinting effect and based on studies conducted with timolol, the binding sites are expected to release its entire drug load within three hours.<sup>104</sup>

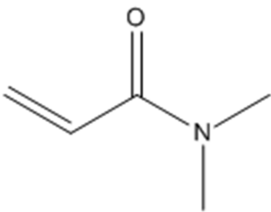
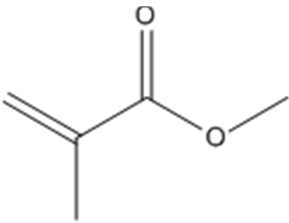
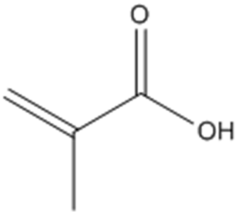
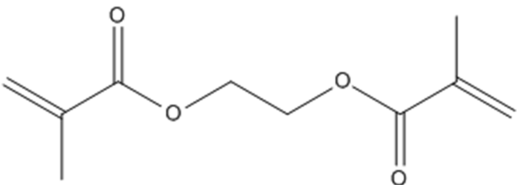
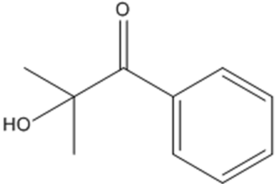
MAA is versatile due to its innate ability to behave as a hydrogen donor and a hydrogen acceptor simultaneously, which is attributed to the presence of the carboxyl group.<sup>110, 252</sup>

EGDMA has been proven to establish stable networks in a wide range of pH and temperature environments.<sup>257</sup> Furthermore, MAA-EGDMA systems have demonstrated high selectivity for propranolol, and moderate selectivity for propranolol metabolites<sup>258</sup> and in general moderate recognition for structurally related beta-blockers.

The structures of all imprinting components are provided in Table 1.7.



**Table 1.7:** Components of the experimental system used in this study.

Component	Structure	Molecular Formula	Molecular Weight (g/mol)
DMAA		C <sub>5</sub> H <sub>9</sub> NO	99.13
MMA		C <sub>5</sub> H <sub>8</sub> O <sub>2</sub>	100.12
MAA		C <sub>4</sub> H <sub>6</sub> O <sub>2</sub>	86.06
EGDMA		C <sub>10</sub> H <sub>14</sub> O <sub>4</sub>	198.22
Darocur 1173		C <sub>10</sub> H <sub>12</sub> O <sub>2</sub>	164.20

#### 1.4.2. *Template Drug*

Propranolol is a  $\beta$ -adrenoreceptor blocker ( $\beta$ -blocker) used in the treatment of angina pectoris, hypertension,<sup>259</sup> cardiac arrhythmia,<sup>260</sup> and myocardial infarctions.<sup>108</sup>  $\beta$ -blockers slow the heart rate down, reduce the force of contraction of the heart muscle, and regulate abnormal rhythms. Angina pectoris attacks can be prevented all together by administration of  $\beta$ -blockers as it reduces the work performed by the heart muscle. High blood pressure is reduced since the rate and force at which the heart pumps blood into the circulation is lowered.  $\beta$ -blockers bind to the  $\beta$ -adrenergic receptors and antagonize the beta effects of epinephrine (EPI) and norepinephrine (NE).<sup>261</sup> By occupying the  $\beta$ -receptors, the  $\beta$ -blockers prevent EPI and NE from producing  $\beta$ -sympathetic effects.

Propranolol, its chemical name ( $\pm$ )-1-isopropylamino-3-(1-naphthyloxy)-2-propanol hydrochloride, is one of the most commonly prescribed  $\beta$ -blockers<sup>262</sup> in the long term treatment of hypertension and cardiovascular diseases and is generally administered orally. Propranolol is effective in lowering blood pressure in mild to moderate hypertension and in severe hypertension is able to prevent reflex tachycardia.<sup>261</sup>

Propranolol is rapidly absorbed by GI tract, however, the oral bioavailability is low, approximately 30%, due to first pass metabolism. Propranolol possesses one chiral center<sup>263</sup> and the (S)-isomer has been indicated to be 100-130 times more active than the (R)-isomer.<sup>264-266</sup> The side chain of the (S)-propranolol molecule is flexible and allows for numerous conformers.<sup>261</sup> The propranolol molecule has three

hydrogen bonding sites, and the more stable conformers exhibit one or two intramolecular hydrogen bonds.<sup>261, 264</sup>

Propranolol is currently on the market today, however due to significant premature drug metabolism and biotransformation prior to the delivery of the target organ, bioavailability is limited.<sup>108</sup> Although oral administration of propranolol is considered safe and well tolerated, the limitation in bioavailability allows significant room to improve the drug's performance.<sup>267</sup>

For this study, propranolol was selected as the template to be imprinted in the cavities because it has been previously non-covalently imprinted by others for drug delivery.<sup>1, 2, 89, 258, 268, 269</sup> Propranolol has also been studied extensively as a template for MIPs in other areas such as to distinguish the enantiomers of the drug in competitive binding assays,<sup>1</sup> solid phase extraction,<sup>270</sup> capillary electrochromatography,<sup>271</sup> HPLC separations,<sup>272</sup> and sensors.<sup>273</sup> Furthermore, propranolol has been demonstrated to respond well in the MMA-DMAA system and interact well with acrylic networks as it is a fairly soluble drug.<sup>274-276</sup> The ease in analysis is also a very attractive feature due its fluorescence.<sup>268</sup> The structure of propranolol and related compounds is provided below in Figure 1.19 and propranolol metabolites can be found in Figure 1.20.

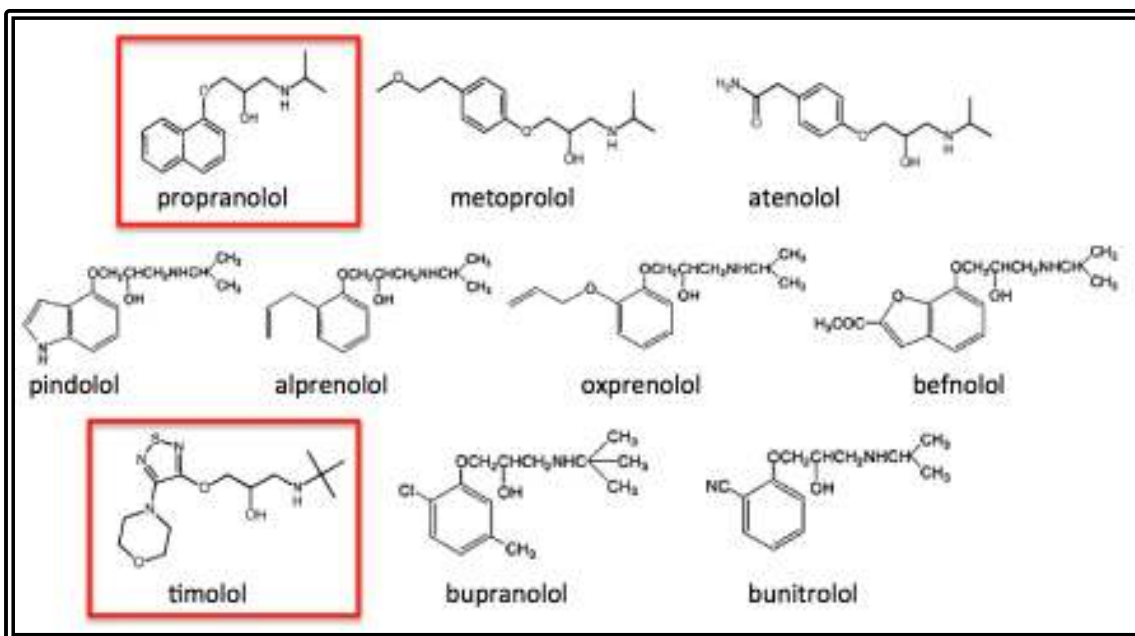


**Figure 1.19:** The chemical structure of propranolol and related compounds.<sup>258</sup>

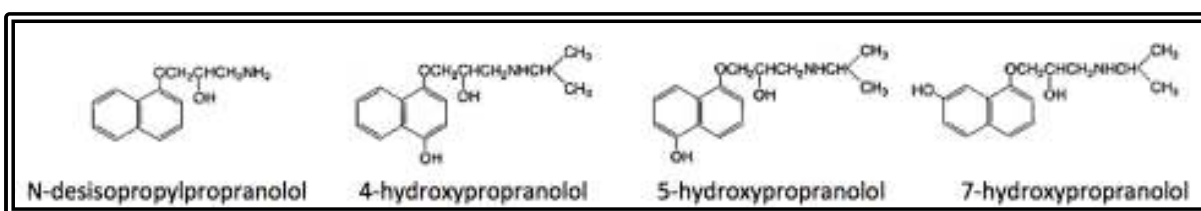


**Figure 1.20:** Chemical structure of propranolol metabolites (adapted from Haginaka, 2000).<sup>258</sup>

#### *1.4.3. Additional Materials Used*

Some of the experiments conducted require the use of a displacement molecule to test the selectivity of MIP for the imprinted template. The materials used in the testing include two Non-Complementary Structures (NCS); benzoic acid and naproxen and two Complementary Structures (CS); timolol, and 1-naphthol, the structure, molecular formula, molecular weight and  $pK_a$  for each can be found in Table 1.8.

##### *1.4.3.1. Benzoic Acid*

Benzoic acid (BA) and its derivatives are commonly used as pharmaceutical and food preservatives, as they inhibit the growth of mold and yeast,<sup>277</sup> and medicinally in the treatment of fungal skin diseases.<sup>278</sup> Various studies have utilized BA in MIP experiments as a model drug and in loading studies.<sup>279, 280</sup> These studies have demonstrated that BA can be adsorbed and released by a polymer network in a controlled manner under certain pH conditions.<sup>281</sup> The molecular weight of BA is significantly smaller than its template counterparts (see Table 1.8) it has a  $pK_a$  value of 4.2, which is similar to naproxen, thus if the interaction with BA is efficient the behaviour of naproxen may also follow a similar pattern.<sup>281</sup> Furthermore, BA maximum absorbance is in the range of 225-232nm,<sup>279, 282</sup> which is quite useful as it does not overlap with the fluorescence of propranolol.

#### 1.4.3.2. *Naproxen*

Naproxen falls under a class of pharmaceuticals known as non-steroidal anti-inflammatory drugs (NSAIDs). NSAIDs are the most commonly used analgesics used across the world today. All NSAIDs have two common features; firstly as the name implies the absence of a steroid structure, and exhibit anti-inflammatory activities that are the basis for their extensive clinical use.<sup>283</sup> NSAIDs are commonly administered to treat pain, inflammation, and fever.<sup>280</sup> The main therapeutic target of NSAIDs is the enzyme cyclo-oxygenase (COX);<sup>284</sup> the COX-1 isoform is involved in homeostasis and the COX-2 is particularly implicated in inflammatory reactions and in promoting tumorigenesis.<sup>285-287</sup>

Naproxen, also known as 6-methoxy- $\alpha$ -methyl- $\omega$ -naphthelene acetic acid, is prescribed to relieve joint pain and stiffness in different types of arthritis (rheumatoid, osteoarthritis, and ankylosing spondylitis), and to hasten recovery following injury to soft tissues.<sup>241</sup> Naproxen mainly exists in the anionic form and has a  $pK_a$  of 4.2,<sup>281</sup> additional properties are listed in Table 1.8. Despite limitations associated with oral administration, naproxen has a high bioavailability of 95% when orally ingested<sup>288</sup> with most of the drug reaching the systemic circulation system in active form.<sup>289</sup> However there are concerns of severe toxic effects from overuse or over dose such as nausea, abdominal pain, and peptic ulcers.<sup>290, 291</sup> Naproxen toxicity and adverse effects can be limited by appropriated encapsulation and as such various research groups have investigation the potential to reduce toxicity.<sup>292-294</sup> Although this is not the objective of the current work, naproxen has

been studied within the same polymer network, although with little success, so there is a level of familiarity surrounding its use.

#### 1.4.3.3. *Timolol*

Timolol, like propranolol, belongs to the class of  $\beta$ -blockers; non-selective  $\beta$ -blockers. Its structure is shown in Table 1.8. Timolol has been widely studied as a template for MIPs and specifically for delivery of ocular therapeutics through contact lenses.<sup>295-297</sup> The chemical name for timolol is (-)-1-(*tert*-butylamino)-3-[(4-morpholino-1,2,5 thiadiazol-3-yl)oxy]-2-propanol maleate and is commonly sold under the name Timoptic®. Timolol has been administered to treat hypertension and angina pectoris, and has also been prescribed after a heart attack to prevent further damage to the heart muscles. Limitations associated with timolol administration include breathlessness (especially in individuals with asthma), chronic bronchitis, emphysema, and masks the body's response to low blood sugar and is therefore prescribed with caution for those with diabetes.<sup>241</sup>

Timolol can also be administered in the form of eye drops for the treatment of glaucoma. The use of timolol for the treatment of glaucoma has been extensively studied by Alvarez-Lorenzo *et al.*, 2011, due to its ability to behave as a donor and acceptor of hydrogen bonds.<sup>90, 298, 299</sup> Timolol offers multiple sites for interaction with the functional monomer allowing for a strong imprinting effect, which make it a suitable template. Also, timolol has been studied in the same polymer system as the one proposed in this work and thus useful information can be obtained from this previous work.<sup>115</sup> Timolol has various structural similarities to propranolol as well

as very comparable physicochemical properties with a  $pK_a$  value of 9.21<sup>300</sup> and an absorbance maximum of 294nm,<sup>301</sup> which would certainly create overlap. The bioavailability of timolol, like propranolol, is quite low when administered orally with only 50% of the active drug reaches the systemic circulation.<sup>237</sup> Therefore, due to the possible side effects and limitations experienced in delivery, a slow sustained delivery mechanism would be advantageous in increasing therapeutic efficacy and reduced systemic toxicity.<sup>302</sup>

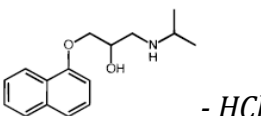
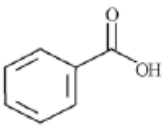
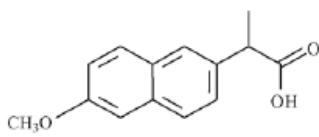
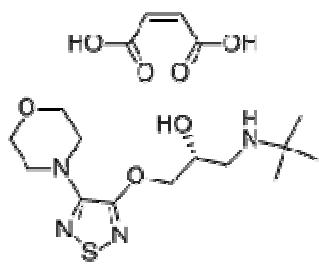
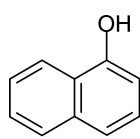
Due to the structural similarities to propranolol and previous reports of effective templating within the MMA-DMAA system,<sup>104</sup> timolol was selected as a complementary structure.

#### *1.4.3.4. 1-Naphthol*

1-Naphthol and its isomer 2-naphthol, have been successfully imprinted using suspension polymerization as mimic templates and applied as selective sorbents for the solid phase extraction of Sudan dyes.<sup>303, 304</sup> Formally known as naphthalen-1-ol, it has a  $pK_a$  value of 9.39.<sup>305</sup> The  $pK_a$  value is very similar to that of propranolol, thus it is possible that it behaves similarly within the polymer network. Like BA, the structure is much smaller in comparison to the principal template, propranolol, and the maximum absorbance is also very similar to that of BA at 228nm<sup>306</sup> and does not overlap with the fluorescence of propranolol.



**Table 1.8:** Structure, molecular formula, molecular weight, and pKa of templates.

Template	Structure	Molecular Formula	Molecular Weight (g/mol)	pK <sub>a</sub>
<b>Propranolol Hydrochloride</b>	 - HCl	C <sub>16</sub> H <sub>21</sub> NO <sub>2</sub> ·HCl	295.80	9.45
<b>Benzoic Acid</b>		C <sub>7</sub> H <sub>6</sub> O <sub>2</sub>	122.12	4.2
<b>Naproxen</b>		C <sub>14</sub> H <sub>14</sub> O <sub>3</sub>	230.26	4.2
<b>Timolol Maleate</b>		C <sub>13</sub> H <sub>24</sub> N <sub>4</sub> O <sub>3</sub> S · C <sub>4</sub> H <sub>4</sub> O <sub>4</sub>	432.49	9.21
<b>1-Naphthol</b>		C <sub>10</sub> H <sub>8</sub> O	144.17	9.39

#### *1.4.4. Experimental Design*

##### *1.4.4.1. Scanning Electron Microscopy*

Scanning electron microscopy (SEM) is a very useful tool to obtain three-dimensional surface morphologies and compositions of organic and inorganic samples on a nanometer (nm) to micrometer ( $\mu\text{m}$ ) scale.<sup>307</sup> Accelerated electrons carry significant amounts of kinetic energy that is dissipated as a variety of signals produced by electron interactions with the sample when the incident electrons are decelerated in the solid sample. Such signals include secondary electrons, back-scattered electrons (BSE), diffracted BSE, photons, visible light, and heat.<sup>308</sup> Secondary electrons are most significant in morphology and topography analysis. The basic components of the SEM include the lens system, the electron gun, the electron collector, the visual and photorecording cathode ray tubes, and the related electronics. The general set up of a SEM is shown in Figure 1.21

BSE signals have been widely used in the investigation of sample morphology in SEM.<sup>309</sup> The three-dimensional appearance of the images obtained is due to the shadow relief effect of the secondary and BSE contrasts.<sup>310</sup> The main use of SEM is to obtain topographic images of a sample at high magnification ranges of 10-10 000X, however, SEM can be used to look inside material and analyze buried structures by selecting only electrons of a certain energy range.<sup>311</sup> Thus, this reconstruction of surface topographies can allow the determination of cavity size and depth and provide information regarding the mechanism of imprinting<sup>312</sup> and how the template interacts with the cavities.

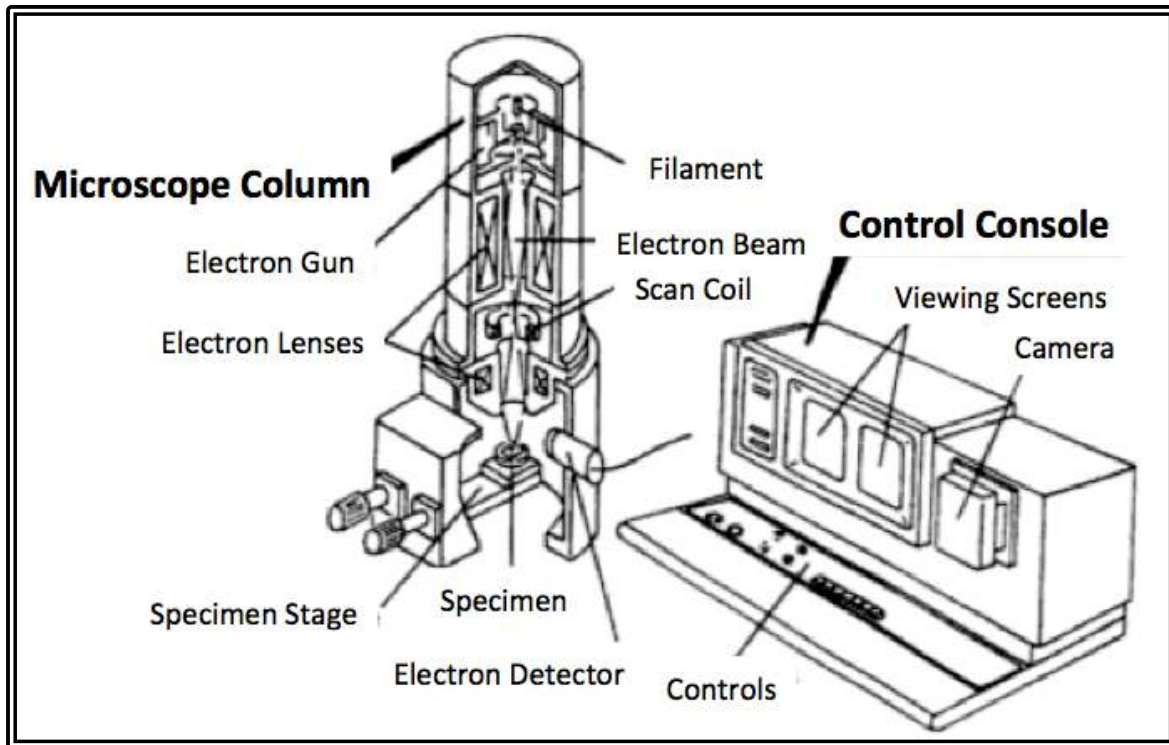


**Figure 1.21:** Major components in a Scanning Electron Microscope set-up.<sup>310</sup>

#### 1.4.4.2. *Fluorescence Spectroscopy*

Fluorescence spectroscopy is a sensitive analytical tool that is used in the detection of fluorescent analytes (e.g., antibiotics, mycotoxins, contaminants).<sup>313</sup> Fluorescence spectral data are commonly presented as emission spectra, the fluorescence intensity is plotted against the wavelength (nm) or wavenumbers ( $\text{cm}^{-1}$ ). Emission spectra are dependent upon the chemical structure of the fluorophore and the solvent in which it is dissolved. A Jablonski diagram, Figure 1.22,<sup>314</sup> illustrates the processes that occur between the absorption and emission of light.<sup>315</sup> Jablonski diagrams are useful in illustrating the variety of molecular processes that can occur in excited states.

Fluorescence is also sensitive to interferences present in the sample and as such direct measurements are often unlikely, especially if the fluorophore is excited in the UV range.<sup>316</sup> When propranolol is bound to a polymer its fluorescence is no longer detectable in the solution in contact with the polymer. As a result, changes in the fluorescence of the external solution can be attributed to changes in propranolol concentration which can be used as an indirect measure of binding to polymer.

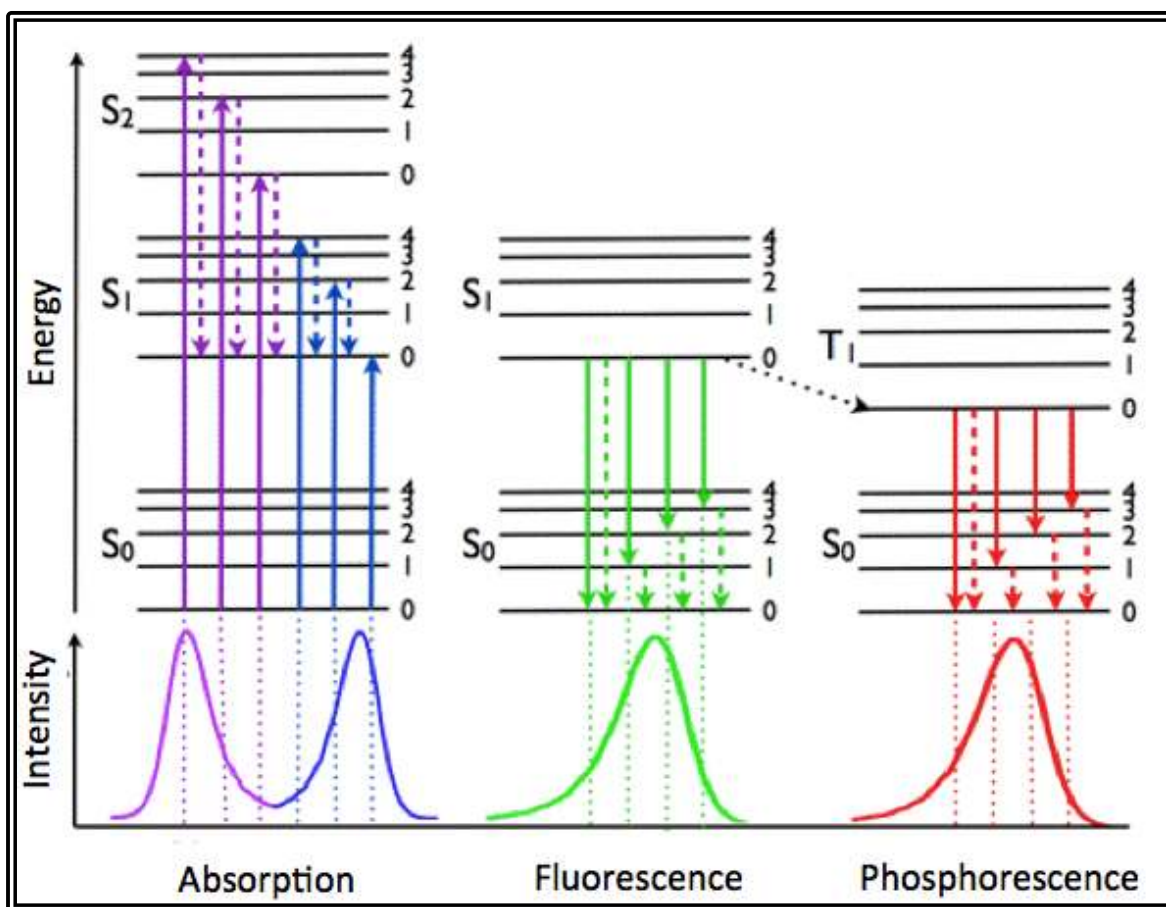


**Figure 1.22:** Jablonski diagram<sup>314</sup> depicting the three singlet states: the ground, first and second electronic states indicated by  $S_0$ ,  $S_1$ , and  $S_2$ , respectively. At each of these electronic energy levels the fluorophores can exist in a number of vibration energy levels depicted by 0, 1, 2, etc. The transitions between the states are depicted by the vertical lines to demonstrate the instantaneous nature of light absorption. Because transitions occur in about  $10^{-15}$  seconds, it is too fast for significant displacement of the nuclei.

### 1.5. Research Objectives

There are a few different goals in this research project. One of the objectives was to understand the imprinted co-polymer system of methyl methacrylate (MMA) and N,N- dimethyl acrylamide (DMAA) through morphological studies. In previous studies, the polymer exhibited a porous like surface and indicated the formation of aggregates. This suggested that molecules may be aggregating in the cavities of the polymer network, and therefore molecular imprinting was not occurring in the manner that is conventionally described in literature. Through the use of SEM, an understanding of interaction of propranolol with the polymer network was attempted. The effect of the Soxhlet cleaning process on the polymers was also examined to establish any morphological modifications that were occurring in the system. Also, the possibility of the formation of propranolol aggregates was examined and an attempt to visualize the aggregates and the cavities was made. It was also observed how the system would be affected if the aggregates were prevented from forming

Another objective of the project was to establish an understanding of the uptake profiles by investigating if preferential uptake of propranolol was exhibited by the system and how various factors influence uptake. The uptake of the template by the polymer system is essential in developing a drug delivery system. Not only does the system have to uptake the drug, it must also *preferentially* uptake the template drug if it was successfully imprinted and created complementary binding sites. If the system is unable to uptake the desired drug template, the polymer is not

a useful drug delivery device. As such, the ability of the system to uptake the drug and various factors related to uptake were examined.

The extent of the molecular affinity and recognition is crucial in establishing a sufficient drug delivery system. The level of affinity and selectivity of propranolol to the system were tested by displacement studies. The displacement studies are of two kinds, competitive displacement and non-competitive displacement.

Along with uptake a given polymer system must also be able to release the template drug to the desired target organ efficiently which is influenced by factors such as temperature and pH, the level of influence of these factors is also observed.

Thus, to summarize the research objectives, the goals were as follows: (i) understand the imprinted co-polymer system of methyl methacrylate and N,N-dimethyl acrylamide through morphological studies, (ii) establish an understanding of uptake profiles by investigating if there is preferential uptake of propranolol by the imprinted polymer and to understand what factors influence uptake, (iii) examine the extent of molecular affinity and recognition through the level of uptake efficiency, and (iv) to investigate the polymer networks release profiles under various conditions.

## 2. EXPERIMENTAL

### 2.1. Materials

*Polymer Components:* N,N-dimethyl acrylamide (DMAA) (99%, stabilized with 500 ppm monomethyl ether hydroquinone (MEHQ)), ethylene glycol dimeth-acrylate (EGDMA) (98%, stabilized with 100 ppm MEHQ), Methacrylic acid (MAA) (99+%, stabilized with 250 ppm MEHQ), and Methyl methacrylate (MMA) (99%, contains  $\leq 30$  ppm MEHQ) were obtained from Sigma-Aldrich (Oakville, Ontario) and were used as received.

*Template:* ( $\pm$ )-propranolol hydrochloride ( $\geq 98\%$ ) was purchased from Sigma-Aldrich (Oakville, Ontario) and used as received.

*Analytical Solvents:* All solvents were purchased from Sigma-Aldrich (Oakville, Ontario), were of analytical grade and were used as received. They included: Acetic acid (99.7%), acetone (99.5%), acetonitrile (MeCN) (anhydrous, 99.8%), chloroform ( $\geq 99.8\%$ , contains 0.5-1.0% ethanol as stabilizer), dichloromethane (DCM) ( $\geq 99.5\%$ , contains 50 ppm amylene as stabilizer), and di-methyl sulfoxide (DMSO) (anhydrous,  $\geq 99.9\%$ ). Ethanol (anhydrous, denatured with 5% isopropanol and 5% methanol) was purchased from VWR (Mississauga, Ontario) and used as received.

*Photoinitiator:* Darocur® 1173 was donated by CIBA Chemicals and was used as received.



*Probe:* Fluorescein (for fluorescence) was obtained from Sigma-Aldrich, Oakville, Ontario and used as received.

*Displacement Molecules:* Benzoic acid ( $\geq 99.5\%$ ), S-(+)-naproxen ( $>98\%$ ), were used in displacement studies as non-complementary structures (NCS), and 1-naphthol ( $\geq 99.0\%$ ) and S-(-) timolol ( $>98\%$ ) were used as complementary structures. All substances were obtained from Sigma-Aldrich (Oakville, Ontario) and used as received.

*Miscellaneous:* The aluminum dishes used as polymerization reactors and the double thickness thimbles used in Soxhlet extraction were purchased from VWR (Mississauga, Ontario). The salts used for buffer preparation include: disodium hydrogen phosphate ( $\text{Na}_2\text{HPO}_4$ ) (99%), sodium chloride (NaCl) (99%), and sodium hydroxide (NaOH) (98%), and were also purchased from VWR (Mississauga, Ontario).

## **2.2. Instrumentation**

Polymerization was accomplished with a Novacur UV light curing system from EFOS. Cleaning of polymer product was achieved with a Soxhlet apparatus and monitored through the use of a Perkin Elmer Lambda 20 spectrophotometer following the absorption of propranolol at 295 nm. The polymers were dried using a Fisher Scientific Vacuum Oven Model 48. Fluorescence data was obtained on a

Perkin Elmer LS50B luminescence spectrometer. Morphology studies were analyzed through the use of a Jeol JS-6380LV Scanning Electron Microscope. Polymer samples were ground into powder form with a tungsten ball mill grinder from Retsch GmbH. Shearing was achieved through the use of an Ultra-Turrax T50 Basic Stirring Motor made by IKA® - Werke. In the uptake and release studies the samples were centrifuged using a Sorvall Legend RT+ centrifuge from Fisher Scientific. In a few select release experiments an ultrasonicator, the Aquasonic 50HT made by VWR, was used.

### **2.3. Analysis**

Measurements were determined through the use of the Perkin-Elmer LS50B Luminescence spectrometer. The ELISA plate reader attachment was installed and sample solutions were placed into the appropriate ELISA cell allowing for multiple measurements to be obtained in a single run. The analysis conditions used were Excitation  $\lambda$ : 285 nm; Scanned ranges: 295-400 nm; Scanned Speed: 100 nm/min; En slit: 5 nm; Ex slit: 4.2 nm.

Scanning Electron Microscopy (SEM) allows for visualization of general morphology, to identify differences between MIPs and NIPS, and examine a sample at a high magnification (10 000 $\times$ , 20 kV). Images were obtained on a Jeol JSM-6380LV SEM. However, at these high magnifications, charging effects are generated. In order to reduce or eliminate the effects of charging, the samples were gold coated, which allows the gold coated samples to be examined at even higher magnification (20 000 $\times$ , 20 kV). Gold atoms come from gold foil that is placed on top of the vacuum

cylinder chamber on the DESK IV sputtering device at 80 mTorr for a time frame of 60 seconds, with the current at 30 mA.

## 2.4. Methods

### 2.4.1. Polymer Synthesis

The functional monomer, MAA (0.401 mmol), and the cross-linking agent, EGDMA (0.583 mmol) were dissolved in 4 mL of backbone monomers, DMAA (19.41 mmol) and MMA (18.78 mmol) in a 50 mL beaker. For the NIP, template was not added, and for the MIP samples 0.029 g of propranolol ( $9.80 \times 10^{-5}$  mol) was dissolved in the 4 mL monomer solution. The photoinitiator, Darocur 1173 (0.4% v/v) was added last. The sample was stirred for five minutes to ensure sufficient mixing. The NIP and MIP samples were poured into separate 20 mL aluminum dishes (4.4 cm in diameter) that were labeled accordingly. The samples were subjected to free radical polymerization that was initiated by UV irradiation using the Novocur curing system. In order to maintain consistency of UV exposure from each polymer batch the lamp was set at a distance of 4 inches above the sample dish for 2.5 minutes. McBain reported the average UV dosage was  $3.80 \text{ J/cm}^2 \pm 0.369$  (A) and  $2.32 \text{ J/cm}^2 \pm 0.242$  (V) and irradiance of  $3.05 \times 10^{-2} \pm 1.90 \times 10^{-3}$  (A) and  $1.90 \times 10^{-2} \pm 1.90 \times 10^{-3}$  (V), where UV(A) and UV(V) correspond to wavelengths in the ranges of 320-390 nm and 395-445 nm, respectively.<sup>317</sup> The UV dosage for the current study was expected to be in the same range.

#### *2.4.2. Polymer Washing*

In order to maximize the uptake of drug the template must be completely removed from the system. A few different approaches to extract the template were utilized, however the most effective method is described below and thus became the “conventional” method of cleaning.

Freshly made polymers underwent a standard washing process through the Soxhlet method, refluxing with ethanol for 10-14 days. The washing solvent was changed every 1-2 days and the liquid in the round bottom flask was measured with UV/Vis spectroscopy to check for un-reacted monomers or remaining residual propranolol. Polymers that were ground immediately after polymerization and then cleaned required extra precaution during the Soxhlet process to avoid sample loss. To prevent sample loss, the powdered polymer was placed in a filter paper and folded a few times and then placed in the thimble. After a day or two the filter paper needed to be changed to prevent any tearing.

Alternative cleaning methods that were investigated include washing in distilled water and a saline (0.9% NaCl) solution. Different washing methods were examined to establish the most effective method that causes minimal or no modifications to the polymer, and to understand the extent of the changes by each method and how these alterations influence uptake and release.

#### *2.4.3. Polymer Drying*

Following cleaning of the samples, the hydrogels were placed into clean 20 mL aluminum dishes and covered with parafilm, and put into the vacuum oven for

drying. The samples were dried at 50°C for 24 hours. A few samples were ground into powder form immediately after polymerization, dried, and then cleaned. To dry samples that were in powder form extra caution was required to prevent sample loss, since the pressure from the vacuum could easily disperse the powder around the oven. Thus, powdered samples were placed on filter paper that was carefully folded, which was then placed into the foil dish and left to dry under the same conditions.

#### *2.4.4. Morphology Studies*

Polymers were prepared as described by the conventional method above and were analyzed by SEM. Samples were examined extensively for the presence of aggregates and to visualize cavities as were seen in previous studies. In the past the cavities were visualized and measured to be 0.25  $\mu\text{m}$  to 0.50  $\mu\text{m}$ .<sup>317</sup> An attempt to reproduce the previous results was made to understand the interaction between the template propranolol and the polymer system. Structure variations between MIPs and NIPs were also examined through SEM.

#### *2.4.5. Shearing Experiments*

The formation of aggregates that was suggested by McBain<sup>317</sup> are not consistent with traditional molecular imprinting that has been described in literature. As such an extensive amount of effort went into trying to understand and identify the cause for the formation of these aggregates. Thus, it was essential to examine how the polymer network would change if the aggregates were prevented from forming by shearing the sample prior to polymerization.

For shearing experiments the polymer components were measured into a 50mL beaker, without the photoinitiator. The aggregates were broken up by applying the shearing device to the mixture (co-polymer and template) at level 1, which is at a speed of 4000 rpm, prior to polymerization. The shearing device essentially behaves like a blender at an extremely high speed, ranging from 4000 – 10 000 rpm. The photoinitiator was added to the sheared sample and polymerized. The system was re-examined once after shearing to get a sense of the effect the aggregates have on the system and how they influence imprinting.

#### *2.4.6. Probe Studies*

In an attempt to visualize the cavities generated in the polymer by the imprinting technique a fluorescent probe was introduced. The objective was to “light” up the cavities or “pockets” to allow for morphological observations to be made. The fluorescent material that was introduced as a probe was fluorescein, which is a dark red synthetic organic compound. Fluorescein has an absorption of 494 nm and emission maximum of 521 nm.

#### *2.4.7. Degradation of Propranolol*

Propranolol is a fluorophore and as such its presence can be detected through the use of fluorescence spectroscopy. However, once propranolol is included into the polymer system, forming the host-guest complex, it can no longer be detected by the instrument. Therefore, the concentrations that are determined for propranolol are determined through an indirect means. The concentration of the propranolol is known at the beginning of an uptake experiment as the solutions are

made to specific concentrations. Therefore, uptake values have been determined by noting the decrease in the concentration of propranolol in the external solution as uptake proceeds. It is necessary to establish if the decrease in detectable propranolol is a result of inclusion into the polymer system or if it is a result of degradation of propranolol. If there is breakdown of propranolol, the extent of degradation must be established and a correction made.

Propranolol (0.029 g) was measured and dissolved in de-ionized water and monitored for concentration changes upon prolonged exposure to ambient lighting. This was accomplished by monitoring the propranolol fluorescence signal every 24 hours for a 7 days period. By determining the propranolol change in the absence of polymer, degradation corrections can be made if necessary.

#### *2.4.8. Uptake*

A series of aqueous solutions with varying propranolol concentrations were prepared (0-250  $\mu$ M). An appropriate quantity of cleaned and dried polymer (0.0500 g – 0.100 g) was added to a 25 mL falcon tube, with 5 mL of the appropriate concentration of solution. Samples for each concentration were prepared for both NIP and MIP. The samples were incubated at 37°C and shaken simultaneously. Prior to analysis the samples were centrifuged at 10 000 rpm for 10 minutes. The tubes were analyzed by fluorescence spectroscopy from day 1 to day 7 at 24 hour intervals.

#### *2.4.9. Preferential Uptake*

A study was conducted to determine if the uptake by the MIP system is preferential to the NIP system. If the polymers have been in fact imprinted, the extent of uptake should be different in the two systems. Uptake studies were conducted with the MIP and NIP system simultaneously and the drug absorption, based on measurement of propranolol fluorescence, was compared between the two systems.

#### *2.4.10. Polymer Form Variation*

The polymers have been studied in both powder and hydrogel form. When the polymer is in powder form it is believed to have greater surface area and therefore it has been speculated to have greater potential for uptake. Thus, a study was conducted and uptake system was set up for both powder form and hydrogel form to determine which form supports greater uptake efficiency.

#### *2.4.11. Effects of Centrifugation*

Each sample was centrifuged prior to analysis by fluorescence spectroscopy as any presence of solid polymer suspended in the external solution greatly affects the fluorescence readings. However, centrifugation can become time consuming as there are 18 samples in a given dilution series (0, 1, 5, 10, 20, 25, 35, 40, 50, 55, 65, 100, 125, 150, 175, 200, 225, 250 $\mu$ M) that each need to be centrifuged. Thus a study was conducted to compare the behaviour of uptake between samples that were not



centrifuged and samples that had been centrifuged to determine if centrifugation is a necessary step.

#### *2.4.12. Maximum Adsorption*

Initially the system was studied for uptake for a period of 72 hours. A study was done to establish the length of time that is required to reach the maximum absorption. The experiments were continued until the uptake by the polymer reached a plateau.

#### *2.4.13. Higher Polymer Concentrations*

The initial dilution series that was created for uptake studies included 12 varying concentration solutions of propranolol; (0, 1, 5, 10, 20, 25, 35, 40, 50, 55, 65, 100 $\mu$ M). It is essential to establish the interaction of the polymer network in a much higher concentration environment. Thus 6 additional concentrations were incorporated, 125, 150, 175, 200, 225, and 250  $\mu$ M, into the dilution series. The affects of the higher concentrations on uptake were examined.

#### *2.4.14. Cavities as Limiting Factor*

Thus far the studies that have been conducted have altered the concentration of drug available for binding, making the quantity of drug the limiting factor. The system was also examined with the quantity of drug kept constant and with the quantity of polymer varied. The concentrations of propranolol solution that were selected for this study were 10, 25, and 50  $\mu$ M.

#### *2.4.15. Displacement Studies*

Displacement studies were conducted to establish the extent of selectivity and affinity for propranolol by the cavities. There were two types of displacement studies; Non-Competitive Displacement (NCD) and Competitive Displacement (CD). In NCD, the system is exposed to propranolol and interacts with the network for the maximum absorption period, previously determined to be 7 days. Following this time, a second molecule is introduced and its ability to replace propranolol and bind to the cavities is investigated after a 24 hour exposure time. Various secondary molecules were examined, two of which had non-complementary structures (NCS), benzoic acid and naproxen, and two of which had complementary structures (CS) to propranolol, 1-naphthol and timolol. In the case of CD, the NCS or CS was introduced to the system at the same time as the propranolol, the behavior was then examined and compared to that of the NCD system.

#### *2.4.16. Release Studies*

Release studies were conducted to establish an understanding of the effectiveness of release of the drug and to distinguish which factors affect release from the polymer. Polymer samples that had gone through the uptake process as described above were obtained and exposed to fresh deionized water. The samples were then tested every 24 hours up to a total of 72 hours, for changes detected in propranolol concentration in the external solvent. Various factors were tested for the release of propranolol such as temperature and pH. These parameters were altered to resemble the internal environment of the body and the changes were

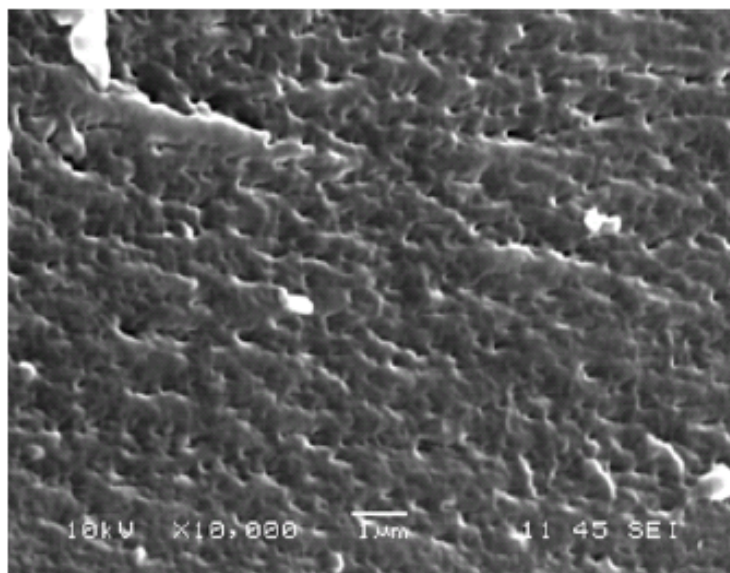
monitored to determine if release became more or less effective under such conditions. Release was also observed when the samples were sonicated. The falcon tubes containing the samples were placed in a tube rack and immersed into the water bath of the sonicator. The samples were sonicated for a total of 72 hours and tested for changes in concentration every 24 hours. Two buffer solutions of  $\text{Na}_2\text{HPO}_4$  were made, adding  $\text{H}_3\text{PO}_4$  or  $\text{NaOH}$  drop wise for pH3 and pH12 respectively. The polymer was then exposed to the respective buffer solution in a falcon tube and tested for propranolol release every 24 hours for a total of 72 hours. The pH studies were performed at room temperature to observe the release effects independently of additional test parameters.

### 3. RESULTS

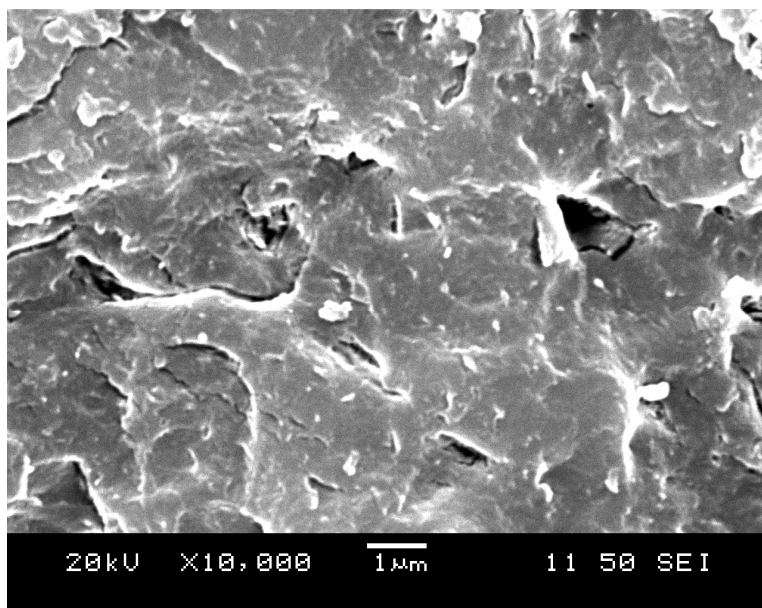
#### 3.1. Morphology Studies

The SEM images obtained from McBain's<sup>317</sup> work, shown in Figure 3.1 (a), indicate that the polymer exhibits a porous surface and the presence of cavities. The cavities were estimated to be approximately 0.25  $\mu\text{m}$  to 0.50  $\mu\text{m}$  in diameter. However, due to the size of propranolol, 1.0 nm to 1.5 nm, McBain suggested that the observed pores reflect spaces created due to the aggregation of propranolol rather than template sites due to individual imprinting events. The subsequent morphology studies conducted in this work were intended to observe, characterize, and understand the formation of cavities and the morphology of the polymer, and ultimately to investigate further McBain's findings.

The SEM image in Figure 3.1 (b) is an image obtained under the same experimental conditions as the image from McBain's work, Figure 3.1 (a). An effort to reproduce McBain's porous surface image was not successful. At no point in the morphological studies was it possible to successfully visualize the presence of any cavities, pores, or clusters of propranolol.



(a)

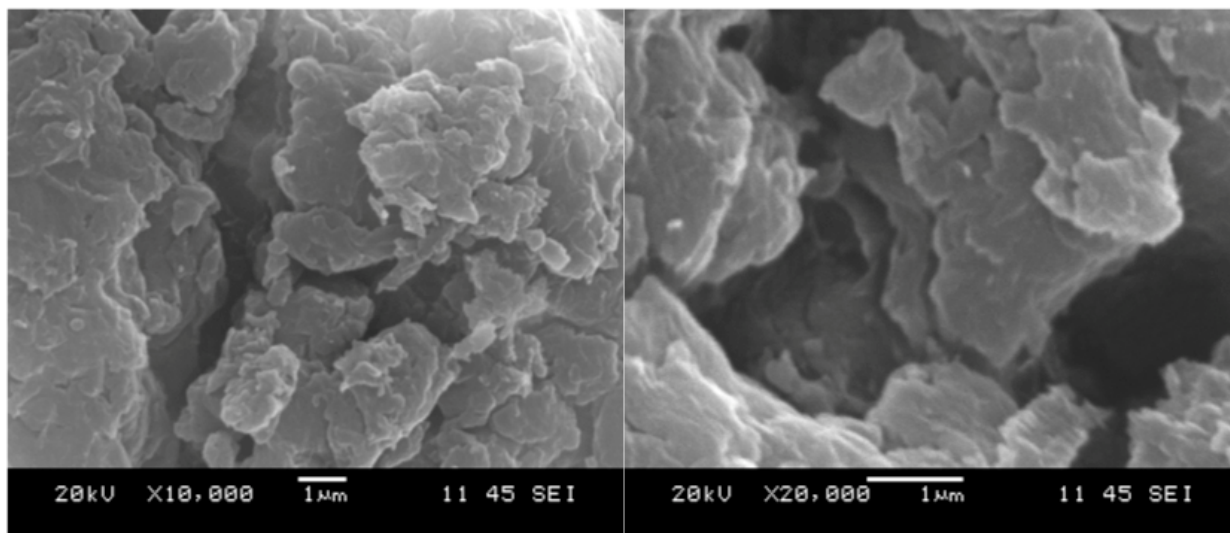


(b)

**Figure 3.1:** Scanning Electron Microscope images of Molecular Imprinted Polymers with Propranolol. Both (a) and (b) are prepared and cleaned in the same manner, as well as at 10 000x magnification with gold coating. Image (a) was obtained in work conducted by McBain that indicates the presence of pores.<sup>317</sup> Image (b) was obtained in the present study.

### *3.1.1. Effects of Cleaning Methods on Polymer Morphology*

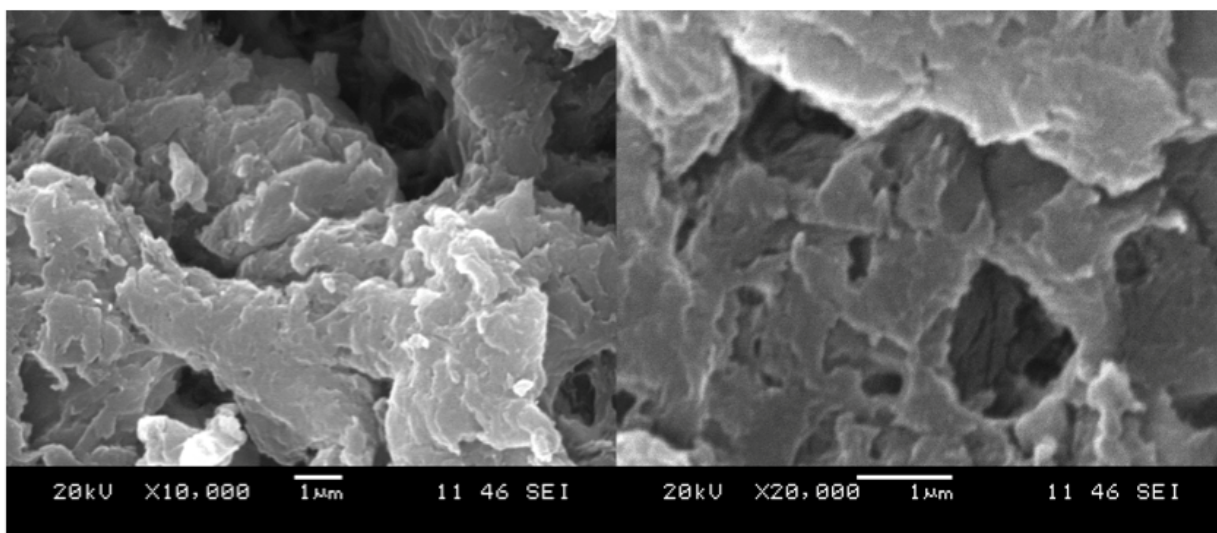
The effects of the Soxhlet cleaning method on the polymer morphology are shown in Figures 3.2 to 3.5. The images obtained from the Soxhlet cleaning method suggest that the process alters the morphology of the polymer. Other cleaning methods such as cleaning with distilled water and a saline solution with shaking were attempted with little success as template extraction proved to be ineffective and excessively time consuming. Thus, the alternative cleaning methods were not examined via SEM. Figures 3.2 and 3.3 display the images of NIP and MIP respectively, prior to cleaning. The images in Figures 3.4 and 3.5 display the NIP and MIP subsequent to the cleaning process at different magnifications.



(a)

(b)

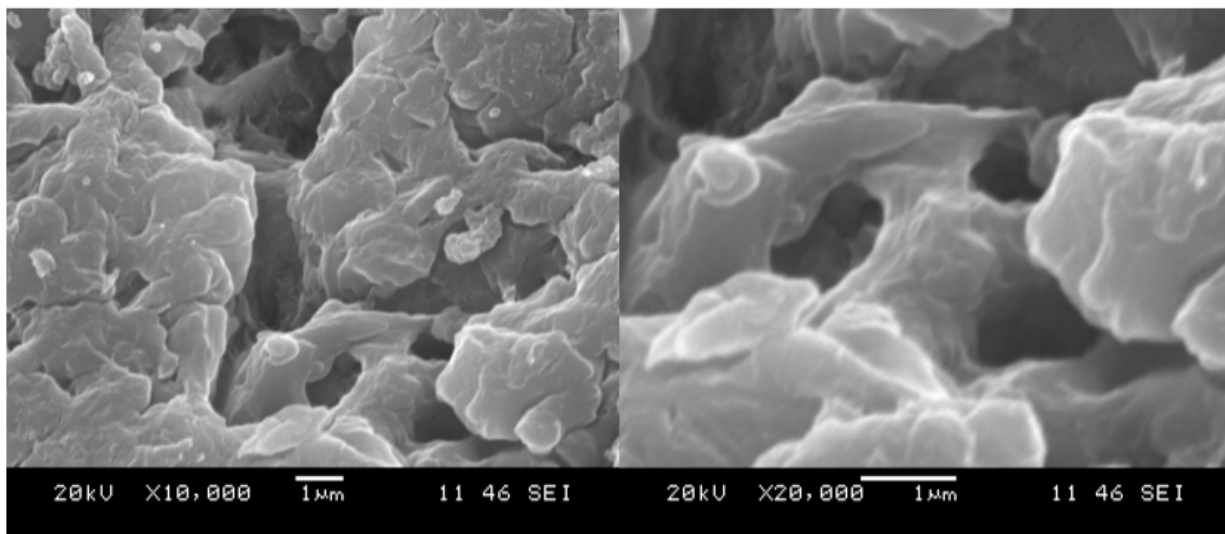
**Figure 3.2:** SEM images of Non-Imprinted Polymers (NIP) that have not been cleaned taken at different magnifications (a) 10 000X, (b) 20 000X.



(a)

(b)

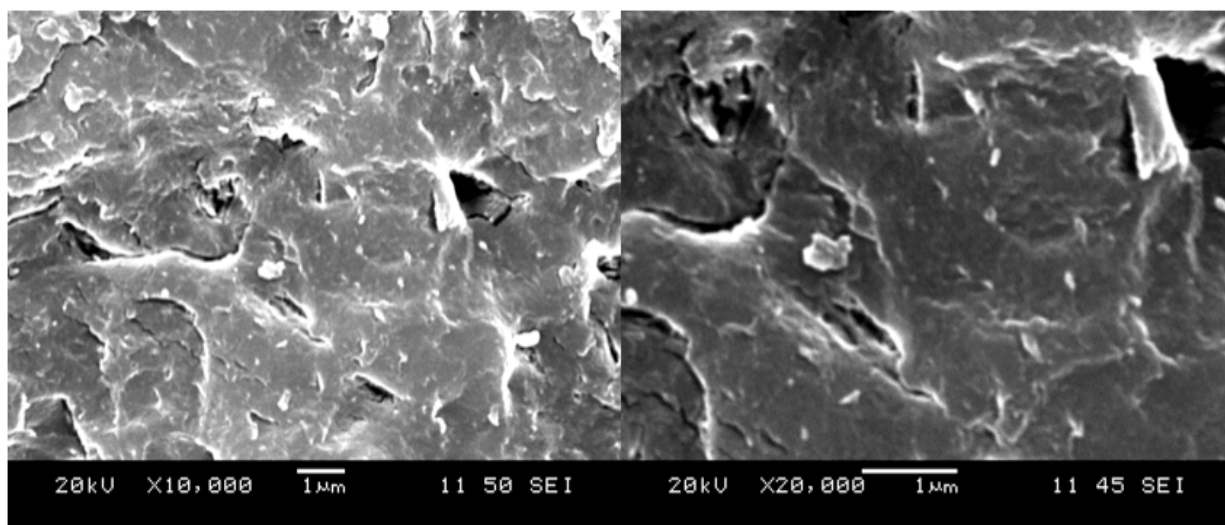
**Figure 3.3:** SEM images of Molecularly Imprinted Polymers with Propranolol (ProMIP) that have not undergone the cleaning process taken at different magnifications (a) 10 000X, (b) 20 000X.



(a)

(b)

**Figure 3.4:** SEM images of NIP subsequent to cleaning taken at different magnifications (a) 10 000X, (b) 20 000X



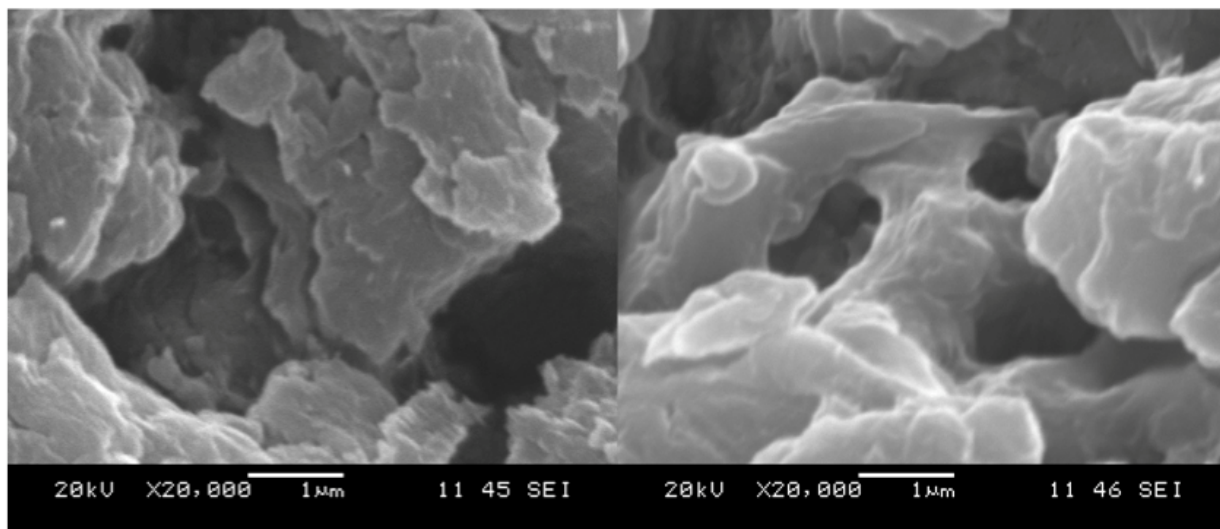
(a)

(b)

**Figure 3.5:** SEM images of ProMIP subsequent to cleaning taken at different magnifications (a) 10 000X, (b) 20 000X.



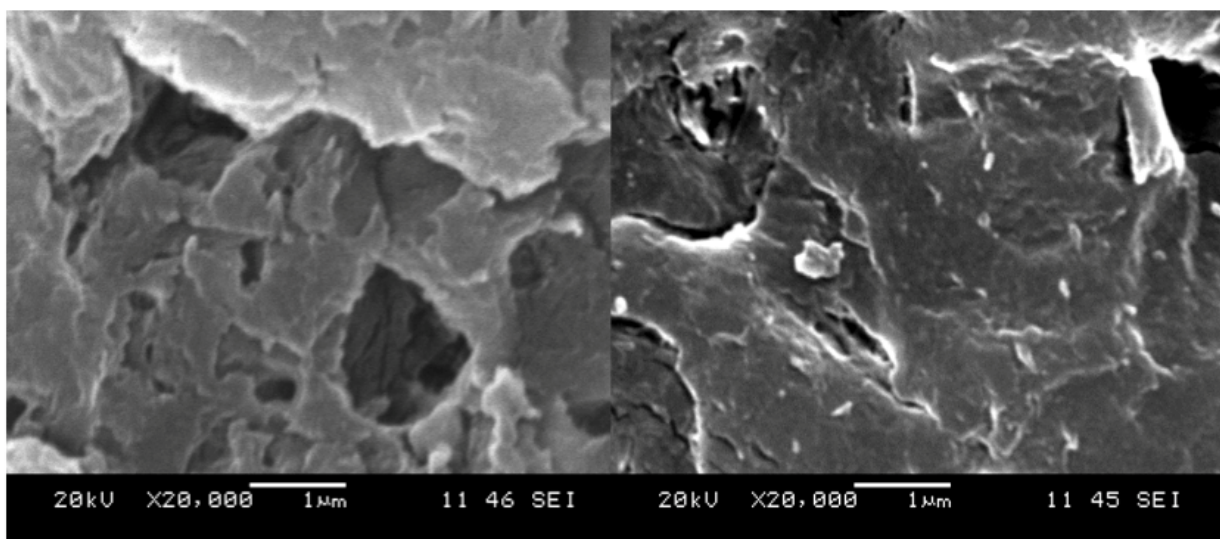
The images in Figures 3.6 and 3.7 allow for a direct comparison of polymers that have been produced in the same manner, however one has been subjected to the cleaning process and one has not. The images in Figure 3.6 are not significantly different from each other. Although the same cannot be said about the cleaned and un-cleaned morphology of the MIP system in Figure 3.7. There is a distinct difference in the appearance of the cleaned vs uncleaned MIP polymers. The surface of the cleaned polymer appears to be rough and dry and as if it were shavings, where as the uncleaned MIP sample has a rubber like appearance. The change observed in the NIP is not significant, although the two are similar, they certainly are not identical.



(a)

(b)

**Figure 3.6:** SEM images of NIP morphology (a) cleaned, (b) un-cleaned at the same magnification, 20 000X. Note the morphological differences are not significant between (a) and (b).



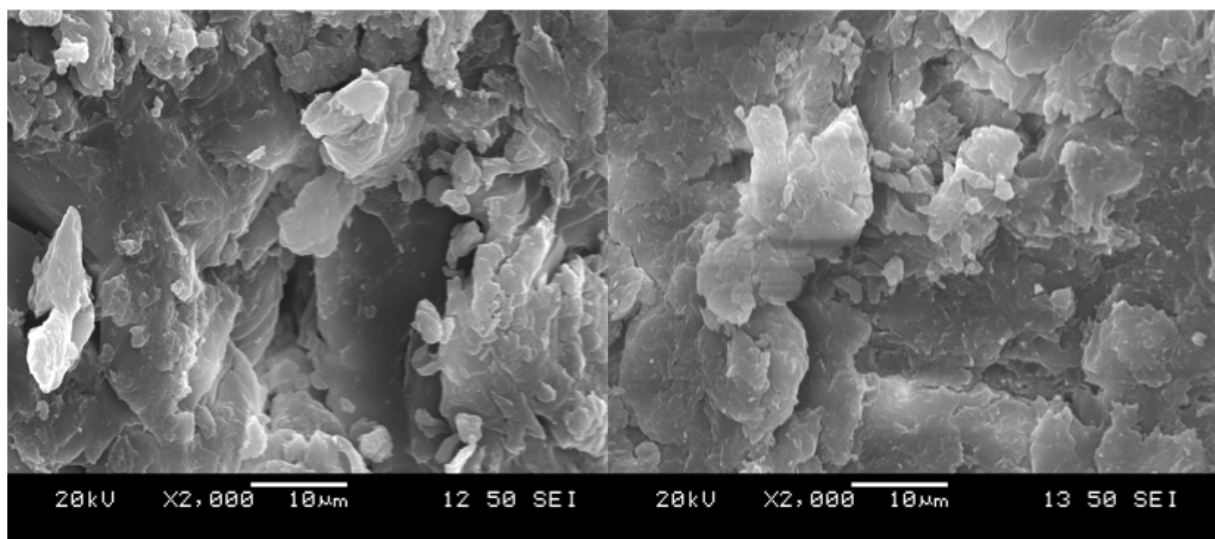
(a)

(b)

**Figure 3.7:** SEM images of ProMIP morphology (a) cleaned, (b) un-cleaned at the same magnification, 20 000X. Note the distinct change in morphology subsequent to cleaning.

### *3.1.2. Effects of Shearing on Polymer Morphology*

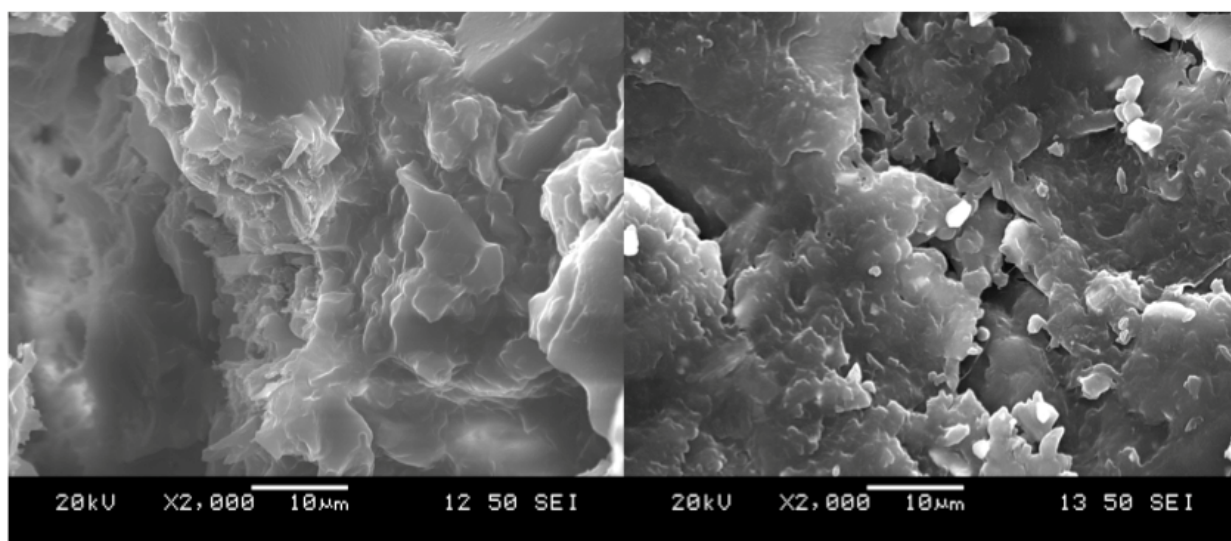
The image of the NIP system that was exposed to the shearing device, seen in Figure 3.8, does not demonstrate any significant morphological changes compared to the un-sheared samples. However, the cleaned MIP sample from the shearing experiment, Figure 3.9, appears to be quite different from the conventionally prepared and cleaned MIP. It appears to have a smooth surface and the edges appear to be rounded. The rough appearance from Figure 3.7 (b) is no longer visible. There is no clear evidence for cavities in any of the images.



(a)

(b)

**Figure 3.8:** SEM images of NIP samples that were sheared at 4 000 rpm prior to polymerization magnified at 2 000X. Image (a) is the raw sheared sample and has not undergone the cleaning process, and (b) is the cleaned sample.



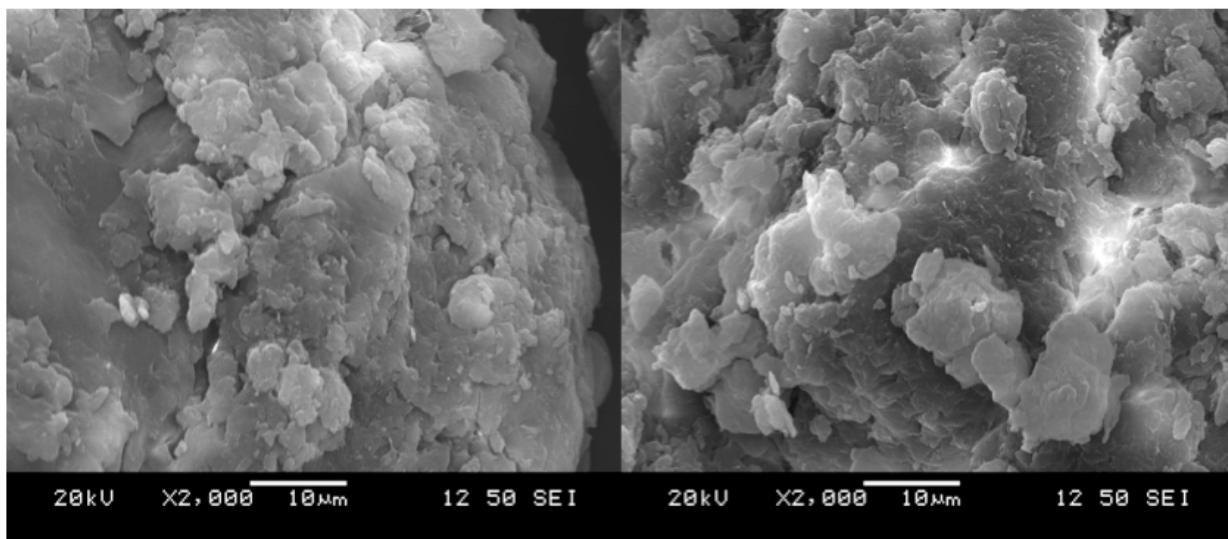
(a)

(b)

**Figure 3.9:** SEM images of ProMIP samples that were sheared at 4 000 rpm prior to polymerization magnified at 2 000X. Image (a) is the raw sheared sample and has not undergone the cleaning process, and (b) is the cleaned sample.

### *3.1.3. Probe Studies*

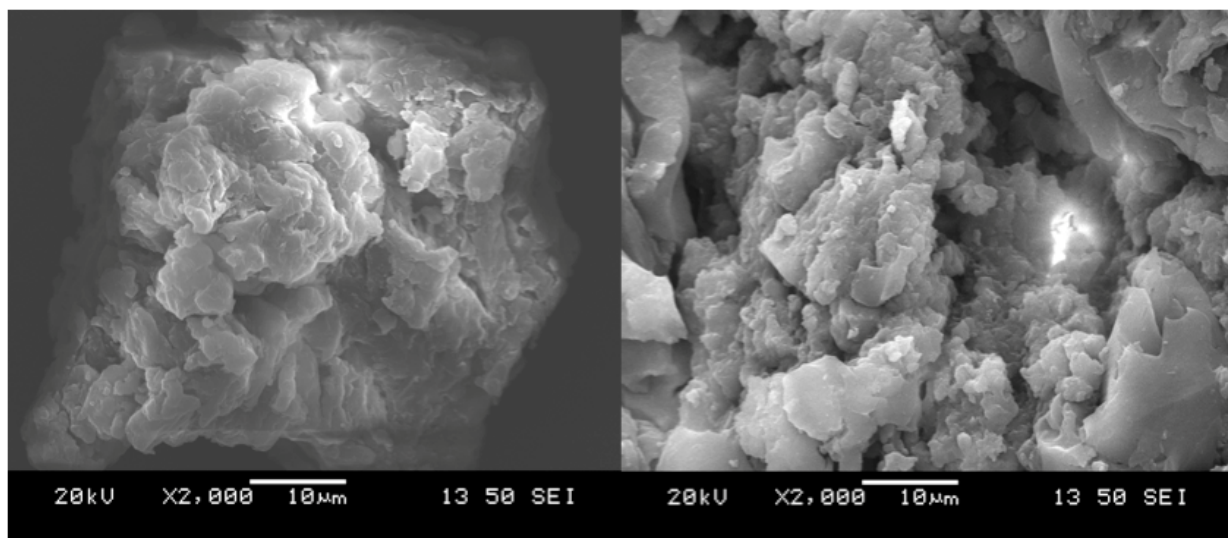
Fluorescein probe experiments were an attempt to visualize the cavities, however the images in Figure 3.11 do not indicate any cavities. The presence of cavities should not be apparent in the NIP system, Figure 3.10, as it was not imprinted. The images in Figure 3.10 and 3.11, obtained without shearing, demonstrate the effect of a fluorescent probe to the NIP and MIP system respectively. The samples demonstrate a greater amount of clustering in comparison to the sheared samples. There is however a distinct difference in the cleaned and un-cleaned structure of both the NIP and the MIP systems with fluorescein present. During the cleaning process, for both NIP and ProMIP, the removal of probe was observed and could be verified by the presence of fluorescein's characteristic red hue in the round bottom flask containing the distilled ethanol.



(a)

(b)

**Figure 3.10:** SEM images of NIP samples in the presence of fluorescein probe magnified at 2 000X. Image (a) is the un-cleaned sample and (b) cleaned sample.



(a)

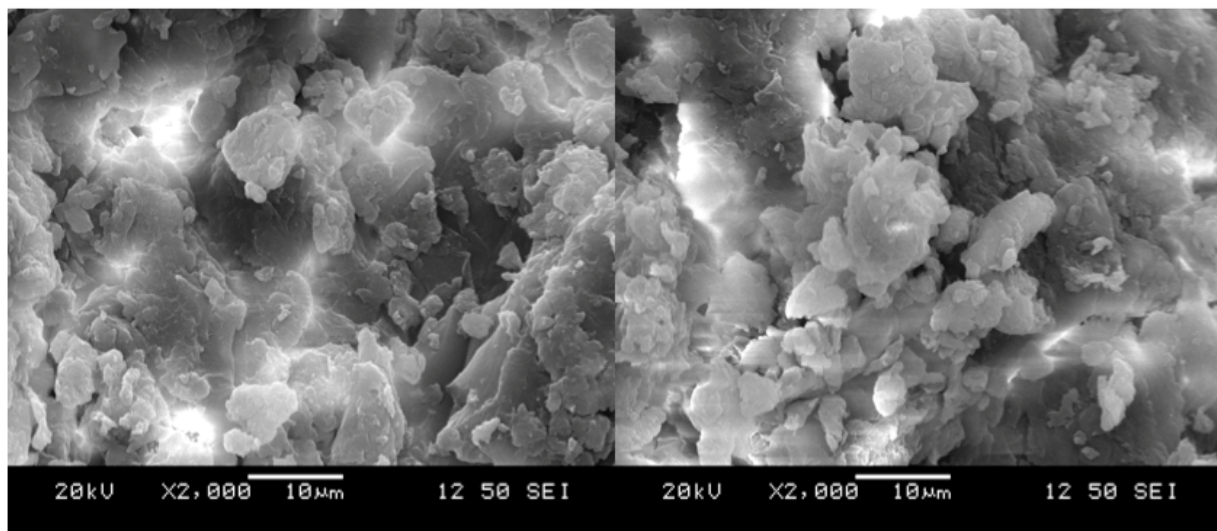
(b)

**Figure 3.11:** SEM images of ProMIP samples in the presence of fluorescein probe magnified at 2 000X. Image (a) is the un-cleaned sample and (b) cleaned sample.

#### *3.1.4. Effects of Shearing in the presence of the Probe*

The images obtained from samples that were prepared in the presence of fluorescein, the fluorescent probe, with shearing are shown in Figures 3.12 and 3.13. All of the images demonstrate a significantly higher amount of clustering in comparison to samples that did not undergo shearing or those that did not have a probe introduced to them such as those samples portrayed in Figures 3.1 to 3.7. The NIP images also exhibit bright patches in certain areas, which may be a result of local charge build up during exposure to the electron beam. No visualization of cavities was achieved.

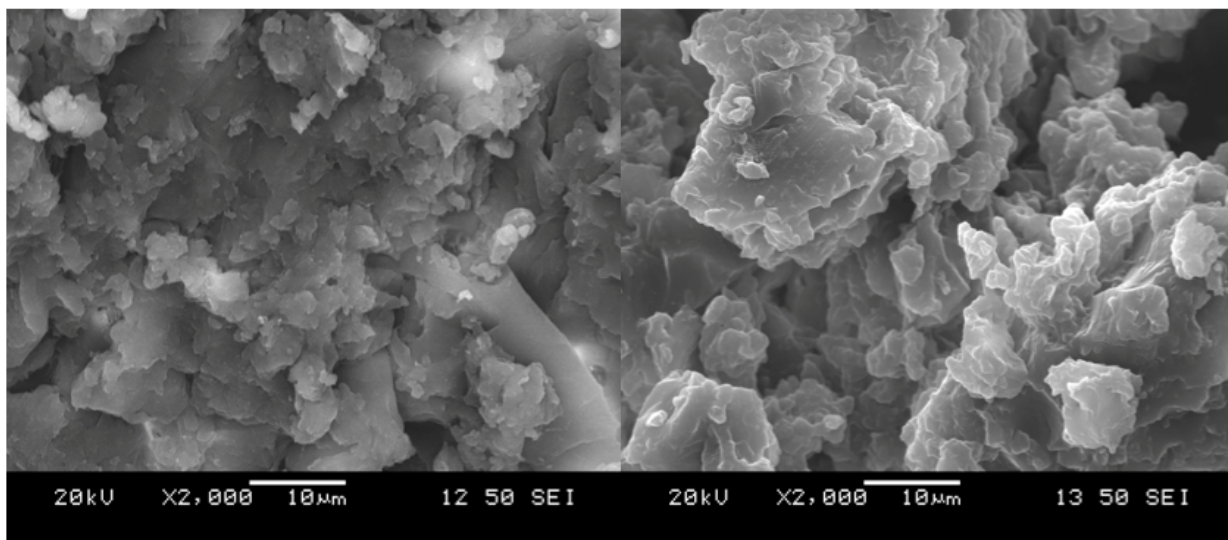




(a)

(b)

**Figure 3.12:** SEM images of NIP samples in the presence of fluorescein probe and sheared at 4 000 rpm and magnified at 2 000X. Image (a) is the un-cleaned sample and (b) cleaned sample.



(a)

(b)

**Figure 3.13:** SEM images of ProMIP samples in the presence of fluorescein probe and sheared at 4 000 rpm and magnified at 2 000X. Image (a) is the un-cleaned sample and (b) cleaned sample.



### 3.2. Degradation of Propranolol

There are several studies that suggest propranolol is light-unstable and a photosensitizing agent.<sup>318-322</sup> In the present work, under the conditions used to prepare the samples, only modest photolysis of propranolol was observed, Figure 3.14 presents the initial and final concentrations of propranolol in a control sample measured when the sample was fresh (Day 0) and after exposure to ambient room lighting for an extended period (Day 7). From the chart, in each of the 18 different concentrations there is a minor decrease in measured concentration of propranolol. Since there is no polymer present in the system the change is attributed to the degradation of propranolol. The overall degradation of propranolol ranges from 0.05% at 250  $\mu\text{M}$  propranolol to 5.8% at 1  $\mu\text{M}$  propranolol. These changes are very minor and it was decided that corrections for such changes in future fluorescence measurements were unwarranted. An additional point from Figure 3.14 is the rather good linearity of the calibration curve up to about 100  $\mu\text{M}$  propranolol for both conditions (Day 0 and Day 7). At concentrations above that, the plot flattens. This represents the saturation of the fluorimeter response at these rather high concentrations.

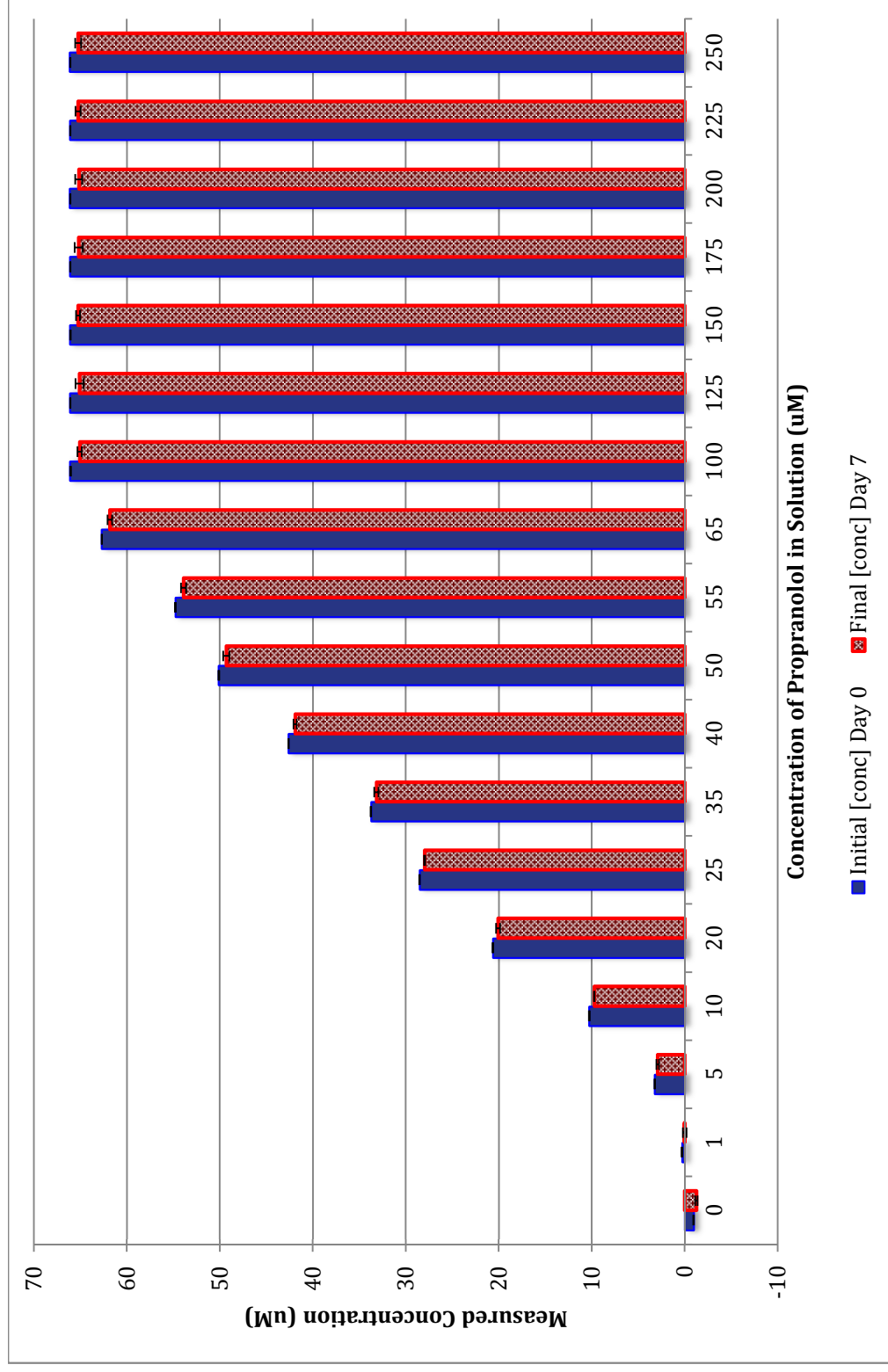


**Figure 3.14:** Graphical representation of photolysis of propranolol observed in control sample at day 0, initial concentration, and day 7, final concentration.

### 3.3. Uptake of Propranolol by Polymer Systems

The results obtained in the uptake experiment demonstrate a level of selectivity for the template, propranolol. It is important to note that the uptake of propranolol was achieved via monitoring changes in concentration of the external environment, i.e., an indirect means. It is crucial that an understanding of how the data is depicted and what inferences can be accurately made from them is established.

Figure 3.15 demonstrates the uptake behaviour of the NIP system for a series of aqueous solutions ranging in concentration from 0-250  $\mu\text{M}$  from 24 hours to 168 hours. Figure 3.15, and subsequent uptake and release plots, should be interpreted as follows: The x-axis demonstrates the concentration that is the known initial concentration of propranolol in the aqueous solutions. The y-axis is the measured concentrations, which were determined by developing a calibration curve (see Appendix A.1) of the fluorescence signals with respect to the known concentrations of propranolol. A system with 0% uptake will have all of the original propranolol unbound in the external solution and have a slope of 1. A system with 100% uptake will have no detectable propranolol in the external solution and have a slope of 0 and the line will fall directly on the x-axis.

Figure 3.15 demonstrates that the uptake is some where between 0 and 100%. It also demonstrates that there are instances where the uptake behaviour is outside of this range. Logically, the uptake simply cannot be less than 0% or more than 100%. The values obtained at low concentrations resulted in a small negative number. The negative number in all of the studies has been interpreted as a

concentration of 0  $\mu\text{M}$ . Also, in the case of higher concentrations, often the fluorescence readings resulted in values that were off-scale, and the values were extrapolated from the calibration curve. Even so, most of the data for solutions with concentrations greater than 100  $\mu\text{M}$  reach a plateau of measured concentration at 24 hours. The concentrations become detectable after several hours, but the behaviour during that time cannot be accurately analyzed. Therefore it is essential to note that there is an upper limit of detection which is outlined in Figure 3.15 by the black dashed lined. It is essential to keep the explanation of the analysis of the uptake charts and the upper detection limit in mind along with the 0% and 100% uptake slopes. In effect, the observed data that lies between the 0% uptake and 100% uptake lines can be viewed as reliable and meaningful. All of the uptake graphs include error bars for each data point, although they may not be distinctly visible.

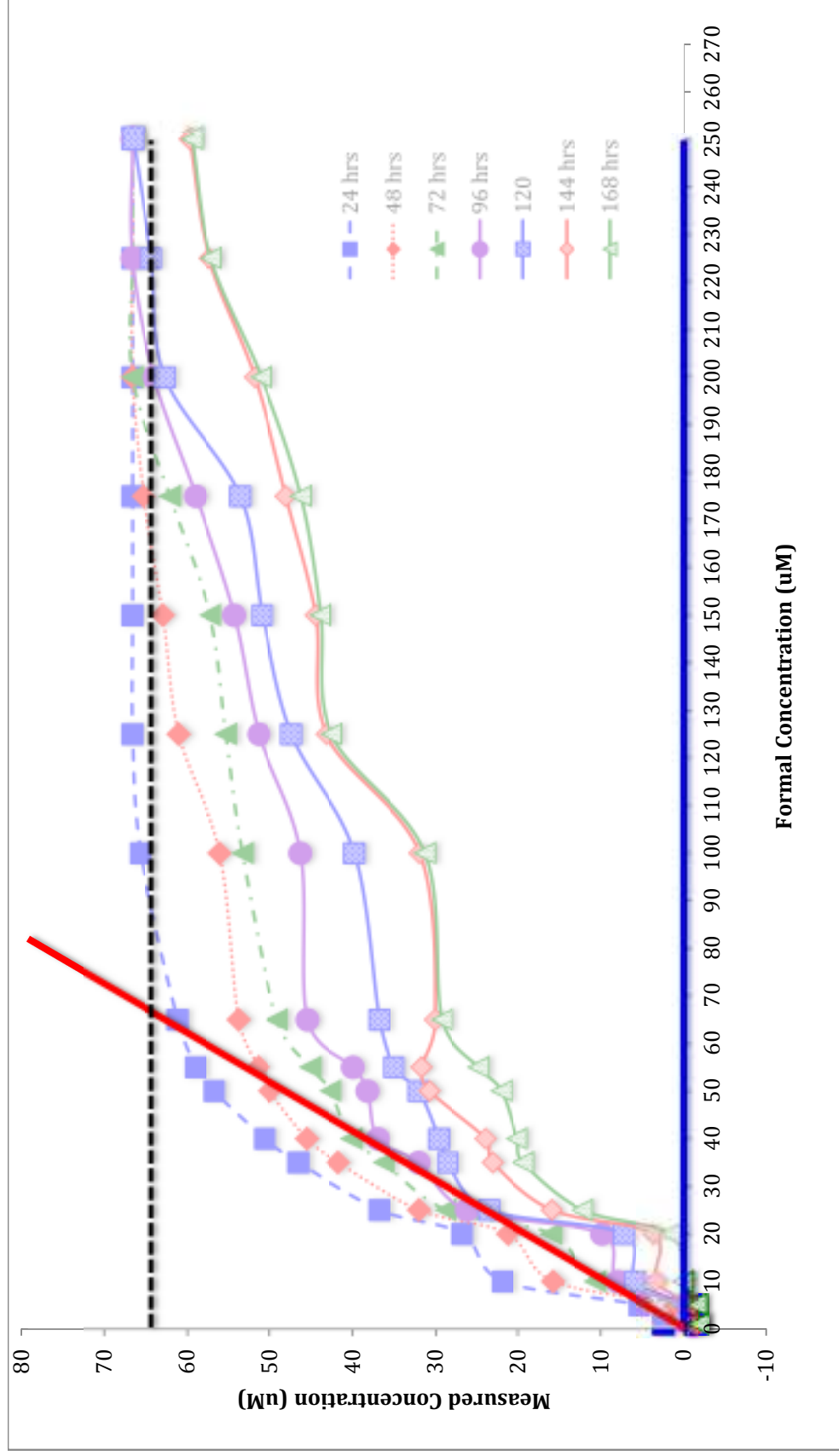


**Figure 3.15:** Explanation of graphical interpretation for NIP network at high concentrations (above 100  $\mu\text{M}$ ) every 24 hours for 168 hours to be applied to all uptake graphs.

### *3.3.1. Preferential Uptake*

In the preferential uptake experiment, the difference in uptake efficiency between the hydrogel NIP and the MIP was compared. The charts in Figure 3.16 and 3.17 display the uptake of the two systems independently and Figure 3.18 allows for a direct comparison of the two systems. The x-axis values are the known analytical concentrations of propranolol at the start of the uptake experiment and the y-axis values are the observed propranolol concentrations in the external medium at equilibrium. Therefore, a lower y-axis value implies greater uptake.

From the charts of the NIP and the MIP individually, Figure 3.16 and 3.17 respectively, the general uptake trend appears to be the similar; uptake increases with exposure time. However, when plotted on the same chart, Figure 3.18, it is obvious that the uptake by the MIP system is far more efficient. The error for the NIP system ranged from 0.05 – 1.16 %. The error for the MIP system ranged from 0.12 - 4.96 %.

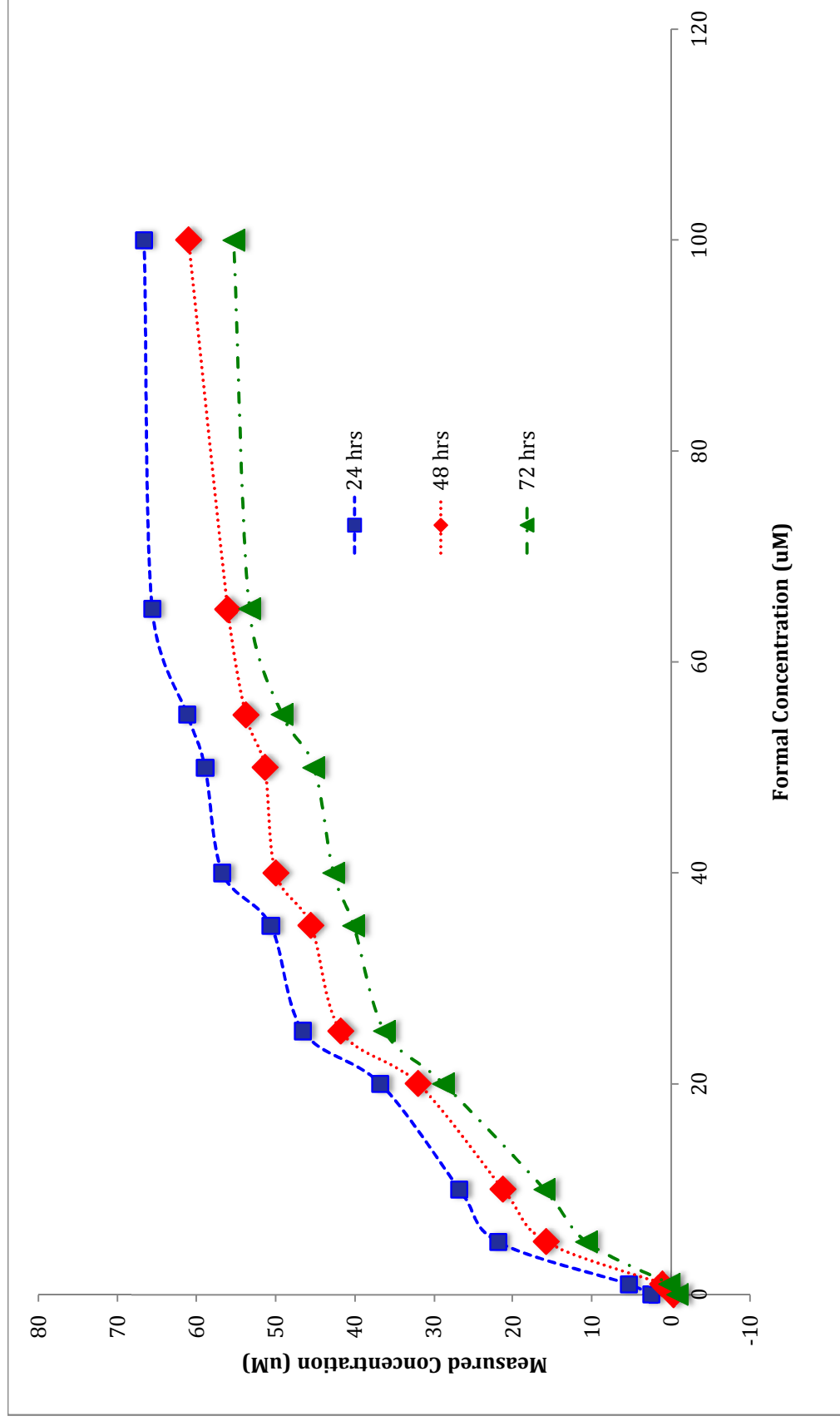


**Figure 3.16:** Graphical interpretation of propranolol preferential uptake by NIP system every 24 hours for a total of 72 hours.

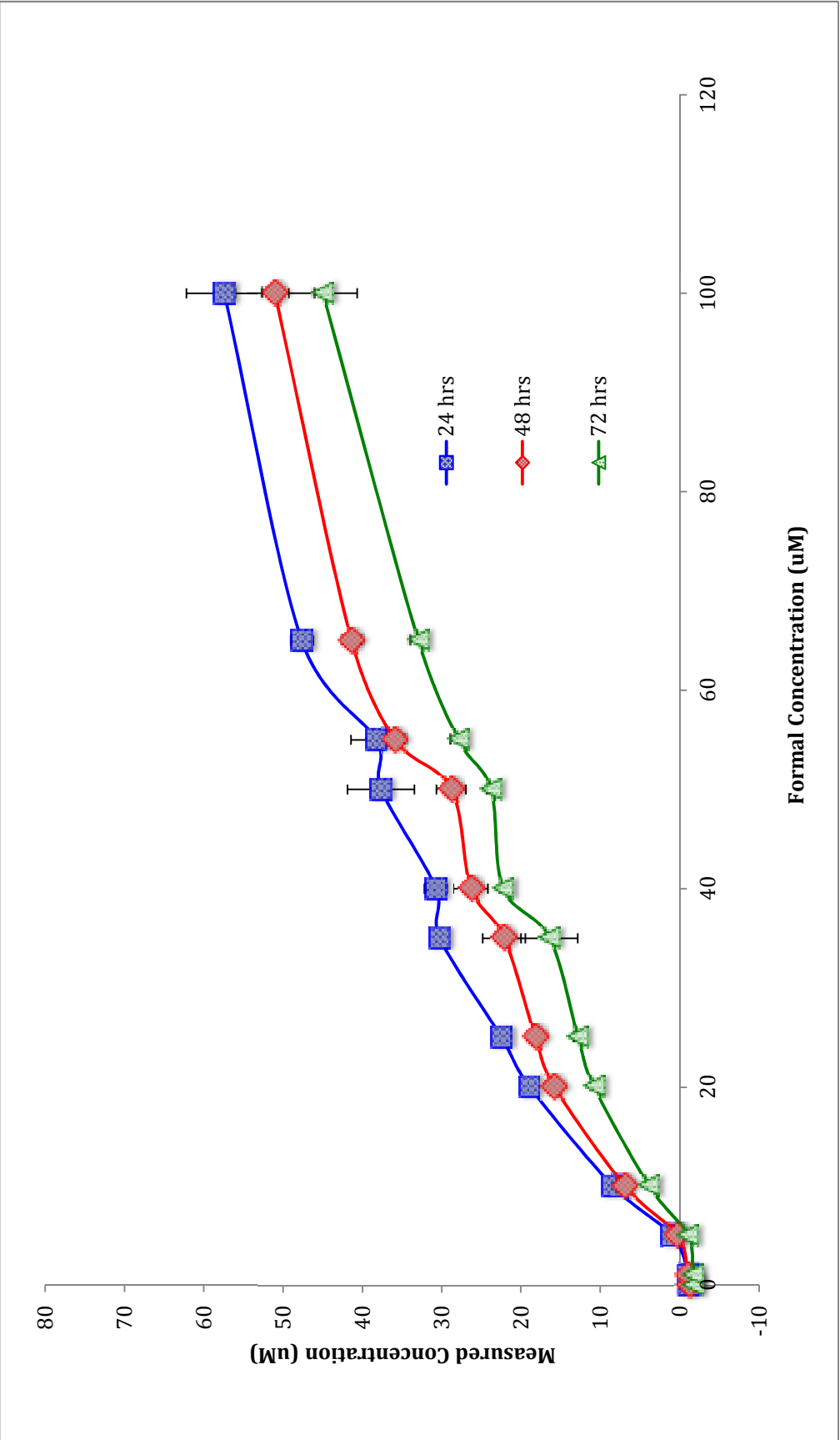


**Figure 3.17:** Graphical interpretation of propranolol preferential uptake by ProMIP system every 24 hours for a total of 72 hours.



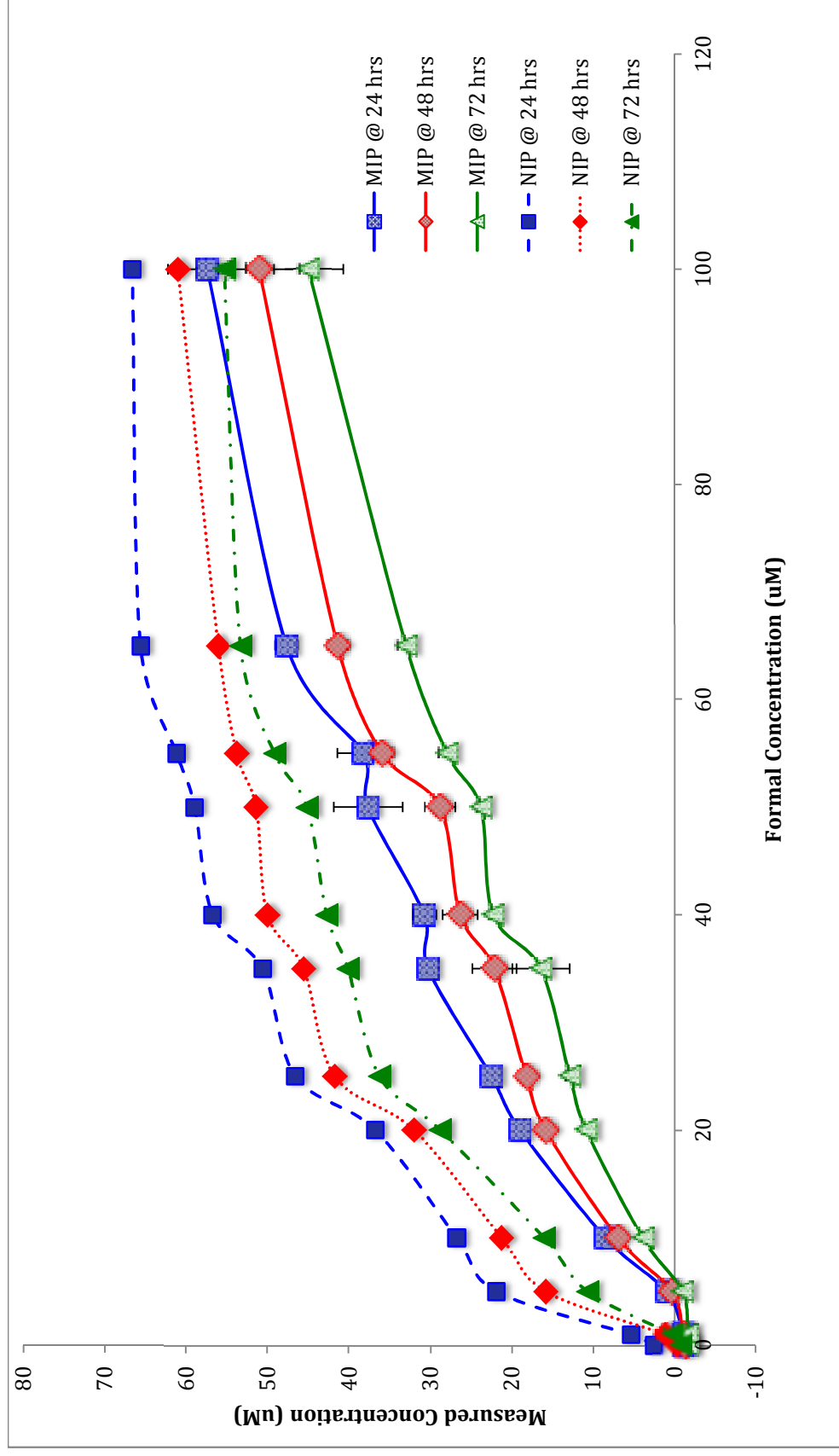


**Figure 3.18:** Graphical comparison of preferential uptake by NIP and ProMIP hydrogel systems every 24 hours for a total of 72 hours.

### 3.3.2. *Structure Variation*

The studies that compare the uptake by the hydrogel (HF) and the powder form (PF) of the system for the NIP network, Figure 3.19, demonstrate that the variation is insignificant. This is also the case in the MIP network, Figure 3.20. Although it was thought that the powder form would have better uptake due to the great surface area, this proved not to be a significant factor. Subsequent uptake experiments were conducted using strictly the hydrogel form, due to the shorter sample preparation time. The error for NIP for HF ranged from 0.03 – 0.48 %, and 0.005 – 0.21 % for PF. The error for MIP for HF ranged from 0.04 – 0.99 %, and 0.007 – 0.23 %.

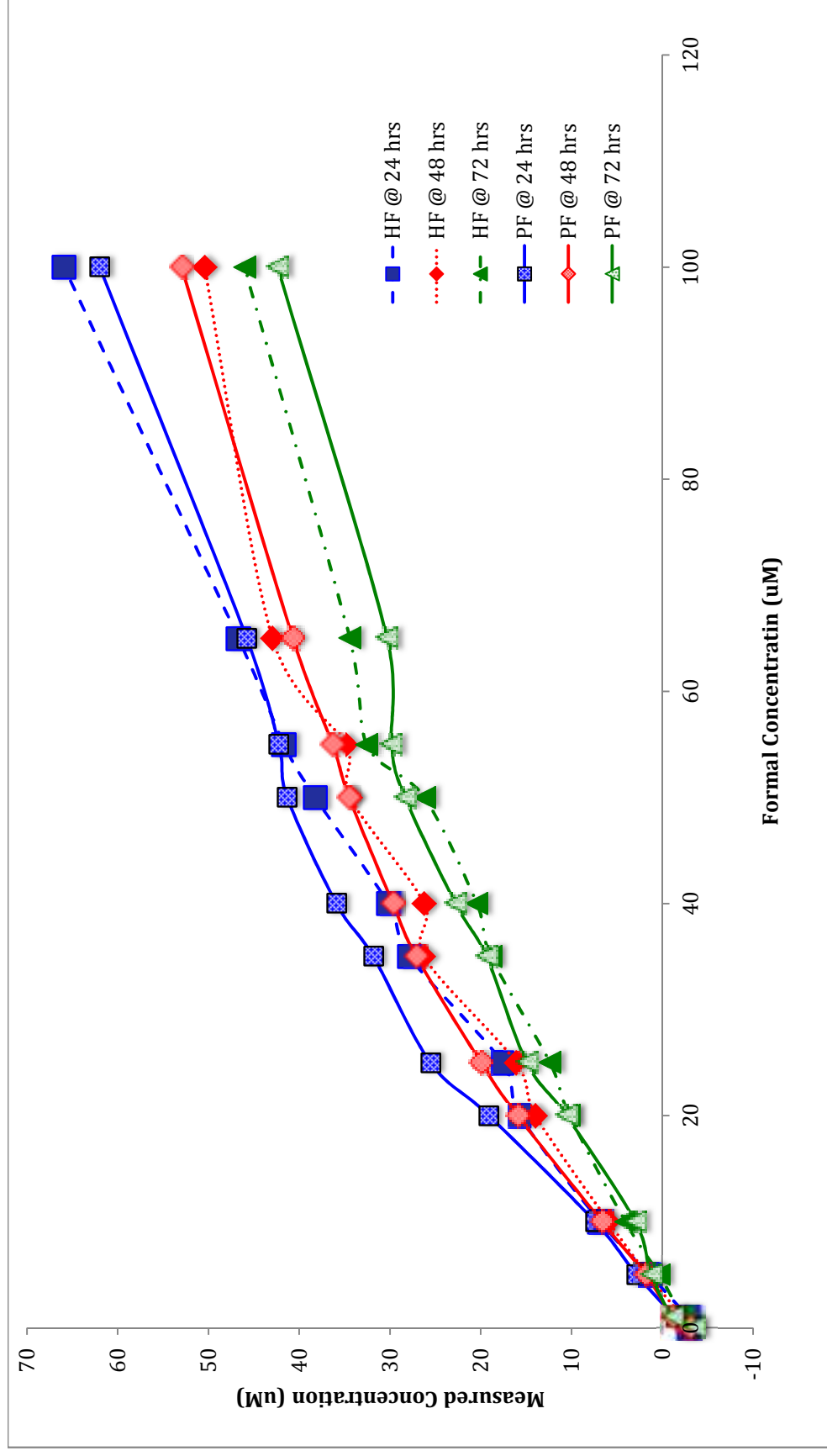


**Figure 3.19:** Graphical comparison of propranolol uptake by HF and PF in NIP network every 24 hours for a total of 72 hours.

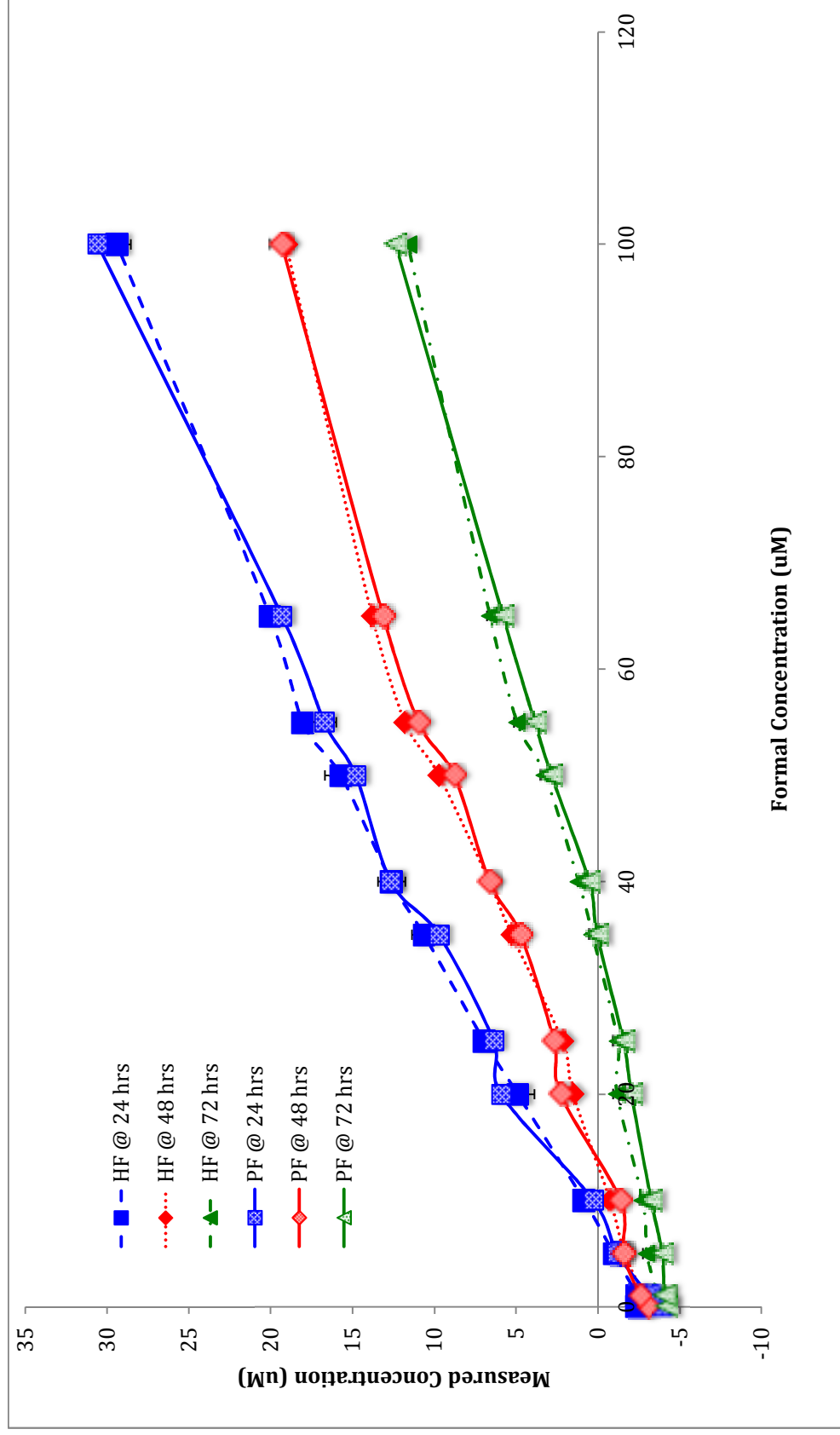


**Figure 3.20:** Graphical comparison of propranolol uptake by HF and PF in ProMIP network every 24 hours for a total of 72 hours.

### *3.3.3. Effects of Centrifugation on Uptake*

The effects of centrifuging samples are described in Figures 3.21 and 3.22. While the MIP sample seems relatively unaffected, the centrifuged (Cent) NIP sample indicates a significantly higher uptake than its non-centrifuged (NCent) counterpart. Thus, due to the observed variation, all samples were centrifuged. The NIP systems error ranged from 0.07 – 2.72 % for the Cent sample, and 0.13 – 2.99 % for the NCent sample. In the MIP system the error ranged from 0.04 – 2.29 % for the Cent sample, and 0.10 – 1.35 % for the NCent sample.

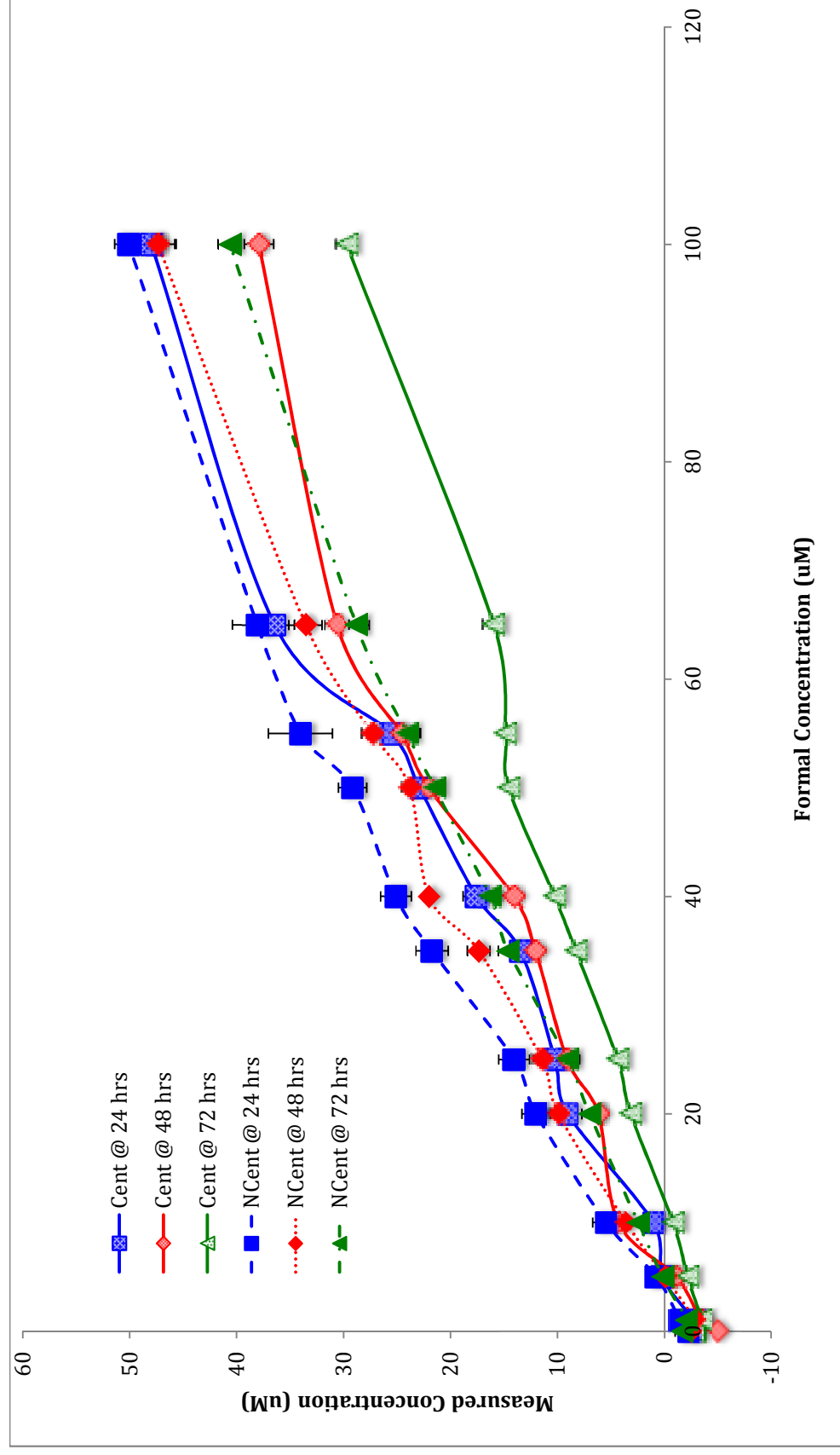


**Figure 3.21:** Graphical interpretation of centrifugation effects on NIP hydrogel networks for every 24 hours for a total of 72 hours.

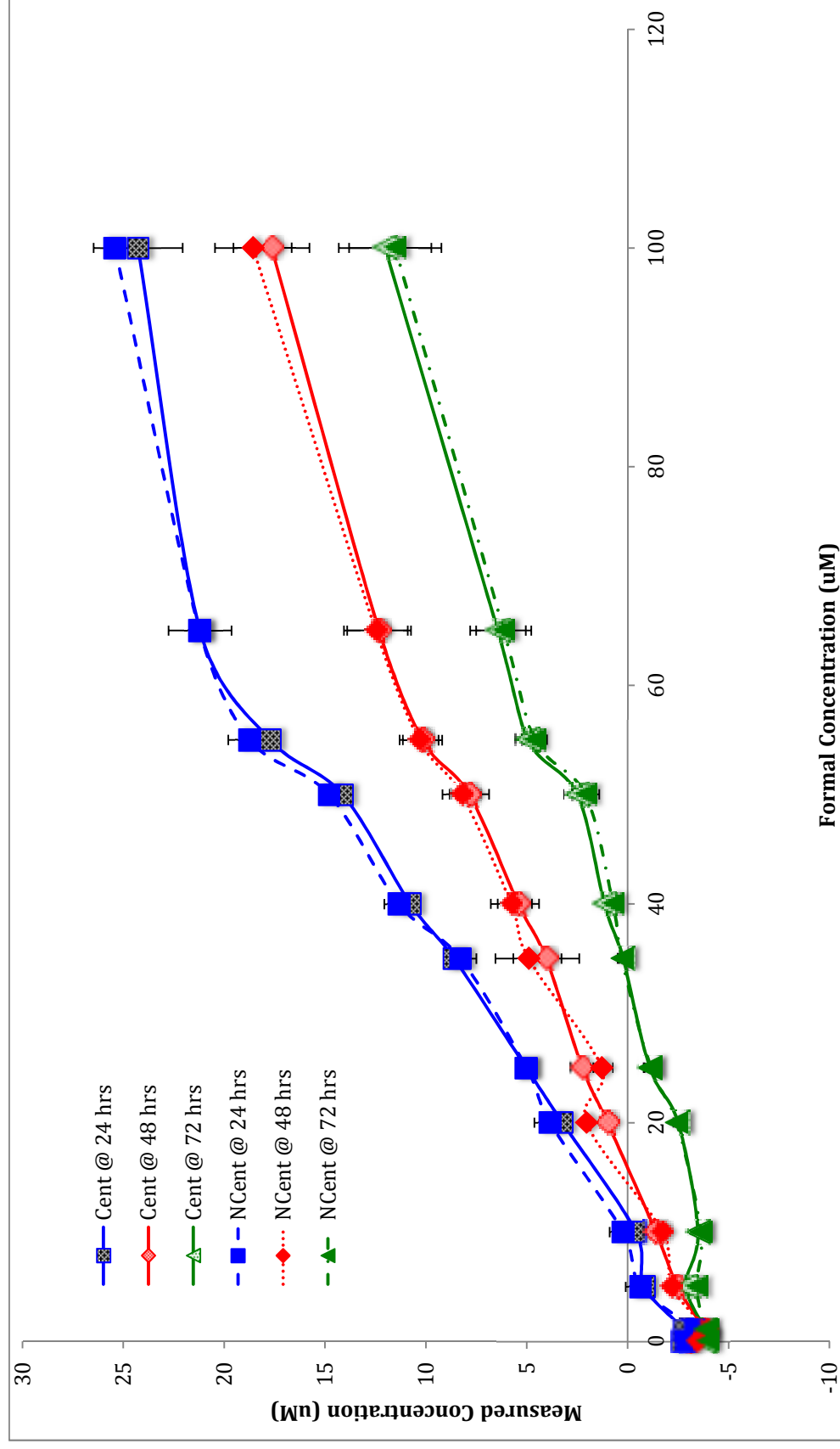


**Figure 3.22:** Graphical interpretation of centrifugation effects on ProMIP hydrogel networks for every 24 hours for a total of 72 hours.

#### 3.3.4. *Maximum Adsorption*

Uptake studies were carried out at different exposure times between 24 hours and 168 hours. The experiments conducted to determine the adsorption maxima demonstrated that in both the NIP and MIP systems saturation of adsorption required about 7 days (168 hours) exposure. The curves for 144 hours and 168 hours for both NIP and MIP, Figure 3.23 and 3.24, are overlapping each other for the most part. Therefore all subsequent uptake experiments were conducted for a period of seven days to allow for the polymer networks to reach the maximum adsorption potentials. The error ranges from 0 % - 1.2 %, and 0.1 % - 4.9 %, for the NIP and MIP system respectively.



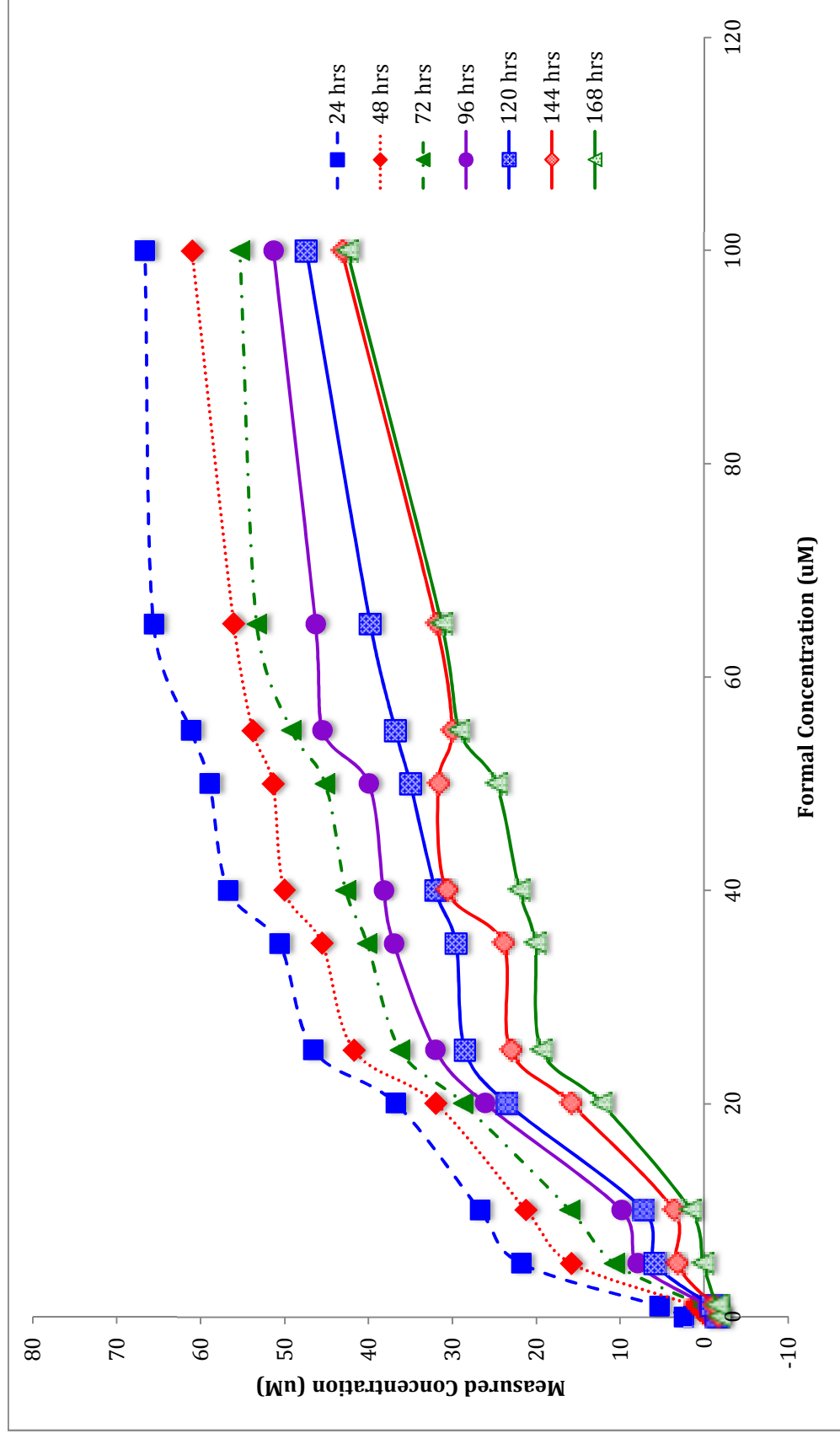


**Figure 3.23:** Plot of propranolol uptake every 24 hours for a maximum of 168 hours in NIP hydrogel network.

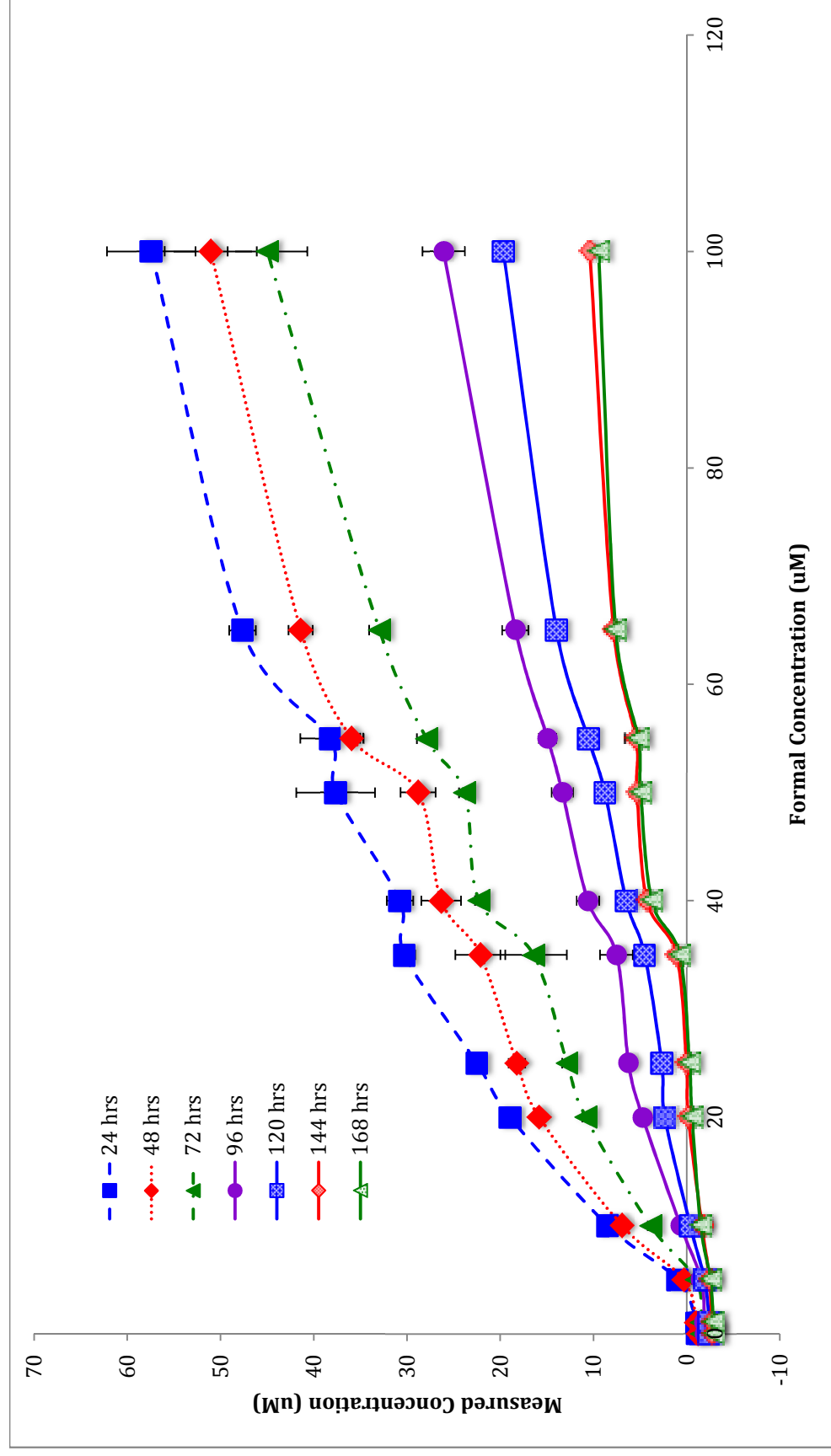


**Figure 3.24:** Plot of propranolol uptake every 24 hours for a maximum of 168 hours in ProMIP hydrogel network.

### 3.3.5. Higher Concentrations

The six additional solutions that were added to the dilution series to observe the influence of higher concentrations on uptake, those above 100  $\mu\text{M}$ , (125, 150, 175, 200, 225, 250  $\mu\text{M}$ ), are displayed in Figures 3.25 and 3.26. The charts are an extension of the preferential uptake studies as well as the maximum adsorption experiments.

The NIP data, illustrated in Figure 3.25, demonstrate that uptake is taking place. The higher concentrations are difficult to decipher as up until 120 hours (day 5), the concentration in the external environment is off-scale and therefore inferring data accurately is challenging. However, the drop in the concentration at 144 hours for 250  $\mu\text{M}$ , indicates that uptake by the system is occurring, and essentially reaches a maximum between 24 -144 hours as there is little change (as seen in previous samples) between 144 and 168 hours. Figure 3.27 illustrates the rate of uptake of NIP at 225  $\mu\text{M}$  over 168 hours in reference to its ProMIP counterpart. From the comparison, it is evident that the rate of uptake for the ProMIP system is significantly greater than the NIP network. The error observed in the uptake of the NIP samples was very low. The error bars are present on the chart, although not obvious, range from 0% to 1.2%.

The uptake observed in Figure 3.26 for MIP system indicates that there is significant uptake between 72 and 96 hours, and again, as in the NIP system, this reaches a plateau by 144 hours as the uptake seen in the subsequent 24 hours is not significantly different. A comparison of the uptake at 144 hours between the NIP

and MIP networks shows the uptake in the MIP system is significantly higher, almost by  $30\mu\text{M}$ . The error in the uptake of the MIP system is much higher and ranges from 0.1% to 4.9%.

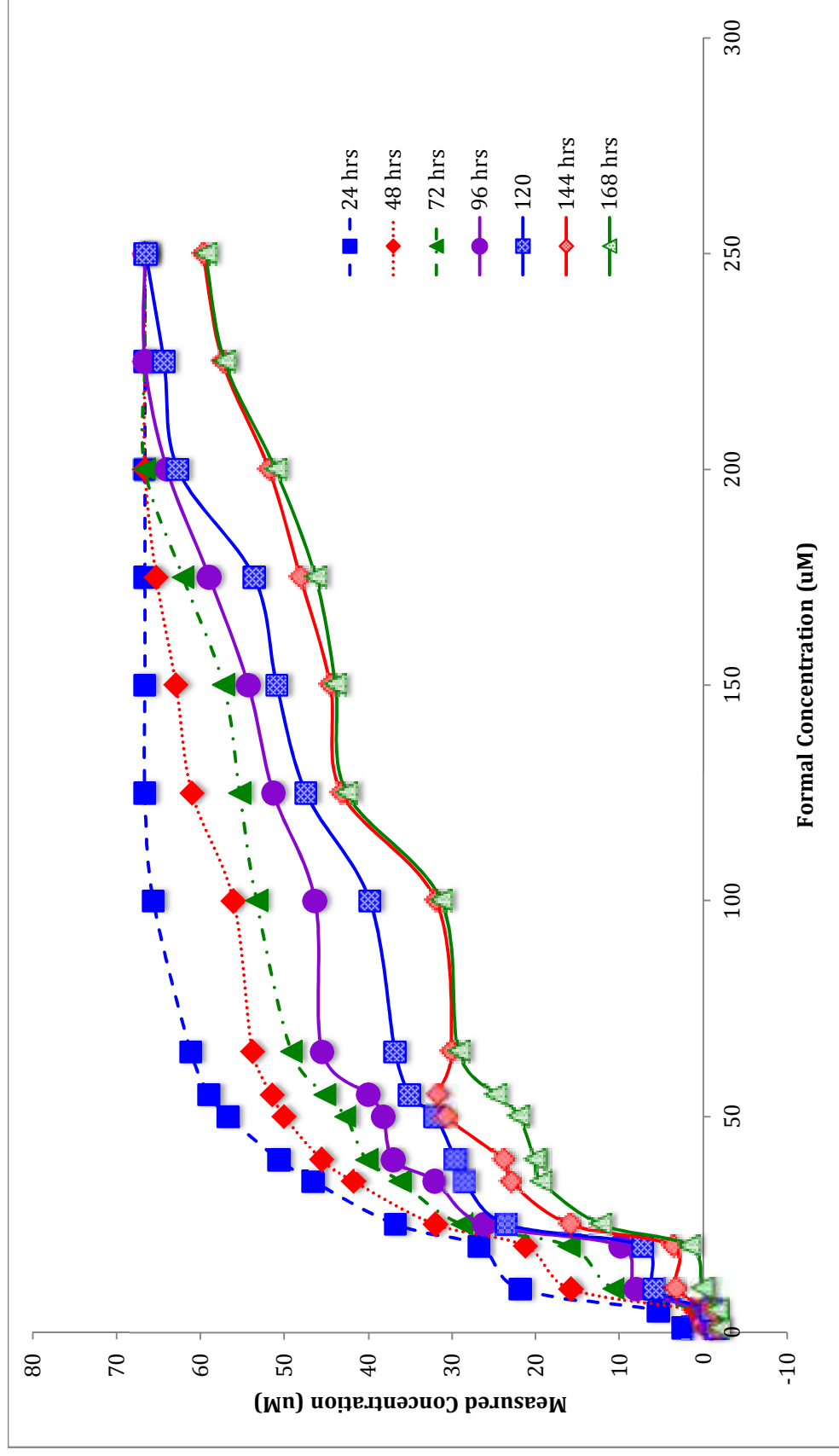


**Figure 3.25:** Graphical representation of behaviour for NIP network at high concentrations (above 100  $\mu\text{M}$ ) every 24 hours for 168 hours.

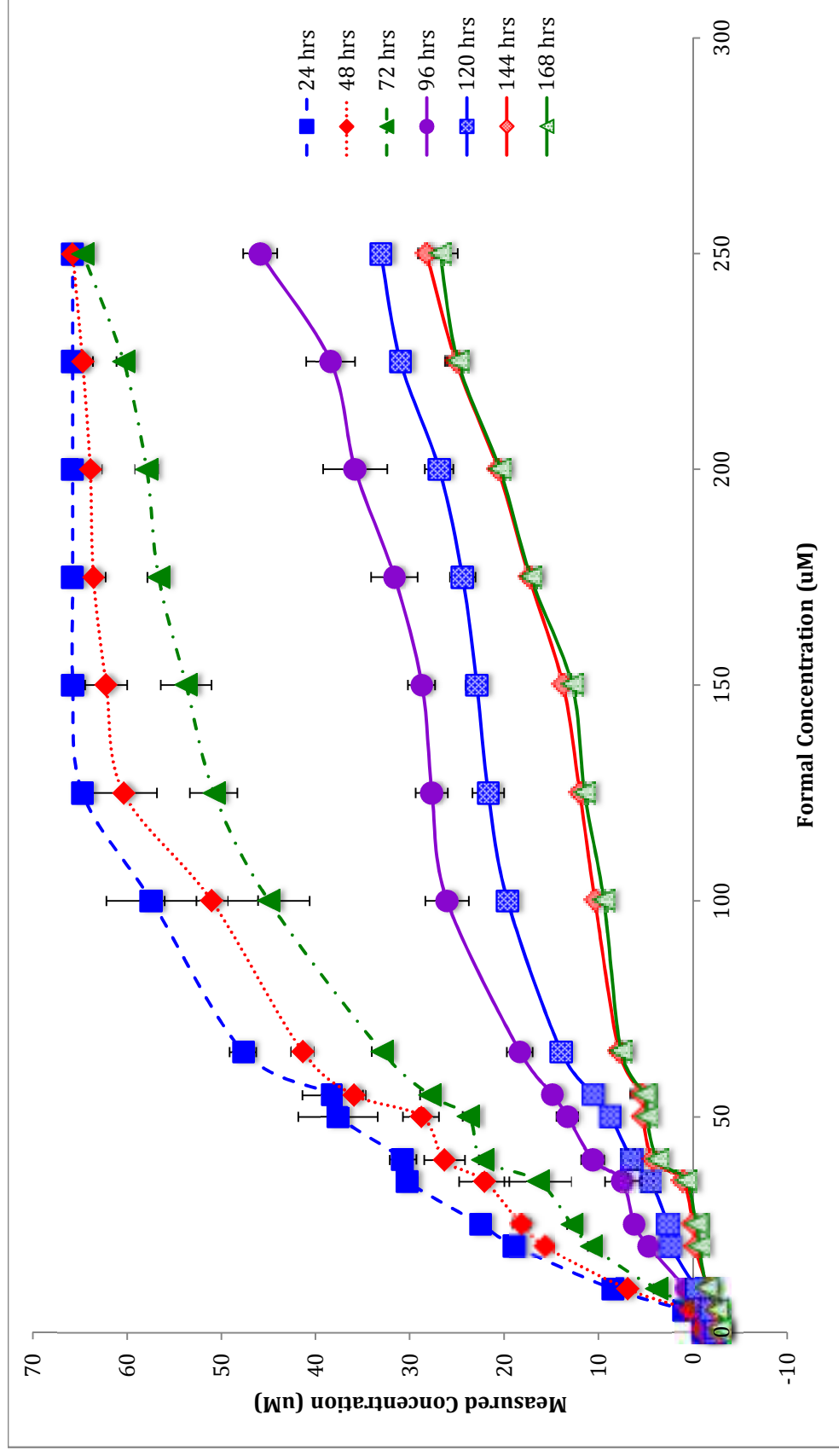


**Figure 3.26:** Graphical representation of behaviour for ProMIP network at high concentrations (above 100  $\mu\text{M}$ ) every 24 hours for 168 hours.

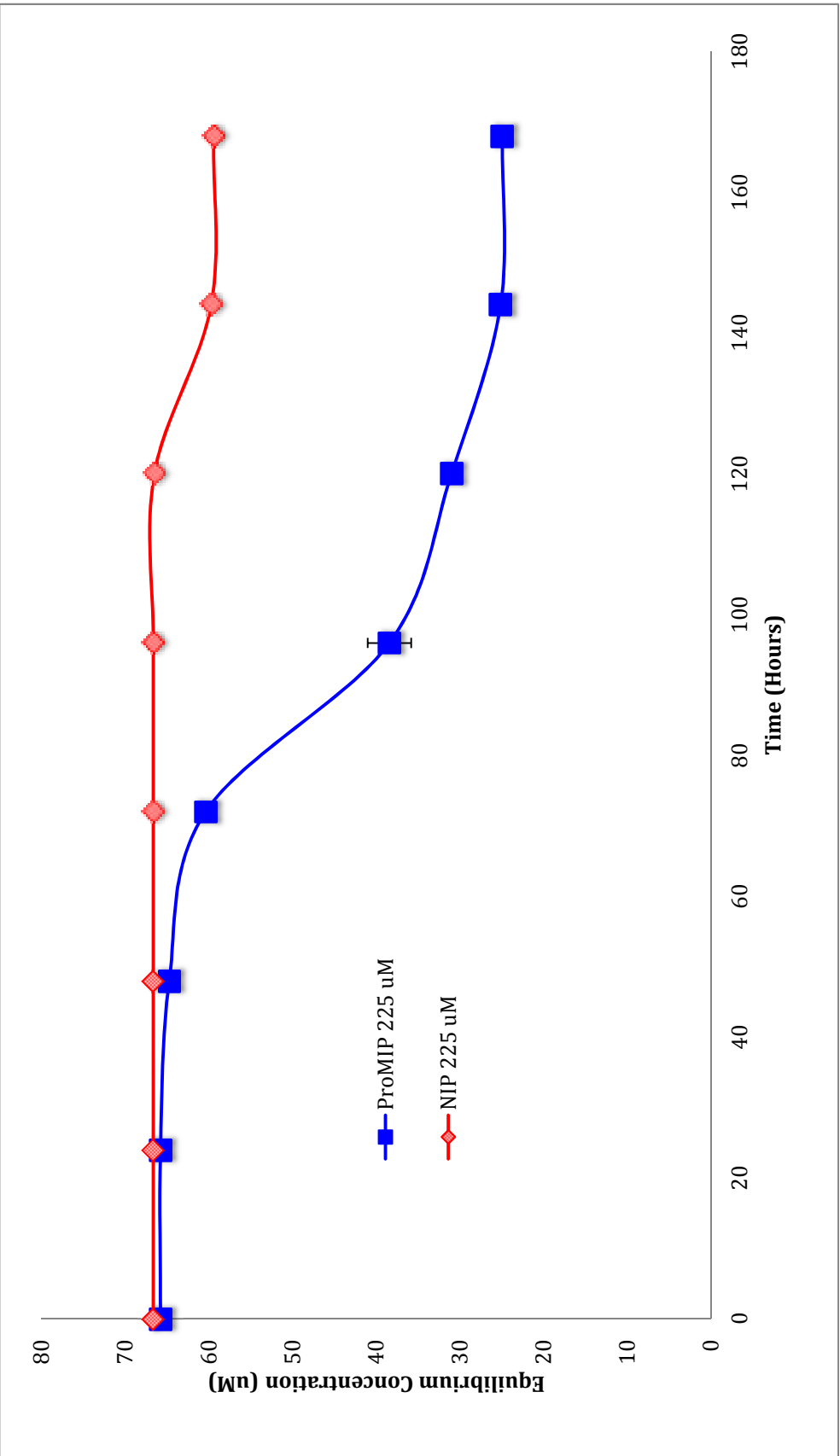


**Figure 3.27:** A comparison of propranolol uptake between the NIP and ProMIP systems in 225  $\mu\text{M}$  propranolol solution as a function of time for every 24 hours for a total of 168 hours.

### 3.3.6. Cavities as Limiting Factor

In this experiment the intention was to alter the amount of MIP and therefore the number of available binding sites. The results were difficult to interpret. In Figure 3.28, the experiment using an analytical concentration of 10  $\mu\text{M}$  propranolol is shown. In the data series of 15 mg of polymer and higher the observed concentration of propranolol greatly exceed 10  $\mu\text{M}$ . Since the concentration of propranolol is constant and controlled, the observed fluorescence should not exceed that for the known analytical concentration. Similar phenomena are also observed in the 25  $\mu\text{M}$ , and 50  $\mu\text{M}$  propranolol solutions in Figure 3.29 and Figure 3.30 respectively. The general trend of the three concentrations is similar and the observed error ranges are 0.08 – 0.79 %, 0.15 – 0.75 %, and 0.45 – 1.70 %, for 10 $\mu\text{M}$ , 25  $\mu\text{M}$ , and 50  $\mu\text{M}$ , respectively. In general the uptake is considerably faster in the samples that have a higher quantity of polymer. However, the uptake between 20 mg, 25 mg, and 50 mg of polymer in all three concentrations overlaps, suggesting that the optimal quantity of polymer is 20 mg, and any quantity beyond that is excessive and renders the same results.



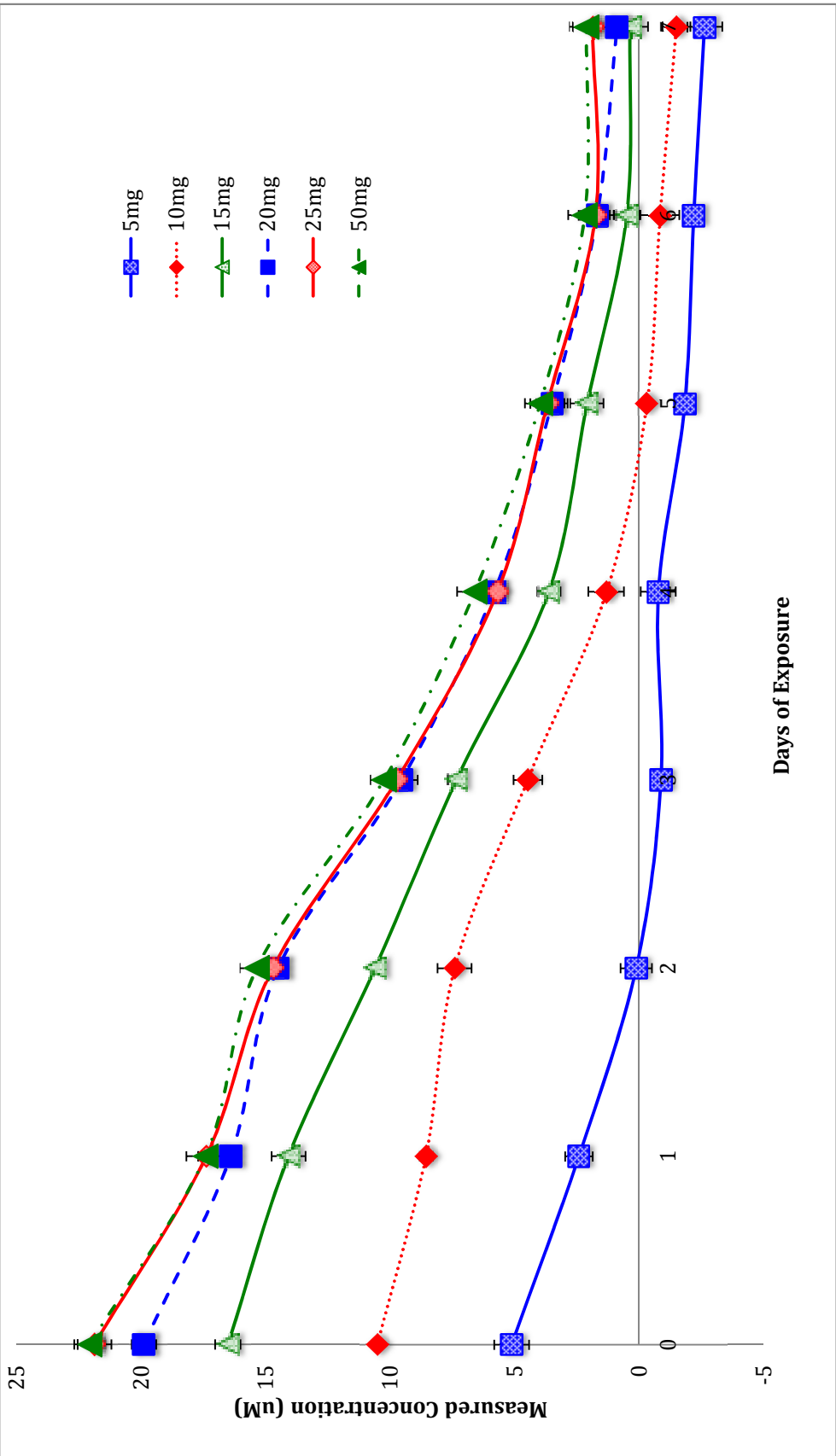


**Figure 3.28:** Graphical uptake comparison of 10 µM Propranolol by varying quantities of ProMIP every 24 hours for a total of 7 days.

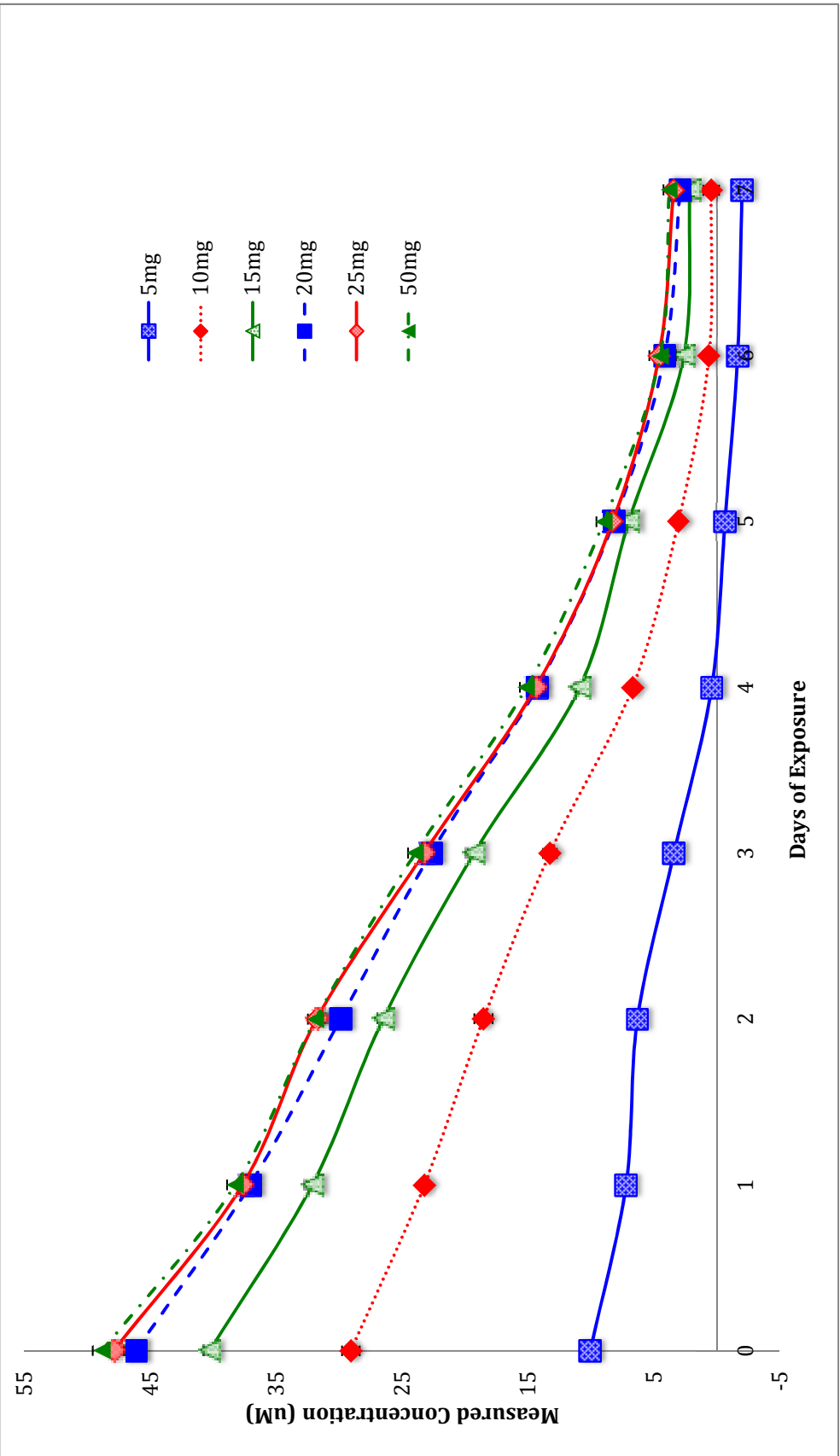


**Figure 3.29:** Graphical uptake comparison of 25 µM propranolol by varying quantities of ProMIP every 24 hours for a total of 7 days.

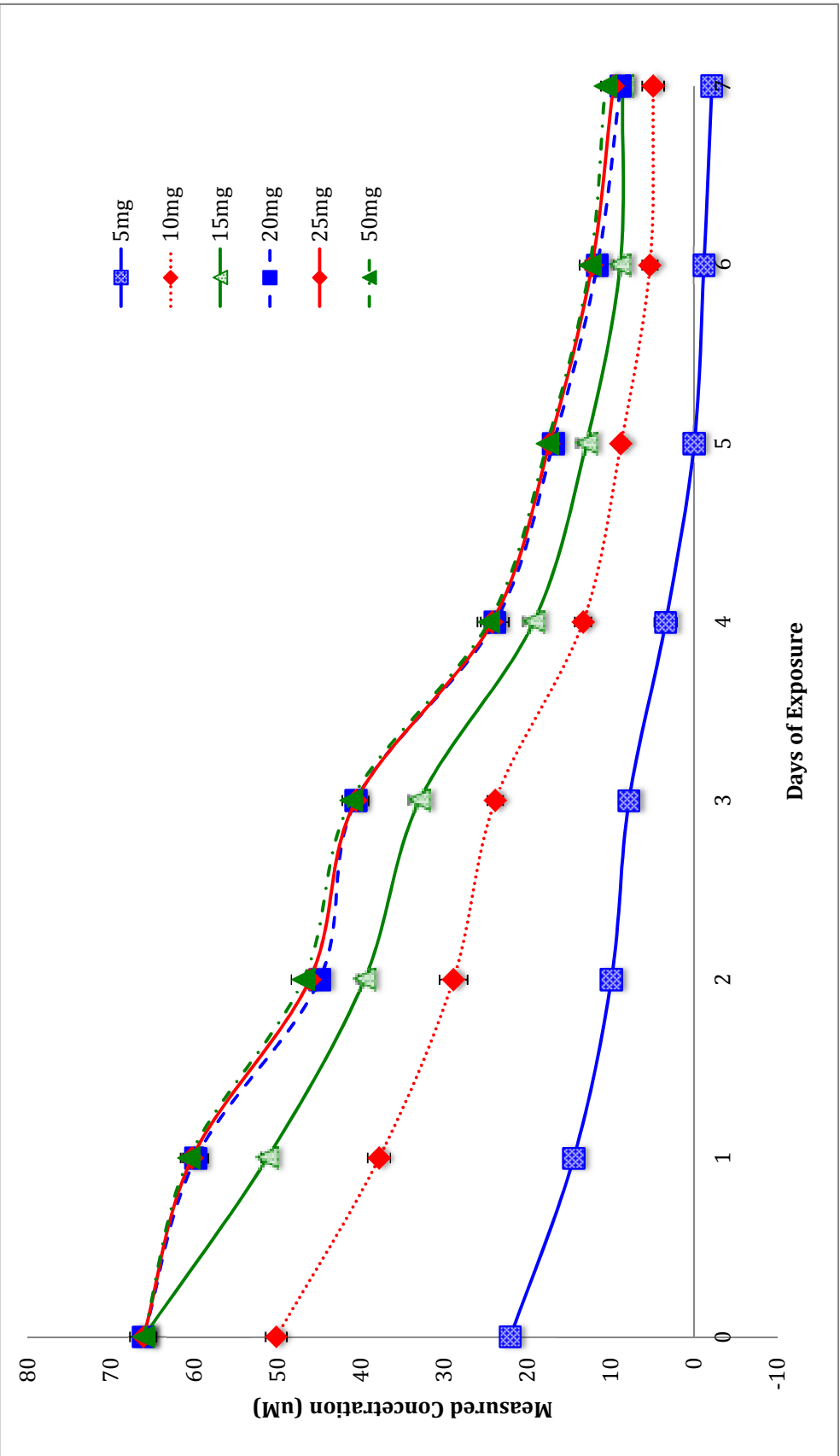


**Figure 3.30:** Graphical uptake comparison of 50  $\mu$ M propranolol by varying quantities of ProMIP every 24 hours for a total of 7 days.

### 3.4. Displacement

The results of the uptake experiments demonstrate the selectivity of the MIP for propranolol compared to the NIP. That selectivity is challenged when a second guest molecule is introduced. In the Non-Competitive Displacement (NCD) experiment, the uptake of propranolol by the MIP was indistinguishable from what was observed in the absence of a displacing agent when a Non-Complementary Structure (NCS) was used, therefore no effective displacement was observed. However, in the case of a Complementary Structures (CS), a slightly higher concentration of propranolol was observed in the external environment, i.e., there was a slight displacement effect.

#### 3.4.1. *Non-Complementary Structures*

##### 3.4.1.1. *Benzoic Acid*

When a NCS, Benzoic Acid (BA), was introduced in the NCD experiment (Figure 3.31), the binding between propranolol is strong and BA did not displace propranolol. If the propranolol molecules are effectively displaced, the concentration of propranolol observed in the external environment would be expected to increase. The addition of BA at day 7 does not cause any significant variation in observed uptake at 7 days compared to what was observed in the absence of BA. This may simply reflect that the binding between the imprints and the template propranolol are exceptionally strong, as suggested by MIP theory. However, it is also possible that the cavity sizes are large relative to the small size of BA and propranolol, and that both are accommodated in the cavity spaces. Alternatively, there may be such an excess of cavities that both propranolol and BA

can be accommodated without them interacting with each other. Error bars are present for all data points although not visible. The error ranged from 0.03 – 1.5 %.

When BA was added at the same time as propranolol (Competitive Displacement, Figure 3.32), the results indicate that BA was able to successfully displace propranolol. Although the displacement is not very large, the fact that displacement by BA was possible suggests that the number of cavity sites relative to the total added propranolol and BA is not excess. Although not visible from Figure 3.32, all data points have error bars and the error ranged from 0.09 to 0.45 % for CD on day 1, and 0.1 – 0.53 % for CD on day 7. This eliminates one of the possible explanations for the observation just noted in the previous paragraph. It also suggests that the binding of propranolol to the polymer is not controlled by as highly specific interactions as the theory of MIP would suggest. As for the possibility of large cavities which can accommodate both guests, we are unable to conclusively establish or refute this possibility.

Although the two sets of data presented here are not entirely consistent, they both suggest that the binding between propranolol and the imprinted cavities is not highly selective.

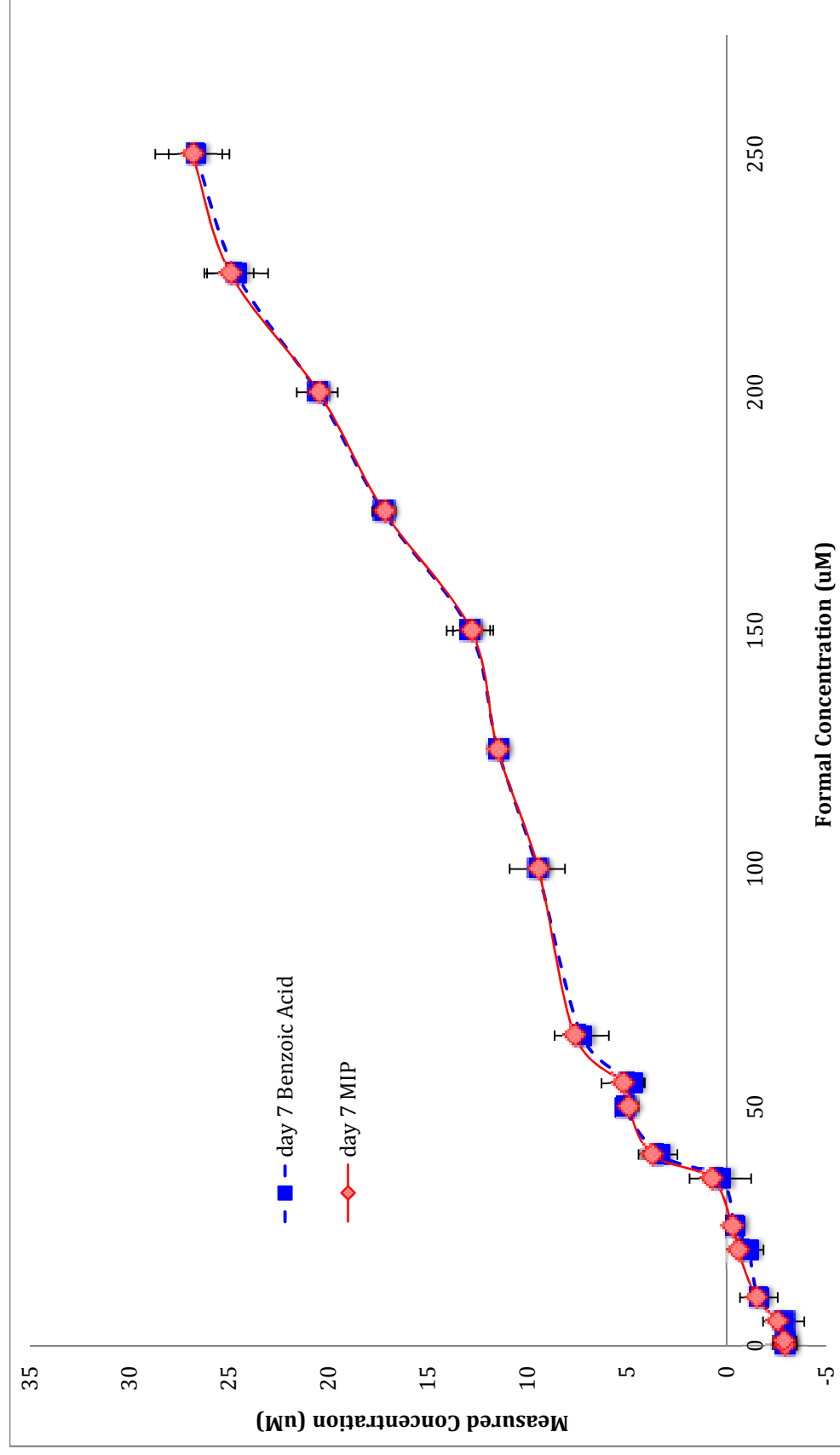


**Figure 3.31:** Non-competitive displacement of propranolol in a MIP network by a non-complementary structure, benzoic acid. BA is introduced seven days after propranolol has reached maximum adsorption.

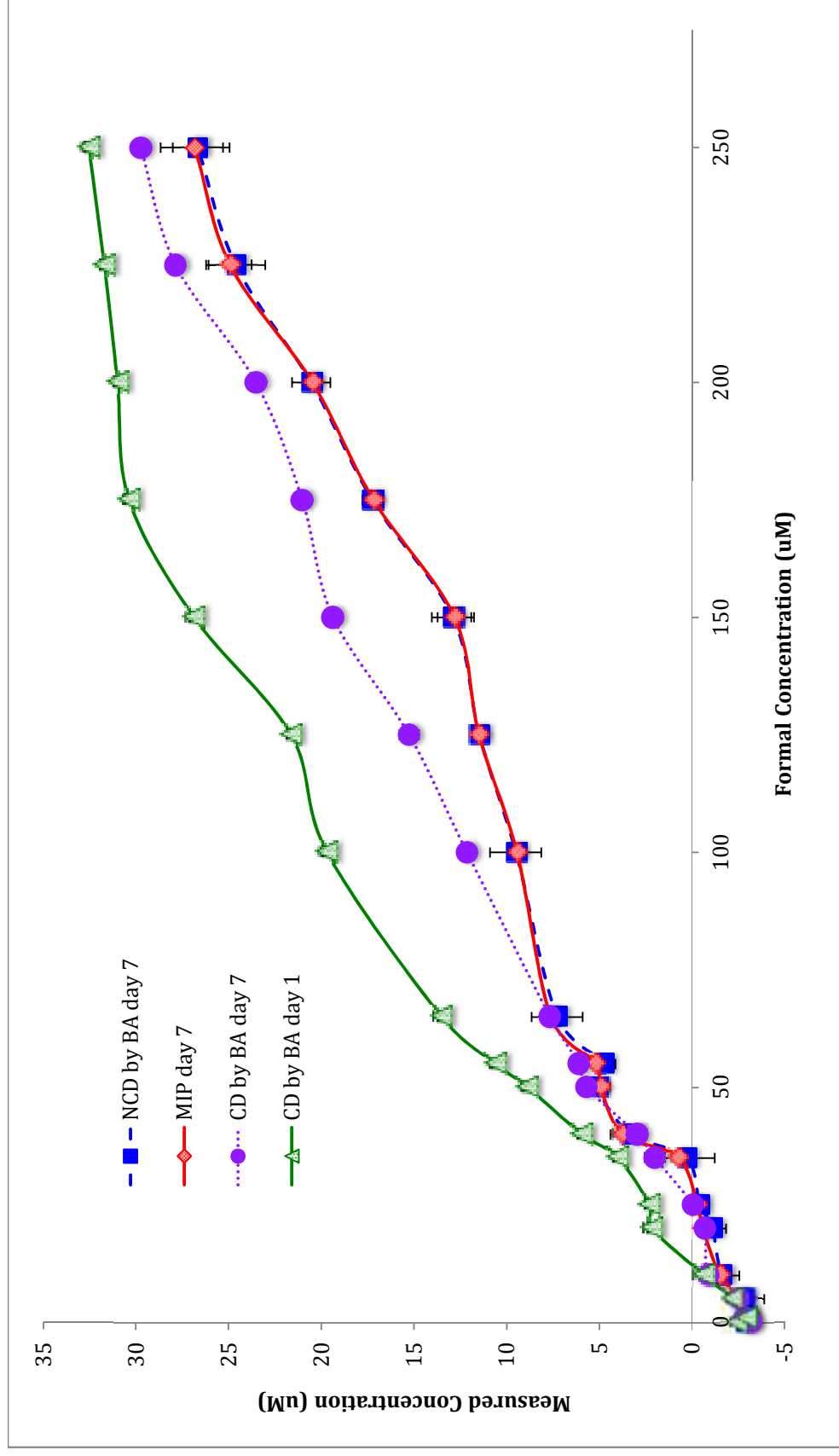


**Figure 3.32:** Competitive displacement of propranolol in a MIP network by a non-complementary structure, benzoic acid. BA is introduced to the MIP at the same time as propranolol.

#### 3.4.1.2. *Naproxen*

The NCD study with naproxen, also a non-complementary substrate, demonstrated (Figure 3.33) that it is unable to successfully displace the bound propranolol. The results for the NCD experiment were similar to the observations with BA. The error ranged from 0.10 – 0.86 %. The variation in the maximum uptake of propranolol under NCD conditions with naproxen is not distinctly different from what is observed in the absence of naproxen; this indicates that the adsorption of naproxen is relatively unchanged. If displacement occurred, the concentration of propranolol in the external environment would be higher than the concentration of propranolol observed in the absence of naproxen. This may demonstrate that the binding of propranolol is strong and therefore displacement under non-competitive conditions are challenging for the NCS. But there are other possible explanations as noted above in the BA analysis.

In CD displacement by naproxen (Figure 3.34), it is clear that the level of unbound propranolol significantly increases and the extent of displacement is higher than what was observed with BA as the displacing agent. Since naproxen is larger than BA, and is closer in size to propranolol, it is possible that when naproxen is included into the MIP cavities, there is no longer sufficient space for propranolol. The fact that the concentration of propranolol increases in the external environment is an indication that the binding of propranolol and the imprinted cavities is not highly selective. Again, this is in contrast to the typical theory of MIP. The error for CD on day 1 ranged from 0.15 – 1.5 % and on day 7 ranged from 0.18 – 1.2 %.



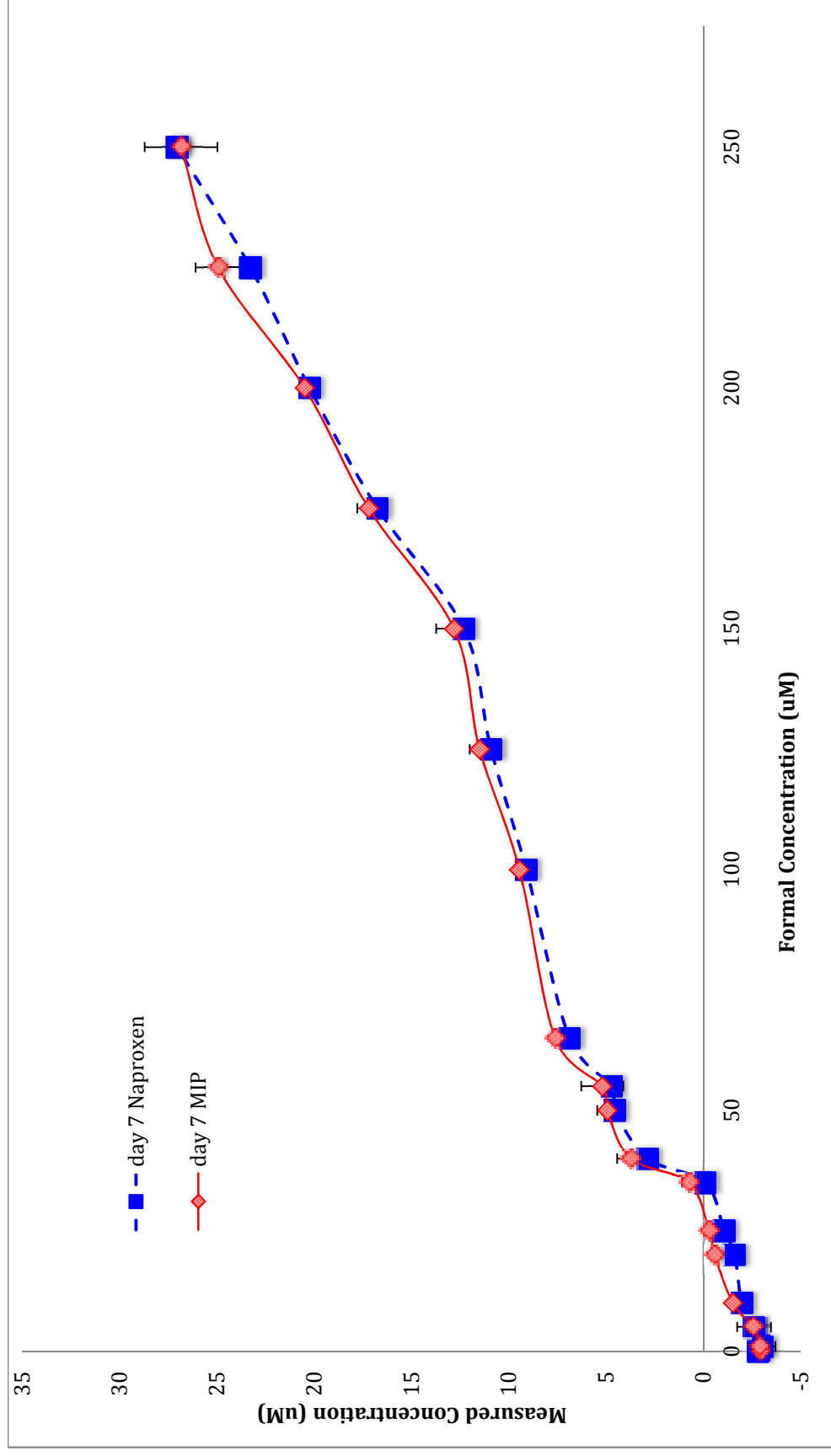


**Figure 3.33:** Non-competitive displacement of propranolol in a MIP network by a non-complementary structure, naproxen. Naproxen is introduced seven days after propranolol has reached maximum adsorption.

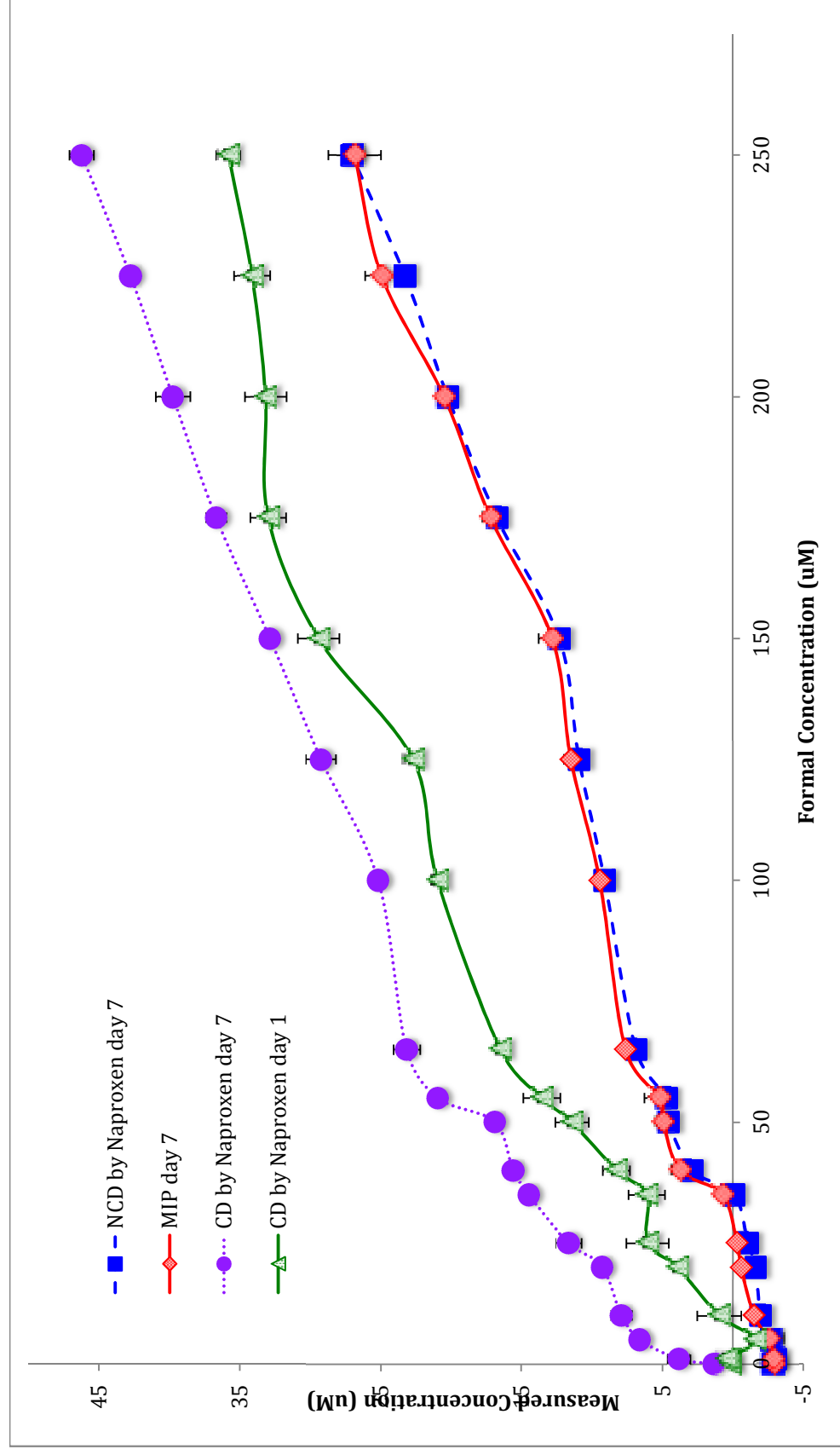


**Figure 3.34:** Competitive displacement of propranolol in a MIP network by a non-complementary structure, naproxen. Naproxen is introduced to the MIP at the same time as propranolol.

### 3.4.2. *Complementary Structures*

The behaviour observed by the system when exposed to a CS also supported the findings from the NCS that the binding of propranolol is not a highly selective process. However both of the CS, 1-naphthol and timolol, that were selected due to their availability are not ideal due to the fact that they both fluoresce in the same region as propranolol. Thus an uptake study of both the CSs had to be done and the adsorption observed in displacement studies were corrected for by the independent uptake resulting in a “corrected” value.

#### 3.4.2.1. *Timolol*

In the NCD experiment (Figure 3.35) the concentration of propranolol in the external environment was slightly lower than NCD experiments with BA and naproxen. One would expect a much higher value in the external value as unbound timolol should also be detectable. The error ranged from 0.08 – 0.75 %.

In the CD experiment (Figure 3.36) the detectable propranolol in the external environment is significantly lower than any other uptake experiment. This change can be attributed to the fact that timolol is also being included into the polymer, since it is a fluorescent molecule, the fluorescence is no longer detectable hence the decrease. The uptake of timolol independently was determined and adjusted to determine its influence on the system. The corrected displacement of propranolol readings with timolol, Figure 3.37, are quite high. The readings in Figure 3.36 are derived from Figures 3.35 and 3.36 to incorporate the corrected readings, thus Figures 3.35 and 3.36 are not corrected. The legitimacy of these results is

questionable. When the independent uptake of timolol by the system was determined, uptake by this system was not particularly strong, which resulted in high concentrations observed in the external solution. However, the results in the displacement studies (prior to correction) indicated much lower fluorescent levels of both timolol and propranolol, which suggests that both timolol and propranolol were being included into the MIP. Once the uptake information was corrected, the detectable propranolol significantly increased, suggesting that timolol was displacing propranolol effectively. While such a result seems reasonable, it has to be stressed that the correction method used here is subject to significant potential error due to the strong overlap of the propranolol and timolol fluorescence signals. Therefore, it is not possible by these means to conclusively determine the cause for the variation in results. The error for the CD for day 1 ranged from 0.10 – 0.99 %, and for day 7 ranged from 0.02 – 0.08 %.

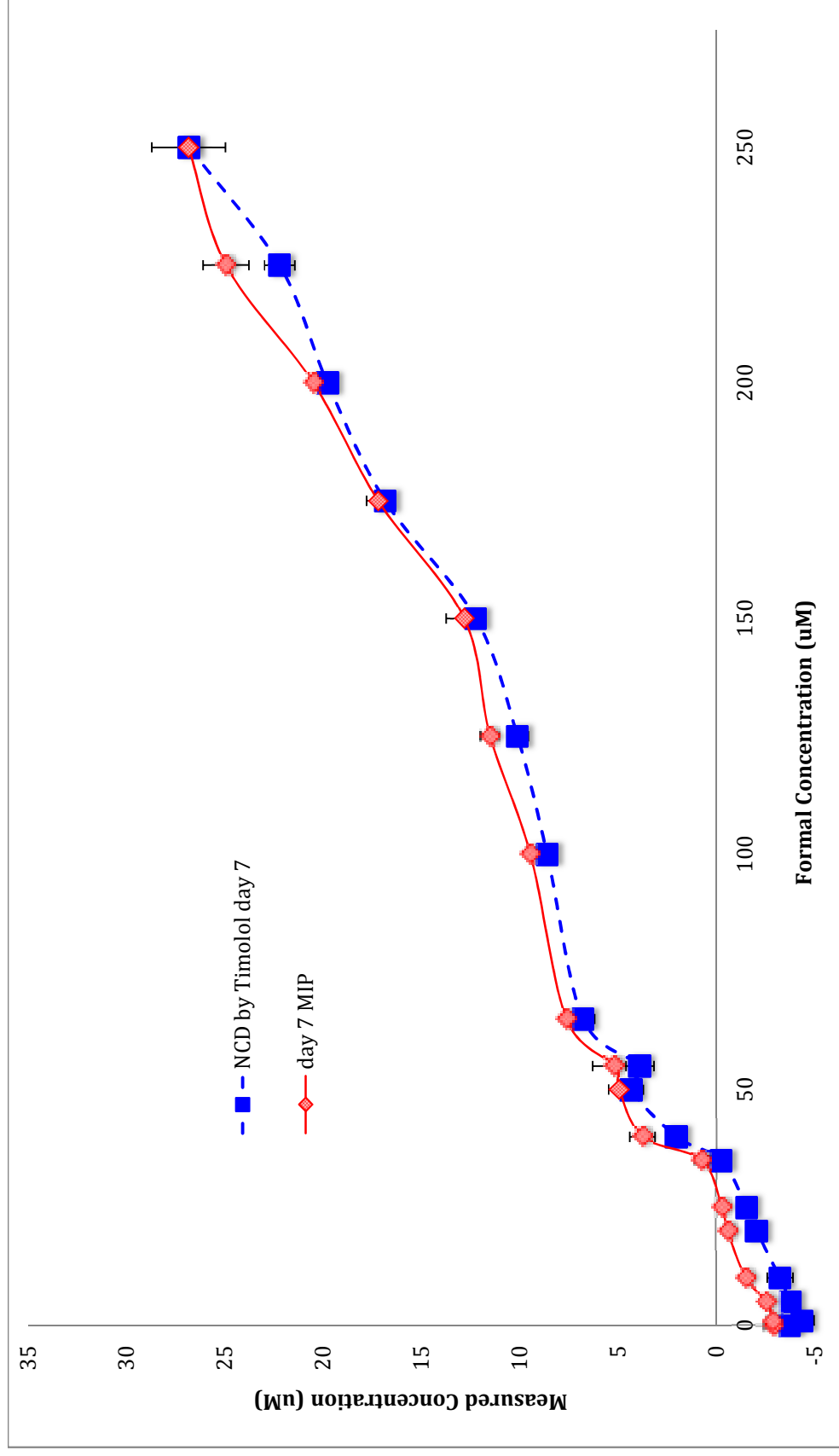


**Figure 3.35:** Non-competitive displacement of propranolol in a MIP network by a complementary structure, timolol. Timolol is introduced seven days after propranolol has reached maximum adsorption.

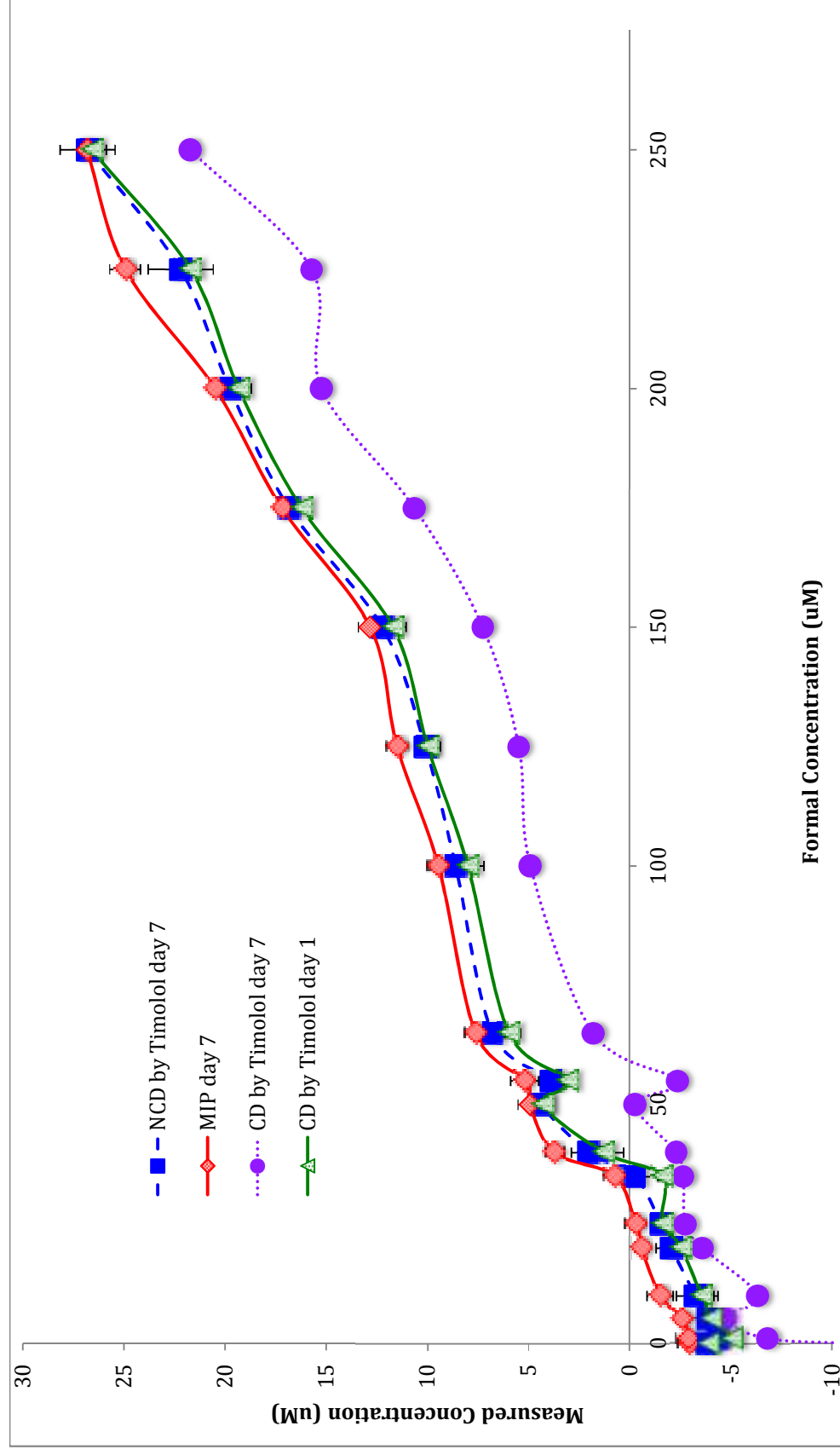


**Figure 3.36:** Competitive displacement of propranolol in a MIP network by a complementary structure, timolol. Timolol is introduced seven days after propranolol has reached maximum adsorption.

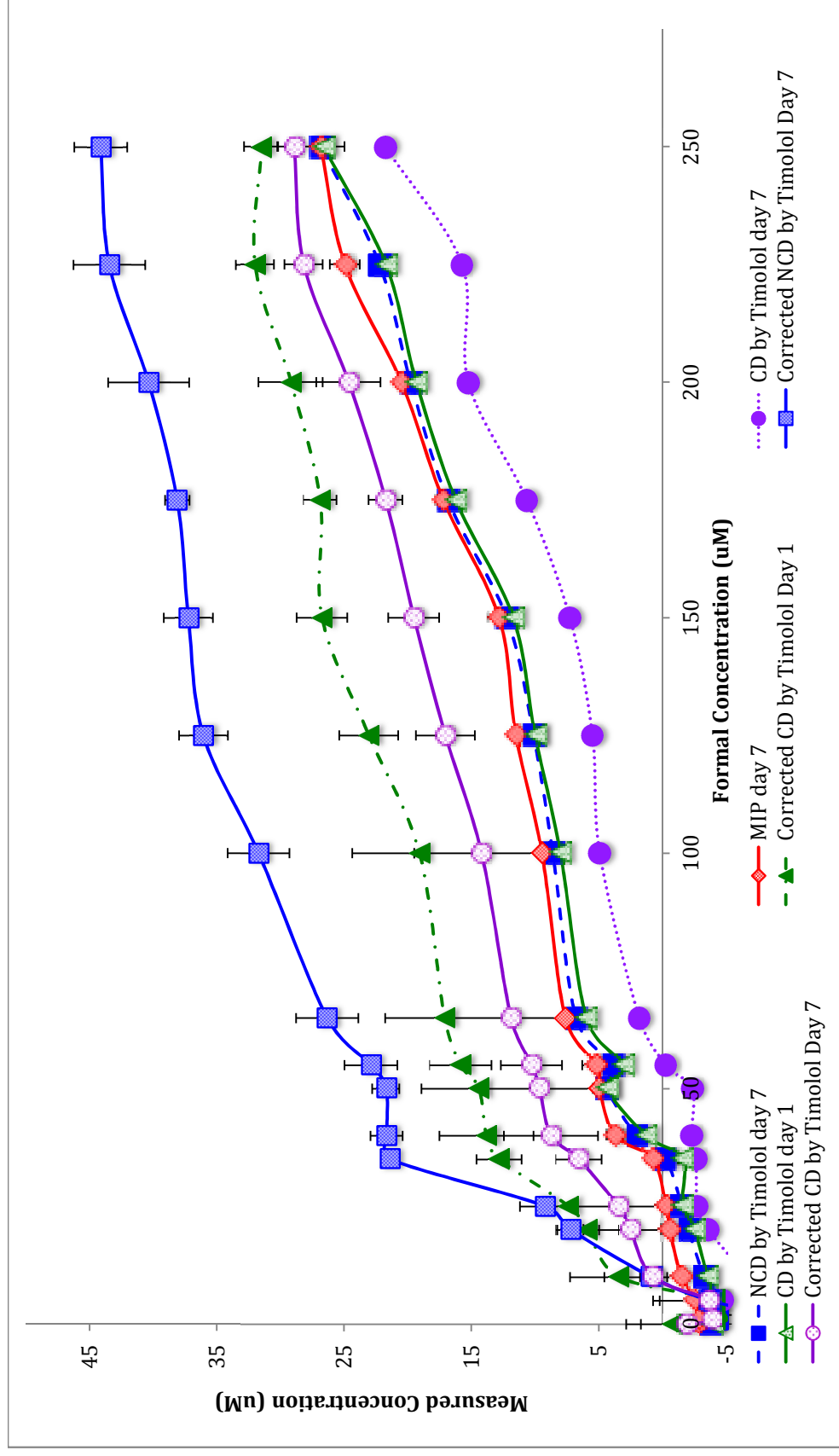


**Figure 3.37:** Corrected competitive and non-competitive displacement of propranolol in a MIP network by a complementary structure, timolol. Timolol is introduced seven days after propranolol has reached maximum adsorption.

#### 3.4.2.2. *1-Naphthol*

The behaviour observed with 1-Naphthol as a complementary displacing agent was similar to that observed with timolol. The correction method was also applied here as there is substantial overlap between the fluorescence spectra of 1-naphthol and propranolol.

In the NCD experiment, Figure 3.38 the results indicate that a higher concentration of propranolol was included into the host MIP. However, a maximum adsorption potential has already been determined and the adsorption by 1-Naphthol in the NCD experiment is higher than that potential. It is entirely possible that 1-Naphthol is contributing to an apparent “increased uptake” due to its fluorescence properties. The error ranged from 0.05 – 0.39 %.

In the CD experiment, Figure 3.39 a similar trend is observed, higher adsorption concentrations than what has been determined to be the maximum adsorption for this polymer with propranolol. Although one would expect to observe the opposite, since there are twice as many fluorescing molecules present, one would expect to see a significantly higher concentration of both molecules in the external solution. The reverse is true until the values are corrected as seen in Figure 3.40. These high concentrations in the external environment cannot be adequately explained, although it can be conclusively stated that the current methodology does not allow to effectively distinguish between displaced propranolol and 1-Naphthol, the secondary guest. The error ranged from 0.10 – 0.57 % for CD on day 1, and 0.09 – 1.29 % on day 7.



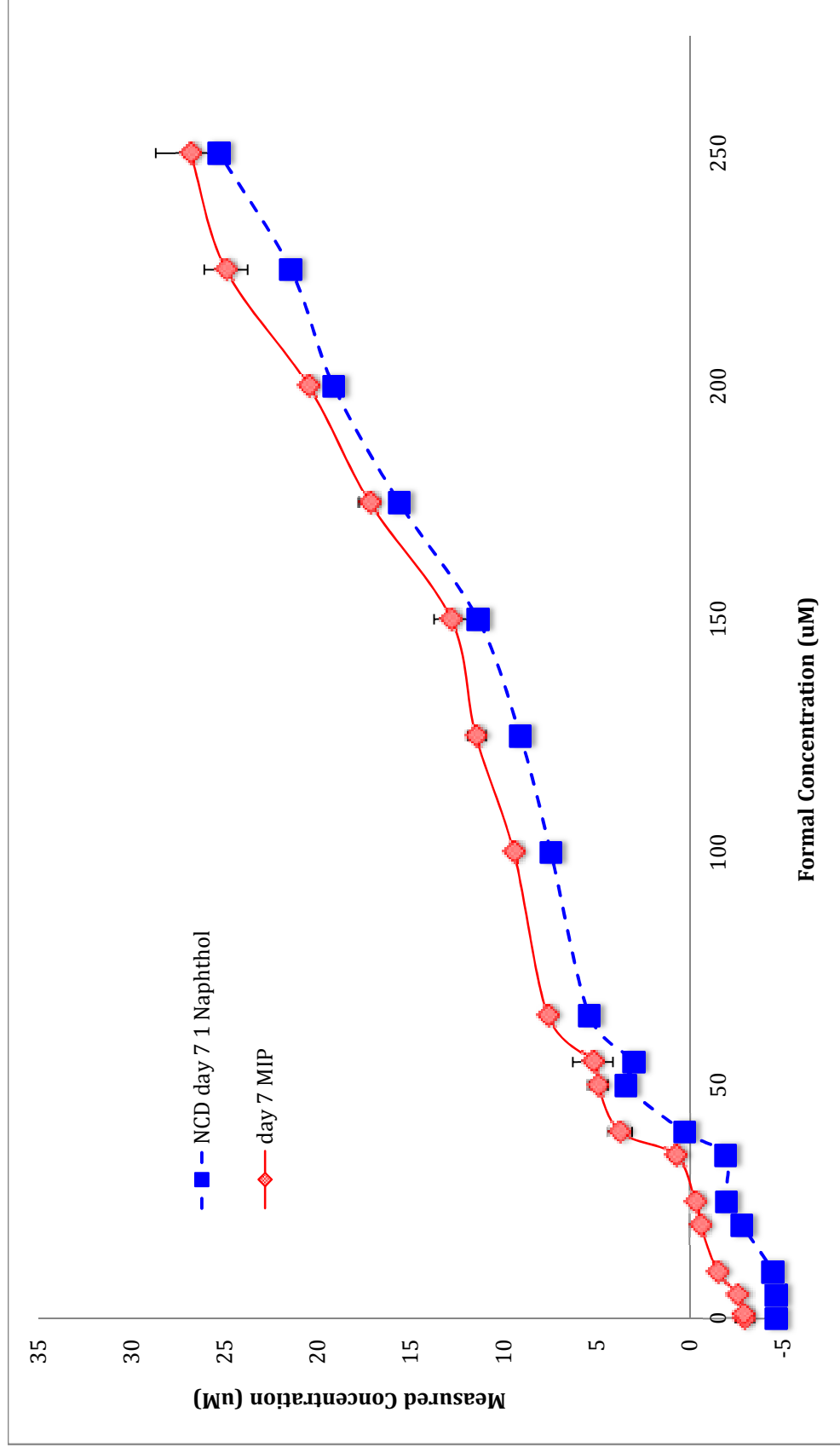


**Figure 3.38:** Non-competitive displacement of propranolol in a MIP network by a complementary structure, 1-naphthol. 1-Naphthol is introduced seven days after propranolol has reached maximum adsorption.

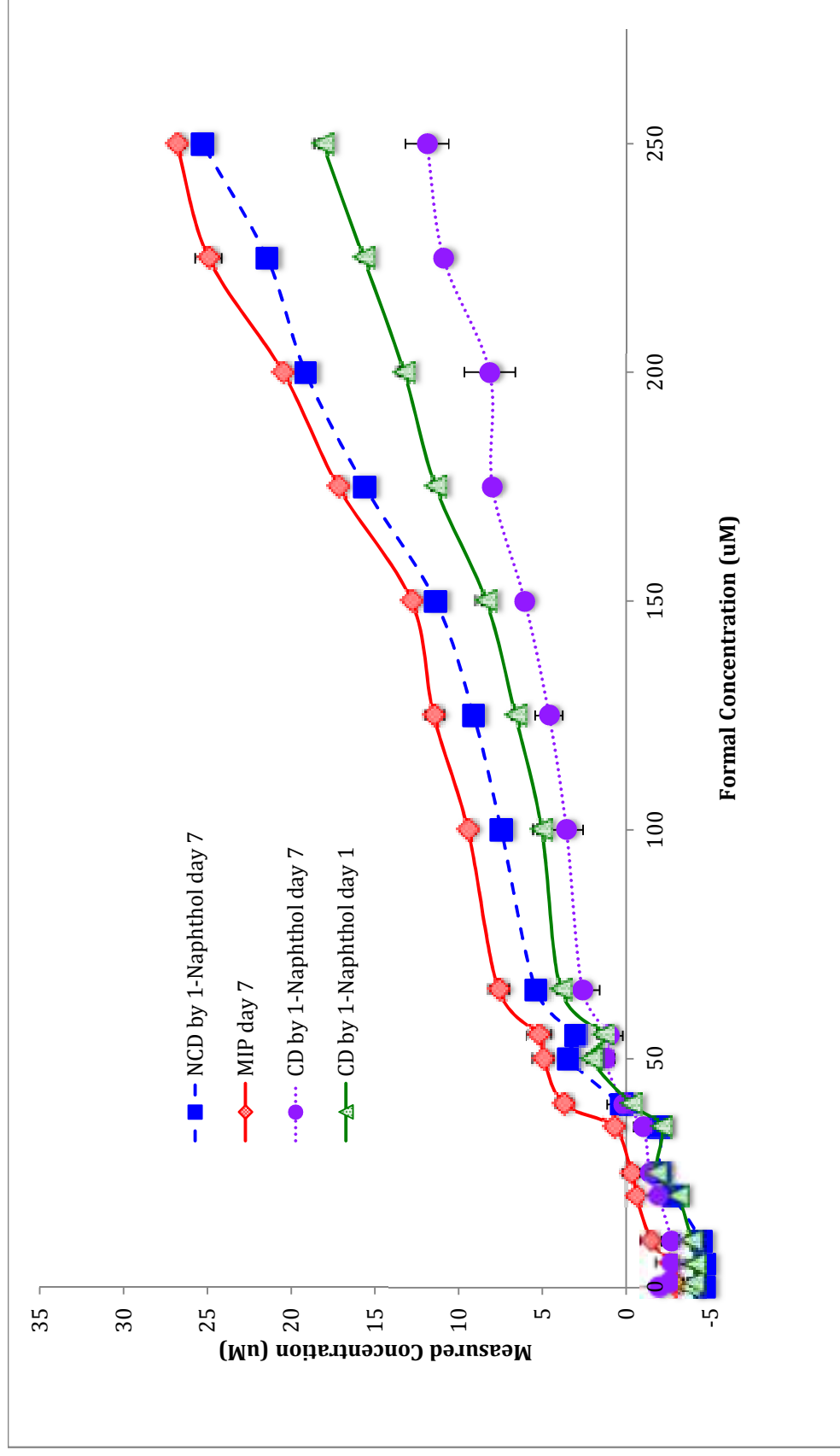


**Figure 3.39:** Competitive displacement of propranolol in a MIP network by a complementary structure, 1-naphthol. 1-Naphthol is introduced seven days after propranolol has reached maximum adsorption.

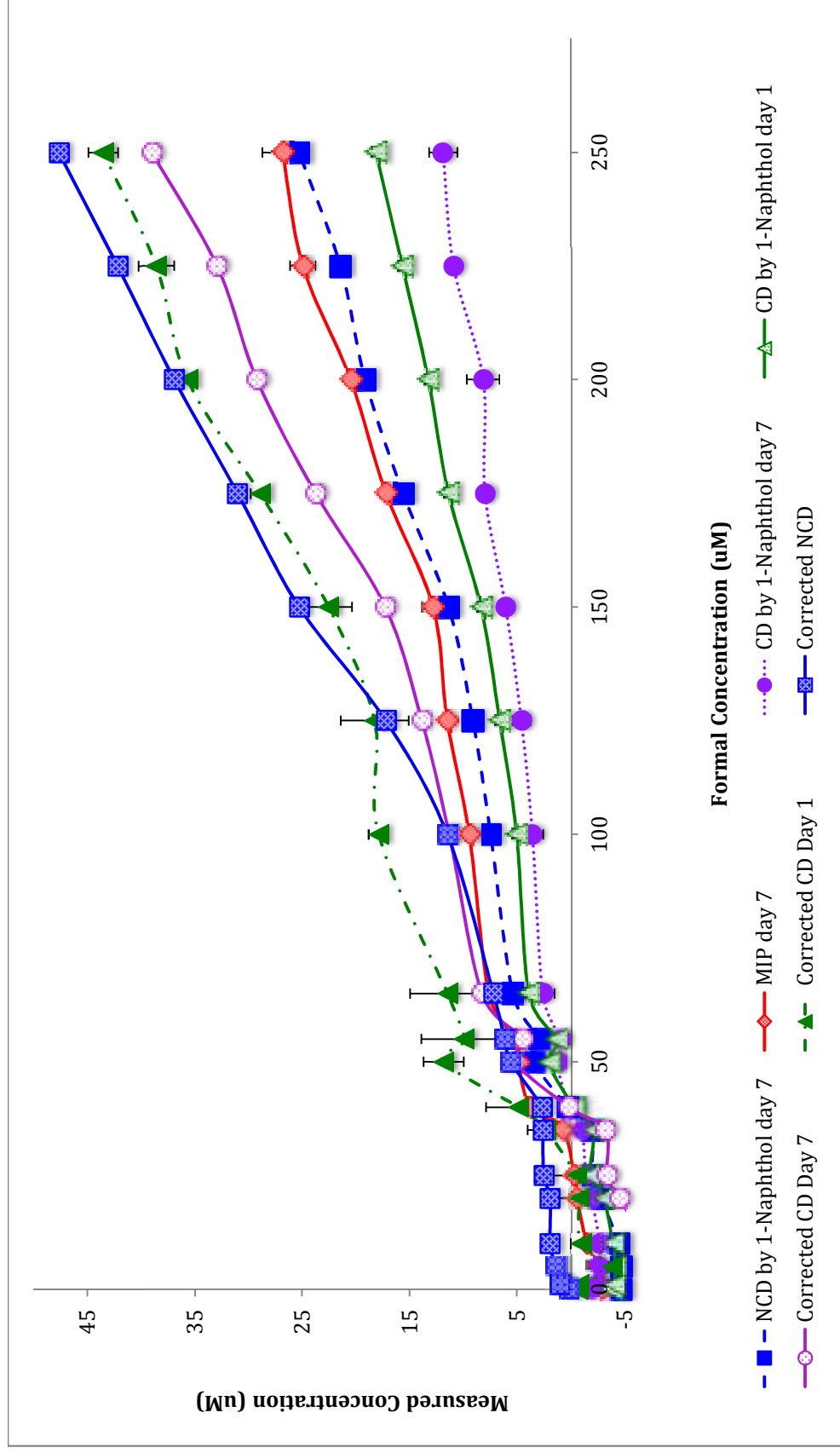


**Figure 3.40:** Corrected competitive displacement of propranolol in a MIP network by a complementary structure, 1-naphthol. 1-Naphthol is introduced seven days after propranolol has reached maximum adsorption.

### 3.5. Release Studies

The release studies demonstrated the strength of binding of propranolol to the imprinted cavities since the release of propranolol was challenging. Error bars have been indicated for each data point for all of the release studies, although may not be visible.

#### 3.5.1. *Temperature (RT, 37 degrees Celsius)*

The results for the release experiment conducted at room temperature, Figure 3.41, demonstrate no change in propranolol observed in the external solution over a three-day period. Perhaps three days is not enough time to observe release from this system. However additional time to observe release would not be representative of a drug delivery system unless it was for exceptionally prolonged drug release. The error for the study conducted at room temperature ranged from 0.005 – 0.58 %. The experiment at 37 degrees Celsius, Figure 3.42, also demonstrates very little release over a three-day period. Heat helps the release of propranolol from the MIP, however the release is not significant enough to be considered an effective drug delivery system. The error for the heated study ranged from 0.01 - 0.45 %.

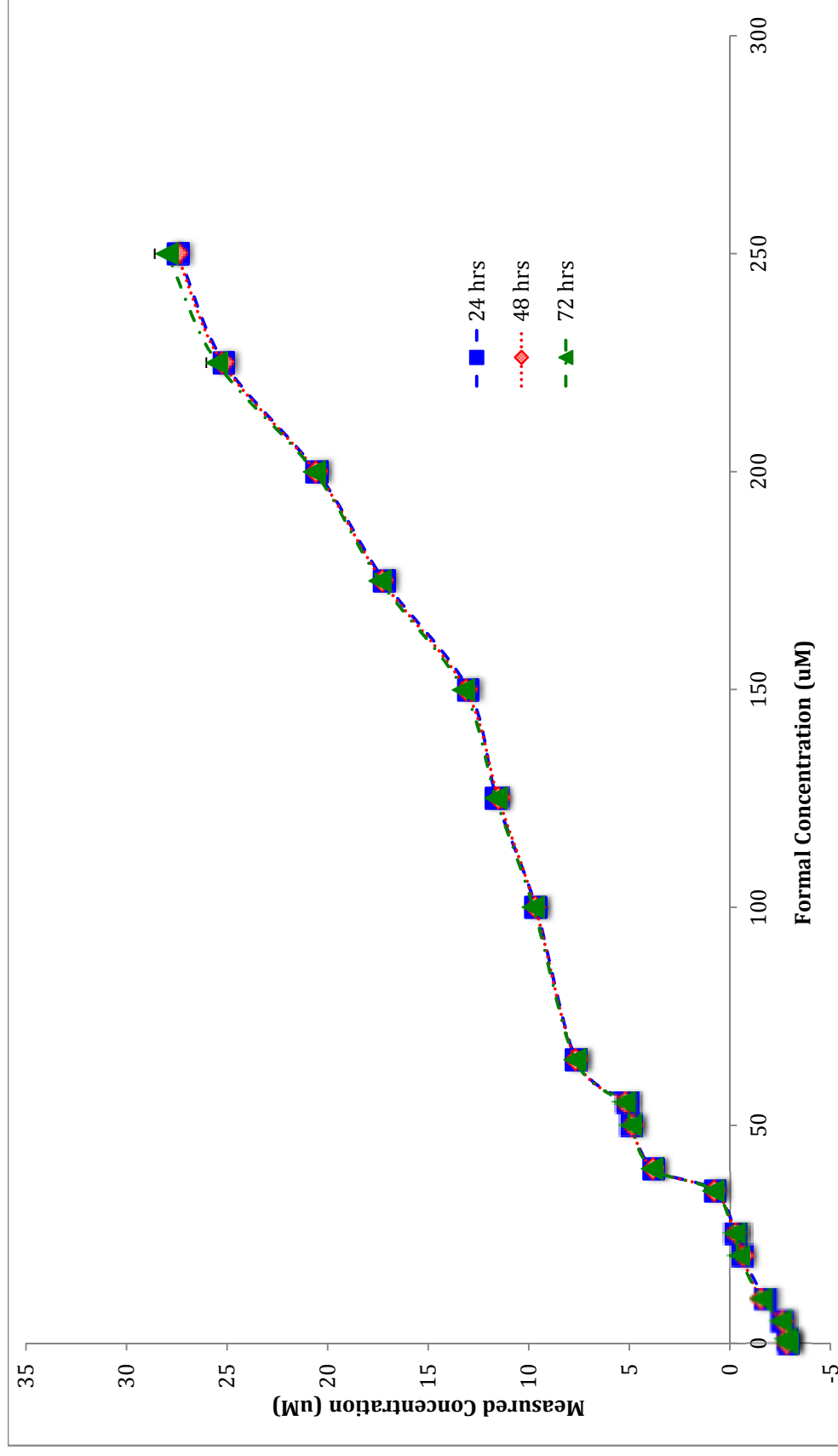


**Figure 3.41:** Release of propranolol from the MIP network every 24 hours for a total of 72 hours at room temperature.

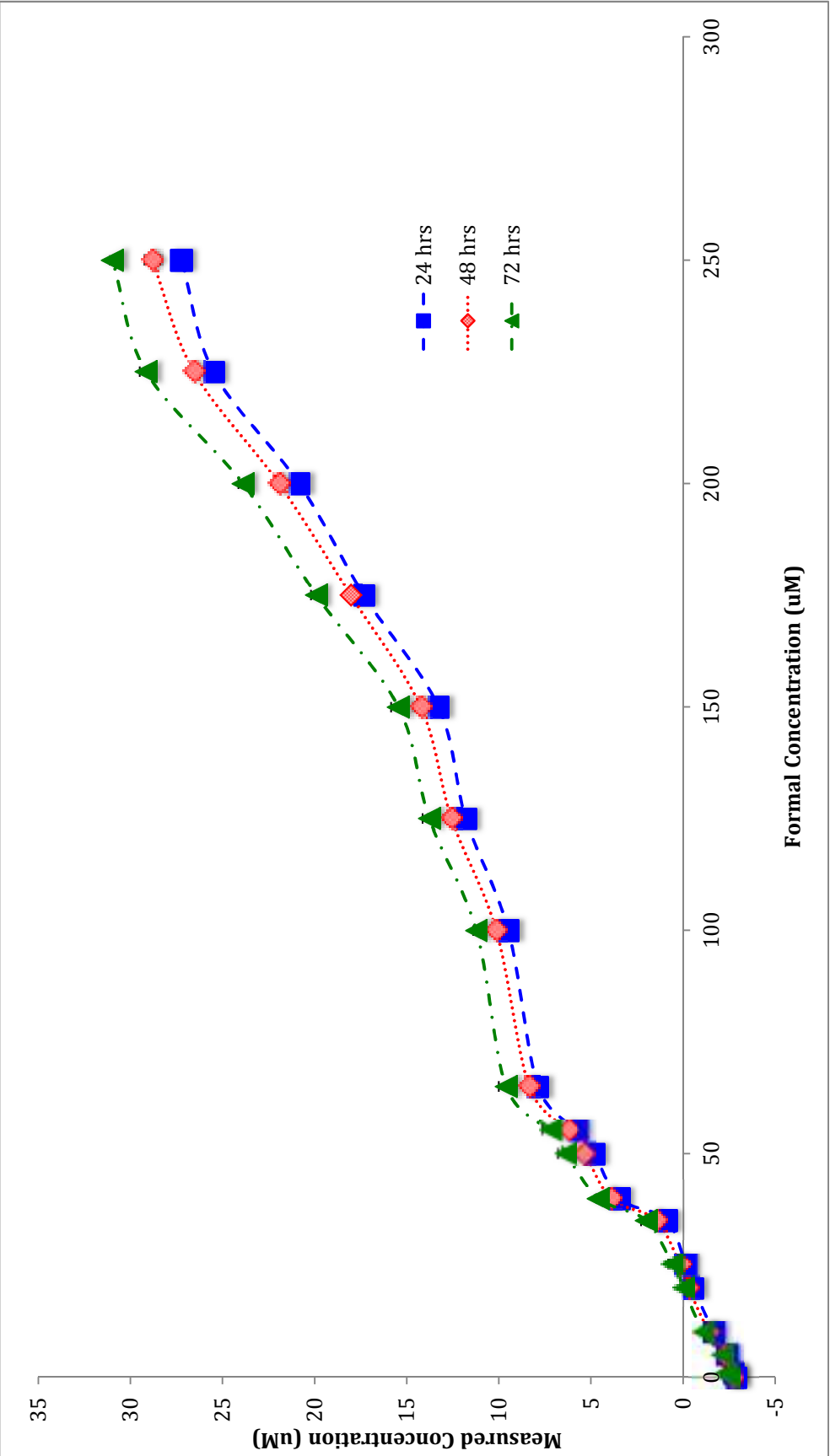


**Figure 3.42:** Release of propranolol from the MIP network every 24 hours for a total of 72 hours at 37 °C.

### 3.5.2. *Agitation (Shaker, Sonicator)*

The shaking method, Figure 3.43, was effective at releasing propranolol, certainly not as effective as the sonicator, however better than the release observed at room temperature and the one with simply heat. This indicates that binding of propranolol to the polymer is relatively strong. The error for the release experiments with shaking ranged from 0.026 – 0.25 %. The release of propranolol with heat (37 degrees Celsius) and sonication, Figure 3.44, demonstrates a more effective release result than shaking. Although it is noteworthy that release within the first 24 hours was not very significant. The error for the release study using the sonicator ranged from 0.02 – 0.30%.

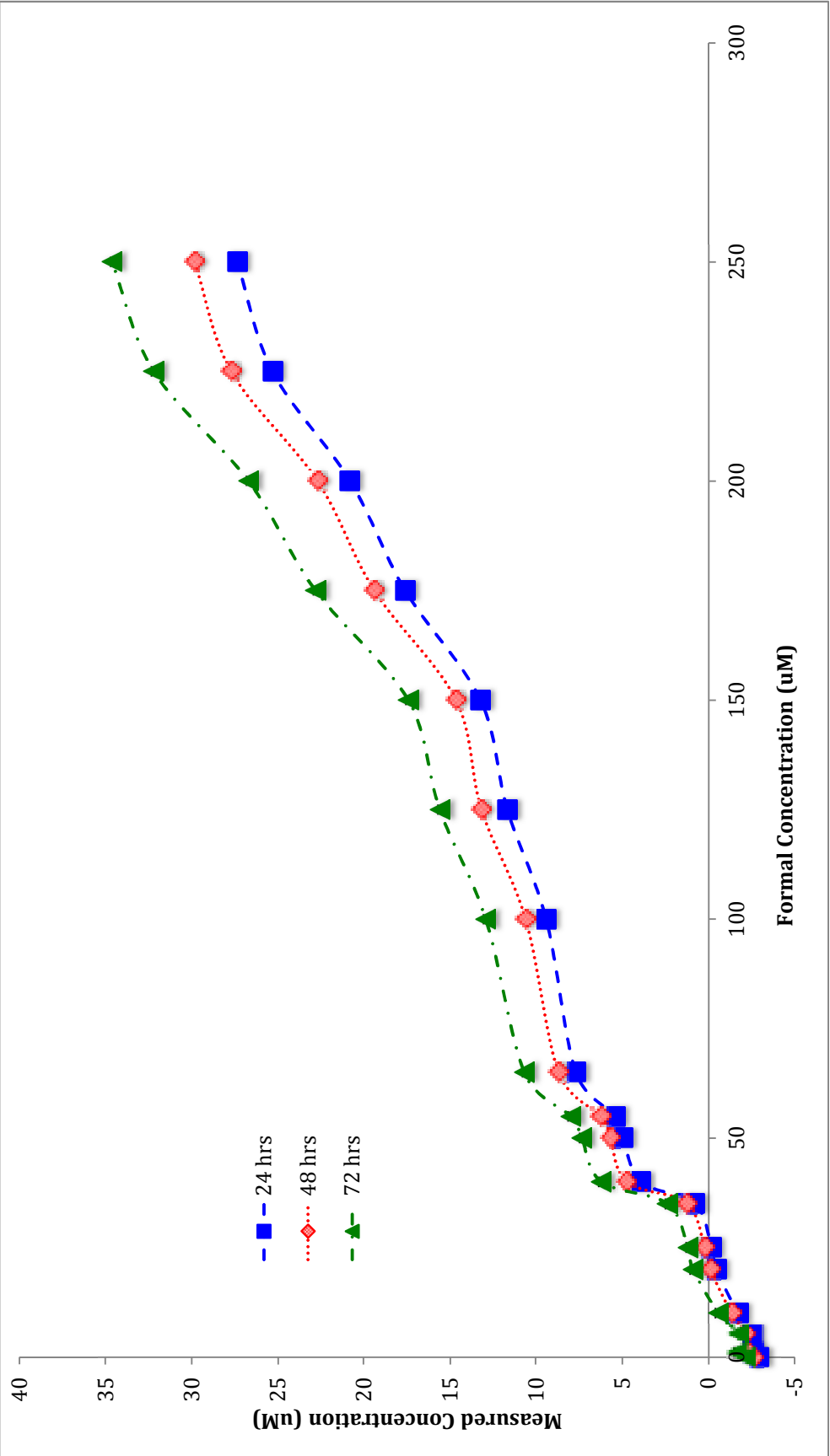


**Figure 3.43:** Release of propranolol from the MIP network every 24 hours for a total of 72 hours with shaking at 37 °C.



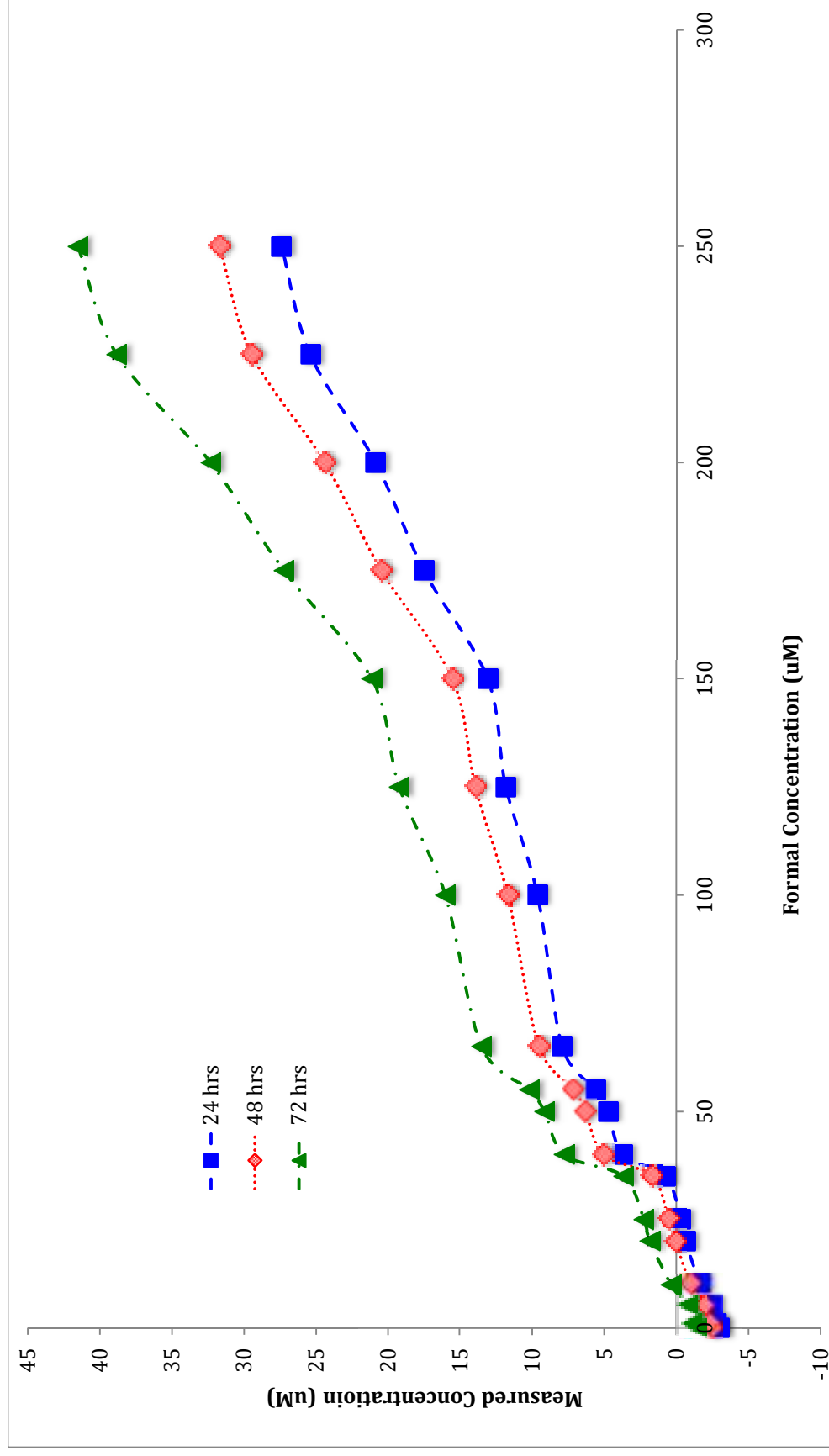


**Figure 3.44:** Release of propranolol from the MIP network every 24 hours for a total of 72 hours with sonicator at 37 °C.

### *3.5.3. pH – Ionic Release*

The results for the pH release experiments demonstrated a significant release of propranolol; pH variation was the most effective release stimuli tested. The release for pH 12, Figure 3.45, was just slightly more effective than the release observed from sonication. The error for pH 12 release study ranged from 0.05 – 0.48 %. The release of propranolol from pH 3, Figure 3.46, was the most effective test condition and the error ranged from 0.005 – 0.54 %.

From a comparison of all of the release methods after 72 hours, Figure 3.47 and Table 3.1, it is clear that the most effective method at propranolol release is the ionic stimulated release followed the sonication approach. Although sonication is an effective release tool, its simulation in the body and ultimately its effectiveness as a drug delivery device is highly questionable.

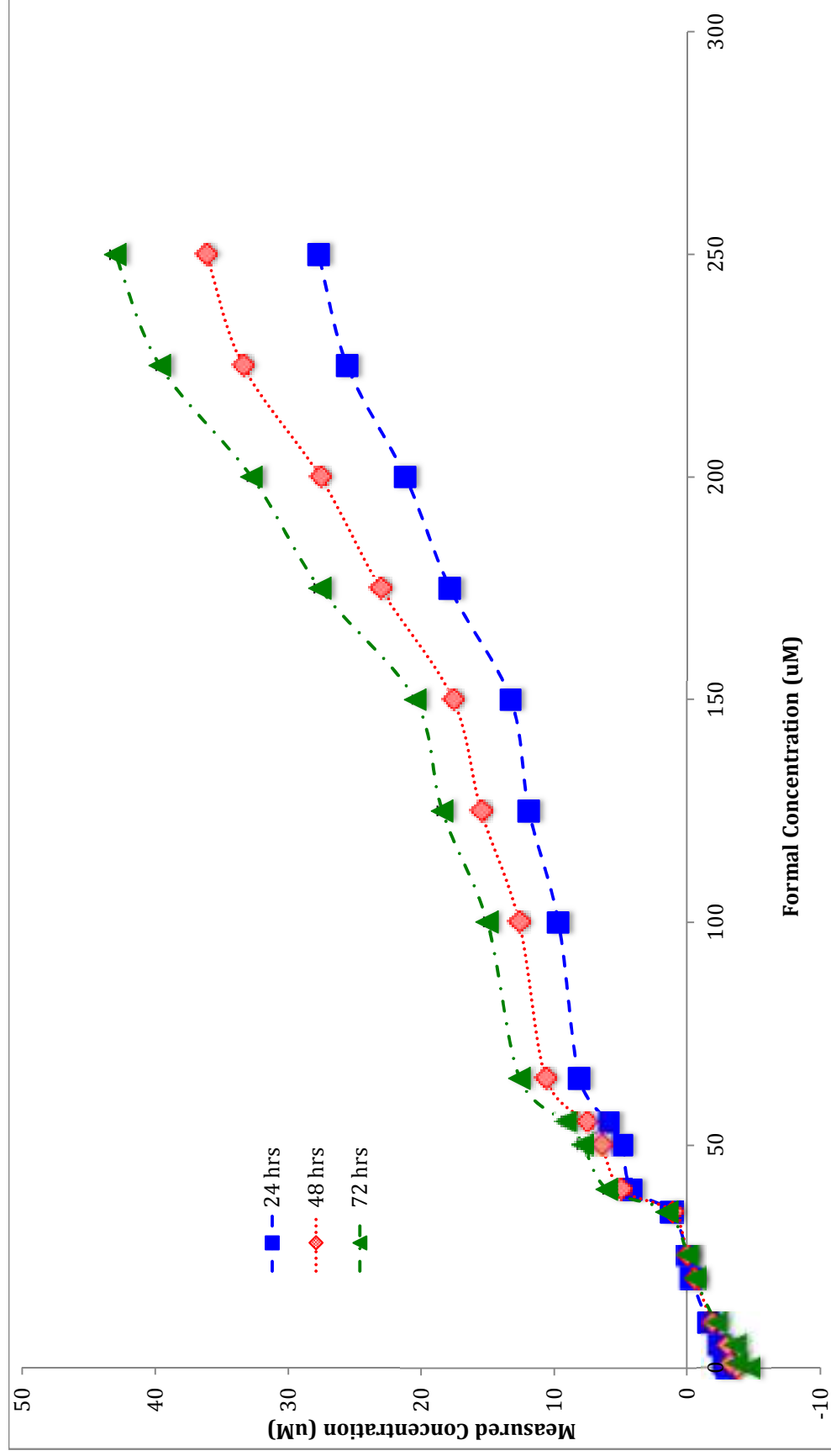


**Figure 3.45:** Ionic release of propranolol from MIP network every 24 hours for a total 72 hours at pH 12.

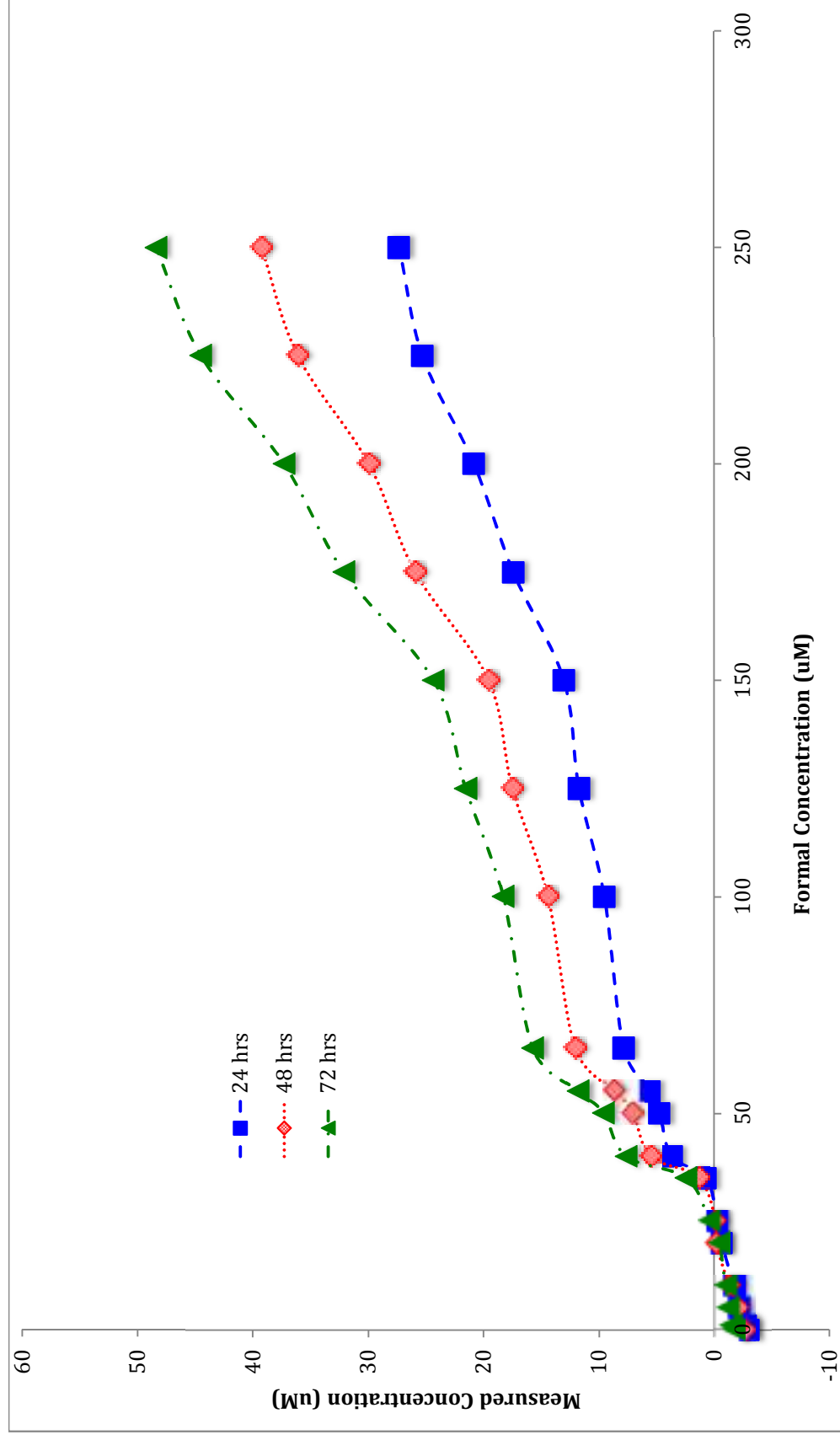


**Figure 3.46:** Ionic release of propranolol from MIP network every 24 hours for a total of 72 hours at pH 3.

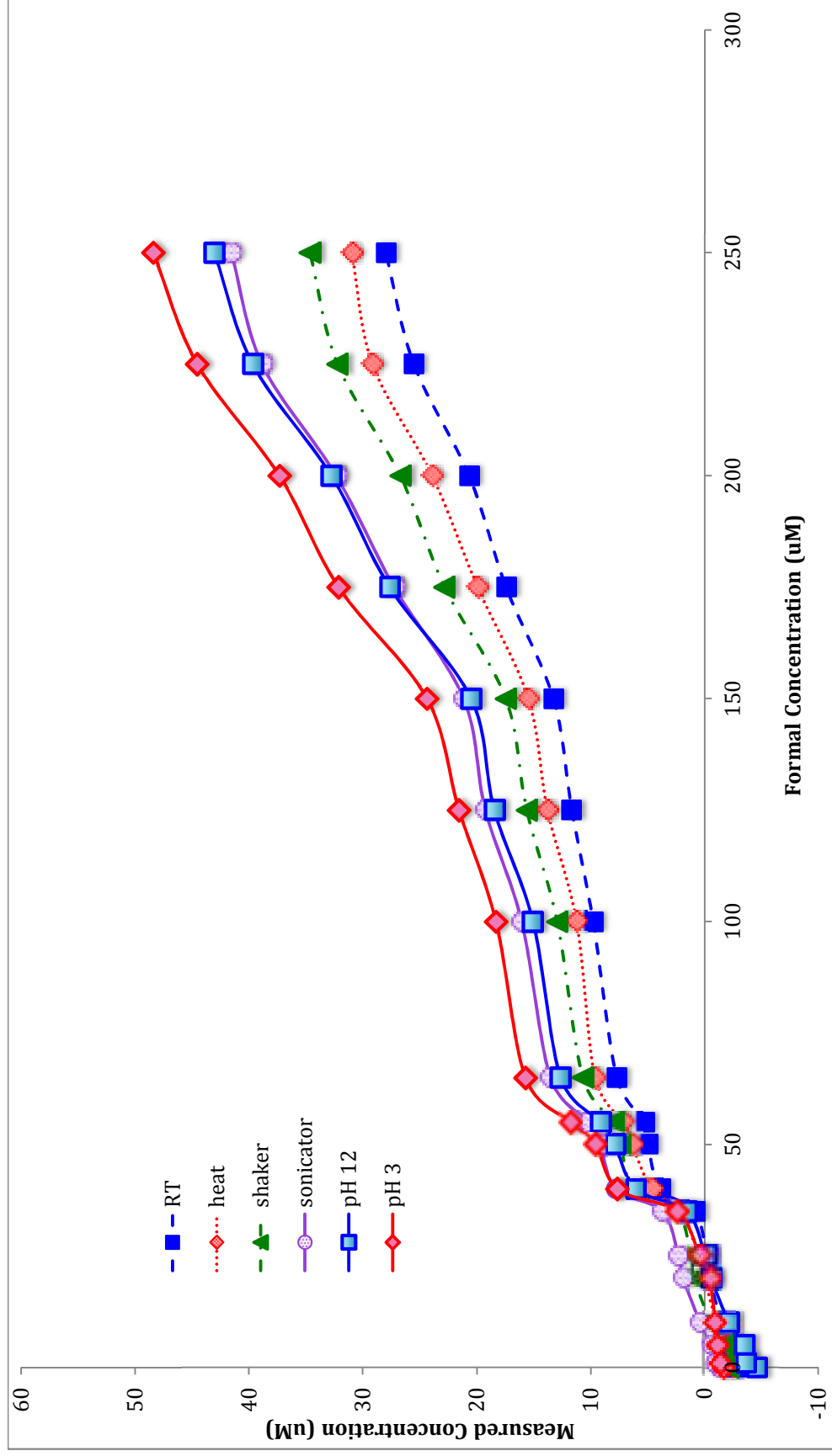


**Figure 3.47:** Release of propranolol from MIP network for all methods, room temperature, heating at 37 °C, sonication, shaking, pH 12 and pH 3 at 72 hours.

**Table 3.1:** Comparison of release method on propranolol release from MIP; 250  $\mu$ M propranolol solution at 72 hours. The release is represented as a percentage of the propranolol released from the system with respect to the total propranolol uptake. A system that reports 100% release would be indicative of all propranolol that was adsorbed during uptake has effectively been removed from the polymer.

<b>Release Method for 250 <math>\mu</math>M Propranolol Solution</b>	<b>Release after 72 hours (%)</b>
Room Temperature	0.04
Heat (37 °C)	14
Shaker	27
Sonication	52
pH12	55
pH3	76

## 4. DISCUSSION

### 4.1. Morphology Studies (Cleaning, Shearing, Probe)

Characterizations performed by SEM, Figure 3.1 to Figure 3.13, to understand the interaction between the MIP and its respective template did not provide much insight. Much effort was put towards an attempt to visualize the cavities that were reported by McBain, shown in Figure 3.1 (a), which were believed to be the imprinted sites. The porous image of the polymer obtained from McBain's work suggested that imprinting was successfully taking place. McBain's complexation studies further supported this conclusion. The fact that the interactions between template and polymer were not characterized and cavities were not visualized raised concerns of whether imprinting was happening at all. One of the goals of the present morphological studies was to try and establish if imprinting was occurring the way it is described in literature, which is one template molecule to one imprinted cavity. After several attempts the results obtained, shown in Figure 3.1 (b), did not reproduce McBain's observations.

SEM allows for images at high magnification to be obtained, however the images from one location of the polymer can look entirely different from another, despite being from the same sample. Also, if the same sample is re-examined at a later time, obtaining the same image can prove to be difficult. Thus, reproducibility with SEM is a challenge in itself. Not only is reproducibility a difficult task, but distinguishing between topographic contrasts and material composition is also a challenge. When inspecting an SEM image, one cannot always determine if features

(e.g., pores) are actually due to topography or as a result of sample arrangement. Kaczmarek stated in his paper from 2001<sup>309</sup> that it can be difficult to separate topographic contrasts and material contrasts in SEM. For instance, the appearance of a cavity may not necessarily be a topographical feature, but rather the result of sample placement. The presence of a cavity as a sample feature can be inaccurately identified as such when it is actually a result of sample particles overlapping on top of one another, giving the perception of a crevice or even depth.

Furthermore, the image of the porous polymer was obtained only once by McBain. It is possible, then, that the sample was not representative. Perhaps it was prepared differently than the method described or differences in the experimental conditions may have lead to an unusual outcome. McBain obtained the porous SEM image during the summer months; the SEM images obtained in this project were during the winter months. Change in atmospheric humidity can have significant effects on the DMAA-MMA hydrogel system that are not necessarily apparent to experimenter.<sup>323, 324</sup> Moisture in the atmosphere during the summer months can cause an increased degree of swelling in the hydrogel.<sup>325</sup> Such environmental changes to experimental conditions might alter the observed morphology of a hydrogel as detected by SEM.<sup>326</sup> Such changes in experimental conditions could be the cause for inconsistency in sample characterization.

Also challenges with the polymerization process may have attributed to the variations experienced relative to McBain's work. Firstly, the bulb of the Novacur light source unexpectedly burst during polymerization and was later replaced with a new bulb. The bulb that burst was the same bulb that McBain used, and the new



bulb might have caused differences in polymerization. While waiting for the replacement bulb to arrive and for the repair to be done, an alternative light source was used; a Hanovia Utility Ultraviolet Quartz Lamp. However, this light source was found to be ineffective. Polymerization took significantly longer (25-30 minutes), whereas it required less than 2 minutes with the Novacur system. The product obtained following Hanovia lamp polymerization was not a hard disk as obtained with the Novacur system, rather its composition was more like a gel. Variations in the polymerization product were likely due to differences in operation parameters of the two light sources. For instance, the Hanovia lamp operated at a very low current of 3.9 amps. A variation in the operating parameters produced a polymer product that was too dissimilar to the original product and raised concerns with respect to reproducibility. To maintain consistency in polymer synthesis all results presented in this paper are from samples polymerized by the Novacur light source; samples prepared by the Hanovia lamp have been excluded.

Another factor that could have caused the variation in polymerization was a decrease in potency of the crosslinking agent. When light curing took more than the standard two minutes to form a polymerized product, an additional portion of the cross-linker EGDMA was added (210 $\mu$ L instead of 105 $\mu$ L) and polymerization occurred almost instantaneously as it had in the past. This caused a concern that the sample of DMAA-MMA contained insufficient quantities of the cross-linker to allow effective polymerization to occur. Since the role of the cross-linking agent is to provide structural scaffolding, it plays a pivotal role in polymerization. However, even with the lower quantity of EGDMA polymerization did occur. Higher quantities

of cross-linker increase the density of the polymer matrix as well as result in the formation of a closer polymer structure around the template according to MIP theory.<sup>327</sup> This results in higher specificity to the template, however template removal may become increasingly difficult.<sup>111</sup> Thus, since additional amounts of cross-linking agent would alter the composition of the network and ultimately would make the results difficult to compare with earlier work, an additional portion of EGDMA was not used in subsequent experiments. Finally, to eliminate the concern that the EGDMA supply was losing its potency, the polymer synthesis was performed with newly ordered reagents, including fresh EGDMA, and polymerization was successfully carried out with the original quantity of EGDMA.

Although imprinting or cavities could not be visualized, one cannot rule out the potential that the template is being imprinted. While characterization of the polymer was not achieved through SEM, perhaps positive results could be obtained through Atomic Force Microscopy (AFM) or Transmission Electron Microscopy (TEM). It is suggested that these tools be used in future efforts.

#### *4.1.1. Cleaning*

The preliminary morphology studies suggested that the surface of the polymers were being altered as a result of the template extraction process, when comparing the cleaned versus the un-cleaned samples from Figures 3.2 to 3.7. The cleaned samples had an appearance of a dry and rough surface, and the un-cleaned samples had a rubber-like appearance with a smooth surface. This difference was more pronounced in the MIP, Figure 3.5, than the NIP, Figure 3.4, and raised

concerns that perhaps the cavities are being destroyed as a result of the harsh conditions of the Soxhlet cleaning process, which ultimately is preventing the visualization of the pores. If the cleaning method was in fact destroying the pores, the cavities should have still been visible in the un-cleaned MIP, which was not the case. Although the modification of the cleaned MIP and NIP compared to un-cleaned is apparent, the destruction of cavities cannot be confirmed, as in the entirety of this project the presence of cavities could never be verified.

Nonetheless alternative cleaning methods were attempted but the milder cleaning methods (distilled water and saline solution while shaking) described were unable to successfully and effectively remove the template, leaving high concentrations of propranolol behind in the polymer. Template removal is a crucial step in the preparation of MIPs. The affinity of the imprinted cavities for the template might make its extraction difficult. However, the association is non-covalent as demonstrated by the fact that the fluorescent material in the polymer (i.e., propranolol) can be washed away. If template molecules are not adequately washed out, there are fewer cavities available for re-binding. It is also possible that template bleeding or leaching could occur which would cause errors in analysis of uptake or release experiments. Residual propranolol that leaches into the external solution during uptake studies would not have been accounted for in concentration measurements, resulting in a low apparent uptake.

Unfortunately, residual amounts of propranolol were detected even after exhaustive washing cycles; this is likely due to poor accessibility of ethanol to the highly cross-linked regions of the polymer.<sup>101</sup> It is also possible that the propranolol

is not sufficiently soluble in ethanol and therefore unable to disrupt the interaction with the imprinted cavities. It is possible that the residual portion of propranolol reflects template that is permanently entrapped in the polymer or is located deep within the polymer network and requires more time to diffuse out. It is also possible that due to polymer/template thermodynamic interactions, the template was not soluble in the pre-polymerization solution, and if it did not adequately dissolve it would not actually be incorporated into the network.<sup>142</sup> Regardless, template extraction was continued with the Soxhlet process and although it may be altering the morphology of the polymer, it was deemed a necessary process to clear residual template as much as possible. Also to maintain consistency with cleaning methods utilized by McBain.

#### *4.1.2. Shearing*

The cavities observed in McBain's SEM image were estimated to be approximately 0.25 $\mu$ m to 0.50 $\mu$ m, in diameter. Since propranolol is significantly smaller (1.0nm to 1.5nm) it was proposed that clusters of propranolol can be accommodated into the cavities that were observed. McBain concluded that either clusters of propranolol were occupying the cavities or that there were smaller pores within the cavities. The shearing experiments were designed to break up any possible aggregates of propranolol prior to polymerization and then to observe any changes in morphology and imprinting. If imprinting were due to the presence of such aggregates, then the nature of the interaction would be hindered or at the very least altered upon shearing of these aggregates prior to polymerization.

While the morphology of the sheared samples, Figures 3.8 and 3.9, was certainly different, the variation did not reveal the presence of cavities. Also the morphological change was again more obvious in the cleaned samples, Figure 3.8 (b), and quite profound in the cleaned MIP, Figure 3.9 (b). The samples gave the appearance of clumping, however, the clumping was not into one large clump rather a series of small “chunks” of polymer clumped on top of each other. Shearing the samples is likely to have created these small chunks.

Whether propranolol aggregates are being disrupted cannot be confirmed, nor can it be verified if breaking up the proposed clusters prevents imprinting. The results obtained from the shearing experiment overall reveal very little information about the nature of the interaction between imprinting components.

#### *4.1.3. Probe*

The probe studies utilized fluorescein as a fluorescent probe to “light” up the cavities. The idea is that polymer pores would accumulate higher quantities of probe molecules, which would cause the imprinted pockets to be brighter than regions that were not imprinted. Prior to examining samples with SEM, the samples were investigated with a handheld UV lamp as a preliminary measure. When inspected with the handheld UV lamp, there were certainly small specks of brightness all over the sample. The observation with the handheld UV lamp was encouraging and prompted further investigation. The samples were then investigated under a confocal microscope. However the images were not magnified enough and

resolution was very poor. Thus confocal microscopy does not allow for morphological observations of the cavities or lit up pockets.

Examination by SEM once again failed to reveal imprint cavities. SEM could not detect any morphological features that could be correlated with the bright specks that were observed with the handheld UV lamp either. In the case of the NIP sample, Figure 3.10, one does not expect to see cavities therefore lit up pockets are not expected to be visualized either, unless there is non-specific binding. However in the MIP samples, the un-cleaned sample, Figure 3.11 (a) would still contain template propranolol and the cleaned samples, Figure 3.11 (b) should have empty imprints, which could accommodate fluorescein in principle. During the Soxhlet process the release of fluorescein was observed. Although specific levels of release were not measured, it can be said with certainty that a sufficient level of the probe remained in the sample following cleaning due to a distinct deep red colour change in the sample from when fluorescein was first introduced.

Overall the probe studies were not successful. Fluorescein was also added to a sample that was sheared prior to polymerization. The results were consistent with the independent findings of the shearing experiments and probe studies. The surface appeared to be full of clusters and gave the appearance of chunks, however, no cavities could be observed. Thus the experiment utilizing the fluorescent probe in conjunction with shearing, shown in Figures 3.12 and 3.13, was also not that informative.

## **4.2. Degradation of Propranolol**

Since decreased fluorescence in the external environment is assumed to be caused by inclusion of propranolol in the polymer during uptake experiments, decreased fluorescence due to other factors produces misleading, inflated estimates of uptake. Photolysis and degradation of propranolol could have attributed to the decrease in detectable fluorescence. In order to avoid skewed observations with respect to uptake, the extent of light-induced degradation of propranolol was determined. It was observed that over a 7 day period that a non-appreciable amount of propranolol was degraded ranging from a low of 0.05% to a high 5.8%, see Figure 3.14. In most cases the degradation was insignificant, and in a mere 10% of readings was the degradation at the high end of this range. A trend could not be established in the samples that had higher degradation. The cause for this degradation could be due to photolysis.<sup>262, 328, 329</sup> The results of this experiment suggest that no correction for template degradation needs to be applied to the uptake measurements.

## **4.3. Uptake Experiment**

In theory, the uptake by a successfully imprinted system should be far superior to its non-imprinted counterpart. Not only should an imprinted system be highly specific for the template, but it also should be highly selective. The uptake experiments performed here demonstrated a level of preference to the MIP network, the extent of which was also demonstrated. The uptake experiments need to take into account the degradation of propranolol as previously demonstrated to be 0.05% to 5.8%, as well as any template leaching of residual propranolol that was

not extracted from the polymer during the cleaning process. Degradation of propranolol would cause the concentration in the external environment to be lower, which may be interpreted as uptake, and on the contrary leaching would result in higher concentrations in the external environment, which would be interpreted as lower uptake. These two potential errors act to cancel out each other's effects. Overall the results from the uptake experiments supports MIPs are adsorbing propranolol more effectively than their NIP counterparts.

#### *4.3.1. Preferential Uptake*

The preferential uptake experiment was designed to demonstrate if imprinting is occurring in the experimental system. Selective binding of propranolol to the MIP suggest that cavities are being locked into place around propranolol during polymerization. Imprinting has not been visualized in the morphology studies, which is raises concerns whether imprinting is occurring at all. The results from the preferential uptake studies demonstrate that there is uptake by both the NIP, Figure 3.16, and the MIP system, Figure 3.17, and that uptake is far more effective in the MIP network. The uptake by the MIP system is almost double the uptake observed by the NIP system. Even taking the potential errors into account (residual template leaching, propranolol degradation), the difference in uptake by the two systems is significant, shown in Figure 3.18. It is likely that the presence of imprints allows for greater binding efficiency, however it is not known if the increased adsorption is a result of the MIP's affinity for propranolol.



#### 4.3.2. *Structure Variation*

When considering preferential uptake various factors relating to sample preparation can influence the re-binding of propranolol. Theoretically, the powder form of the MIP should allow for greater surface area and exposure of the cavities to allow for ease of re-binding of propranolol to the highly cross-linked pockets. However, polymers in their hydrogel form are highly sensitive to changes in environmental conditions such as moisture and swell when added to propranolol solutions, allowing for cavities to expand. This may also facilitate re-binding of propranolol.

The results obtained, shown in Figures 3.19 and 3.20, demonstrate no preference for either form with uptake efficiencies essentially overlapping for both the powder and hydrogel forms. Although little information was revealed regarding which structure of polymer lead to preferential uptake, the time consuming process of preparing powdered samples could be eliminated. Although sample preparation for the powder form is not by any means challenging, the hydrogel by contrast, can be used immediately after drying; the hydrogel is more convenient. Furthermore, when samples were ground using the ball mill grinder, sample loss was always experienced. Thus, since the uptake was relatively similar in both forms the uptake studies were carried out with the hydrogel form of the polymer. All subsequent experiments were carried out in the hydrogel form.

#### 4.3.3. *Centrifugation*

Prior to fluorescence testing, the samples were centrifuged to avoid any possible influences of light scattering by suspended polymer on the observed fluorescence signal. It was observed that when samples were retrieved from the incubator, the hydrogel had settled at the bottom of the falcon tube prior to centrifugation. In hopes of eliminating centrifugation of the twelve tubes (0, 1, 5, 10, 20, 25, 35, 40, 50, 55, 65, 100 $\mu$ M) before every fluorescence reading, the effect of centrifugation on uptake was tested.

It was found that the uptake in the MIP system, Figure 3.22, was not greatly influenced by centrifugation as the results were overlapping between the centrifuged and un-centrifuged samples. However the NIP system, Figure 3.21, at 72 hours demonstrated a significantly higher apparent uptake when centrifuged then its non-centrifuged counterpart. As a result, all samples in this work were centrifuged to avoid any interference in fluorescence readings.

#### 4.3.4. *Maximum Adsorption*

The uptake experiments were designed such that readings for re-binding were taken every 24 hours for a maximum of 72 hours. The results obtained in the preferential uptake experiment, Figures 3.16 and 3.17, demonstrated that uptake continues after 72 hours, as a plateau is not reached. To stop testing for uptake at 72 hours is therefore premature and further uptake readings were conducted to determine the point at which maximum uptake is achieved.

The results indicate that a significant jump in uptake is achieved between 72 hours and 96 hours, Figure 3.23, and is especially pronounced in the MIP network, shown in Figure 3.24, almost twice as much uptake is achieved in this time frame. The jump in uptake between 72 hours and 96 hours could be due to swelling in the hydrogel reaching a maximum. The DMAA-MMA system is reported to swell to 64%<sup>104</sup> in water. And McBain reported the DMAA-MMA system to swell to  $66.91 \pm 2.35 \%$  when imprinted with propranolol.<sup>317</sup> Beyond 96 hours uptake continues and reaches a plateau at 144 hours. The uptake remains constant from 144 hours to 168 hours or a negligible increase is observed. To ensure that a plateau was achieved all samples following the maximum adsorption experiments were carried out to 168 hours.

#### 4.3.5. *High Concentrations*

The concentration of the twelve drug solutions that were tested for uptake ranged from 0-100  $\mu\text{M}$ . In an effort to determine the nature of uptake at higher concentrations, six additional concentrations were introduced, increasing in 25  $\mu\text{M}$  increments from 100  $\mu\text{M}$ ; 125, 150, 175, 200, 225, 250  $\mu\text{M}$ . In the NIP experiment, Figure 3.24, at times less than 120 hours the fluorescence signal is so strong that it is off scale and not detectable. After 120 hours the uptake by the polymer is sufficient to reduce the signal so that it is measurable. The decrease in concentration of the higher drug solutions after 120 hours indicates that the system is continuing to adsorb drug but the uptake only reaches detectable levels after 120 hours for 200, 225 and 250  $\mu\text{M}$ . However, the system also demonstrates that after 144 hours it

reaches a plateau as no significant change in uptake is observed beyond 144 hours. This suggests that propranolol concentration is not the limiting factor in uptake.

With respect to the MIP system, Figure 3.26, the uptake is again more efficient and therefore the higher concentration tests reach detectable levels quicker than with its NIP counterpart. The 250 $\mu$ M solution remains at undetectable levels for only 48 hours in comparison to 120 hours in the NIP system. This suggests that uptake at higher concentrations is more rapid and apparent in the MIP, presumably due to the availability of imprinted cavities. The greater efficiency of MIP uptake is apparent in Figure 3.27, which makes a direct comparison of uptake by NIP and MIP in a 225  $\mu$ M propranolol solution. The MIP also suggests that perhaps the concentration of propranolol concentration is not the limiting factor in uptake.

#### *4.3.6. Cavities as limiting Factor*

One of two things could be happening in the MIP system, either the uptake does not increase any further beyond 144 hours due to the fact that all propranolol in solution has been included already, or that there are no longer any available binding sites left for propranolol to bind to. Since the results from the high concentration experiments suggest that propranolol concentration is not the limiting factor, the cavities as the limiting factor were tested.

Concentrations that were detectable from day 1 were carefully selected, so that they could be compared to previous uptake experiments. The propranolol solutions tested were 10, 25, and 50 $\mu$ M, Figures 3.28, 3.29, and 3.30 respectively. To test if cavities were the limiting factor, the quantity of polymer was altered. In

previous experiments 10mg of polymer had been added to the solution. The experiment that had half as much polymer added; 5mg, appeared to reach maximum uptake significantly faster. This supported the claim that the available binding sites were the limiting factor in uptake.

By the same logic, the system that had twice as much polymer added to it would reach maximum uptake slower than the usual 10mg. The results are consistent with the hypothesis and the uptake does reach a maximum at a slightly slower rate. However, an interesting observation in each of the three concentrations tested (10, 25, and 50 $\mu$ M) was the fact that detectable propranolol prior to testing in samples containing higher quantities of polymer (20, 25, and 50mg), exhibited higher concentrations of propranolol than the initial concentration of the solution it was suspended in.

Contamination during testing was considered as a probable source of the higher fluorescence observed. However, the experiment was conducted in triplicate and exhibited deviations of less than 2%. Since the deviation in the results was so low, it supported that the solutions were made adequately and testing was being performed effectively. Therefore it is believed that at higher quantities of polymer template leaching has a more severe and apparent effect.

Sellergren and co-workers demonstrated that increasing the number of binding sites on the imprinted polymer increased selectivity and uptake.<sup>330</sup> However, due to the errors observed with the higher polymer quantities, the current experiment could not conclusively demonstrate if available binding sites are the limiting factor in propranolol uptake by the MIP system. The observations that the

system reaches maximum uptake significantly faster when half as many binding sites are available does support the hypothesis, but cannot alone allow for a conclusion to be made.

#### **4.4. Displacement**

Since selective uptake by the MIP has been positively established, the extent of the selectivity for propranolol was determined by introducing a secondary competitor molecule. The efficiency with which the secondary molecule can or cannot displace the bound propranolol provides an indication of the level of affinity the imprinted cavities for propranolol. The displacement studies were conducted in one of two ways; non-competitive, or competitive. The displacement studies with non-complementary structures were not successful despite being very informative. The lack of selectivity of the imprinted cavities for propranolol makes the use of the system as a DDS unlikely.

##### *4.4.1. Non Complementary Structures (NCS)*

The non-competitive displacement (NCD) experiments for both BA, Figure 3.31, and naproxen, Figure 3.33, demonstrate that propranolol could not be displaced and insignificant to no change is observed in uptake when the NCS are introduced after propranolol has achieved binding equilibrium with the polymer. This is to be expected as propranolol has been allowed to interact with the polymer for 168 hours which has been previously demonstrated to be the maximum adsorption period. Since propranolol has been given a binding advantage over the

NCS molecules, the fact that propranolol cannot be displaced demonstrates that the interaction is quite strong and specific. However, the displacement by the NCS is investigated after a 24 hour exposure time. It is also possible, based on uptake studies, that 24 hours is not a sufficient amount of time to allow for displacement.

However, when the NCS molecules are introduced at the same time as propranolol, which reflects competitive displacement (CD), the results do not support that interaction is specific to propranolol. With both NCS test molecules the fluorescence in the external solution increases, suggesting that propranolol is being displaced from the imprinted cavities and therefore becoming detectable again. The fact that the NCS can successfully occupy the imprinted cavities, means fewer binding sites are available for propranolol to bind; hence, the displacement effect.

In the case of BA, Figure 3.32, the molecule is significantly smaller than propranolol and both are significantly smaller than the cavities proposed by McBain, which suggests that both molecules can be accommodated into a cavity at the same time. However, if they are both being accommodated into a given cavity the concentration of propranolol in the external solution would not increase in the presence of BA. Although there may be some cavities that have both BA and propranolol, enough propranolol molecules are being displaced that the observed external concentration is increasing. Therefore BA is successfully displacing propranolol when added competitively.

In the case of naproxen, Figure 3.34, the size of the molecule is similar to that of propranolol as shown in Table 1.8. If imprints are specific to one molecule of propranolol, then only one molecule of propranolol or naproxen could be

accommodated at a given time. However, if the cavities are of a size that was depicted by McBain, then again both naproxen and propranolol could be accommodated. However, the increase in detectable concentration of propranolol following the competitive introduction of naproxen, demonstrates that propranolol is successfully being displaced. Therefore the imprinted cavities are not highly selective for propranolol.

Overall, the displacement studies by the NCS demonstrate that the selectivity of cavities for propranolol is not very high and that the template can effectively be displaced. As such, the systems application as a DDS is not very likely.

#### *4.4.2. Complementary Structures*

Selectivity is expected to decrease when a CS is introduced, as it becomes more challenging for the imprinted cavities to distinguish between the propranolol molecule and the molecule with the related structure to propranolol. Timolol and 1-naphthol were used in CS displacement studies. The results for both molecules indicated a significantly lower detectable fluorescence in the external solution, implying that higher quantities of the drug were being included. However, the maximum adsorption of propranolol has already been determined, and the apparent displacement values observed initially for CD were significantly higher than that. Overtime, additional apparent inclusion was observed in the case of timolol and 1-naphthol because they fluoresce in the same region as propranolol does. This makes it difficult to interpret propranolol displacement by these CS.



An attempt to correct for the overlap was made, by quantifying the uptake by both CS by the polymer independently and subtracting from the displacement data for propranolol. The corrected data would then reflect the displacement of propranolol by the relevant CS. The corrected data suggested that appreciable quantities of propranolol was displaced, contrary to the un-corrected data mentioned above, and as such the imprinted cavities were not selective.

In the case of timolol, shown in Figures 3.36, 3.37 and 3.38, the NCD also demonstrated that timolol was able to successfully displace propranolol as the corrected concentration of propranolol was higher in the external solution. It is noteworthy that the error associated with the corrected displacement of timolol is quite high, 0.1 to 5.2%, in comparison to other experiments within this project. With respect to the CD, the concentration observed was even higher than in the NCD experiments. Since timolol is able to successfully displace propranolol when propranolol had a 7 day binding advantage, it can be concluded that the cavities are not highly selective.

In the case of 1-naphthol, shown in Figures 3.38, 3.39, and 3.40, the trends were not consistent with those in timolol. Prior to the correction the results appear to be consistent with timolol, however the corrected data is not consistent and cannot fully be rationalized. The independent uptake of 1-naphthol was rather sporadic and thus the correction was sporadic also. Perhaps the independent uptake of 1-naphthol is not very effective in this particular system and therefore a correction of the displacement data cannot be made by this means. It cannot

conclusively be determined if 1-naphthol is successfully displacing propranolol, the general trend implies that it is but also has high error associated to it.

It is important to note that the measurements of displacement for both CS are not by direct measurement and this could attribute to the high error observed. Perhaps timolol and 1-naphthol are not good NCSs since they fluoresce in the same region and the method to correct the data is likely not adequate. As such, the selectivity or lack thereof cannot conclusively be ascertained for 1-naphthol, but displacement by timolol suggests that the system is not highly selective for propranolol.

#### **4.5. Release**

The release studies demonstrated that the drug is effectively released from the MIP system and to some extent can be controlled. In the release experiment conducted at room temperature with no shaking, Figure 3.41, no release was demonstrated over a 72 hour period. This raised concerns that the drug interaction with the polymer is strong as suggested by the relatively long adsorption period (7 days). The release experiments were conducted to a maximum of 72 hours. Perhaps for release at room temperature a longer analysis period is required. However, in the context of drug release, this system might be useful in prolonged drug delivery.

The experiment conducted at 37°C, Figure 3.42, demonstrated very slight release; although not efficient enough to be used as a DDS, the release was certainly greater than that observed at room temperature. This was not expected, as higher temperatures are known to induce a compressed state of the polymer. This effect

should enhance binding to propranolol, thus release would arguably be more difficult than at room temperature. Although release was successfully observed, it was not significant enough to be considered an effective DDS.

The agitation (shaking and sonication) experiments were also conducted at 37°C. The shaking experiment, shown in Figure 3.44, demonstrated only slightly more release than the study with just heat, over a 72 hour period. The release of the sonicated samples, Figure 3.43, was effective, releasing nearly 20  $\mu\text{M}$  propranolol from the system. The release after 48 hours in either shaking or sonication is not very high, which demonstrates that this system may be better suited for prolonged drug delivery. Sonication has demonstrated a very effective release mechanism. Some may argue that the process of sonication is not easily reproducible in the body; the harsh conditions that the drug encounter following ingestion may not be equivalent but can be further studied to establish similarities to sonication.

The pH experiments demonstrate the most effective release mechanism in the MIP network, specifically pH 3 seen in Figure 3.46. Release was observed at pH 12, Figure 3.47, but was not as extensive as in pH 3. This was expected, as the polymer system is cationic, and cationic hydrogels swell at a pH that is lower than the gel  $pK_a$  due to ionization within the network. In both of the pH experiments, the release between 24 hours and 48 hours is greater than between 48 hours and 72 hours. This is evident from the graph as the data series for 24 hours and 48 hours are further apart for both pH 12 and pH 3. The graph also indicates that the rate of release slows down after 48 hours as the data series for 48 hours and 72 hours are

closer than 24 hour and 48 hour series. Overall the pH experiments successfully released propranolol and the results that were expected were observed.

Hiratani *et al.*, express the total loading capacity of their polymer as the total amount of template that could be released.<sup>5</sup> Similarly the release determined in Table 3.1 is based on the total uptake by the network and not the total quantity of propranolol that was present in the uptake solution. Therefore, 100% release would reflect a complete release of included propranolol from the uptake study. The release studies overall demonstrate that under appropriate conditions the polymer system can effectively release propranolol, and modifications to release conditions can allow for prolonged controlled release.

## 5. CONCLUSION

The MMA-DMAA polymer was successfully synthesized and imprinted. Although the nature of the interaction between the components could not be characterized and the imprinted cavities could not be visualized, the system was successfully imprinted as demonstrated through preferential uptake studies. The morphology studies by SEM conducted to understand the topography of the polymer and to visualize imprinting as seen by McBain were not particularly informative and could not be used to confirm that the polymer network was being imprinted.

Uptake studies proved to be more definitive. Although there were various factors that needed to be accounted for that might give rise to errors, such as propranolol degradation and template leaching, the preferential uptake studies demonstrated without any doubt that the MIP system rebinds propranolol more effectively than the NIP. Presumably this is a result of some sort of imprinting sites being created during polymer synthesis. The structure variation experiments demonstrated that there is no significant difference in the uptake between the powder or the hydrogel form, and as such all uptake studies were performed in the hydrogel form due to ease of sample preparation. The centrifugation experiment demonstrated that centrifugation is a necessary process to avoid errors in fluorescence analysis. Maximum adsorption of propranolol was achieved after an uptake period of 7 days. Furthermore, it was not conclusively determined if the binding sites are the limiting factor due to the unexplainable high concentrations of

propranolol observed in solution which may be due to leaching when high quantities of polymer are present.

The displacement studies demonstrated the extent of imprinting for propranolol was not highly selective. In the non-competitive displacement (NCD) experiments with the non-complementary structures (NCS), benzoic acid and naproxen, propranolol was not effectively displaced. However, when introduced competitively the NCS could displace propranolol. Therefore the imprinted cavities are not highly selective. The complementary structures (CS), timolol and 1-naphthol, were difficult to analyze to due their own fluorescent properties causing interference in analysis. Once the timolol displacement was corrected, it demonstrated that it effectively displaced propranolol. Therefore, although the MIP behavior is consistent with successful imprinting of cavities, the selectivity of these imprints for propranolol seems to not be very high. Martin *et al.*, also report similar results with complementary structures to propranolol. They demonstrate that structural analogues of propranolol exhibit a degree of “cross-reactivity”.<sup>331</sup>

The limitations observed with selectivity might be attributed to the formation of cavities as a result of the presence of propranolol during polymerization. During uptake studies these cavities are able to capture a wide range of molecules as a result of “holes” or “pores” being present, but they don’t specifically bind for propranolol. That is, the template seems to induce some type of cavity formation, but it appears the cavities are ones that encourage non-specific binding as opposed to selective binding. This in an interesting outcome as it is not

consistent with the standard model of molecular imprinting described in the Introduction of this thesis.

The release experiments demonstrated the system can be utilized to deliver a dose of propranolol over an extended time period and release factors can be modified to control the release. It was also observed that pH had the greatest effect and the system would likely be effective in pH-stimulated prolonged drug release. However, in light of the non-specificity of template binding just noted, it is unlikely this particular system could be harnessed as a viable drug delivery system for clinical applications.

Although some of the studies did not demonstrate the expected results, overall the experiments established selective uptake and that the DMAA-MMA system has potential for controlled release. Both of these key results are indicative of a successful molecularly imprinted system. However, the mechanisms of recognition are not entirely understood, which limits the optimization of imprinting strategies.

## 6. FUTURE STUDIES

The current study demonstrates some potential for establishing the MMA-DMAA system as an efficient drug delivery device for propranolol. By making some modifications to the system, some of its limitations can be addressed. For instance, further work on displacement studies would be useful. If complementary structures that do not fluoresce in the same region as propranolol can be introduced, results that do not require correction can be obtained and this would give additional insight into the specificity, or lack thereof, of the polymer binding sites.

Perhaps by adjusting the quantities of polymer components greater selectivity can be achieved. For instance, by increasing the quantity of cross linker greater selectivity around propranolol might be achieved, as the polymerization would be more tightly structured; although it is possible that increase in EGDMA may pose challenges in template extraction. Experiments can be conducted to determine the optimal quantities of each component.

With respect to release studies, fillers like dextrose or lactose can be added during the uptake phase to increase the rate of drug release by producing a burst effect,<sup>332</sup> which implies immediate and sudden release of a drug.<sup>333, 334</sup> In controlled release systems, the DDS upon exposure to the release medium immediately releases an initial large bolus of drug before the release rate reaches a stable profile and a schematic representation of such drug release is presented Figure 6.1.<sup>335</sup> Both fillers have been found to increase the rate of drug release. The incorporation of fillers to promote the burst effect would be favorable for certain applications such as wound treatment, encapsulated flavors, targeted delivery and pulsatile release.<sup>336</sup>



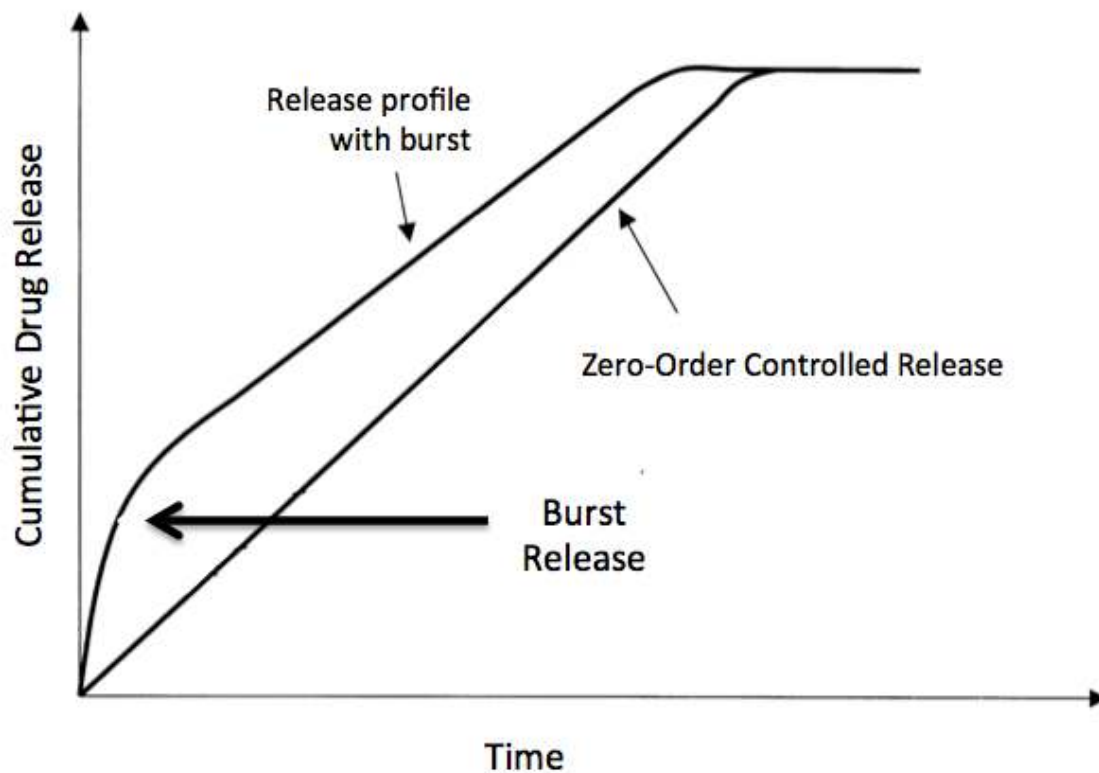


**Figure 6.1:** Schematic representation of the burst effect in a zero-order (constant drug delivery) controlled release system.<sup>335</sup> The burst release leads to a higher initial drug delivery and also reduces the effective lifetime of the device.

Mathematical models of release kinetics can predict drug release rates, drug diffusion and elucidate the physical mechanisms of drug transport by simply comparing the release data to mathematical models.<sup>337</sup> Drug release through controlled delivery polymer systems has been modeled predominantly by steady-state and transient description of drug diffusion by use of Fick's Law.<sup>338</sup> The release kinetics from such drug-release models depends on the mechanism of the release itself, the polymer microstructure, and the conditions of the experiment.<sup>339</sup> In order to further understand the release behaviour of propranolol in the DMAA-MAA network a mathematical model approach may be useful.<sup>340</sup>

The competitive displacement studies demonstrated that propranolol could effectively be displaced. In regards to selectivity, displacement was not the desired outcome. However, Lauten *et al.*, suggest the use of the displacement molecule to assist in template release.<sup>142</sup> They reported that when the imprinted system is in the presence of the displacing agent it binds to it by first releasing the template molecule. Thus the behaviour of displacement, although undesirable, can be used strategically to produce a desired outcome, release.

Also, with respect to cleaning, tests can be done to establish whether the cleaning methods are destroying the cavities; an outcome which would suggest alternative cleaning strategies. If the uptake by polymers cleaned by an alternative process is faster and more efficient it is possible that the hypothesis, that cavities are being destroyed during Soxhlet extraction, has some basis and should be further investigated. If not, it is not necessary to continue investigating this further since uptake has been observed in the MMA-DMAA system. It is possible that template

removal is not as efficient and successful due to the insolubility of propranolol in ethanol and alternative organic solvents can be tried and tested in the cleaning process. Quantifying the amount of propranolol removed from the system during extraction could be essential, but may need to be conducted at very high concentrations, precluding the use of fluorescence as the analytical tool. Perhaps a few cleaning methods need to be tested in conjunction to achieve 100% extraction, to avoid any template bleeding. Other extraction methods as described by Lorenzo *et al.* and in Figure 6.2 can be utilized.<sup>101</sup> It is not possible to state that any of these methods would not be destructive to the template until specifically tested.

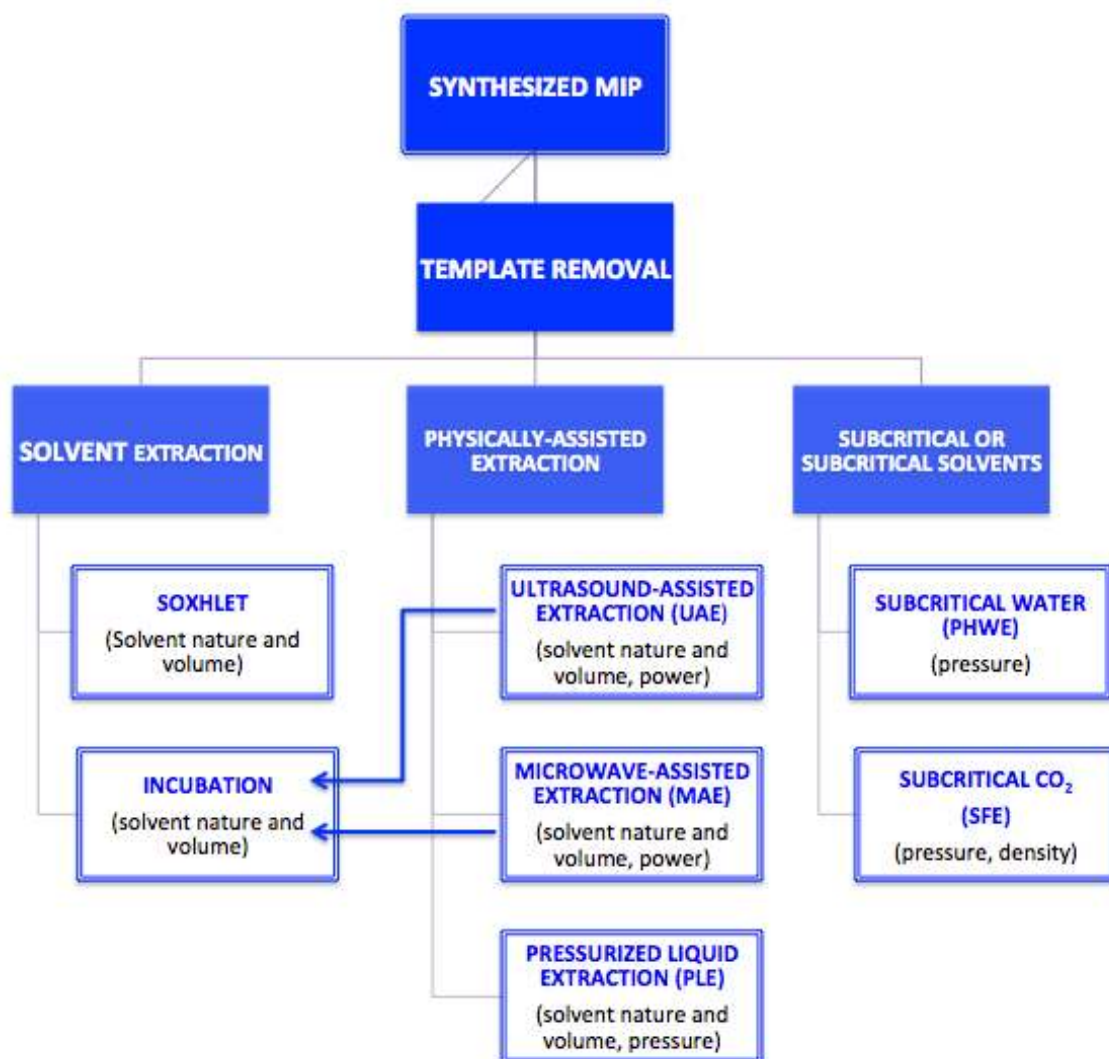


**Figure 6.2:** Potential alternative approaches available for template extraction.<sup>101</sup>

With respect to morphology studies, Atomic Fluorescence Microscopy (AFM) or Transmission Electron Microscopy can be used to establish surface topography and to potentially visualize the imprinted cavities. There have been a few reports that aim to improve the morphology of MIPs to enhance the imprinting effect. Improving the inner morphology of the polymer could increase the visualization of cavities.<sup>341</sup> Steinke and co-workers argue that statistically and the kinetically-driven nature of the network-forming process in traditional free radical polymerization (FRP) makes it impossible to achieve a homogenous distribution of binding sites in MIPs.<sup>342</sup> As a solution they recommend a thermodynamically controlled process *via* ring-opening metathesis polymerization (ROMP). Steinke *et al.*, have also reported that by using a covalent imprinting approach they were able to demonstrate that a MIP with higher selectivity for the template could be synthesized by the ROMP method.<sup>343</sup> The concept of enhancing inner polymer morphology and improving individual cavities as a way to improve molecular imprinting and MIPs is an appealing approach and should be investigated.

Despite the wealth of literature on molecular imprinting technology that has been published in the last several years, there are still a lot of areas of development. The additional experiments suggested in this chapter may offer potential to enhance understanding of the interaction of propranolol with the DMAA-MMA polymer network.

## APPENDIX

### A.1. Calculating the Measured Concentration

A calibration curve of the known concentrations of the aqueous dilutions series is plotted against the fluorescence signals produced. The solutions that experience uptake will have decreasing levels of propranolol in the external environment. The concentration of propranolol in the external solution is determined by measuring the fluorescence signal and converting the signal to a concentration using the line of best fit from the calibration curve. By subtracting the observed concentration after uptake equilibrium has been achieved from the known initial concentration, the concentration of propranolol that is adsorbed by the polymer is determined. A calibration curve was made for each set of aqueous solutions as it was also used as a means to monitor any major fluctuations in the fluorimeter lamp intensity.

Due to the upper detection limit for concentrations of 100  $\mu\text{M}$  and beyond, these solutions were excluded from the calibration curve in order to obtain a reliable fit. In order to determine measured concentrations, the line of best fit was extrapolated and concentrations were determined accordingly.

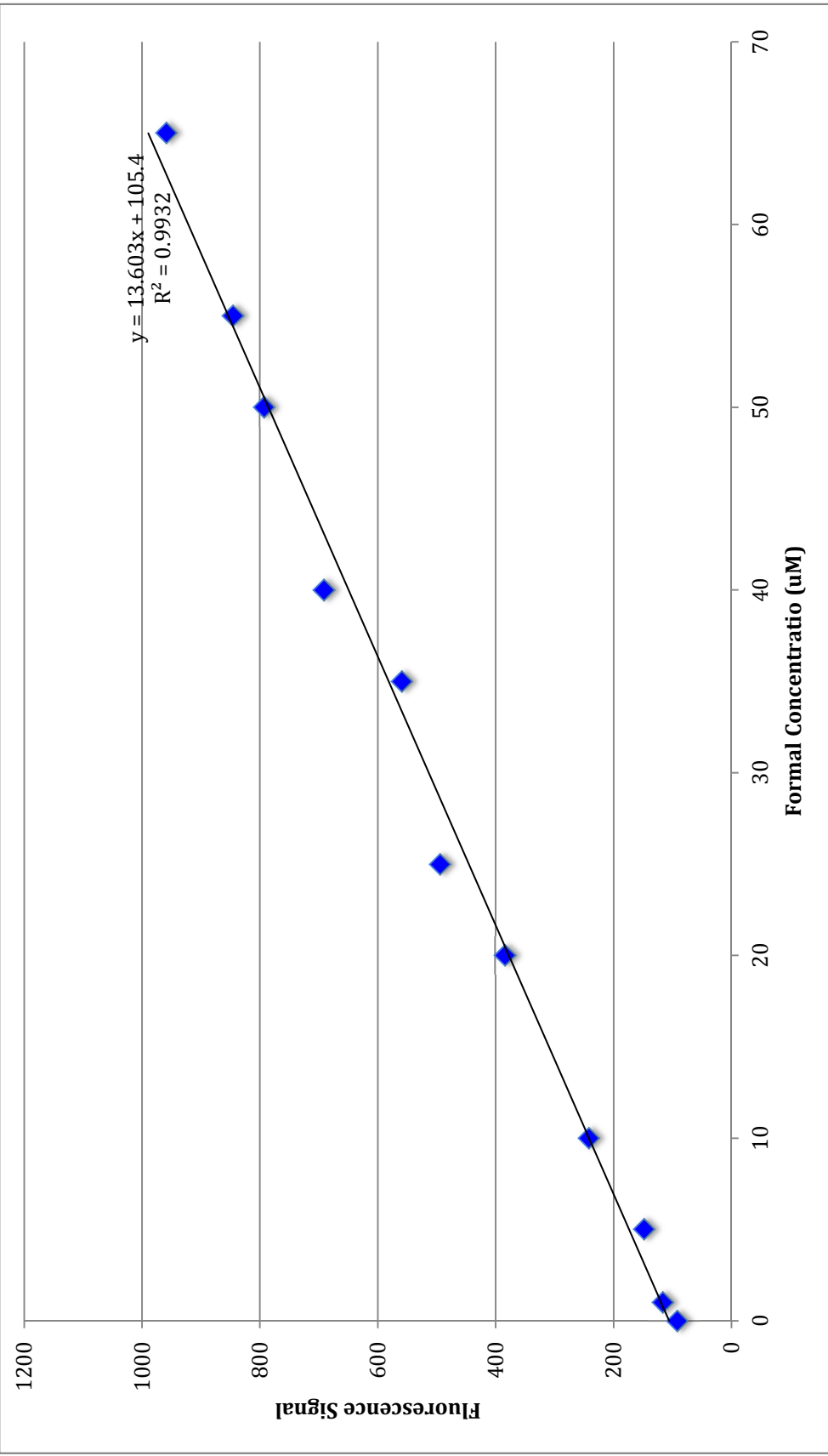


**Figure A.1:** Calibration curve used for the determination of measured concentrations.

## REFERENCES

1. Andersson, L.I. *Anal. Chem.* **1996**, 68 (1), pp. 111-117
2. Moral, N.P., Mayes, A.G. *Mat. Res. Soc. Symp. P.* **2002**, 723, pp. 61-66
3. Vasapollo, G., Sole, R.D., Mergola, L., *et al.* *Int. J. Mol. Sci.* **2011**, 12 (9), pp. 5908-5945
4. Alvarez-Lorenzo, C., Yañez, F., Concheiro, A. *J. Drug Del. Sci. Tech.* **2010**, 20 (4), pp. 237-248
5. Hiratani, H., Fujiwara, A., Tamiya, Y., Mizutani, Y., Alvarez-Lorenzo, C. *Biomaterials* **2005**, 26 (11), pp. 1293-1298
6. Otero-Espinar, F.J., Torres-Labandeira, J.J., Alvarez-Lorenzo, C., *et al.* *J. Drug Del. Sci. Tec.* **2010**, 20 (4), pp. 289-301
7. Puoci, F., Cirillo, G., Curcio, M., *et al.* *Expert Opin. Drug Del.* **2011**, 8 (10), pp. 1379-1393
8. Conn, M., Rebek, J. *Chem. Rev.* **1997**, 97 (5), pp. 1647-1668
9. Lehn, J.-M. *J. Inclusion Phenom.* **1988**, 6 (4), pp. 351-396
10. Lehn, J.-M. In *The Concepts and Language of Supramolecular Chemistry*; M. Volcan Kisakürek, M.V., Ed.; Organic Chemistry: Its Language and its State of the Art. John Wiley and Sons Inc.: New York, NY, 1993.
11. Pedersen, C. J. *Angew. Chemi. Int. Edit.* **1988**, 27, pp. 1021-1027
12. Cram, D. J. *J. Inclusion Phenom.* **1988**, 6 (4), pp. 397-413
13. Hofmeier, H., Schubert, U. *Chem. Soc. Rev.* **2004**, 33 (6), pp. 373-399
14. Chakrabarty, R., Mukherjee, P., Stang, P. *Chem. Rev.* **2011**, 111 (11), pp. 6810-6918
15. Albrecht, M. *Naturwissenschaften* **2007**, 94 (12), pp. 951-966
16. Jasat, A., Sherman, J.C. *Chem. Rev.* **1999**, 99 (4), pp. 931-968



17. Lehn, J.-M. *P. Natl. Acad. Sci. USA.* **2002**, 99 (8), pp. 4763-4768
18. Fyfe, M.C.T., Stoddart, J.F. *Accounts Chem. Res.* **1997**, 30 (10), pp. 393-401
19. Schluter, A.D., Ed.; In *Functional Molecular Nanostructures*; Topics in Current Chemistry, Springer: New York, **2005**; pp 151-191
20. Whitesides, G.M., Mathias, J.P., Seto, C.T. *Science* **1991**, 254 (5036), pp. 1312-1319
21. Gellman, S.H. *Chem. Rev.* **1997**, 97 (5), pp. 1231-1232
22. Lehn, J.-M. *J. Mol. Graphics* **1989**, 7 (2), pp. 95
23. Sakamoto, T., Ojida, A., Hamachi, I. *Chem. Commun.* **2009**, 2, pp. 141-152
24. Francklyn, C. S., Schimmel, P. *Chem. Rev.* **1990**, 90 (7), pp. 1327-1342
25. Linton, B., Hamilton, A.D. *Chem. Rev.* **1997**, 97 (5), pp. 1669–1680
26. Goshe, A.J., Steele, I.M., Ceccarelli, C., *et al.* *P. Natl. Acad. Sci. USA.* **2002**, 99 (8), pp. 4823-4829
27. Liu, S., Gibb, B.C. *Chem. Commun.* **2008**, 32, pp. 3709-3716
28. Chandler, D. *Nature* **2005**, 437, pp. 640-647
29. Pratt, L.R., Pohorille, A. *Chem. Rev.* **2002**, 102 (8), pp. 2671-2691
30. Ghaddar, T.H., Castner, E.W., Isied, S.S. *J. Am. Chem. Soc.* **2000**, 122 (6), pp. 1233-1234
31. Chou, H.C., Hsu, C.H., Cheng, Y.M., *et al.* *J. Am. Chem. Soc.* **2004**, 126 (6), pp. 1650-1651
32. Schalley, C.A., Ed.; In *Analytical Methods in Supramolecular Chemistry*; Wiley-VCH:Weinheim, **2007**, Chapter 1, pp. 1-15
33. Stauffer, David Alan. *The Ion-Dipole Effect is a Force for Molecular Recognition and Biomimetic Catalysis*, California Institute of Technology – Ph. D. Dissertation, **1989**
34. König, B. *J. für praktische Chemie* **1995**, 337 (1), pp. 339-346
35. Bosshard, H.R. *News Physiol. Sci.* **2001**, 16 (4), pp. 171-173

36. Lichtenthaler, F.W. J. *Angew. Chemi. Int. Edit.* **1994**, 33 pp. 2364-2374
37. Klebe, G. In *NATO Science for Peace and Security Series A: Chemistry and Biology*, Springer: Germany, **2009**, pp. 79-101
38. Chen, B., Piletsky, S., Turner, A.P.F. *Comb. Chem. High T. Scr.* **2002**, 5 (6), pp. 409-427
39. Cramer, F. *Pharm. Acta Helv.* **1995**, 69 (4), pp. 193-203
40. Musgrave, I. Spetner and Biological Information. The Talk Origins Archive. **2005**
41. Hentze, H.-P., Antonietti, M. *Curr. Opin. Solid St. M.* **2001**, 5 (4), pp. 343-353
42. Halley, J.D., Winkler, D.A. *Complexity* **2008**, 13 (5), pp. 10-15
43. Rebek Jr., J. *Chem. Soc. Rev.* **1996**, 25 (4), pp. 255-264
44. Wagner, R.W., Brown, P.A., Johnson, T.E., *et al.* *J. Chem. Soc. Chem. Comm.* **1991**, 20, pp. 1463-1466
45. Ball, P. *Nature* **2001**, 409, pp. 413-416
46. Lebeurier, G., Nicolaieff, A., Richards, K.E. *P. Natl. Acad. Sci. USA.* **1977**, 74 (1), pp. 149-153
47. Lehn, J.-M. *J. Angew. Chemi. Int. Edit.* **1988**, 27, pp. 89-112
48. Lehn, J.-M. In *Supramolecular Chemistry: Concepts and Perspectives*, Wiley-VCH: Weinheim Germany, **1995**, pp. 1-271
49. Davis, A.V., Yeh, R.M., Raymond, K.N. *P. Natl. Acad. Sci. USA.* **2002**, 99 (8), pp. 4793-4796.
50. Fiedler, D., Leung, D.H., Bergman, R.G., *et al.* *Accounts Chem. Res.* **2005**, 38 (4), pp. 349-358
51. Pluth, M.D., Bergman, R.G., Raymond, K.N. *Accounts Chem. Res.* **2009**, 42 (10), pp. 1650-1659

52. Albrecht, M., Frochlich, R. *B. Chem. Soc. Jpn.* **2007**, *80* (5), pp. 797-808
53. Albrecht, M., Janser, I., Burk, S., Weis, P. *Dalton T.* **2006**, *23*, pp. 2875-2880
54. Stang, P.J. *J. Org. Chem.* **2009**, *74* (1), pp. 2-20
55. Stang, P.J. *Chem.-Eur J.* **1998**, *4* (1), pp. 19-27
56. Stang, P.J., Olenyuk, B. *Accounts Chem. Res.* **1997**, *30* (12), pp. 502-518
57. Stang, P.J., Cao, D.H. *J. Am. Chem. Soc.* **1994**, *116* (11), pp. 4981-4982
58. Lindsey, J.S. *New J. Chem.* **1991**, *15*(2-3), pp. 153-80
59. Skobridis, K., Theodorou, V., Seichter, W., Weber, E. *Cryst. Growth Des.* **2010**, *10* (2), pp. 862-869
60. Szejtli, J. *Chem. Rev.* **1998**, *98* (5), pp. 1743-1753
61. Salorinne, K., Nissinen, M. *Org. Lett.* **2006**, *8* (24), pp. 5473-5476
62. Zheng, B., Wang, F., Dong, S., Huang, F. *Chem. Soc. Rev.* **2012**, *41* (5), pp. 1621-1636
63. Viton, F., White, P.S., Gagné, M.R. *Chem. Commun.* **2003**, *9* (24), pp. 3040-3041
64. Miyauchi, M., Harada, A. *J. Am. Chem. Soc.* **2004**, *126* (37), pp. 11418-11419
65. Kano, K., Nishiyabu, R., Asada, T., *et al.* *J. Am. Chem. Soc.* **2002**, *124* (33), pp. 9937-9944
66. Sakina, H., Abdelaziz, B., Leila, N., *et al.* *J. Incl. Phenom. Macro.* **2012**, *74* (1-4), pp. 1-10
67. Gopalsamuthiram, V., Predeus, A.V., Huang, R.H., Wulff, W.D. *J. Am. Chem. Soc.* **2009**, *131* (50), pp. 18018-18019
68. Notestein, J.M., Andrini, L.R., Kalchenko, V.I., Requejo, F.G., Katz, A., Iglesia, E. *J. Am. Chem. Soc.* **2007**, *129* (5), pp. 1122-1231
69. Atwood, J.L., Barbour, L.J., Jerga, A. *J. Am. Chem. Soc.* **2002**, *124* (10), pp. 2122-2123
70. Li, W.S., Aida, T. *Chem. Rev.* **2009**, *109* (11), pp. 6047-6076

71. Boyd, P.D.W., Reed, C. A. *Accounts Chem. Res.* **2005**, 38 (4), pp. 235 - 242
72. Rothmund, P. J. *Am. Chem. Soc.* **1936**, 58 (4), pp. 625-627
73. Hardie, M.J. *Isr. J. Chem.* **2011**, 51 (7), pp. 807-816
74. Kirchhoff, P. D.; Bass, M. B.; Hanks, B. A.; Briggs, J. M.; Collet, A.; McCammon, J. A. *J. Am. Chem. Soc.* **1996**, 118 (13), pp. 3237 - 3246
75. Kirchhoff, P. D.; Dutasta, J. P.; Collet, A. McCammon, J. A. *J. Am. Chem. Soc.* **1997**, 119 (34), pp. 8015 - 8022
76. Davis, M.E., Brewster, M.E. *Nat. Rev. Drug Discov.* **2004**, 3 (12), pp. 1023-1035
77. Steed, J.W. *Nat. Chem.* **2011**, 3 (1), pp. 9-10
78. Szejtli, J. In *Cyclodextrins and their Inclusion Complexes*, Akademiai Kiado: Budapest, **1982**
79. Weber, E. *J. Mol. Graphics* **1989**, 7 (1), pp. 12-27
80. Le Roex, T., Nassimbeni, L.R., Weber, E. *New J. Chem.* **2008**, 32 (5), pp. 856-863
81. Wulff, G. *J. Am. Chem. Soc.* **1985**, 26 (1), pp. 203
82. Wulff, G. . J. *Angew. Chemi. Int. Edit.* **1995**, 34 (17), pp. 1812-1832
83. Wulff, G. *Mol. Cryst. Liq. Crys. A.* **1996**, 276-277, pp. 1-6.
84. O'Shannessy, D.J., Ekberg, B., Andersson, L.I., Mosbach, K. *J. Chromatogr.* **1989**, 470 (2), pp. 391-399.
85. Mosbach, K. *Trends Biochem. Sci.* **1994**, 19 (1), pp. 9-14
86. Mayes, A.G., Mosbach, K. *TrAC.* **1997**, 16 (6), pp. 321-332
87. Dvorakova, G., Haschick, R., Chiad, K., *et al. Macromol. Rapid Comm.* **2010**, 31 (23), pp. 2035-2040

88. Allender, C.J., Richardson, C., Woodhouse, B., *et al. Int. J. Pharm.* **2000**, 195 (1-2), pp. 39-43
89. Kempe, H., Kempe, M. *Anal. Bioanal. Chem.* **2010**, 396 (4), pp. 1599-1606
90. Hiratani, H., Mizutani, Y., Alvarez-Lorenzo, C. *Macromol. Biosci.* **2005**, 5 (8), pp. 728-733
91. White, C.J., Byrne, M.E. *Expert Opin. Drug Del.* **2010**, 7 (6), pp. 765-780
92. Dickert, F.L., Hayden, O. *TrAC.* **1999**, 18 (3), pp. 192-199
93. Wulff, Guenter. *Pure Appl. Chem.* **1982**, 54 (11), pp. 2093-2102
94. Arshady, R., Mosbach, K. *Makromol. Chemie.* **1981**, 182 (2), pp. 687 - 692
95. Salian, V.D., Vaughan, A.D., Byrne, M.E. *J. Mol. Recognit.* **2012**, 25 (6), pp. 361-369
96. Kryscio, D.R., Peppas, N.A. *Acta Biomater.* **2012**, 8 (2), pp. 461-473
97. Shi, X., Wu, A., Qu, G., *et al. Biomaterials* **2007**, 28, pp. 3741-3749.
98. Haupt, K. *Nat. Mater.* **2010**, 9 (8), pp. 612-614
99. Wulff, G., Biffis, A. In *Molecular imprinting with covalent or stoichiometric non-covalent interactions; Sellergren, B., Ed.; Molecularly Imprinted Polymers; Elsevier: Amsterdam*, **2001**, pp. 71-111
100. Zhang, Y., *et al. J. Membrane Sci.* **2010**, 346 (2), pp. 318-326
101. Lorenzo, R.A., Carro, A.M., Alvarez-Lorenzo, C., Concheiro, A. *Int. J. Mol. Sci.* **2011**, 12 (7), pp. 4327-4347
102. Alvarez-Lorenzo, C., Concheiro, A. *Mini-Rev. Med. Chem.* **2008**, 8 (11), pp. 1065-1074
103. Peppas, N.A., Huang, Y. *Pharmaceut. Res.* **2002**, 19 (5), pp. 578-587
104. Hiratani, H., Alvarez-Lorenzo, C. *Biomaterials* **2004**, 25 (6), pp. 1105-1113

105. Cunliffe, D., Kirby, A., Alexander, C. *Adv. Drug Deliver. Rev.* **2005**, 57 (12), pp. 1836- 1853
106. Takeoka, Y., Berker, A.N., Du, R., *et al. Phys. Rev. Lett.* **1999**, 82 (24), pp. 4863-4865
107. Ito, K., Chuang, J., Alvarez-Lorenzo, C., Watanabe, T., *et al. Prog. Polym. Sci.* **2003**, 28 (10), pp. 1489-1515
108. Byrne, M.E., Salian, V. *Int. J. Pharm.* **2008**, 364 (2), pp. 188-212
109. Sellergren, B. *TrAC.* **1999**, 18 (3), pp. 164-174
110. Yan, H., Kyung, H.R. *Int. J. Mol. Sci.* **2006**, 7 (5-6), pp. 155-178
111. Warriner, K., Lai, E. P. C., Namvar, A., *et al. In Molecular Imprinted Polymers for Biorecognition of Bioagents*; Zourob, M, Elwary, S. and Turner, A., Ed.; Principles of Bacterial Detection: Biosensors, Recognition Receptors and Microsystems; Springer: New York, **2008**, 29, pp. 785 – 814.
112. Kim, H., Spivak, D.A. *J. Am. Chem. Soc.* **2003**, 125 (37), pp. 11269-11275
113. Olsson, G.D., Karlsson, B.C.G., Shoravi, S., Wiklander, J.G., Nicholls, I.A. *J. Mol. Recognit.* **2012**, 25 (2), pp. 69-73
114. Bandyopadhyay, A., Odegard, G.M. *Model. Simul. Mat. Sci. Eng.* **2012**, 20 (4), pp. 45018
115. Alvarez-Lorenzo, C., Concheiro, A. *J. Chromatogr. B.* **2004**, 804 (1), pp. 231-245
116. Miyata, T., Hayashi, T., Kuriu, Y., Uragami, T. *J. Mol. Recognit.* **2012**, 25 (6), pp. 336-343
117. Wulff, G. *Trends Biotechnol.* **1993**, 11 (3), pp. 85-87
118. Muhammad, T., Nur, Z., Elena V. *et al. S.A., Analyst* **2012**, 137 (11), pp. 2623-2628

119. Mollnelli, A., O'Mahony, J., Nolan, K., *et al.* *Anal. Chem.* **2005**, 77 (16), pp. 5196-5204
120. Navarro-Villoslada, F., San Vicente, B., Moreno-Bondi, M.C. *Anal. Chim. Acta* **2004**, 504 (1), pp. 149-162
121. Yoshimatsu, K., Yamazaki, T., Chronakis, I.S., Ye, L. *J. Appl. Polym. Sci.* **2012**, 124 (2), pp. 1249-1255
122. Nicholls, I.A. *Chem. Lett.* **1995**, 24 (11), pp. 1035-1036
123. Monroe, B.M., Weed, G.C. *Chem. Rev.* **1993**, 93 (1), pp. 435-448
124. Fouassier, J.P., Rabek, J.F., Ed.; In *Fundamentals and Methods, Radiation Curing in Polymer Science and Technology*; Elsevier Science: Essex, **1993**, pp. 2-46
125. Rudin, A. In *Introductory Concepts and Definitions, The Elements of Polymer Science and Engineering: An Introductory Text and Reference for Engineers and Chemists*; Academic Press: California, USA, **1999**, pp. 1-28
126. Decker, C. *Macromol. Rapid Comm.* **2002**, 23 (18), pp. 1067-1093
127. Allen, N.S. *J. Photoch. Photobio. A.* **1996**, 100 (1-3), pp. 101-107
128. Rouillard, A.D., Berglund, C.M., Lee, J.Y., *et al.* *Tissue Eng. Pt. C-Meth.* **2011**, 17 (2), pp. 173-179
129. Yagci, Y., Jockusch, S., Turro, N.J. *Macromolecules*, **2010**, 43 (15), pp. 6245-6260
130. Davidson, S.R. *J. Photoch. Photobio. A.* **1993**, 69 (3), pp. 263-275
131. Gruber, H.F. *Progress Polym. Sci.* **1992**, 17 (6), pp. 953-1044
132. Hageman, H.J. *Prog. Org. Coat.* **1985**, 13 (2), pp. 123-150
133. Allen, N.S. In *Photopolymerisation and Photoimaging Science and Technology*; Elsevier Applied Science: London, **1989**, pp. 5-71

134. Randell, D.R. In *Radiation Curing of Polymers II*; Royal Society of Chemistry: Cambridge, **1991**, pp. 2-132
135. Fouassier, J.P. In *Photoinitiation, Photopolymerisation and Photocuring: Fundamentals and Applications*; Hanser Publishers: Munich-Vienna-New York, 1995,
136. Fuchs, Y., Soppera, O., Haupt, K. *Anal. Chim. Acta* **2012**, 717, pp. 7-20
137. Kuhlmann, R., Schnabel, W. *Angew. Makromol. Chem.*, **1978**, 70 (1), pp. 145-157
138. Hageman, H. J. In *Photoinitiators and Photocatalysts for Various Polymerisation and Crosslinking Processes*; Randell, D. R., Ed.; Radiation Curing of Polymers II. Royal Society of Chemistry, London, **1987**, pp. 47-60
139. Arsu, N., Reetz, I., Yagci, Y., Mishra, M.K. *Handbook of Vinyl Polymers: Radical Polymerization, Process, and Technology* **2009**, 20, pp. 141-204
140. O'Shannessy, D.J., Ekberg, B., Mosbach, K. *Anal. Biochem.* **1989**, 177 (1), pp. 144-149
141. Piletska, E.V., Guerreiro, A.R., Whitcombe, M.J., Piletsky, S.A. *Macromolecules* **2009**, 42 (14), pp. 4921-4928
142. Lauten, E.H., Peppas, N.A. *J. Drug Del. Sci. Tech.* **2009**, 19 (6), pp. 391-399
143. Turiel, E.; Martín-Esteban, A.; Tadeo, J.L. *J. Chromatogr. A* **2007**, 1172 (2), pp. 97-104.
144. Luque de Castro, M.D., Priego-Capote, F.J. *J. Chromatogr. A* **2010**, 1217 (16), pp. 2383-2389
145. Pichon, V., Chapuis-Hugon, F. *Anal. Chim. Acta* **2008**, 622 (1-2), pp. 48-61
146. Kempe, M. *Anal. Chem.* **1996**, 68 (11), pp. 1948-1953
147. Sedláček, J. *Cesk. Oftalmol.* **1965**, 21 (6), pp. 509-512



148. Lee, W.-C., Cheng, C.-H., Pan, H.-H., *et al. Anal. Bioanal. Chem.* **2008**, 390 (4), pp. 1101-1109
149. Remcho, V.T., Tan, Z.J. *Anal. Chem.* **1999**, 71 (7), pp. 248A-255A
150. Tamayo, F.G., Turiel, E., Martín-Esteban, A. *J. Chromatogr. A* **2007**, 1152 (1-2), pp. 32-40
151. Haginaka, J. *J. Chromatogr. B.* **2008**, 866 (1-2), pp. 3-13
152. Haginaka, J., Sanbe, H., Takehira, H. *J. Chromatogr. A* **1999**, 857 (1-2), pp. 117-125
153. Vallano, P.T., Remcho, V.T. *J. Chromatogr. A* **2000**, 887 (1-2), pp. 125-135
154. Turiel, E., Martín-Esteban, A. *J. Sep. Sci.* **2005**, 28 (8), pp. 719-728
155. Turiel, E., Martín-Esteban, A. *Anal. Chim. Acta* **2010**, 668 (2), pp. 87-99
156. Caro, E., Marcé, R.M., Borrull, F., Cormack, P.A.G., Sherrington, D.C. *TrAC*. **2006**, 25 (2), pp. 143-154
157. Del Sole, R., Scardino, A., Lazzoi, M.R., Vasapollo, G. *J. Appl. Polym. Sci.* **2011**, 120 (3), pp. 1634-1641
158. Javanbakht, M., Attaran, A.M., Namjumanesh, M.H., Esfandyari-Manesh, M., Akbari-adergani, B. *J. Chromatogr. B.* **2010**, 878 (20), pp. 1700-1706
159. Ričanyová, J., Gadzala-Kopciuch, R., Reiffova, K., *et al. Adsorpt.* **2010**, 16 (4-5), pp. 473-483
160. Qi, P., Wang, J., Jin, J., Su, F., Chen, J. *Talanta* **2010**, 81 (4-5), pp. 1630-1635
161. Le Moullec, S., Bégos, A., Pichon, V., *et al. Chromatogr. A* **2006**, 1108 (1), pp. 7-13
162. Chianella, I., Piletsky, S.A., Tothill, I.E., *et al. Biosens. Bioelectron.* **2003**, 18 (2-3), pp. 119-127
163. Farrington, K., Magner, E., Regan, F. *Anal. Chim. Acta* **2006**, 566 (1), pp. 60-68

164. Cacho, C., Turiel, E., Martín-Esteban, A., *et al.* *J. Chromatogr. A* **2006**, *1114* (2), pp. 255-262
165. Turiel, E., Martín-Esteban, A., Fernández, P., *et al.* *Anal. Chem.* **2001**, *73* (21), pp. 5133-5141
166. Javanbakht, M., Fard, S.E., Mohammadi, A., *et al.* *Anal. Chim. Acta* **2008**, *612* (1), pp. 65-74
167. Piletsky, S.A., Turner, N.W., Laitenberger, P. *Med. Eng. Phys.* **2006**, *28* (10), pp. 971-977
168. Piletsky, S.A., Andersson, H.S., Nicholls, I.A. *Macromolecules* **1999**, *32* (3), pp. 633-636
169. Piletska, E.V., Romero-Guerra, M., Guerreiro, A.R., *et al.* *Anal. Chim. Acta* **2005**, *542* (1), pp. 47-51
170. Piletska, E.V., Guerreiro, A.R., Romero-Guerra, *et al.* *Anal. Chim. Acta* **2008**, *607* (1), pp. 54-60
171. Scorrano, S., Longo, L., Vasapollo, G. *Anal. Chim. Acta* **2010**, *659* (1-2), pp. 167-171
172. Longo, L., Vasapollo, G., Scardino, A., *et al.* *J. Porphyr Phthalocya* **2006**, *10* (8), pp. 1061-1065
173. Longo, L., Scorrano, S., Vasapollo, G. *J. Polym. Res.* **2010**, *17* (5), pp. 683-687
174. Longo, L., Vasapollo, G. *Metal-Based Drugs*, **2008**, pp. 281843-281845
175. Ye, L., Weiss, R., Mosbach, K. *Macromolecules* **2000**, *33* (22), pp. 8239-8245
176. Yoshimatsu, K., Reimhult, K., Krozer, A., *et al.* *Anal. Chim. Acta* **2007**, *584* (1), pp. 112-121
177. Mayes, A.G., Mosbach, K. *Anal. Chem.* **1996**, *68* (21), pp. 3769-3774

178. Urraca, J.L., Moreno-Bondi, M.C., Hall, A.J., Sellergren, B. *Anal. Chem.* **2007**, 79 (2), pp. 695-701
179. Dirion, B., Cobb, Z., Schillinger, E., Andersson, L.I., Sellergren, B. *J. Am. Chem. Soc.* **2003**, 125 (49), pp. 15101-15109
180. Urraca, J.L., Hall, A.J., Moreno-Bondi, M.C., Sellergren, B. *Angew. Chemi. Int. Edit.* **2006**, 45 (31), pp. 5158-5161
181. Ramström, O., Mosbach, K. *Curr. Opin. Chem. Biol.* **1999**, 3 (6), pp. 759-764
182. Kandimalla, V.B., Ju, H. *Anal. Bioanal. Chem.* **2004**, 380 (4), pp. 587-605
183. Langer, R., Vacanti, J.P. *Science* **1993**, 260 (5110), pp. 920-926
184. Slaughter, B.V., Khurshid, S.S., Fisher, O.Z., *et al. Advanced Materials* **2009**, 21 (32-33), pp. 3307-3329
185. Von Der Mark, K., Park, J., Bauer, S., *et al. Cell Tissue Res.* **2010**, 339 (1), pp. 131-153
186. Caldorera-Moore, M., Peppas, N.A. *Adv. Drug Delivery Rev.* **2009**, 61 (15), pp. 1391-1401
187. Elisseeff, J., Anseth, K., Sims, D. *et al. P. Natl. Acad. Sci. USA.* **1999**, 96 (6), pp. 3104-3107
188. Elisseeff, J., McIntosh, W., Anseth, K., *et al. R. J. Biomed. Mater. Res.* **2000**, 51 (2), pp. 164-171
189. Nguyen, K.T., West, J.L. *Biomaterials* **2002**, 23 (22), pp. 4307-4314
190. Young L, Medina D, DeOme K, *et al. Exp. Gerontol.* **1971**, 6 (1), pp. 49-56
191. Ifkovits J, Burdick J. *Tissue Eng.* **2007**, 13 (10), pp. 2369-2385
192. Hilt, J.Z., Byrne, M.E. *Adv. Drug Delivery Rev.* **2004**, 56 (11), pp. 1599-1620

193. Puoci, F., Iemma, F., Picci, N. *Curr. Drug Deliver.* **2008**, 5 (2), pp. 85-96
194. Spizzirri, U.G., Peppas, N.A. *Chem. Mater.* **2005**, 17 (26), pp. 6719-6727
195. Tong, K., Xiao, S., Li, S., Wang, J. *J. Inorg. Organomet. Polym. Mater.* **2008**, 18 (3), pp. 426-433
196. Schoener, C.A., Hutson, H.N., Peppas, N.A. *Polym. Int.* **2012**, 61 (6), pp. 874-879
197. Dill, K.A. *Nature* **1999**, 400, pp. 309-310
198. Brannon-Peppas, L. In *Absorbent Polymer Technology*; Elsevier: Amsterdam, **1990**, pp. 45-66.
199. Steed, J. W. In *Core Concepts in Supramolecular Chemistry and Nanochemistry*; Turner, D. R., Wallace, K.J., Eds.; John Wiley; Hoboken, NJ, **2007**
200. Lowman, A.M., Peppas, N.A. In *Encyclopedia of Controlled Drug Delivery*; Mthiowitz, E., Ed.; Wiley: New York **1999**, pp. 397-418
201. Peppas, N.A. In *Hydrogels in Medicine and Pharmacy*; CRC Press: Boca Raton, FL, **1987**
202. Hamcerencu, M., Desbrieres, J., Popa, M., *et al.* *Carbohydr. Polym.* **2012**, 89 (2), pp. 438-447
203. Peppas, N.A. In *Radiation Synthesis of Intelligent Hydrogels and Membranes for Separation Purposes*; Guven, G., Eds.; IAEA; Vienna, **2000**, pp. 1-14.
204. Flory, P.J. *J. Chem. Phys.* **1950**, 18 (1), pp. 108-111
205. Lin, C.-C., Metters, A.T. *Adv. Drug Delivery Rev.* **2006**, 58 (12-13), pp. 1379-1408
206. Alkayyali, L.B., Abu-Diak, O.A., Andrews, G.P., *et al.* *Ther. Del.* **2012**, 3 (6), pp. 775-786
207. Peppas, N.A., Langer, R. *Science* **1994**, 263 (5154), pp. 1715-1720

208. Peppas, N.A. *Curr. Opin. Coll. Int. Sci.* **1997**, 2 (5), pp. 531-537
209. Hunginger, H.E. *Pharm. Ind.* **1991**, 53 (11), pp. 1056-1065
210. Park, H., Park, K. *Pharmaceut. Res.* **1996**, 13 (12), pp. 1770-1776
211. Ratner, B.D., Hoffman, A.S. *J. Am. Chem. Soc.* **1976**, 31 (1), pp. 1-36
212. Chowdhury, S.M., Hubbell, J.A. *J. Surg. Res.* **1996**, 61 (1), pp. 58-64
213. Lu, S., Ramirez, W.F., Anseth, K.S. *J. Pharm. Sci.* **2000**, 89 (1), pp. 45-51
214. Stanojević, M., Krušić, M.K., Filipović, J., Parojčić, J., Stupar, M. *J. Deliv. Target. Thera. Agents* **2006**, 13 (1), pp. 1-7
215. Hoffman, A.S. *Adv. Drug Delivery Rev.* **2002**, 54 (1), pp. 3-12
216. Gupta, P., Vermani, K., Garg, S. *Drug Discov. Today* **2002**, 7 (10), pp. 569-579
217. Qiu, Y., Park, K. *Adv. Drug Delivery Rev.* **2001**, 53 (3), pp. 321-339
218. Taşdelen, B., Kayaman-Apohan, N., Güven, O., Baysal, B.M. *Int. J. Pharm.* **2004**, 278 (2), pp. 343-351
219. An, Y., Hubbell, J.A. *J. Control. Release* **2000**, 64 (1-3), pp. 205-215
220. Peppas, N.A. *MRS Bull.* **2006**, 31 (11), pp. 888-893
221. Peppas, N.A., Kim, B. *J. Drug Del. Sci. Tech.* **2006**, 16 (1), pp. 11-18
222. Bergmann, N.M., Peppas, N.A. *Progress Polym. Sci.* **2008**, 33 (3), pp. 271-288
223. Tonge, S.R., Tighe, B.J. *Adv. Drug Delivery Rev.* **2001**, 53 (1), pp. 109-122
224. Haraguchi, K., Farnworth, R., Ohbayashi, A., Takehisa, T. *Macromolecules* **2003**, 36 (15), pp. 5732-5741
225. Peppas, N.A., Bures, P., Leobandung, W., Ichikawa, H. *Eur. J. Pharm. Biopharm.* **2000**, 50 (1), pp. 27-46
226. Peppas, N.A., Khare, A.R. *Adv. Drug Delivery Rev.* **1993**, 11 (1-2), pp. 1-35

227. Peppas, N.A., Colombo, P. *J. Control. Release* **1997**, 45 (1), pp. 35-40
228. Betancourt, T., Pardo, J., Soo, K., Peppas, N.A. *J. Biomed. Mater. Res. A* **2010**, 93 (1), pp. 175-188
229. Jeong, S. H.; Huh, K. M.; Park, K. In *Hydrogel Drug Delivery Systems*; Uchegbu, I. F., Schatzlein, A. G., Eds.; Polymers in Drug Delivery; CRC/Taylor & Francis: Boca Raton, FL, **2006**
230. Davis, K.A., Anseth, K.S. *Crit. Rev. Ther. Drug.* **2002**, 19 (4-5), pp. 385-423
231. Hennink, W.E., Van Nostrum, C.F. *Adv. Drug Delivery Rev.* **2002**, 54 (1), pp. 13-36
232. Robinson, J.R. In *Controlled Drug Delivery – Challenges and Strategies*; Park, K., Ed.; American Chemical Society: Washington DC, **1997**, pp. 1-7
233. Langer, R., Peppas, N.A. *AIChE J.* **2003**, 49 (12), pp. 2990-3006
234. Peppas, N.A. *Adv. Drug Delivery Rev.* **2004**, 56 (11), pp. 1529-1531
235. Langer, R. *Nature* **1998**, 392 pp. 5-10
236. Mustata, G., Dinh, S.M. *Crit. Rev. Ther. Drug.* **2006**, 23 (2), pp. 111-135
237. Brenner, G. M., Stevens, C.W. In *Pharmacology*; Elsevier Inc.: Philadelphia, PA, **2006**
238. Hanson, Glen R., Venturelli, Peter J.; Fleckenstein, Annette E. In *How and Why Drugs Work; Drugs and Society*; Jones and Bartlett Inc.: Sudbury, Massachusetts, **2005**
239. Calcagno, Anna Maria; Siahaan, Teruna J. In *Physiological, Biochemical and Chemical Barriers to Oral Drug Delivery*; Wang, Binghe; Siahaan, Teruna; Soltero, Richard, Ed.; Drug Delivery: Principles and Applications; John Wiley and Sons Inc.: NJ, **2005**

240. Owens III, D.E., Peppas, N.A. *Int. J. Pharm.* **2006**, *307* (1), pp. 93-102
241. Berner, M.S, Rotenberg, G.N. Ed.; In The Canadian Medical Association. Guide to prescription and over the counter drugs, Montreal, Canada, **1990**
242. Elmquist, W. F. In *Targeted Bioavailability: A Fresh Look at Pharmacokinetic and Pharmacodynamic Issues in Drug Delivery*; Wang, Binghe; Siahaan, Teruna; Soltero, Richard, Ed.; Drug Delivery: Principles and Applications; John Wiley and Sons Inc.: NJ, NY, **2005**
243. Gulsen, D., Chauhan, A. *Invest. Ophth. Vis. Sci.* **2004**, *45* (7), pp. 2342-2347
244. Vandamme, T.F. *P. Ret. Eye Res.* **2002**, *21* (1), pp. 15-34
245. Zurowska-Pryczkowska, K., Sznitowska, M., Janicki, S. *Eur. J. Pharm. Biopharm.* **1999**, *47* (3), pp. 255-260
246. Siepmann, F., Siepmann, J., Walther, M., MacRae, R.J., Bodmeier, R. *J. Control. Release* **2008**, *125* (1), pp. 1-15
247. Dinçer, S., Türk, M., Pişkin, E. *Gene Ther.* **2005**, *12* (1), pp. S139-S145
248. des Rieux, A., Fievez, V., Garinot, M., Schneider, Y.-J., Préat, V. *J. Control. Release* **2006**, *116* (1), pp. 1-27
249. Liechty, W.B., Peppas, N.A. *Eur. J. Pharm. Biopharm.* **2012**, *80* (2), pp. 241-246
250. Duncan, R. *Nat. Rev. Drug Discov.* **2003**, *2* (5), pp. 347-360
251. Liechty, W.B., Kryscio, D.R., Slaughter, B.V., Peppas, N.A. *Annu. Rev. Chem. Biomol.* **2010**, *1*, pp. 149-173
252. Khurshid, S.S., Schmidt, C.E., Peppas, N.A. *J. Biomat. Sci.-Polym. E.* **2011**, *22* (1-3), pp. 343-362

253. Schneider, F., Piletsky, S., Piletska, E., *et al.* *J. Appl. Polym. Sci.* **2005**, *98* (1), pp. 362-372
254. Aydin, O., Attila, G., Dogan, A., *et al.* *Toxicol. Pathol.* **2002**, *30* (3), pp. 350-356
255. Fiume, M.Z. *Int. J. Toxicol.* **2002**, *21* (3), pp. 1-50
256. Lin, Z., Cheng, Y., Lü, H., *et al.* *Polymer* **2010**, *51* (23), pp. 5424-5431
257. Svenson, J., Nicholls, I.A. *Anal. Chim. Acta* **2001**, *435* (1), pp. 19-24
258. Haginaka, J., Sakai, Y. *J. Pharmaceut. Biomed.* **2000**, *22* (6), pp. 899-907
259. Claerhout, I., Buijsrogge, M., Delbeke, P., *et al.* *Brit. J. Ophthalmol.* **2011**, *95* (9), pp. 1199-1202
260. Nguyen, J., Fay, A. *Sem. Ophthalmol.* **2009**, *24* (3), pp. 178-184
261. Sadlej-Sosnowska, N., Dobrowolski, J.Cz., Mazurek, A.P. *J. Mol. Str.* **2000**, *520* (1-3), pp. 165-171
262. Piram, A., Faure, R., Chermette, H. *et al.* *Int. J. Env. Anal. Chem.* **2012**, *92* (1), pp. 96-109
263. Powell, J.R., Ambre, J.J., Ruo, T.I. In *The efficacy and toxicity of drug stereoisomers*, I.W. Wainer, & D.E. Dreyer, Ed.; Drug Stereochemistry, New York, NY, **1988**
264. Barrett, A.M., Cullum, V.A. *Br. J. Pharmacol.* **1968**, *34*, pp. 43-55
265. Jantararat, C., Tangthong, N., Songkro, S., *et al.* *Int. J. Pharm.* **2008**, *349* (1-2), pp. 212-225
266. Stoschitzky, K., Lindner, W., Rath, M., *et al.*, *N-S Arch Pharmacol.* **1989**, *339* (4), pp. 474-478
267. Love, J.N., Sikka, N., Klein-Schwartz, W., Curtis, L. *J. Emerg. Med.* **2004**, *26* (3), pp. 309-314



268. Hunt, C.E., Ansell, R.J. *Analyst* **2006**, *131* (5), pp. 678-683
269. Schweitz, L., Spegel, P., Nilsson, S. *Analyst* **2000**, *125* (11), pp. 1899-1901
270. Martin, P., Wilson, I.D., Morgan, D.E., Jones, G.R., Jones, K. *Anal. Comm.* **1997**, *34* (2), pp. 45-47
271. Walshe, M., Garcia, E., Howarth, J., Smyth, M.R., Kelly, M.T. *Anal. Comm.* **1997**, *34* (4), pp. 119-122
272. Haginaka, J., Sakai, Y., Narimatsu, S. *Anal. Sci.* **1998**, *14*, pp. 823-826
273. Haupt, K., Noworyta, K., Kutner, W. *Anal. Comm.* **1999**, *36* (11-12), pp. 391-393
274. Blanco-Fuente, H., Esteban-Fernández, B., Blanco-Méndez, J., Otero-Espinar, F.-J. *Chem. Pharma. Bull.* **2002**, *50* (1), pp. 40-46
275. Fundueanu, G., Constantin, M., Mihai, D., *et al.* *J. Chromatogr. B.* **2003**, *791* (1-2), pp. 407-419
276. Wang, N.X., Von Recum, H.A. *Macromol. Biosci.* **2011**, *11* (3), pp. 321-332
277. Warth, A.D. *App. Environ. Microbio.* **1991**, *57* (12), pp. 3410-3414
278. Somerville, D.A., Noble, W.C., White, P.M., *et al.* *Br. J. Derm.* **1971**, *85*, pp. 450-453
279. Paradee, N., Sirivat, A., Niamlang, S., Prissanaroon-Ouajai, W. *J. Mat. Sci.* **2012**, *23* (4), pp. 999-1010
280. Caro, E., Marcé, R.M., Cormack, P.A.G., *et al.* *J. Chromatogr. B.* **2004**, *813* (1-2), pp. 137-143
281. Papaphilippou, P., Christodoulou, M., Marinica, O.-M., *et al.* *ACS App. Mat.* **2012**, *4* (4), pp. 2139-2147
282. Hu, L.Y., Orwoll, R.A. *Sep. Sci. Tech.* **2010**, *45* (16), pp. 2337-2344
283. Hussain, M., Javeed, A., Ashraf, M., *et al.* *Pharmacol. Res.* **2012**, *66* (1), pp. 7-18

284. Vane, J.R. *Nature: New Bio.* **1971**, 231 (25), pp. 232-235
285. Lipsky, P.E. *Am. J. Orthoped.* **1999**, 28 (3), pp. 8-12
286. Adelizzi, R.A. *J. Am. Osteop. Assc.* **1999**, 99 (11), pp. 7-12
287. Zha, S., Yegnasubramanian, V., Nelson, W.G., *et al. Canc. Lett.* **2004**, 215 (1), pp. 1-20
288. Juber, A.; Legarto, M.L.; Massa, N.E.; *et al. J. Mol. Str.* **2006**, 783 (1-3), pp. 34-51
289. Mishra, A., Agrawal, S., Pathak, K. *Dr. Deliv.* **2012**, 19 (2), pp. 102-111
290. Roth, S.H. *Drugs* **2012**, 72 (7), pp. 873-879
291. Kristensen, S.L., Fosbøl, E.L., Kamper, A.-L., *et al. Pharmacoepidem. Dr. S.* **2012**, 21 (4), pp. 428-434
292. Roth, S.H. *Arch. Intern. Med.* **1986**, 146 (6), pp. 1075-1076.
293. Lanas, A., Garcia-Tell, G., Armada, B., Oteo-Alvaro, A. *BMC Med.* **2011**, 9, art. no. 38
294. Massó González, E.L., Patrignani, P., Tacconelli, S., *et al. Arthritis Rheum.* **2010**, 62 (6), pp. 1592-1601
295. Gupta, H., Aqil, M. *Drug Discov. Today* **2012**, 17 (9-10), pp. 522-527
296. Kompella, U.B., Kadam, R.S., Lee, V.H.L. *Thera. Deliv.* **2010**, 1 (3), pp. 435-456
297. Liu, S., Jones, L., Gu, F.X. *Macromol. Bio.* **2012**, 12 (5), pp. 608-620
298. Hiratani, H., Alvarez-Lorenzo, C. *J. Control. Release* **2002**, 83 (2), pp. 223-230
299. Alvarez-Lorenzo, C., Hiratani, H., Gómez-Amoza, J.L., *et al. J. Pharm. Sci.* **2002**, 91 (10), pp. 2182-2192
300. Poulin, P., Theil, F.-P. *J. Pharm. Sci.* **2009**, 98 (12), pp. 4941-4961
301. Mohammedi, H., Shyale, S., Shanta Kumar, S.M. *Int. J. Pharm. Sci. Rev. Res.* **2011**, 6 (2), pp. 163-166

302. Saettone, M.F., Chetoni, P., Bianchi, L.M., *et al. Int. J. Pharm.* **1995**, 126 (1-2), pp. 79-82
303. Yan, H., Qiao, J., Pei, Y., *et al. Food Chem.* **2012**, 132 (1), pp. 649-654
304. Zhang, Z., Xu, S., Li, J., *et al. J. Agric. Food Chem.* **2012**, 60 (1), pp. 180-187
305. Ahmad, E., Rabbani, G., Zaidi, N. *et al., PLoS ONE* **2011**, 6 (11), pp. 26186
306. Wu, W., Jiang, W., Xia, W., Yang, K., Xing, B. *J. Colloid. Interf. Sci.* **2012**, 374 (1), pp. 226-231
307. Wassink, D.A., Raski, J.Z., Levitt, J.A., *et al. Scanning Microscopy* **1991**, 5 (4), pp. 919-926
308. Schwarz, A.J., Kumar, M., Adams, B. L., Eds. In *Electrons Backscatter Diffraction in Materials Science*, Kluwer Academic/Plenum Publishers, New York, **2000**
309. Kaczmarek, D. *Opt. Appl.* **2001**, 31 (3), pp. 649-658
310. Goldstein, J. In *Scanning electron microscopy and x-ray microanalysis*. Kluwer Academic/Plenum Publishers, **2000**, pp. 689
311. Radzinski, Z.J., Russ, J.C. *J. Comput. Assist. Micros.* **1989**, 1 (2), pp. 181-193
312. Beil, W., Carlsen, I.C. *J. Micros.* **1990**, 157 (1), pp. 127-133
313. Harz, S., Schimmelpfennig, M., Tse Sum Bui, B., *et al. Eng. Life Sci.* **2011**, 11 (6), pp. 559-565
314. Lakowicz, J.R. In *Principles in Fluorescence Spectroscopy*. Vol. I; Springer: New York, **2006** pp. 3
315. Szudy, J., Ed.; In *Born 100 years ago: Aleksander Jablonsi (1898-1980)*, Uniwersytet Mikołaja Kopernika: Torun, Poland, **1998**
316. Ton, X.-A., Acha, V., Haupt, K., *et al. Biosens. Bioelectron.* **2012**, 36 (1), pp. 22-28

317. McBain, K. Molecular Imprinting of Hydrogels: Improved Drug Delivery Vehicles.  
Ryerson University – M.Sc. Thesis, **2009**
318. Sortino, S., Petralia, S., Boscà, F., Miranda, M.A. *Photochem. Photobio. Sci.* **2002**, *1* (2), pp. 136-140
319. Dantas, R.F., Rossiter, O., Teixeira, A.K.R., *et al.* *Chem. En. J.* **2010**, *158* (2), pp. 143-147
320. Liu, Q.-T., Williams, H.E. *Enviro. Sci. Tech.* **2007**, *41* (3), pp. 803-810
321. Piram, A., Salvador, A., Verne, C., *et al.* *Chemosphere* **2008**, *73* (8), pp. 1265-1271
322. Petrovic, M., Petrovic, M., Barceló, D. *TrAC*. **2007**, *26* (6), pp. 486-493
323. Russo, M.A.L., Strounina, E., Waret, M., *et al.* *Biomacromol.* **2007**, *8* (1), pp. 296-301
324. Ferree, B.A. Pat. App. Pub. **2003**, 623, 17.16
325. Zhao, C., He, P., Xiao, C., *et al.* *J. Appl. Polym. Sci.* **2012**, *123* (5), pp. 2923-2932
326. Geever, L.M., Cooney, C.C., Lyons, J.G., *et al.* *Eur. J. Pharm. Biopharm.* **2008**, *69* (3), pp. 1147-1159
327. Arima, T., Hamada, T., McCabe, J.F. *J. Dent. Res.* **1995**, *74* (9), pp. 1597-1601
328. Uwai, K., Tani, M., Ohtake, Y., *et al.* *Life Sci.* **2005**, *78* (4), pp. 357-365
329. Lin, A.Y.-C., Lin, C.-A., Tung, H.-H., *et al.* *J. Haz. Mat.* **2010**, *183* (1-3), pp. 242-250
330. Sellergren, B., Nilsson, K.G.I. *Meth. Mol. Cel. Bio.* **1989**, *1* (2), pp. 59-62
331. Martin, P., Wilson, I.D., Jones, G.R. *J. Chromatogr. A* **2000**, *889* (1-2), pp. 143-147
332. Streubel, A., Siepmann, J., Bodmeier, R. *Eur. J. Pharm. Sci.* **2003**, *18* (1), pp. 37-45
333. Pygall, S.R., Kujawinski, S., Timmins, P., Melia, C.D. *Int. J. Pharm.* **2009**, *370* (1-2), pp. 110-120

334. Williams III, R.O., Reynolds, T.D., Cabelka, T.D., *et al. Pharma. Dev. Tech.* **2002**, 7 (2), pp. 181-193
335. Huang, X., Brazel, C.S. *J. Control. Release* **2001**, 73 (2-3), pp. 121-136
336. Fu, Y., Kao, W.J. *Expert Opin. Drug Del.* **2010**, 7 (4), pp. 429-444
337. Mallapragada, S.K., Pandit, N. *Am. Soc. Mech. Eng. BED* **1999**, 42, pp. 675-676
338. Siepmann, J., Siepmann, F. *J. Control. Release* **2012**, 161 (2), pp. 351-362
339. Narasimhan, B. *Adv. Drug Delivery Rev.* **2001**, 48 (2-3), pp. 195-210
340. Narasimhan, B.; Mallapragada, SK; Peppas, N.A., *Release Kinetics, Data interpretation*, In: Encyclopedia of Controlled Drug Delivery, Vol. 2, Mathiowitz, E., Ed., John Wiley & Sons, New York, **1999**, pp. 921-935
341. Haupt, K., Linares, A.V., Bompert, M., Bui, B.T.S. *T. Curr. Chem.*; Haupt, K., Ed., Springer, Berlin, Heidelberg, **2012**, 325, pp. 1-28
342. Patel, A., Fouace, S., Steinke, J.H.G. *Anal. Chim. Acta* **2004**, 504 (1), pp. 53-62
343. Patel, A., Fouace, S., Steinke, J.H.G. *Chem. Comm.* **2003**, 9 (1), pp. 88-89